

Photochemical Expulsion of Leaving Groups from a Naphthothiophene-2-Carboxamide Linked to a Chromophore

Lingzi Li
Marquette University

Recommended Citation

Li, Lingzi, "Photochemical Expulsion of Leaving Groups from a Naphthothiophene-2-Carboxamide Linked to a Chromophore" (2018). *Dissertations (2009 -)*. 803.
https://epublications.marquette.edu/dissertations_mu/803

PHOTOCHEMICAL EXPULSION OF LEAVING GROUPS FROM A
NAPHTHOTHIOPHENE-2-CARBOXAMIDE LINKED TO A CHROMOPHORE

by
Lingzi Li

A Dissertation submitted to the Faculty of the Graduate School,
Marquette University,
in Partially Fulfillment of the Requirement
for the Degree of Doctor of Philosophy

Milwaukee, Wisconsin
August 2018

ABSTRACT

PHOTOCHEMICAL EXPULSION OF LEAVING GROUPS FROM A NAPHTHOTHIOPHENE-2-CARBOXAMIDE LINKED TO A CHROMOPHORE

Lingzi Li

Marquette University, 2018

Two bichromophoric systems were synthesized which have thioxanthone as the chromophore that absorbs the incident light and a naphthothiophene-2-carboxanilide, which serves as a triplet excited state energy acceptor. Upon excitation the triplet excited state of the thioxanthone is populated via intersystem crossing, which is efficient with $\Phi_{isc} = 0.68$. Based on the relative energies of the triplet excited states of thioxanthone ($E_T = 65 \text{ kcal mol}^{-1}$) and naphthothiophene ($E_T = 51 \text{ kcal mol}^{-1}$), the subsequent triplet excited state energy transfer to generate the triplet excited state of the naphthothiophene-2-carboxamide should be a very rapid process that is 14 kcal mol^{-1} exothermic. Computational studies have shown that the triplet excited state of the naphthothiophene-2-carboxanilide undergoes an electrocyclic ring closure to ultimately generate an intermediate with zwitterionic character. This intermediate is thought to be responsible for the elimination of a leaving group that is attached to the C-3 position of the thiophene ring. When the thioxanthone chromophore is linked to naphthothiophene-2-carboxanilide via a trimethylene linkage, the release of a leaving group originally attached to the C-3 position of the thiophene ring occurs with $\Phi = 0.13 - 0.15$. These efficiencies can be compared to the thioxanthone sensitized photolysis, in which the triplet energy transfer is intermolecular. The triplet sensitized quantum yield is $\Phi = 0.13$. The close similarity in efficiencies for the linked and unlinked systems indicates that the triplet energy transfer is as efficient when it occurs by a through-bond mechanism involving the trimethylene linker as when it is intermolecular and occurs collisionally between donor and acceptor, which instead requires overlap of the donor and acceptor orbitals. In both cases the energy transfer efficiency is $\Phi_{et} = 1$, given that $\Phi = \Phi_{isc}\Phi_{et}\Phi_r$. On the other hand, when the thioxanthone directly replaces the phenyl group of the naphthothiophene-2-carboxanilide the quantum yield is two-fold less than the trimethylene-linked system. Either $\Phi_{et} < 1$ or $\Phi_r < 0.19$ due to an unfavorable substituent effect that discourages electrocyclization with the thioxanthone ring.

ACKNOWLEDGEMENTS

Lingzi Li

First and foremost, I would like to express my deepest gratitude to my advisor, Dr. Mark G. Steinmetz, who has been a tremendous mentor ever since I joined the chemistry lab. This thesis would not have been possible without his patient guidance.

I am thankful to my thesis committee members, Dr. William Donaldson, Dr. James Gardinier, Dr. Evgueni Kovrigin and Dr. Chae S. Yi for their time, patience and suggestions through my graduate studies. I would like to thank Marquette University Chemistry Department for providing me with the unrestricted facilities and constant financial support during this period. My special thank goes to Dr. Sergey Lindman for his help in X-ray crystallography, Dr. Sheng Cai for help with NMR, Dr. Shama P. Mirza and Dr. Anna Benko of the Shimadzu Laboratory for Advanced and Applied Analytical Chemistry at the University of Wisconsin, Milwaukee for the HR-MS analyses. I would like to thank my group member Dr. Gilbert Ndzeidze and former member Dr. Himali Devika Jayasekara for their help and friendship. My special gratitude to Dr. Sandra Lukaszewski-Rose, Mr. Paul Dion and Ms. Lori Callaghan for their kind help.

I would like to thank my family for their continuous support. I am grateful to my grandmother for her unconditional love. I am forever indebted to my father for providing me with the education opportunity and life experiences that made me who I am today. This journey to graduate school would not have started if not for their encouragement ever since my childhood. I want to dedicate the thesis to my family.

Finally, I would like to thank the National Science Foundation for the financial support of this work (Grant No. CHE-1055339).

TABLE OF CONTENTS

ACKNOWLEDGEMENTS	i
TABLE OF CONTENTS.....	iii
LIST OF TABLES	vi
LIST OF FIGURES	vii
LIST OF SCHEMES.....	ix
LIST OF NMR SPECTRA IN APPENDIX 3.	xi
CHAPTER 1.	1
INTRODUCTION	1
1.1. The goal of the project.	1
1.2. Brief introduction on photoremovable protecting groups.	4
1.3. Background on release of leaving groups via photogenerated zwitterionic intermediates.	6
1.3.1. The mechanism for the photorelease of leaving groups.	8
1.3.2. Background on Chemical Actinometry	14
1.4. Background on photochemistry	15
1.4.1. Background on the sensitized release of leaving group.	18
1.5. Introduction to some PRPGS and the Mechanism of Photorelease.	20
1.6. Applications of the caged compounds in biological studies.	25
1.6.1. Caged neurotransmitters.	25
1.6.2. Caged calcium ions.....	27
1.6.3. Caged nucleotides and nucleosides.	28
1.6.4. Caged peptides and proteins.....	29
1.6.5. Caged mRNA and DNA.....	31
1.6.6. Summary.....	32
CHAPTER 2.	33

CAGED COMPOUND INVOLVED NAPHTHO(2,3-B)THIOPHENE-2-CARBOXANILIDE WITH THIOXANTHONE AS PHOTO SENSITIZER	33
2.1. Introduction	33
2.2. Results	36
2.2.1. Synthesis.....	36
2.2.2. Synthesis of compound 12 and 13.....	39
2.2.3. Crystal Structures.	42
2.2.4. Photolyses	44
2.2.5. Absorption Spectroscopy.....	46
2.3. Experimental section.....	51
CHAPTER 3.	77
PHOTOCHEMISTRY OF THE SYSTEM INVOLVING THIOXANTHONE AND NAPHTHOTHIOPHENE-2-CARBOXAMIDE.....	77
3.1. Introduction.	77
3.2. Results	78
3.2.1. Quantum Yields.....	78
3.2.2. Quenching Studies.....	80
3.2.3. Intermolecular sensitized photolysis with thioxanthone as the sensitizer.	84
3.2.4. Intermolecular Sensitized Photolysis with xanthone as the sensitizer.	85
3.2.5. Intermolecular Sensitized Photolysis with acriflavine as the sensitizer.	86
3.3. Discussion	87
3.4. Conclusions.	90
3.5. Experimental Section.	92
3.5.1. Potassium Ferrioxalate Actinometry.	92
3.5.2. Determination of light output (LOP).....	93
3.5.3. General Procedure for Quantum Yield Determination.....	94
3.5.4. Preparation of 100 mM KH ₂ PO ₄ buffer pH 7 solution.....	95
3.5.5. Photochemical Studies.....	95
APPENDIX 1.....	101

SYNTHESIS OF 3-BROMO-7-OXO-7H-CYCLOPENTA [1,2-b:4,3-b']DITHIOPHENE-2-CARBOXYLIC ACID WITH POTENTIAL TO BE SENSITIZED WITH CHROMOPHORE THAT ABSORBS AT LONGER WAVELENGTH.	101
4.1. Introduction	101
4.2. Results	103
4.3. Experimental Section.	106
APPENDIX 2.....	110
X-RAY CRYSTALLOGRAPHY.....	110
APPENDIX 3.....	113
NMR SPECTRA.....	113
BIBLIOGRAPHY.....	177

LIST OF TABLES

CHAPTER 1.

Table 1.1. Quantum yields with various leaving groups.....	9
Table 1.2. Some examples of previously reported caged compounds. ²³	26
Table 1.3. A list of commercial available caged compounds.....	32

APPENDIX 2.

Table 5.1. Crystal data and structure refinement for direct-linked cage compound 11b	110
Table 5.2. Crystal data and structure refinement for tethered caged compound 12a	111
Table 5.3. Crystal data and structure refinement for methylated Boc animo thioxanthone 27	112

LIST OF FIGURES

CHAPTER 1.

Figure 1.1. Depiction of photactivation of caged compound..... 4

Figure 1.2. Typical examples of caged bioeffectors reported previously. a. nitrophenyl-EGTA(caged calcium)²²; b. P³-1-(2-nitro)phenyl-ethyl-ATP (caged ATP); c. 6-bromo-7-hydroxycoumarin-4-ylmethyl caged²⁷; d. 4-Methoxy-7-nitroindolyl-caged-L-glutamate¹²; e. 4-hydroxy-phenacyl (HP) bromide caged P_ST¹⁹⁷Ca.²⁹ 5

Figure 1.3. Plot of log Φ vs p K_a of the LG⁻conjugate acid for the photolysis in Scheme 1.4).¹ 10

Figure 1.4. Relative enthalpies of the stationary points on the ground-state S₀ and the lowest triplet T₁ surfaces relevant for formation of the ring closure product from **3**. Unpaired spin density isosurfaces are shown for open-shell species.² 12

Figure 1.5. Examples of some PRPGs. 20

Figure 1.6. Chemical structure of NB, NPE, NBOC, MeNBOC caged compounds with different functional groups..... 21

Figure 1.7. Selected caged Glutamate..... 26

Figure 1.8. Examples of Ca²⁺ cages with their parent chelators (EDTA, EGTA, BAPTA) 27

Figure 1.9. Uncaging of caged Ca²⁺. a. Ca²⁺ uncaging by photolysis of nitr-2. b. Ca²⁺ uncaging by photolysis of NP-EGTA. 28

Figure 1.10. Three caging strategies for nucleotides according to the structures of the nucleotides. 29

Figure 1.11. Preparation of caged protein using chemical modification. 30

Figure 1.12. Synthesis of caged AIP..... 31

CHAPTER 2.

Figure 2.1. Three cases studied in this project. **Error! Bookmark not defined.**

Figure 2.2. Direct-linked caged compound **11b**. (a. Crystal structure. b. Crystal packing.) 42

Figure 2.3. X-ray structure of direct-linked caged compound **12a**. (a. Crystal structure. b. Crystal packing.) 43

Figure 2.4. X-ray structure of methylated Boc amino thioxanthone **27**. (a. Crystal structure. b. Crystal packing.) 44

Figure 2.5. ^1H NMR COSY for photoproduct of compound 11b in DMSO- d_6	45
Figure 2.6. Absorption spectra of photoreactant 11b (—) and photoproduct 43b (----). Concentrations were 2.54×10^{-5} M and 2.97×10^{-5} M, respectively in dioxane containing 17% 100 mM phosphate buffer at pH 7.....	47
Figure 2.7. Absorption spectra of reactant 12a (—) and photoproduct 45b (----). Concentrations were 2.01×10^{-5} M and 1.75×10^{-5} M, respectively in dioxane containing 17% 100 mM phosphate buffer at pH 7.....	48
Figure 2.8. Absorption spectra of anilide 13a (—), photoproduct 46a (·····), and thioxanthone (----).....	49
Figure 2.9. Absorption spectra of trimethylene – linked thioxanone 12a (—) and an equimolar mixture of thioxanthone and anilide 13a (·····).....	50
Figure 2.10. Absorption spectra of anilide 13b (—) and thioxanthone (·····).....	50
Figure 2.11. The Absorption spectra of anilide 12a (—) and acriflavine (·····).	51

CHAPTER 3.

Figure 3.1. Stern-Volmer plot for quenching of the photochemistry of 12a by ferrocene. Fit of the data to a line (—), calculated curves (eq. 3.2) for $\tau_1 = 200$ ns (- - -) or $\tau_1 =$ 500 ns (·····) using $\tau_2 = 11.5$ μs	81
Figure 3.2. Stern-Volmer plot for quenching of the photochemistry of 13a by ferrocene.	83
Figure 3.3. Depiction of Semi-micro optical bench set up for quantum yield determination.	95

APPENDIX 1.

Figure 4.1. Compound 47 and its corresponding caged compound.....	102
---	-----

LIST OF SCHEMES

CHAPTER 1.

Scheme 1.1. Photorelease of various leaving groups from benzothiophene carboxamide via a putative zwitterionic intermediate.....	1
Scheme 1.2. The proposed cage compounds involve photochemical electrocyclic ring closure.....	7
Scheme 1.4. The mechanism of the photorelease of leaving groups.....	8
Scheme 1.5. Photoexpulsion of various leaving groups from benzothiophene-2-carboxamide.....	9
Scheme 1.6. The summary of the mechanism.....	11
Scheme 1.7. Photolysis quantum yields for different triplet energy transfer (ET) from thioxanthone to thiophene rings.....	13
Scheme 1.8. A global paradigm for the overall photophysical and photochemical pathways from $*R$. ⁴⁹	17
Scheme 1.9. The Jablonski diagram (state energy diagram) for organic photochemical reactions.....	17
Scheme 1.10. General scheme for photosensitization.....	18
Scheme 1.11. Intermolecular Triplet Sensitization of the 2-(2-Nitrophenyl)propyl Chromophore. ⁵¹	19
Scheme 1.12. Nitrobenzyl-protected adenosine triphosphate(ATP).....	20
Scheme 1.13. The photodeprotection mechanism of o-Nitrobenzyl group. ³⁶⁻³⁸	21
Scheme 1.14. The photodeprotection mechanism of benzoin group.....	23
Scheme 1.15. The photodeprotection mechanism of p-hydroxyphenacyl group.	24
Scheme 1.16. The deprotection mechanism of coumarin group	25
Scheme 1.17. Synthesis of caged mRNA.....	31

CHAPTER 2.

Scheme 2.1. Photoremovable protecting groups based on zwitterionic intermediate from benzothiophene-2 carboxanilide.	Error! Bookmark not defined.
--	-------------------------------------

Scheme 2.2. Synthesis of compound 20	Error! Bookmark not defined.
Scheme 2.3. Synthesis of 28	39
Scheme 2.4. Synthesis of 33	40
Scheme 2.5. Sythesis of 39	41
Scheme 2.6. Synthesis of 42	41
Scheme 2.7. Photolysis of direct-linked caged compound 11	45
CHAPTER 3.	
Scheme 3.1. Photolysis of 11b	78
Scheme 3.2. Photolysis of 12 with various leaving groups.....	79
Scheme 3.3. Energy diagram for photolysis of tehtered thioxathone anilide 12a	Error! Bookmark not defined.
Scheme 3.4. Intermolecular sensitized photolysis of thioxanthone with naphthothiophene-2-carboxanilide 13b	85
Scheme 3.5. Intermolecular sensitized photolysis of xanthone and anilide 13b	85
Scheme 3.6. Intermolecular sensitized photolysis of acriflavine and anilide 13a	86
APPENDIX 1.	
Scheme 4.1. Retrosynthesis of 48a	103
Scheme 4.2. Retrosynthesis of compound 47	104
Scheme 4.3. Attempted sysnthesis of 47	105
Scheme 4.4. Original attempted synthesis of 47	106

LIST OF NMR SPECTRA IN APPENDIX 3.

Figure 1. ^1H NMR Spectra of Compound 14 in CDCl_3	114
Figure 2. ^{13}C NMR Spectra of Compound 14 in CDCl_3	115
Figure 3. ^1H NMR Spectra of Compound 15 in DMSO-d_6	116
Figure 4. ^{13}C NMR Spectra of Compound 15 in DMSO-d_6	117
Figure 5. ^1H NMR Spectra of Compound 16 in CDCl_3	118
Figure 6. ^{13}C NMR Spectra of Compound 16 in CDCl_3	119
Figure 7. ^1H NMR Spectra of Compound 18 in CDCl_3	120
Figure 8. ^{13}C NMR Spectra of Compound 18 in CDCl_3	121
Figure 9. ^1H NMR Spectra of Compound 19 in DMSO-d_6	122
Figure 10. ^{13}C NMR Spectra of Compound 19 in DMSO-d_6	123
Figure 11. ^1H NMR Spectra of Compound 21 in DMSO-d_6 Error! Bookmark not defined.	
Figure 12. ^{13}C NMR Spectra of Compound 19 in DMSO-d_6	125
Figure 13. ^1H NMR Spectra of Compound 23 in DMSO-d_6	126
Figure 14. ^1H NMR Spectra of Compound 25 in CDCl_3	127
Figure 15. ^{13}C NMR Spectra of Compound 25 in CDCl_3	128
Figure 16. ^1H NMR Spectra of Compound 26 in CDCl_3	129
Figure 17. ^{13}C NMR Spectra of Compound 26 in CDCl_3	130
Figure 18. ^1H NMR Spectra of Compound 27 in CDCl_3	131
Figure 19. ^1H NMR Spectra of Compound 27 in CDCl_3	132
Figure 20. ^1H NMR Spectra of Compound 28 in CDCl_3	133
Figure 21. ^{13}C NMR Spectra of Compound 28 in CDCl_3	134
Figure 22. ^1H NMR Spectra of Compound 11a in CDCl_3	135
Figure 23. ^{13}C NMR Spectra of Compound 11a in CDCl_3	136

Figure 24. ^1H NMR Spectra of Compound 43a in CDCl_3	137
Figure 25. Expanded (8.90 – 7.30 ppm) ^1H NMR Spectra of Compound 43a in CDCl_3	138
Figure 26. ^1H NMR Spectra of Compound 11b in DMSO-d_6	139
Figure 27. ^1H NMR Spectra of Compound 43b in DMSO-d_6	140
Figure 28. Expanded (8.80 – 7.20 ppm) ^1H NMR Spectra of Compound 43a in DMSO-d_6	141
Figure 29. ^{13}C NMR Spectra of Compound 43b in DMSO-d_6	142
Figure 30. Cosy Spectra of Compound 43b in DMSO-d_6	143
Figure 31. ^1H NMR Spectra of Compound 31 in CDCl_3	144
Figure 32. ^{13}C NMR Spectra of Compound 31 in CDCl_3	145
Figure 33. ^1H NMR Spectra of Compound 33 in CDCl_3	146
Figure 34. ^{13}C NMR Spectra of Compound 33 in CDCl_3	147
Figure 35. ^1H NMR Spectra of Compound 12 in CDCl_3	148
Figure 36. ^{13}C NMR Spectra of Compound 12 in CDCl_3	149
Figure 37. ^1H NMR Spectra of Compound 45 in CDCl_3	150
Figure 38. ^{13}C NMR Spectra of Compound 45 in CDCl_3	151
Figure 39. ^1H NMR spectra of compound 40 in CDCl_3	152
Figure 40. ^1H NMR Spectra of Compound 41 in CDCl_3	153
Figure 41. ^{13}C NMR Spectra of Compound 41 in CDCl_3	154
Figure 42. ^1H NMR Spectra of Compound 13a in CDCl_3	155
Figure 43. ^{13}C NMR Spectra of Compound 13a in CDCl_3	156
Figure 44. ^1H NMR Spectra of Compound 13b in DMSO-d_6	157
Figure 45. ^{13}C NMR Spectra of Compound 13b in DMSO-d_6	158
Figure 46. ^1H NMR Spectra of Compound 46b in DMSO-d_6	159
Figure 47. ^1H NMR Spectra of Compound 46a in CDCl_3	160

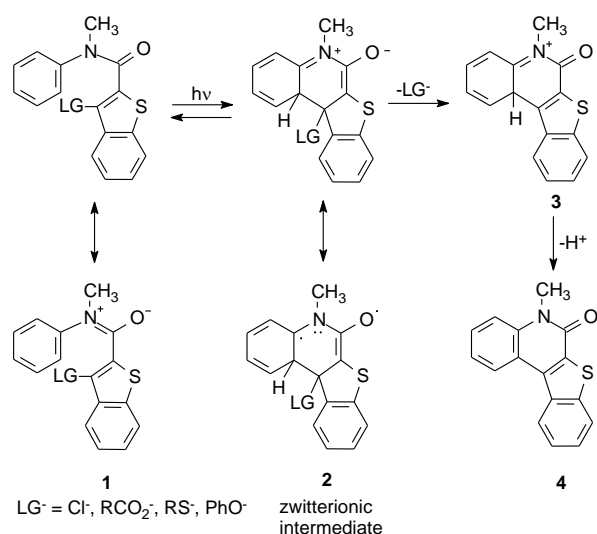
Figure 48. ^1H NMR Spectra of Compound 34 in CDCl_3	161
Figure 49. ^{13}C NMR Spectra of Compound 34 in CDCl_3	162
Figure 50. ^1H NMR Spectra of Compound 35 in CDCl_3	163
Figure 51. ^{13}C NMR Spectra of Compound 35 in CDCl_3	164
Figure 52. ^1H NMR Spectra of Compound 36 in CDCl_3	165
Figure 53. ^{13}C NMR Spectra of Compound 36 in CDCl_3	166
Figure 54. ^1H NMR Spectra of Compound 37 in CDCl_3	167
Figure 55. ^{13}C NMR Spectra of Compound 37 in CDCl_3	168
Figure 56. ^1H NMR Spectra of Compound 38 in CDCl_3	169
Figure 57. ^{13}C NMR Spectra of Compound 38 in CDCl_3	170
Figure 58. ^1H NMR spectra of compound 51 in CDCl_3	171
Figure 59. ^{13}C NMR spectra of compound 51 in CDCl_3	172
Figure 60. ^1H NMR spectra of compound 52 in CDCl_3	173
Figure 61. ^1H NMR spectra of compound 53 in CDCl_3	174
Figure 62. ^1H NMR spectra of compound 54 in CDCl_3	175
Figure 63. ^1H NMR spectra of compound 55 in CDCl_3	176

CHAPTER 1.

INTRODUCTION

1.1. The goal of the project.

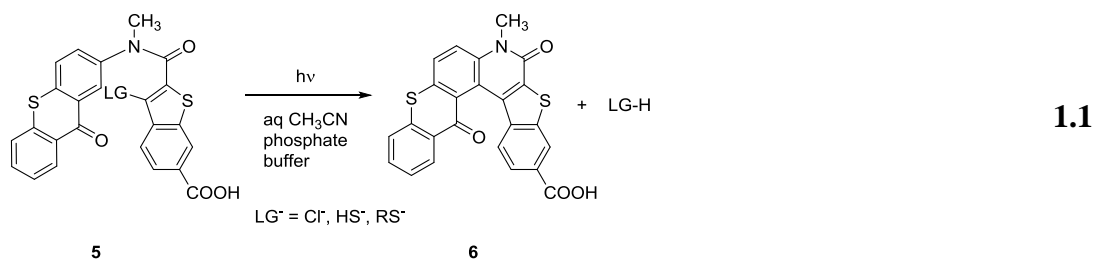
The anilide of benzothiophene-2-carboxamide has been found to efficiently expel a wide variety of leaving group anions from the C-3 position of the ring system upon photolysis.¹ The LG⁻ release step is thought to take place from a putative zwitterionic intermediate, which is generated upon excited state electrocyclic ring closure of the thiophene ring with the phenyl group attached to carboxamide nitrogen. (Scheme 1.1)



Scheme 1.1. Photorelease of various leaving groups from benzothiophene carboxamide via a putative zwitterionic intermediate.

Efforts turned to incorporating a chromophore that absorbs at longer wavelengths than 300-320 nm that was used for compound **1**. Thus, the *N*-phenyl was replaced by a thioxanthone chromophore², which absorbs light in the 380-410 nm region. (Equation 1.1) The C-6 carboxylic acid group also provides aqueous solubility. These modifications

resulted in a system that expels leaving groups quantitatively. However, the quantum yields were found to be $\Phi = 0.01-0.06$, depending on the leaving group to be expelled.



The goal of the dissertation research is to improve quantum yields for LG^- expulsion by improving the energetics of an energy transfer step that is involved in the above reaction with the thioxanthone chromophore. The aforementioned photoreaction in Scheme 1.1 occurs in the triplet excited state. The initial triplet excited state is localized on the thioxanthone chromophore, which has a triplet energy $E_T = 64 \text{ kcal mol}^{-1}$.³ For the electrocyclicization to occur, triplet energy transfer must generate the triplet excited state of the benzothiophene ring system, according to a recent computational study. Since the latter triplet excited state has $E_T = 69 \text{ kcal mol}^{-1}$,^{4,5} the energy transfer step is unfavorable and 5 kcal mol^{-1} endothermic. The dissertation project facilitates the energy transfer by replacing the benzothiophene ring system with a naphththiophene ring system that has an estimated $E_T = 51 \text{ kcal mol}^{-1}$.⁶

The first hurdle to overcome in the dissertation project was to synthesize the naphthothiophene-2-carboxamide ring system with a leaving group at the C-3 position. Literature only exists for the synthesis of unsubstituted naphthothiophene ring, which was considered impractical for the dissertation project, because it provided no opportunities for incorporating the necessary carboxamide group or the leaving group. A practical synthesis was thus devised for this dissertation.

The anilide *N*-phenyl was replaced with a thioxanthone chromophore and the photochemistry was studied. Quantum yields are only modestly higher than found for the previously studied benzothiophene-2-carboxamide bearing a thioxanthone chromophore. It was considered possible that the short linkage between thioxanthone and naphthothiophene rings inhibited the energy transfer step from the triplet excited thioxanthone. Thus, the thioxanthone was attached to the carboxamide group via a flexible trimethylene linker. This last modification resulted in significant improvement of the efficiencies for the photoreaction.

Quenching studies were conducted using ferrocene as a triplet state quencher. The quenching kinetics were derived, and Stern-Volmer plots were obtained. However, quantum yields for the closely linked thioxanthone naphthothiophene-2-carboxamide system were too low for an analogous quenching study to be successful.

Work turned to incorporating useful leaving groups than bromide at the C-3 position of the naphthothiophene ring system. Nucleophilic substitution of the bromide with a methoxy group was successful upon oxidation of the thiophene sulfur to a sulfoxide. Subsequent reduction of the sulfoxide and further elaboration of the functionality followed by attachment of the tethered thioxanthone ultimately afforded a naphthothiophene ring system with a C-3 hydroxyl group. The C-3 hydroxyl group could then be coupled to produce a C-3 carboxylate leaving group.

Other work was performed to determine whether the photoelimination could be sensitized by a diaminoacridinium salt⁷ that absorbed light in the 450 nm wavelength region. Photoproduct was observed after photolysis. Time did not permit modifying the sensitizer by incorporating a bromine heavy atom to increase Φ_{isc} . In addition, the effort

to replace the benzothiophene with a cyclopentadithiophene-7-one ring system⁸ having $E_T = 38 \text{ kcal mol}^{-1}$ would have enabled the use of chromophores absorbing at $>500 \text{ nm}$ wavelengths. The synthesis progressed, but time ran out to fulfill that goal.

1.2. Brief introduction on photoremovable protecting groups.

Photoremovable protecting groups (PRPGs) are a type of protecting groups that can be removed upon light irradiation. The ability to photorelease various substrates with spatial, temporal and concentration control in variety environments has allowed the photoremovable protecting groups to be applied widely in synthesis⁹⁻¹¹, physiology^{12,13}, and molecular biology¹⁴ since they were first reported in 1962.¹⁵ Specifically, in biological studies, researchers use PRPGs in “caged” compounds to protect biomolecules whose bioactivity can be restored once released upon the irradiation.(Figure 1.1)

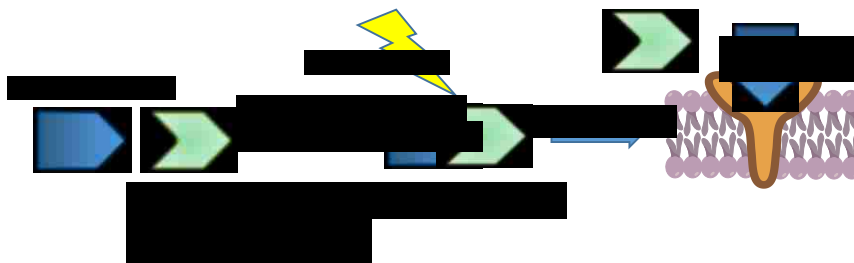


Figure 1.1. Depiction of photactivation of caged compound.

These photoreleased bioeffector leaving groups may be small molecules and ions like neurotransmitters¹⁶⁻¹⁸, nucleotides and nucleosides,^{9,19,20} and calcium ion²¹⁻²⁴, or they may be macromolecules such as peptides²⁵, proteins²⁵⁻²⁶, mRNA and DNA^{21,22}. Some typical examples of caged compounds are given in Figure 1.2.

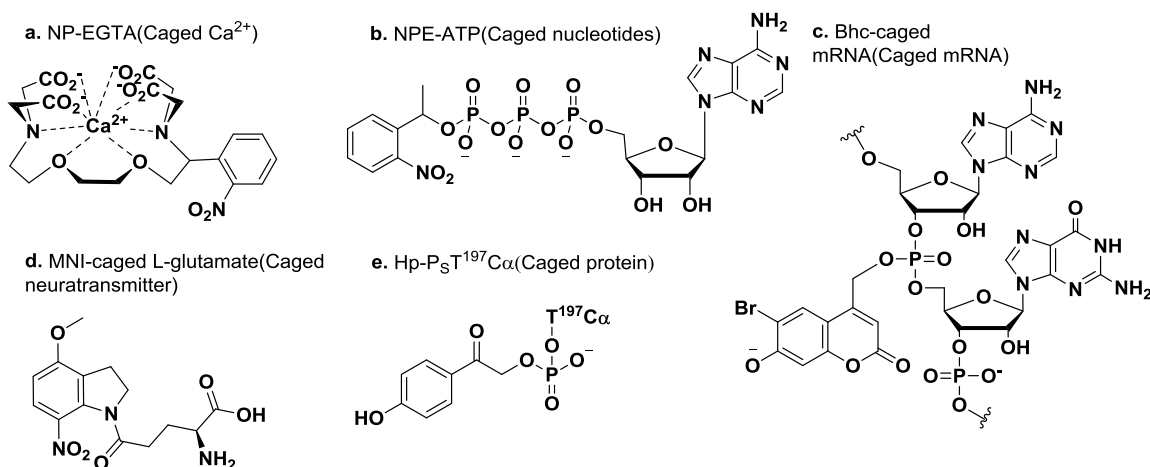


Figure 1.2. Typical examples of caged bioeffectors reported previously. a. nitrophenyl-EGTA(caged calcium)²²; b. P^3 -1-(2-nitro)phenyl-ethyl-ATP (caged ATP); c. 6-bromo-7-hydroxycoumarin-4-ylmethyl caged²⁷; d. 4-Methoxy-7-nitroindolinyl-caged-L-glutamate¹²; e. 4-hydroxy-phenacetyl (HP) bromide caged $\text{P}_S\text{T}^{197}\text{Ca}$.²⁹

The ability of precisely photoreleasing wide range of leaving groups allows caged compounds to facilitate numerous studies of biological processes. Caged neurotransmitters are used in investigations of the mechanisms of neurotransmitter-mediated reactions on cell surfaces. The roles of calcium ions in biological process has been studied using caged calcium compounds^{21,22}. Caged ATP can be used to study the Na^+/K^+ -ATPase pump for ion transport across the cell membrane.^{30,31} Targeting gene expression is also achieved with Caged mRNA and DNA.^{27,32}

Different application will require different properties of photoprotecting groups. Extensive research on PRPGs, notably the work by Sheehan and Umezawa³³, and Lester and Nerbonne³⁴ has led to the following criteria for what makes a suitable PRPG:

1. The irradiation wavelength should be over 300 nm and should not be absorbed by the photoproduct, the media and the photoprotected substrate.
2. The photoprotected substrates and byproducts should be soluble in the

aqueous media, which in most cases, will be an aqueous buffer of high ionic strength. Moreover, they should be inert to the aqueous media before irradiation.

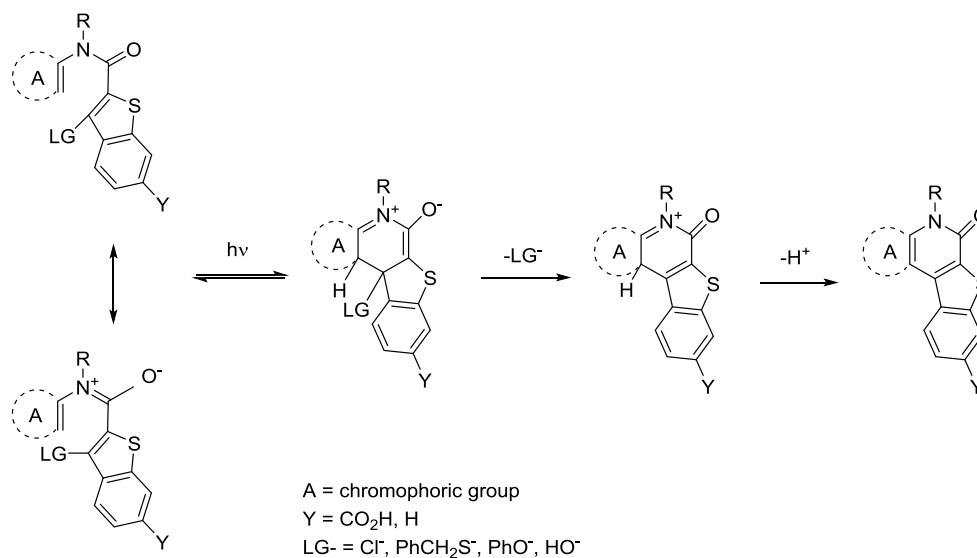
3. The photochemical reaction should have high quantum efficiency, (e.g. $\Phi > 0.1$) or alternatively, high photosensitivity, $\Phi\epsilon > 50$.
4. The caged compounds and the photochemical byproducts should be harmless to the biological system.
5. The release of the bioeffectors should be fast (in microseconds or shorter)
6. The synthesis of the caged compounds should be with reasonable yields and inexpensive.

While the above criteria are desirable, it is unlikely that a particular PRPG will have all of these properties. Researchers have proposed a wide range of different photoremovable protecting groups having properties suitable for particular applications. Some common photoremovable protecting groups are o-nitrobenzyl, benzoin, p-hydroxyphenacyl and coumarin-4-ylmethyl compounds. A brief introduction on the mechanism of their photoreaction and the application was attempted in section 1.5.

1.3. Background on release of leaving groups via photogenerated zwitterionic intermediates.

Our group focus on the caged compounds which expel leaving groups via zwitterionic intermediates produced through electrocyclic ring closure reactions of benzothiophene carboxamides. (Scheme 1.2) The objectives of the proposed research are listed as follow:

1. Extend photolysis wavelength for achieving release of bioeffectors from the 350 nm region out to the visible wavelength ranging from 350 nm to 650nm.
2. Release basic bioeffector leaving groups, such as thiolates, phenolate carboxylates and phosphate leaving groups which are conjugate bases of essential side chains functionality in peptides and proteins.
3. Reduce or eliminate the problem of premature solvolytic release of the bioeffectors under aqueous conditions at high ionic strength.

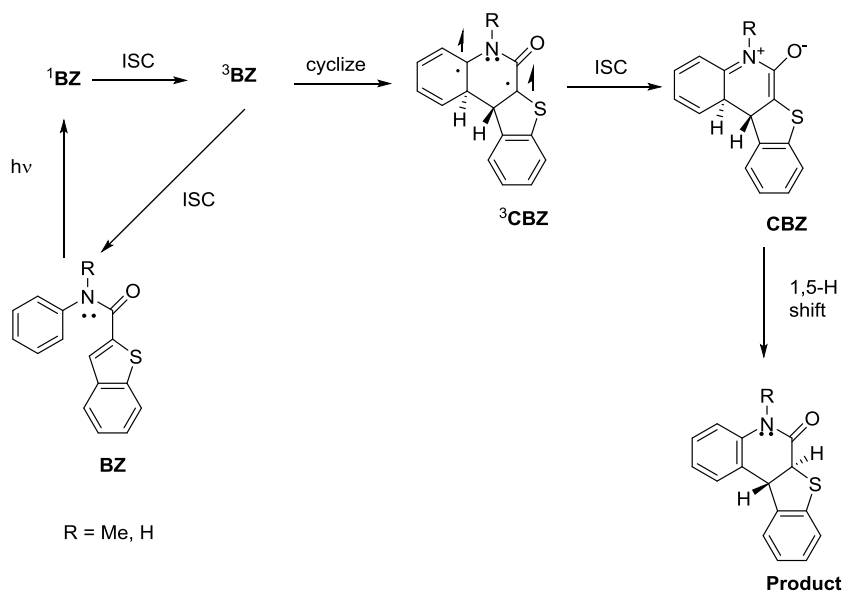


Scheme 1.2. The proposed cage compounds involve photochemical electrocyclic ring closure.

The above PRPG allows the photolysis wavelength to be varied by attaching different chromophoric A structures to the nitrogen of the amide linker. Various leaving group anions of biological importance can be released from the zwitterionic intermediates.

1.3.1. The mechanism for the photorelease of leaving groups.

The electrocyclic ring closure should be a photochemically allowed conrotatory process to form a six-membered ring. This has been demonstrated by Witkop and coworkers.³⁵ (Scheme 1.3).

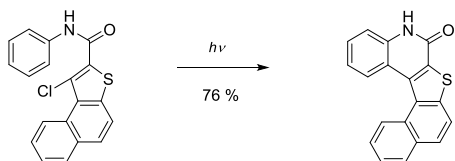


Scheme 1.3. The mechanism of photocyclization.

Despite the absence of a leaving group at C-3 carbon, their study still provides information for this project. In that example the initial cyclization is followed by 1,5-H migration, which occurs suprafacially to give a tetracyclic product. The conrotatory motion involved in the first step of the reaction is inferred from the stereochemistry at the ring junction in the photoproduct.

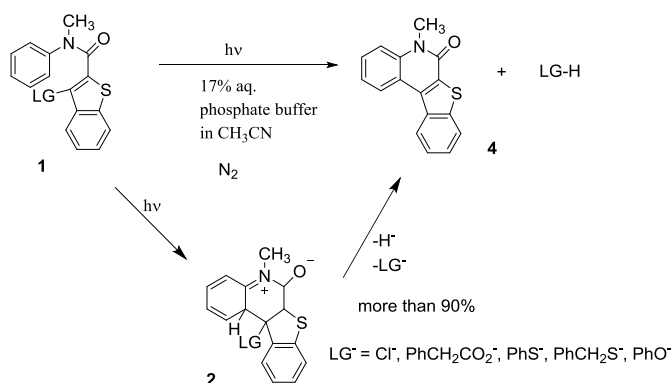
Witkop's benzothioindole **BZ** does not have a leaving group at the C-3 position. However, Castle and coworkers³⁶ reported studies that have chloride as a leaving group at this position in the benzothioindole ring. The photochemical reaction observed by Castle and coworkers is essentially the same as that studied in the project, although the

mechanism was not discussed or studied in their paper. In that work no quantum yields were determined either. Furthermore, the triplet multiplicity was never specified or established experimentally. The focus of the research by Castle was to take advantage of the photocyclization reaction for the synthesis of heterocyclic ring systems for medicinal studies of their mutagenicity. An example of synthesis steps is shown in Equation 1.5.



1.3.1.1. The dependency of Φ on the basicity of leaving group (LG^-)

The dependency of Φ on the basicity of leaving group (LG^-) was studied previously.¹ A variety of leaving groups (Cl^- , $\text{PhCH}_2\text{CO}_2^-$, PhS^- , PhCH_2S^- , PhO^-) attached at the C-3 carbon in the benzothiophene ring could be released with various quantum yield in high chemical yield once irradiated at $\lambda = 310$ nm. (Scheme 1.5)



Scheme 1.3. Photoexpulsion of various leaving groups from benzothienopyridinone-2-carboxamide

LG^-	Cl^-	$\text{PhCH}_2\text{CO}_2^-$	PhS^-	PhO^-	PhCH_2S^-	HO^-
Φ	0.23	0.16	0.10	0.074	0.075	0.007

Table 1.1. Quantum yields with various leaving groups.¹

As the basicity of the leaving group increases, the quantum yield Φ decreases evidently. (Table 1.1). There is a proximate dependence of the $\log \Phi$ on the pK_a of the LG^- conjugate acid. (Figure 1.3). This led to the rationale that the electrocyclic ring closure reaction to form the zwitterion is reversible. The LG^- expulsion competes with the ring opening reaction which regenerates the starting material. For another case, DFT calculations show that there is a barrier of ca. 10 kcal mol⁻¹ for this reverse reaction of **3**. (Figure 1.1)

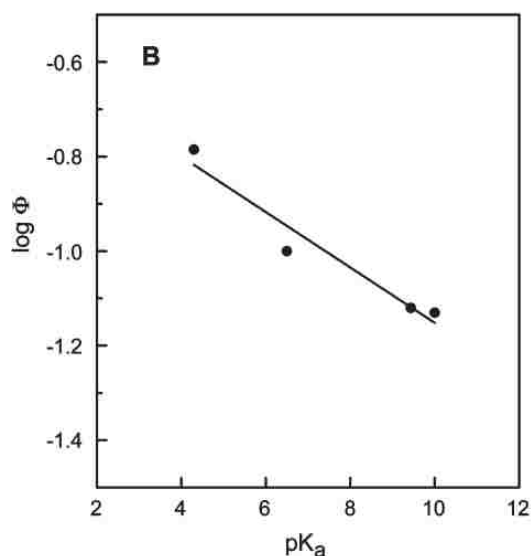
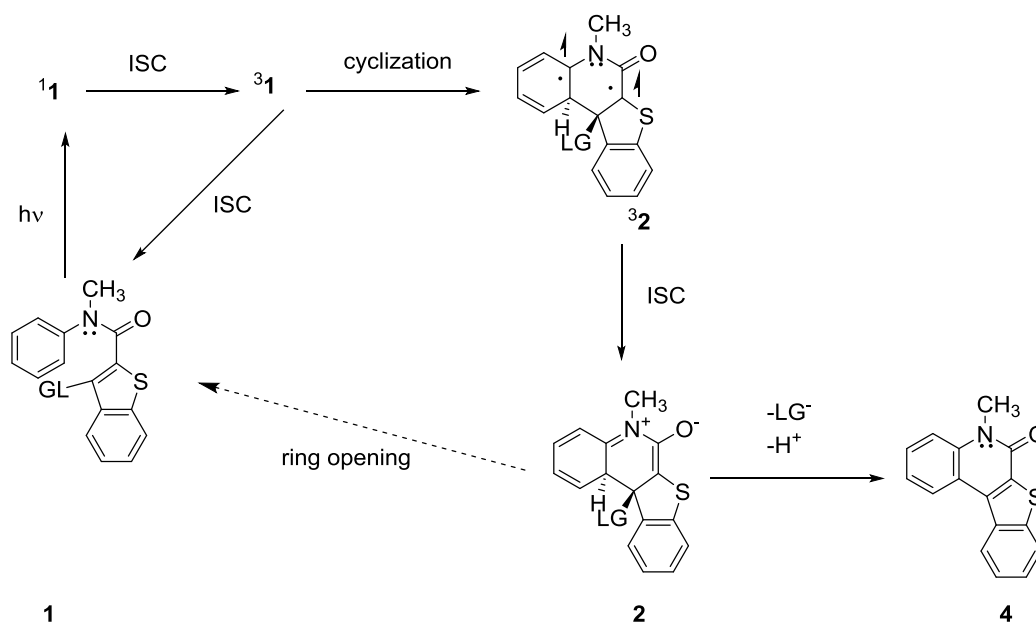


Figure 1.3. Plot of $\log \Phi$ vs pK_a of the LG^- conjugate acid for the photolysis in Scheme 1.5).¹

A higher barrier might have been expected, because the ring opening is formally forbidden thermally. The relatively low barrier can be due to the reaction being analogous to expulsion of a leaving group comprised of a positively charged iminium ion nitrogen species in compound **2** in Scheme 1.5.

Chemical yields do not behave in the same way quantum yields do. For the reaction in Scheme 1.5, the chemical yields are more than 90% for all of the LG^- shown.

This is true for even $\text{LG}^- = ^-\text{OH}$ (93%).¹ This is because the photoproduct absorbs at longer wavelengths than the reactant. During photolysis the photoproducts do not compete with the reactant for the light. The whole mechanism for this project is summarized as scheme 1.6.



Scheme 1.4. The summary of the mechanism.

1.3.1.2. Photolysis efficiency.

As mentioned above (Scheme 1.5), the anilide of benzothiophene-2-carboxamide can expel various leaving groups at the C-3 of the thiophene ring. The light is absorbed directly by benzothiophene ($\lambda = 310$ nm). Chemical yields of photoreleased leaving groups vary from 0.1 - 0.23. To extend the photolysis wavelength to more than 310 nm, the N-phenyl group was replaced by thioxanthone chromophore (eq 1.1).² The photorelease of chlorides and thiolates occurred quantitatively at 386 nm, but there was a decrease in the quantum yields (0.01-0.06).

DFT calculation showed that the triplet excitation transfer from thioxanthone chromophore to benzothiophene was necessary for the reaction to proceed. According to Figure 1.4, the initial lowest excited state, $^3\text{Thiox}$, is located 59 kcal mol⁻¹ in enthalpy above the S_0 state.

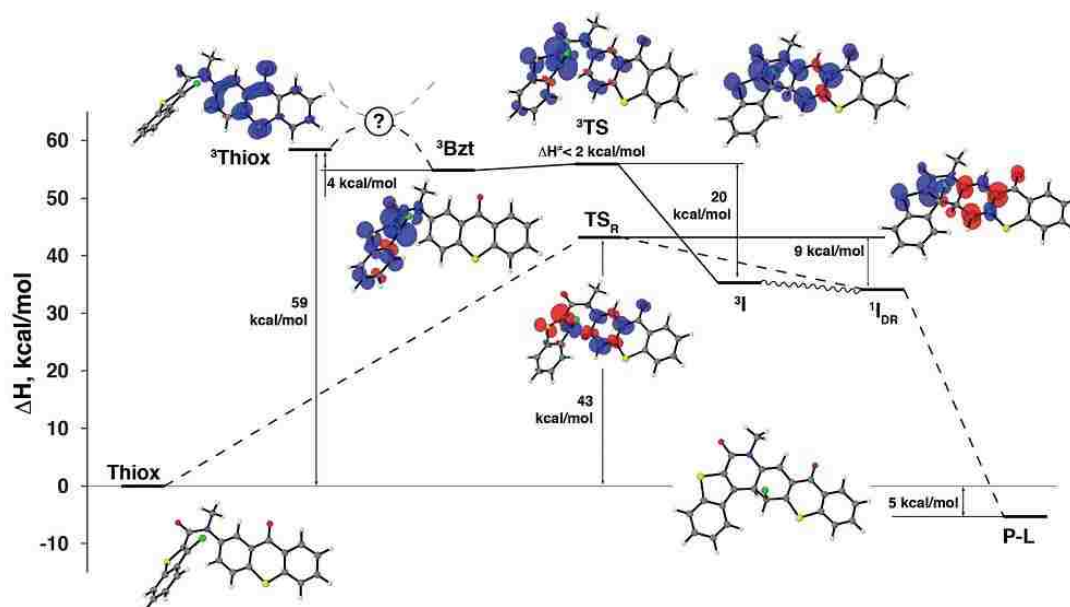
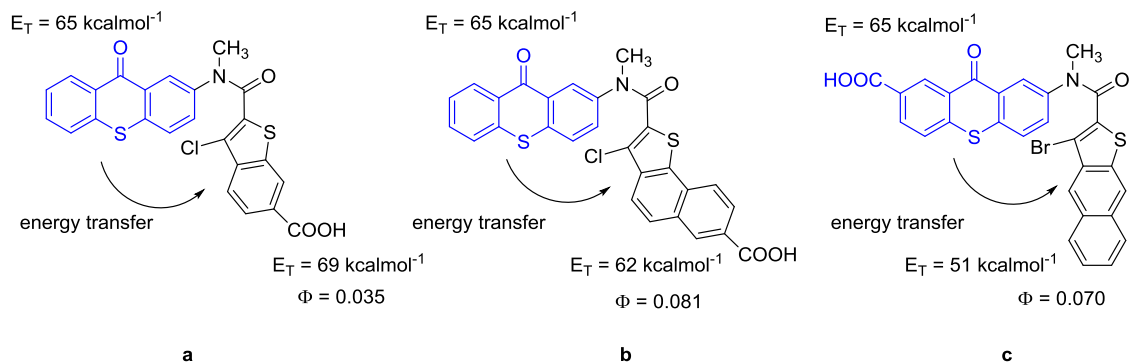


Figure 1.4. Relative enthalpies of the stationary points on the ground-state S_0 and the lowest triplet T_1 surfaces relevant for formation of the ring closure product from **3**. Unpaired spin density isosurfaces are shown for open-shell species.²

Experimentally, the energy may be 65 kcal mol⁻¹.³ The $^3\text{Thiox}$ is not of much geometric difference from the S_0 state. Another minima with the triplet excitation localized mostly on the benzothiophene (^3Bzt), is located about 4 kcal mol⁻¹ below the $^3\text{Thiox}$. This latter energy may be as high as 69 kcal mol⁻¹ for benzothiophenes, according to the literature⁴. Geometrically, ^3Bzt is different from $^3\text{Thiox}$ that in ^3Bzt C-3 carbon bearing the leaving group is pyramidal. The pyramidalized carbon apparently then attacks the C-1' carbon or the C-3' carbon to cyclize.

These DFT calculations suggest a reasonable way of increasing the quantum

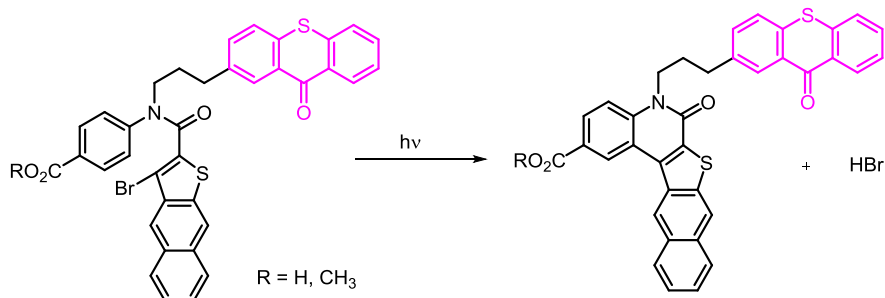
yields: replacing benzothiophene with other thiophene groups that have lower triplet excited energies than the chromophore triplet excited states. Thioxanthone chromophore



Scheme 1.5. Photolysis quantum yields for different triplet energy transfer (ET) from thioxanthone to thiophene rings.

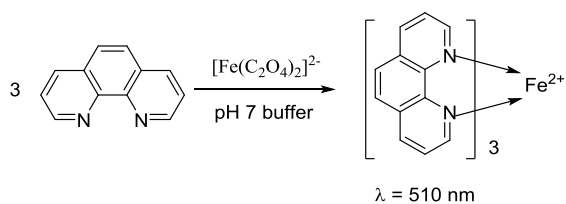
has a triplet energy $E_T = 65 \text{ kcal/mol}$ ³ while benzothiophene has triplet energy $E_T = 69 \text{ kcal/mol}$.⁴ Previous work on naphthothiophene $E_T = 62 \text{ kcal mol}^{-1}$ gave reasonable increase in quantum yield. (Scheme 1.15) Therefore, naphthothiophene with $E_T = 51 \text{ kcal mol}^{-1}$ ⁶ is proposed in this project to further improve the quantum yield. This work will be discussed in chapter 3.

However, recent work in our group shows that the intermolecular sensitization of thioxanthone with benzothiophene-2-carboxanilide could have quantum yields as high as 0.4³⁷. Therefore, a similar system where the thioxanthone chromophore connects to the naphthothiophene rings via a flexible trimethylene linker is proposed to facilitate the triplet energy transfer (eq. 1.6). (Equation 1.6) The results will be discussed in chapter 3.



1.3.2. Background on Chemical Actinometry

Light output in this project was measured using potassium ferrioxalate³⁸ as a chemical actinometry. When potassium ferrioxalate is irradiated, Fe^{3+} is converted to Fe^{2+} (Eq. 1.7). Fe^{2+} can form a complex with 1,10-phenanthroline that absorbed at 510 nm while Fe^{3+} only forms a weak complex with 1,10-phenanthroline, which is transparent at 510 nm. (Eq. 1.8). Measuring the absorbance of the complex at 510 nm, we can calculate the amount of ferrous produced and therefore mE of light absorbed based on the quantum yield of the ferrous production at wavelength of light used (irradiation light of the photolysis) (Eq. 1.10).



$$[\text{Fe}^{2+}] = \frac{\text{Optical Density at 510nm}}{\epsilon \text{ of the } \text{Fe}^{2+} \text{ complex}}$$

$$mE = \frac{\text{mmol of } \text{Fe}^{2+}}{\Phi \text{ of } \text{Fe}^{2+} \text{ at irradiation wavelength}}$$

The advantages of using potassium ferrioxalate Actinometry could be summarized as follows:

1. Easy and fast to use.
2. Does not depend on difference readings between large numbers to determine amount of conversion.
3. Quantum yields are accurately known
4. Can be used in the blue region of the visible spectrum.
5. Stirring is not necessary.
6. Oxygen does not have to be excluded.
7. Quantum yields are relatively insensitive to wavelength, concentration, temperature and light intensity.

1.4. Background on photochemistry

For the photolysis of a caged compound, light acts as the trigger to initiate a series of reactions. The first step is the absorption by the caged compound of a photon of energy (E),

$$E = h\nu \qquad \qquad \qquad \mathbf{1.11}$$

where h is Planck's constant and ν is the frequency of the light.

Since only light that is absorbed by the caged molecule can trigger photochemical reactions, the higher the proportion of molecules absorbing the light, the more product will be formed. Absorbance (A) of a caged molecule in solution is determined by Beer-Lambert Law.

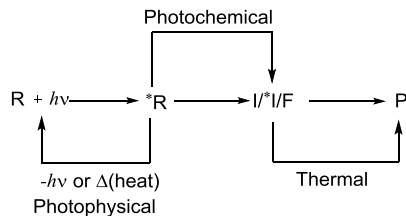
$$A = \epsilon cl \qquad \qquad \qquad \mathbf{1.12}$$

where ε is the extinction coefficient, c is the concentration of the caged compound, and l is the length of the light path through the solution. Thus for efficient photolysis, ε should be high at wavelengths triggering the photochemical reactions. It is not sufficient that the caged compound absorbs light well, but each time a photon is absorbed it should be likely to result in formation of the photoproduct. A measure of the efficiency of a photochemical reaction is given by the quantum yield (ϕ), which is the ratio of amount of product formed over the number of photons (of a certain wavelength) absorbed.

$$\phi = \frac{\text{product molecules formed}}{\text{photons absorbed}} \quad \mathbf{1.13}$$

Thus, the caged compounds with a high extinction coefficient and a high quantum yield will require less light to photolyze.

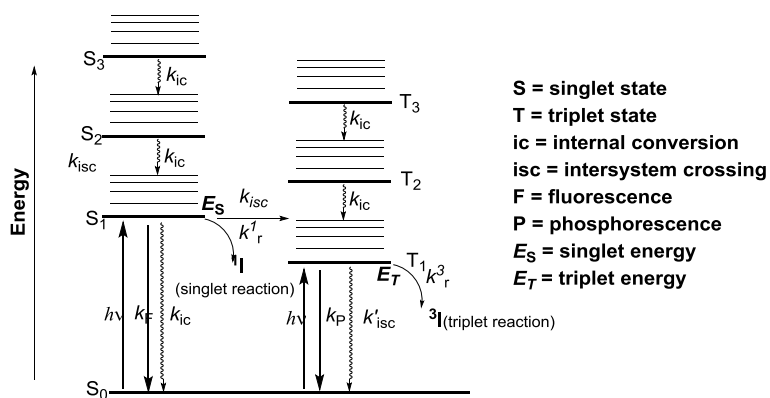
To better understand the factors that influence the quantum yield of the photorelease of the leaving group, it is necessary to look at the overall process after the absorption of a photon by a caged compound. (Scheme 1.7)³⁹ As a result of absorbing the photon, the caged molecule (R) is promoted to an excited state (*R). Photochemical processes can take place from the highly reactive chemical species *R to give stable products, while photophysical processes directly from *R result in no chemical change of the photoreactant. These photophysical processes can be radiative (fluorescence and phosphorescence) and non-radiative. The most commonly observed pathway that leads to a product is *R \rightarrow I \rightarrow P, where the intermediates I can be a radical pair, a biradical, or a zwitterion.



Scheme 1.6. A global paradigm for the overall photophysical and photochemical pathways from $*R$.³⁹

Other photochemical processes like $*R \rightarrow *I \rightarrow P$, where $*I$ could be an electronically excited intermediate, or processes like $*R \rightarrow F \rightarrow P$, where $*R$ leads to P through a “funnel” (F), are less common and will not be discussed in this dissertation.

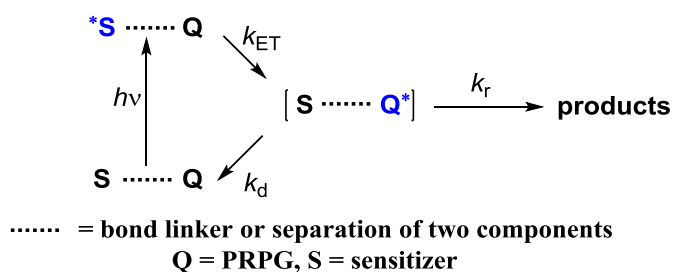
The excited states during the photochemical reaction may be classified as singlet or triplet based on their electronic configuration. Excited states undergo internal conversion to lower energy states of the same multiplicity rapidly with loss of heat (relaxation), while the intersystem crossing from a singlet state to a lower energy triplet state is slower than internal conversion. The important electronic states and pathways during an organic photochemical reaction are presented in Scheme 1.8.



Scheme 1.7. The Jablonski diagram (state energy diagram) for organic photochemical reactions.

1.4.1. Background on the sensitized release of leaving group.

Non-radiative decays mentioned above may take place by triplet energy transfer to other molecules (quenching/ sensitization). For most PRPGs, the leaving groups can be expelled directly from the protecting groups, which are also chromophores. However, not all the molecules can undergo very efficient intersystem crossing from S_1 to T_1 , and if T_1 is the only pathway for the desired chemical reaction to proceed, the overall quantum yield for release the leaving group can be low. Moreover, the caged compound under study may not absorb the light at the preferable wavelength. The introduction of a photosensitizer with high intersystem crossing quantum yield can help resolve the problem and extend the photolysis wavelength to where the sensitizer absorbs. Research on the indirect photolysis has been reported.⁴⁰ In such a system, there are two components. (Scheme 1.9) They can be linked together or just separated in the media. One of the components (quencher) will get activated through (most commonly) triplet energy transfer from the excited component (sensitizer) that is directly activated by the light.

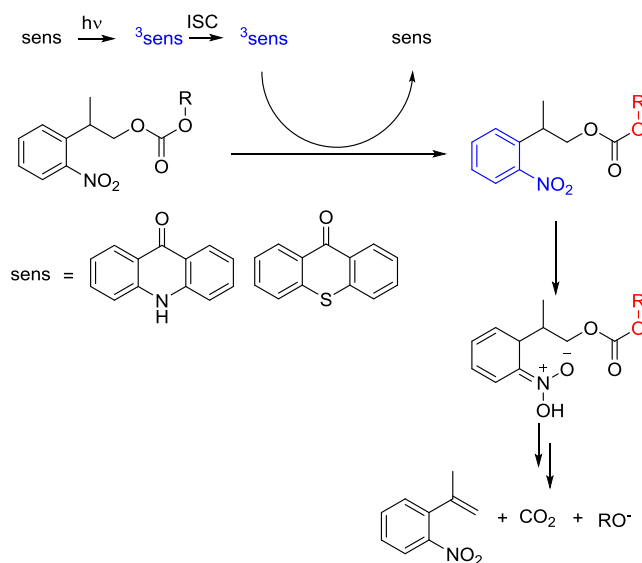


Scheme 1.8. General scheme for photosensitization.

The photosensitizer should be the major light absorber. To make the triplet energy transfer efficient, the energy transfer process must be exergonic (5 kcal/mol). Besides, the

sensitizer should be able to undergo the intersystem crossing efficiently, in other words, the triplet quantum yield Φ_T should be high enough to populate enough triplet excited states and the triplet lifetime should be long enough to enable the triplet energy transfer.²⁵

In the current project, the chromophores benzophenone or thioxanthone are attached to the nitrogen of an amide linker. The results of sensitized photolysis can complement those of direct photolysis, where the chromophore intramolecularly transfers its triplet energy to the reactive aromatic naphthothiophene-2-carboxanilide that eventually releases the leaving group. The intermolecular energy transfers (sensitization) are also possible. An example of intermolecular energy transfer has been provided by Steinmer, Creen, and co-workers.⁴¹ They reported that with a sensitizer such as thioxanthone can increase the sensitivity of 2-(2-nitrophenyl)propyl group to two-photon excitation.



Scheme 1.9. Intermolecular Triplet Sensitization of the 2-(2-Nitrophenyl)propyl Chromophore.⁴¹

are modified from *o*-Nitrobenzyl group to photorelease amino groups.

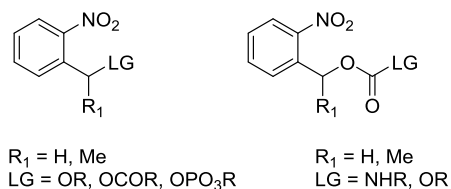
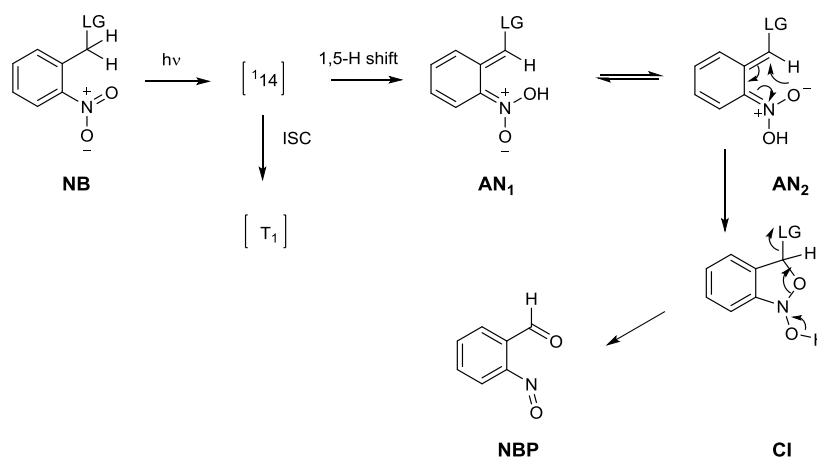


Figure 1.6. Chemical structure of NB, NPE, NBOC, MeNBOC caged compounds with different functional groups.

The uncaging of the *o*-nitrobenzyl compounds is thought to follow the mechanism shown in Scheme 1.13. The *o*-nitrobenzyl groups bear a leaving group at the benzylic position. The singlet aci-nitro intermediate **AN₁** is formed by hydrogen shift from the *o*-methylene group once irradiated by the light. There is a high energy barrier to rotate the bond C=N to cyclize into the intermediate **I**. So, hydrogen transfer to form the other aci-nitro isomer **AN₂** is necessary to generate the cyclic intermediate **CI**. The cyclic intermediate **CI** will undergo a concerted process to expel the leaving group and form the nitroso-substituted benzaldehyde **NBP**.

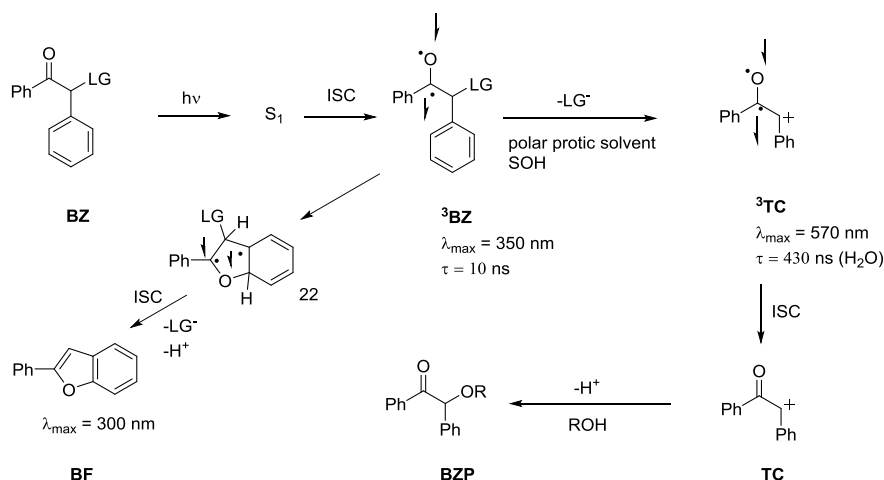


Scheme 1.11. The photodeprotection mechanism of *o*-Nitrobenzyl group.⁴³⁻⁴⁵

o-Nitrobenzyl generally have good absorption and photochemical properties. Quantum yields for photorelease of leaving groups are fairly high and absorption extends out past 300 nm. However, the release of the leaving group LG⁻ from *o*-nitrobenzyl protecting groups produces the byproduct nitrosoarenes, which are toxic to cells.⁴⁶ Nitrosoarenes also can oxidize thiols that are newly released or already exist in the biological system.⁴⁷ Thus, the *o*-nitrobenzyl derivatives may not be suitable for protecting sulfhydryl groups.

1.5.2. Benzoin derivatives

Benzoin compounds were first reported by Sheehan and Wilson⁴⁸ to photochemically to expel acetate. Phosphates can be expelled quantitatively from the corresponding benzoin cages too.⁴⁹ Givens and Matuszewski⁵⁰ studied the mechanism of the photorelease of diethylphosphate from unsubstituted benzoin derivatives (Scheme 1.14). The photolytic reaction can be quenched by the well-known triplet quenchers such as naphthalene and piperylene. This indicates the reaction proceeds via a triplet excited state. Two reaction paths compete in diethylphosphate elimination from triplet benzoin diethyl phosphate. Path A dominates in most solvents except water and fluorinated alcohols and generates 2-phenylbenzofuran **BF** within 25 ns. This is supported by 2-phenylbenzofuran's strong absorption at 300 nm. Flash photolysis in ethanol at reduced temperature gives the triplet-triplet absorption as a broad band 300 ~ 440 nm. Path B dominates in polar and protic solvent such as water and fluorinated alcohol and generates compound **BZP** via a transient triplet cation **TC**, $\lambda_{\text{max}} = 570$ nm with a lifetime about 500 ns. The triplet cation **TC** decayed to give the singlet ground state of the cation **TC** which reacts with the protic solvent to form compound **BZP**.



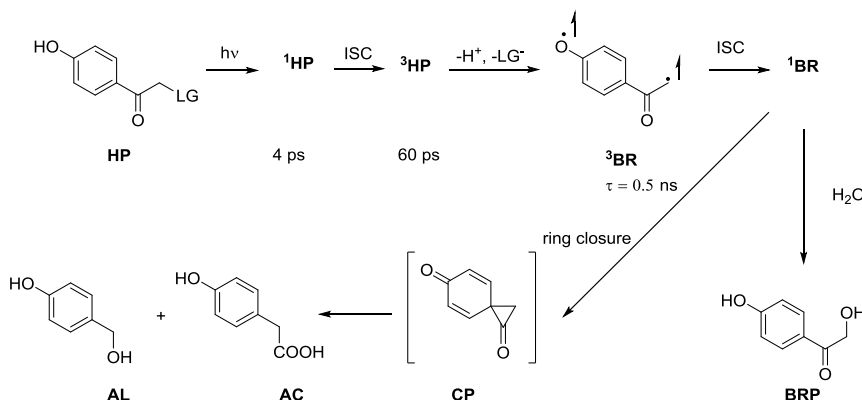
Scheme 1.12. The photodeprotection mechanism of benzoin group.

The protection of chiral molecules with benzoin compounds can be problematic since the benzoin bears a chiral center too. Thus, incorporation of the chiral leaving group will result in the formation of diastereomers. Enantioselective synthesis of benzoin cages is necessary if the high purity is required to avoid complicating the latter photolysis. Another problem is that benzofuran **BF** is formed as a byproduct in the photoreaction. The benzofuran absorbs strongly at the same wavelength used to photolyze the reactant and thus, it can act as an internal filter. This internal filter effect will cause photolysis to slow down as the photolysis proceeds, possibly reducing the achievable chemical yield.

1.5.3. p-Hydroxyphenacyl derivatives.

p-Hydroxyphenacyl groups have been reported to cage ATP, GABA, glutamic acid⁵¹ and proteins²⁹. The mechanism of the photolysis is understood as Scheme 1.15.⁵² The triplet chromophore rearranges to generate the triplet biradical with a lifetime less than 1 ns by concerted expulsion of the leaving group. The triplet biradical undergoes

intersystem crossing to give its ground state which either hydrolyzes to give **BRP** or cyclizes to form cyclopropanone **CP**. Hydrolysis of the propanone **BR** intermediate generates the carboxylic acid **AC** while decarbonylation gives the alcohol **AL**.



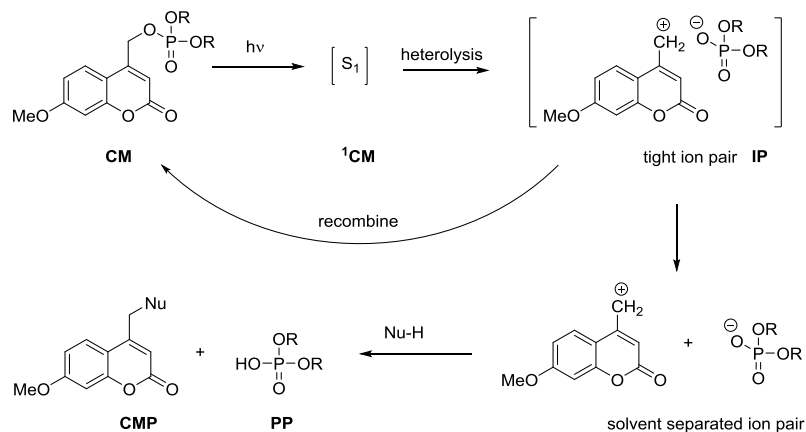
Scheme 1.13. The photodeprotection mechanism of p-hydroxyphenacyl group.

The photolysis reactions of p-hydroxyphenacyl compounds often have high quantum yields and chemical yields. But the disadvantage is that the photolysis wavelength lies deep in the UV. This limits their application.

1.5.4. The coumarin derivatives.

The coumarin groups have been attractive to the researchers since their first discovery because they absorb at very long wavelengths, even longer than 400 nm. Some also have the feature of being able to undergo two-photon photolysis, so that photolysis can occur with near IR light of wavelengths 700-800 nm. However, the coumarin groups rely on an $\text{S}_{\text{N}}1$ reaction that occurs in the short lived singlet excited state.⁵³ With the leaving group anion's basicity increasing, the excited state $\text{S}_{\text{N}}1$ elimination of the leaving group slows, and the reaction becomes inefficient.⁵⁴ So the coumarin has its disadvantage that the leaving groups are limited to fairly weak bases such as carboxylates and

phosphates. The mechanism of photorelease of coumarin-caged phosphates is as Scheme 1.16.⁵⁵ After initial irradiation, the lowest $^1(\pi, \pi^*)$ excited singlet state ^1CM , which undergoes the heterolytic C-O bond cleavage to form a tight ion pair. The initially formed tight ion pair **IP** is the key intermediate. The coumarinylmethyl cation either reacts directly with nucleophiles or solvent to generate a new stable coumarylmethyl product **CMP**. Alternatively, the tight ion pair can recombine to form the ground state **CM**. It is the similar mechanism with the carboxylates.



Scheme 1.14. The deprotection mechanism of coumarin group

1.6. Applications of the caged compounds in biological studies.

Caged compounds are valuable tools for biologist because the light activation provide the full control over the timing, location and amplitude of bioeffectors release. Examples of important caged compounds will be discussed in the following paragraphs.

1.6.1. Caged neurotransmitters.

Neurotransmitters are essential in a neuron's signaling. They cause the opening of ion channels by binding to the neurotransmitter receptors on the cell membrane,

producing a localized change in the membrane potential of the targeting cell. By measuring the resulting circuit, it is possible to study the kinetics of the process.

Previously reported caged neurotransmitters include glutamate, γ -aminobutyric acid (GABA), glycine, carbamoylcholine, aspartate, phenylephrine, and kainic acid. Some selected examples are listed in Table 1.2.

Neurotransmitters	Assay system
γ -Aminobutyric acid	γ -Aminobutyric acid receptor in Purkinje cells ⁵⁶
Glutamate	Glutamate receptor in hippocampus ⁵⁷
Glycine	A subunit of human glycine receptor ⁵⁸
Phenylephrine	Adrenergic receptor ⁵⁹
N-Methyl-D-aspartic acid	N-Methyl-D-aspartic acid receptor in hippocampus ⁶⁰
5-Hydroxytryptamine	5-Hydroxytryptamine (3) receptor in NIE-115 cells rombin ⁶¹

Table 1.2. Some examples of previously reported caged compounds.²⁵

The most widely used neurotransmitter is Glutamate. Various PRPGs have been reported to cage glutamate. Some common ones¹⁷ are N-nitrophenethoxycarbonyl (Noc), carboxynitrobenzyl (CNB), propylmethoxynitro-biphenyl (PMNB), diethylaminocoumarin (DEAC), bromohydroxycoumarin (Bhc) and ruthenium-bipyridine (RuBi). (Figure 1.7)

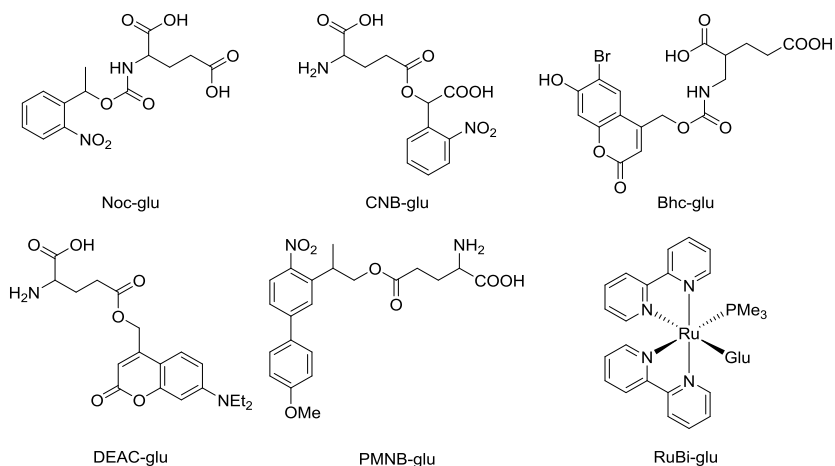


Figure 1.7. Selected caged Glutamate.

1.6.2. Caged calcium ions.

Calcium ion play important roles in cellular processes such as muscle contraction, ion channels regulation, nonmuscle motility, and synaptic transmission⁶². Caged Ca^{2+} are widely used to define these roles. Excellent reviews have been published by Ellis-Davies.^{62,63} Unlike other organic caged compound covalently modified by a PRPG, inorganic calcium cation utilizes photoliable derivatives of high-affinity calcium chelators like EDTA, EGTA and BAPAT (ethylenediaminetetraacetic acid, ethylene glycol-bis(2-aminoethylether)-N,N,N,N-tetraacetic acid, and 1,2-bis(2-aminophenoxy)ethane-N,N,N,N-tetraacetic acid). They have been used so widely in neurobiology that a lot of them are commercially available. (Figure 1.8)

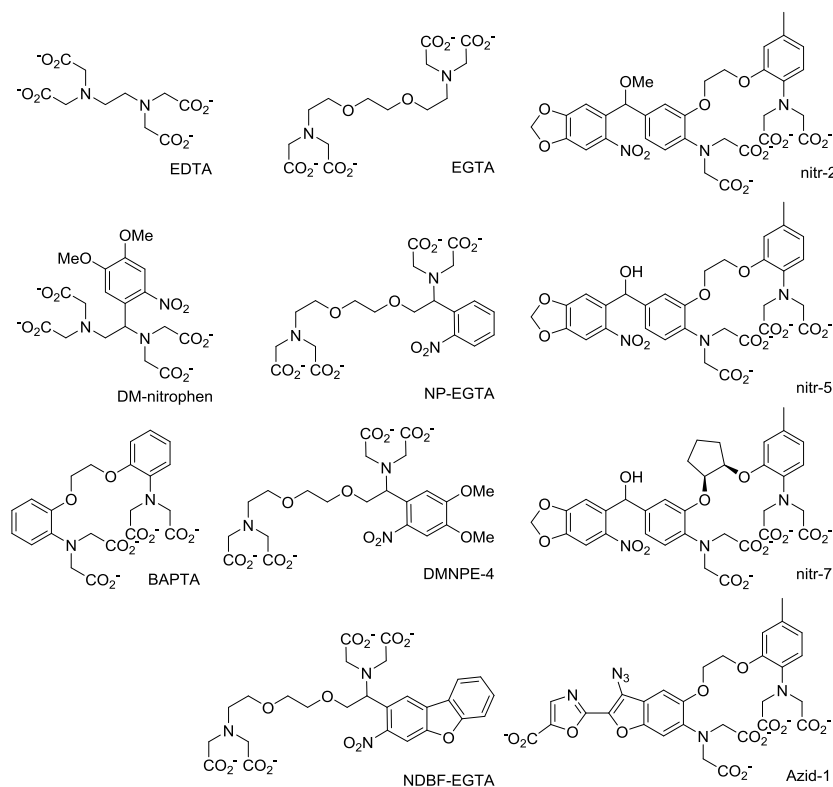


Figure 1.8. Examples of Ca^{2+} cages with their parent chelators (EDTA, EGTA, BAPTA)

For BAPTA derivatives⁶⁴, the buffering capacity of calcium chelators is lowered by the conjugation formed on the aromatic ring after the irradiation. (Figure 1.9a). For EDTA and EGTA derivatives¹⁴, the calcium ion is released from the photochemical cleavage of the backbone of the calcium chelators. (Figure 1.9b).

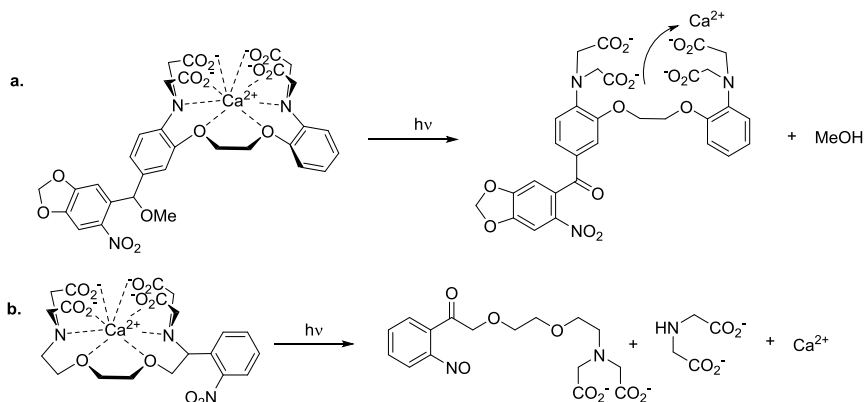


Figure 1.9. Uncaging of caged Ca^{2+} . a. Ca^{2+} uncaging by photolysis of nitr-2. b. Ca^{2+} uncaging by photolysis of NP-EGTA.

1.6.3. Caged nucleotides and nucleosides.

The first synthesized caged compound that is bioactive were nucleotides and nucleosides.^{19,30} They regulate many biological processes such as cell metabolism, ion transport, signal transduction, proliferation and differentiation. With the unique properties of caged nucleotides and nucleosides, it is possible to analyze the mechanisms of these processes. For example, caged ATPs were used to study the mechanisms of ion transport processes, such as Na,K-ATPase, CaATPs, KdpATPs and H,K-ATPase.⁶⁵⁻⁶⁷

There are three strategies¹⁹ when it comes to caging nucleotides and nucleosides: caging phosphate groups of nucleotides, caging the 2' and/or 3' position of nucleotides, and caging nucleobases of nucleotides and nucleosides.

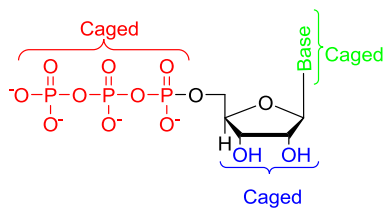


Figure 1.10. Three caging strategies for nucleotides according to the structures of the nucleotides.

1.6.4. Caged peptides and proteins.

Peptides and proteins play important roles in a lot of biological processes such as muscle contraction, intracellular signaling, and neurotransmission. Therefore, caged proteins and peptides provide researchers with powerful tools to study the mechanism of these processes. Caged proteins and peptides could be prepared by three methods²⁵: (1) chemical modification, (2) nonsense codon suppression and (3) solid-phase peptide synthesis. The chemical modification method, which covalently modifies the reactive amino acid residues (amino-reactive, thiol-reactive, and carboxylic acid-reactive), is the easiest and most common way to make caged proteins and peptides. (Figure 1.11). However, it is difficult to selectively protect the reactive residues because there are multiple of these reactive groups in most peptides and proteins.

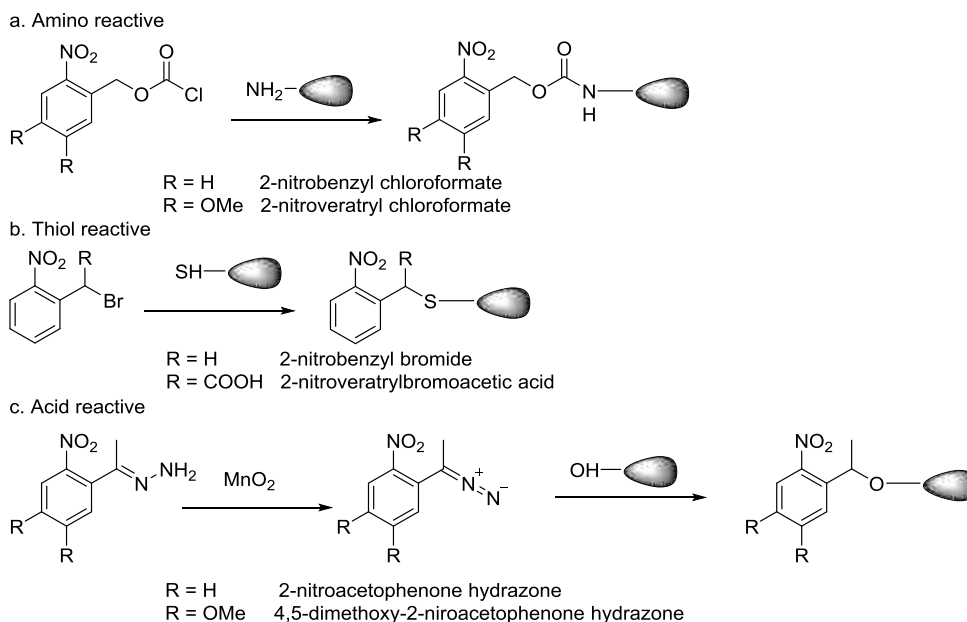


Figure 1.11. Preparation of caged protein using chemical modification.

The nonsense codon suppression technique was established by Schultz's group⁶⁸ and was improved by Lester's group to be used *in vivo*.⁶⁹ By using this nonsense codon suppression technique, the selective photoprotection of amino acids at a desired site could be achieved in any peptide and protein. This technique is the most sophisticated way to prepare caged peptides and proteins.

Solid-phase peptide synthesis (SPPS) provides a straightforward way to synthesize peptides in large quantities.^{70,71} In this technique, an amino acid previously protected with a PRPG is introduced at the desired site. Tatsu et al. used this method to prepare caged AIP ([Lys(NB)1,2]AIP) from N-Fmoc-N-(2-nitrobenzyl-oxycarbonyl)-Lys.⁷² (Figure 1.12)

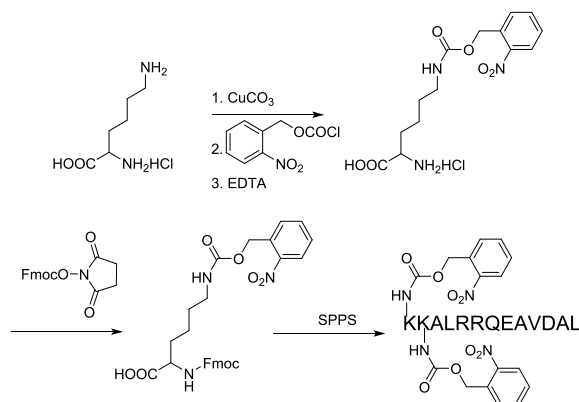
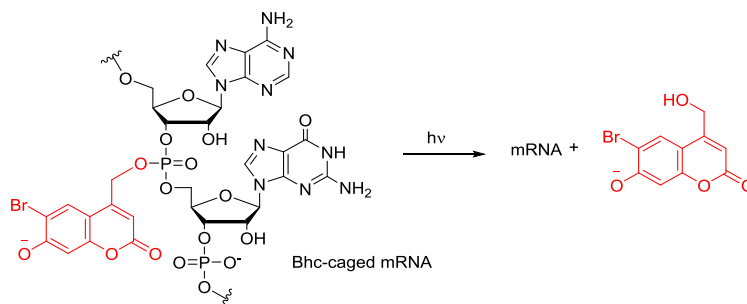


Figure 1.12. Synthesis of caged AIP.

1.6.5. Caged mRNA and DNA.

Caged mRNA and DNA allow the photoactivation of the gene expression in a temporally and spatially controlled manner.⁷³ A function of any gene of interest can be photoactivated by using the chemistry of caged compounds. For example, 6-bromo-4-diazomethyl-7-hydroxy-coumarin (Bhc-diazo) could be used as the caging agent for mRNA (Scheme 1.17)²⁷. MacMillan and Chaulk⁷⁴ reported the first photochemical control of a ribozyme reaction with O-(2-nitrobenzyl) caged RNA.

Monroe et al.³² reported the inactivation and site-specific light induction of plasmid expression using caged DNA photoprotected by 1-(4,5-dimethoxy-2-nitrophenyl) diazoethane (DMNPE).



Scheme 1.15. Synthesis of caged mRNA.

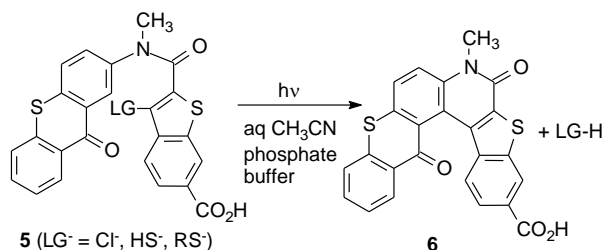
1.6.6. Summary

The synthesis of caged compounds could be complicated. Biologists have limited choices on commercially available caged compounds. For commercially unavailable caged compounds, they must collaborate with research groups who are able to do the synthesis. Ellis-Davies and co-workers¹³ summarized a list of commercial available caged compounds with their properties. (Table 1.3)

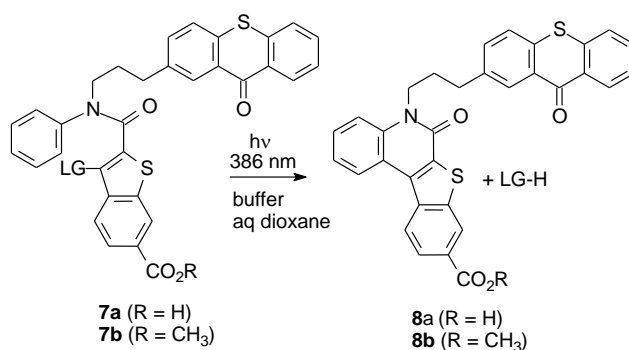
Caged compound	ϕ	ϵ ($M^{-1} \text{ cm}^{-1}$)	$\phi \epsilon$	Rate (S^{-1})	Stability
Calcium chelators					
DM-nitrophen	0.18	4300	774	38000	Complete
NP-EGTA	0.23	970	223	68000	Complete
nitr-5	0.01	5500	66	2500	Complete
diazo-2	0.03	22800	684	2300	Complete
Neurotransmitters					
CNB-Glu	0.14	500	70	48000	Fair
CNB-GABA	0.16	500	80	36000	Fair
CNB-carbamoylcholinea	0.8	430	344	17000	Excellent
MNI-Gluc	0.09	4300	366	100000	Excellent
Phosphates					
NPE-IP ₃	0.65	430	280	225/280	Excellent
NPE-cAMP	0.51	430	219	200	Fair
DMNPE-cAMP	0.05	5000	250	300	Poor
NPE-cADPribos	0.11	430	47	18	Excellent
NPE-ATP	0.63	430	271	90	Excellent
DMNPE-ATP	0.07	5000	350	18	Fair

Table 1.3. A list of commercial available caged compounds.¹³

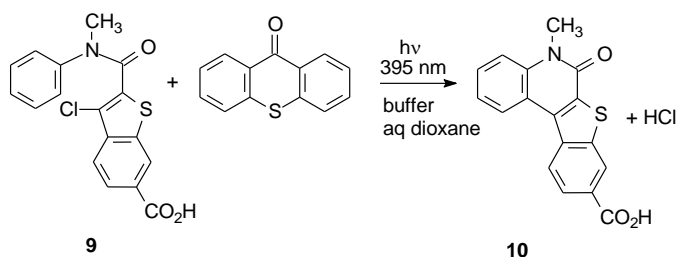
Initial attempts to extend the photolysis wavelength with benzothiophene-2-carboxamides involved replacing the N-phenyl group of the anilide with a chromophoric group such as a thioxanthone moiety (eq. 2.1)². With thioxanthone as the chromophore as in compound **5**, quantum yields were found to be low.² The low quantum yields for the photoexpulsion reaction of **5** were attributed² to the need for triplet excitation transfer to take place from the initial triplet excited state of the thioxanthone energy donor to generate the triplet excited state of the benzothiophene as energy acceptor. This energy transfer step is energetically unfavorable by ca. 4 kcal mol⁻¹. However, it was later found⁷⁵ that linking the chromophore to the anilide nitrogen via a trimethylene chain as in **7** led to highly efficient leaving group expulsions (eq. 2.2) with



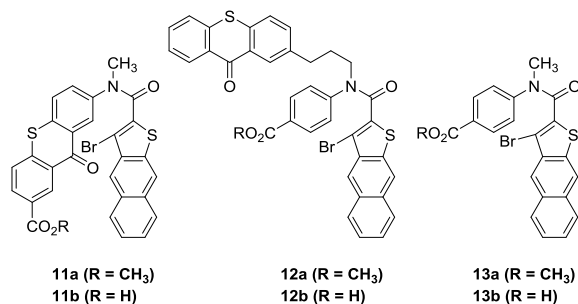
quantum yields ranging from 0.14-0.41 for thiolates, carboxylates, phosphates, and chloride as LG.³⁷ The trimethylene chain evidently facilitated triplet excitation transfer via a through-bond mechanism.



Moreover, equilibration of the donor and acceptor triplet excited states together with subsequent leaving group expulsion could effectively compete with the relatively slower decay of the thioxanthone triplet excited state. The low quantum yields for **5** are presumably due to a combination of effects, an unfavorable geometry for through-bond triplet energy transfer and a substituent effect for electrocyclization between thioxanthone and benzothiophene ring systems. It is worth noting that the bimolecular sensitized photolysis of anilide **9** with thioxanthone as the sensitizer proceeds with quantum yields of 0.4, provided the concentrations of the anilide is sufficiently high to efficiently quench the thioxanthone triplet excited state during its triplet excited state lifetime (eq. 2.3).



Further increases in photolysis wavelength will require replacing the benzothiophene ring system, which has a triplet energy of 69 kcal mol^{-1} , with an aromatic thiophene that has a much lower E_T . This will be true so long as triplet excitation transfer from the chromophore to the thiophene ring system must take place prior to electrocyclization in the triplet excited state. In this chapter the benzothiophene ring system was replaced with a naphthothiophene ring system⁶, which is estimated to have $E_T = \text{ca. } 51 \text{ kcal mol}^{-1}$. Use of the naphthothiophene ring system as the triplet energy acceptor would allow the use of chromophores that absorb at much longer wavelengths than thioxanthone, which has $E_T = 65 \text{ kcal mol}^{-1}$.



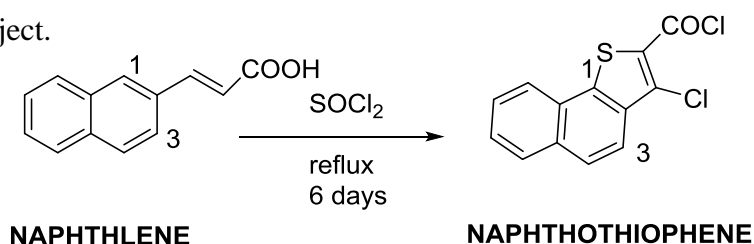
In this chapter the synthesis and spectra data are reported for three cases (Figure 2.1) where triplet excitation transfer from thioxanthone chromophore to the naphthothiophene ring system is highly exothermic: (1) the thioxanthone chromophore is directly attached to the naphthothiophene-2-carboxamide at the amide nitrogen (compound **11**), (2) the thioxanthone chromophore is tethered to the amide nitrogen via a trimethylene linkage (compound **12**), and (3) the thioxanthone bimolecularly sensitizes the photochemistry of the naphthothiophene-2-carboxanilide **13**.

2.2. Results

2.2.1. Synthesis.

The above caged compound **11a** (Figure 2.1) requires the synthesis of 3-bromonaphtho[2.3.b]thiophene-2-carboxylic acid, which will need to be coupled to the methyl 7-(methylamino)-9-oxo-9H-thioxanthene-2-carboxylate. Demethylation of the methyl ester **11a** on its thioxanthone chromophore will give the caged compound **11b**, 7-(3-bromo-N-methylnaphtho[2,3-b]thiophene-2-carboxamido)-9-oxo-9H-thioxanthene-2-carboxylic acid.

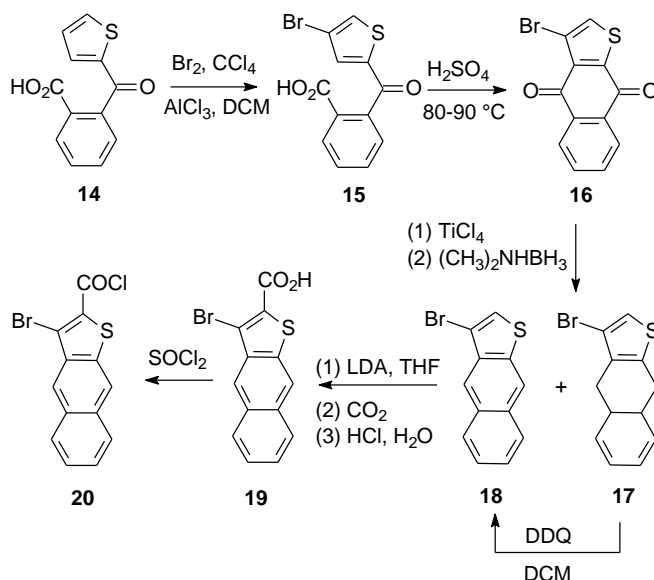
In previous work the thiophene ring generally had chloride at the C-3 position, whereas acid **19** has a C-3 bromide. This is because the naphthothiophene ring in **34** cannot be formed by the Higa reaction, which uses thionyl chloride and results in the C-3 chloride.⁷⁶ The Higa reaction can produce the 3-chloronaphtho[2.1.b]thiophene carbonyl chloride **37** because cyclization exclusively occurs at the C-1 rather than C-3 position of the naphthalene ring as shown in Equation 2.4. Literature search gave only one literature for the synthesis of substituted naphthothiophene ring,⁷⁷ which is not suitable for this project.



The synthesis of 3-bromonaphtho[2.3.b]thiophene-2-carboxylic acid **6** starts with Friedel Crafts acylation of thiophene with a yield of 86%⁷⁸. The literature provides precedence for selective C-3 monobromination of the thiophene ring when a keto group is attached to the C-5 position.⁷⁹ Therefore, bromination was performed with keto acid using liquid bromine in anhydrous dichloromethane. The monobromide was obtained in 89%. 1,2-dichloroethane and chloroform could also be the solvent.

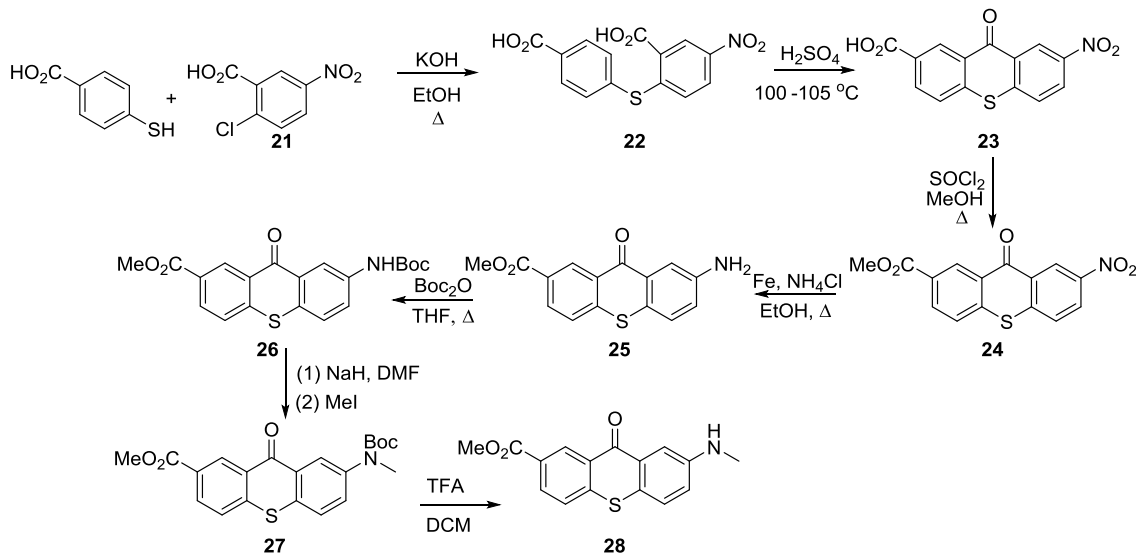
The synthesis of **19** hinges on the reduction of quinone **16**, which can be accomplished smoothly with borane dimethylamine complex at 0 °C in the presence of the Lewis acid, TiCl₄ (Scheme 2.2).⁸⁰ The only other method that was used with some success involved reduction by Al(Hg) in cyclohexanol,⁸¹ but this method was problematic, in that the yields of **18** were considerably lower and higher temperatures and

reaction times were required. As shown in Scheme 2.2, compounds **17** and **18** were both formed in comparable yields from **16**. The two were inseparable by silica gel column chromatography, so **17** in the mixture was converted to **18** upon further treatment with DDQ. The overall yield of **18**, starting from **16**, was 63%. Further metallation with LDA followed by carboxylation with CO₂ gave the naphthothiophene-2-carboxylic acid **19**.



An important element in the synthesis of compound **28** (Scheme 2.3) was the use of the Boc group at nitrogen to achieve the monomethylation of the C-4 amide, followed by its selective removal with TFA in the presence of the methyl ester at C-7. Otherwise, the synthesis is adapted from a similar, earlier reported route involving nucleophilic aromatic substitution of 2-chloro-5-nitrobenzoic acid **21** using mercaptobenzoic acid under basic conditions.⁸² The esterification of **23** to give **24** was problematic, because both compound had poor solubility in methanol. Despite that fact, **24** was obtained in

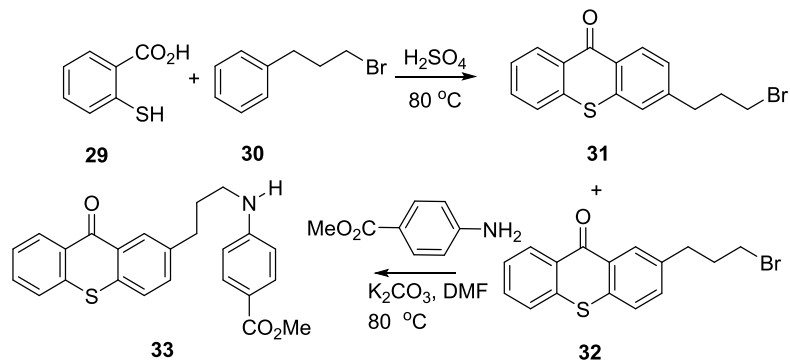
reasonable yield, but was always contaminated with a minor amount of **23**, since the product precipitated along with some starting material during the reaction.



Scheme 2.1. Synthesis of **28**.

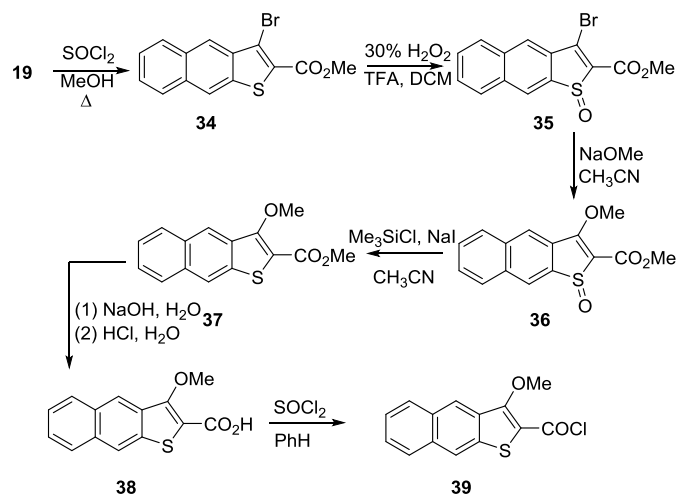
2.2.2. Synthesis of compound **12** and **13**.

To synthesize compound **12** and **13**, the corresponding aniline **33** was a prerequisite. Compound **33** was synthesized by alkylation with 4-bromopropylthioxanthone **32** (Scheme 2.4). The 4-bromopropylthioxanthone was the major product of reaction between 3-bromo-1-phenylpropane and thiosalicylic acid in concentrated sulfuric acid. (Scheme 2.4) The procedure is adapted from a known reaction that typically favors the regioisomer depicted as **32** over regioisomer **31** by a 4 : 1 ratio.⁸³



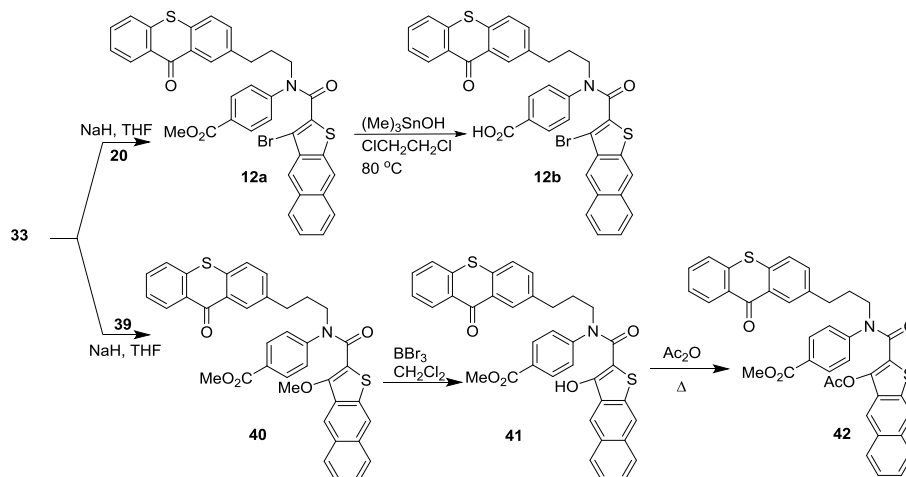
Scheme 2.2. Synthesis of **33**.

In the case of the trimethylene-linked thioxanthone compound **12** the C-3 bromide ultimately needed to be replaced with a hydroxyl group in order to provide functionality for the incorporation of biologically important leaving groups such as carboxylate or phosphate. The strategy for incorporating a C-3 hydroxyl group would entail first replacing the C-3 bromo group of **34** with CH_3O^- and later converting it to a hydroxyl group. Attempts to substitute the C-3 bromide of **34** by reaction with CH_3ONa failed and returned unreacted starting material. However, the thiophene ring could be activated towards nucleophilic substitution oxidizing⁸⁴ to the sulfoxide using hydrogen peroxide with TFA (Scheme 2.8). This successfully produced **36**. Subsequent reduction regenerated the thiophene ring in **37**. Hydrolysis of the methyl ester furnished the acid **38**.



Scheme 2.3. Synthesis of **39**.

The trimethylene-linked thioxanthone compound **12a** ($\text{LG}^- = \text{Br}^-$) was obtained by deprotonating the aniline derivative **33** (Scheme 2.6) with sodium hydride and reacting with **20** acid chloride derived from naphthothiophene-2-carboxylic acid **19** (Scheme 2.6). Similarly, coupling of acid chloride **39** with **33** gave the C-3 methoxy derivative **40**, which was converted to the C-3 alcohol **41** with BBr_3 . Acylation of the alcohol gave the C-3 acetate derivative **42** for photochemical studies. Similar procedures were used to obtain the anilides **13a,b**.



Scheme 2.4. Synthesis of **42**.

2.2.3. Crystal Structures.

2.2.3.1. Crystal structure of direct-linked cage compound **11b**.

The molecule has a folded cis-conformation with the amide group almost perpendicular both to the thioxanthone and naphthothiophene moieties. The carboxy group makes a hydrogen bond with DMSO solvate molecule. The structure contains large residual electron density peaks at C20, S1 and DMSO molecules. However, the peaks correspond to no feasible disorder model and most probably represent “ghost” peaks from twin.

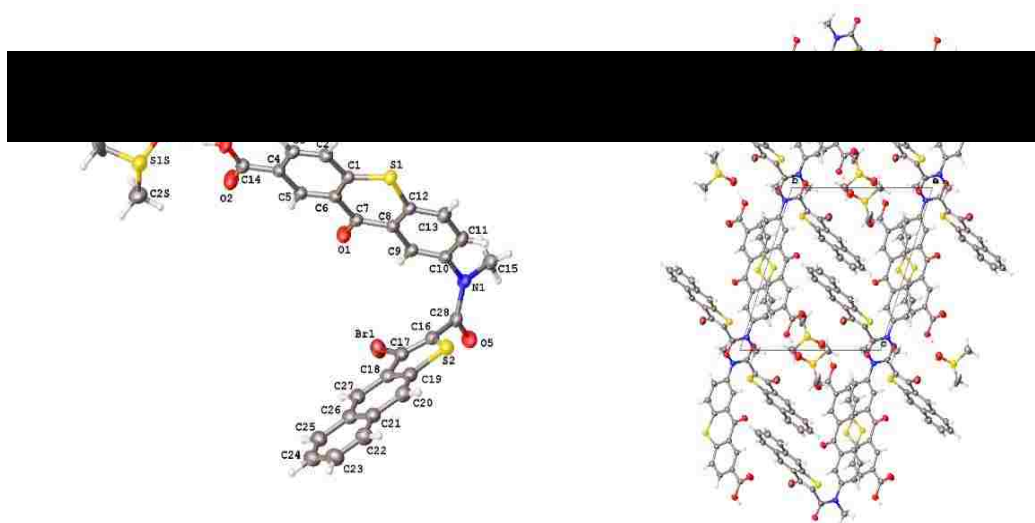


Figure 2.1. Direct-linked caged compound **11b**. (a. Crystal structure. b. Crystal packing.)

Both thioxanthone and naphthothiophene moieties form separate centrosymmetric dimers in crystal with parallel overlap of their pi-systems. The structure contains channels along x axis filled out by the solvent.

2.2.3.2. Crystal structure of tethered caged compound 12a.



Figure 2.2. X-ray structure of direct-linked caged compound **12a**. (a. Crystal structure. b. Crystal packing.)

The molecule has a conformation with trans-arrangement of the trimethylene-thioxanthone and naphthothiophene moieties. The cis-positioned naphthothiophene and p-carbomethoxyphenyl substituents are almost perpendicular to the plane of the central amide group. The trimethylene bridge is also essentially orthogonal to the adjacent thioxanthone and amide groups. The brominated naphthothiophene moiety shows some signs of disorder (librational motion). Both thioxanthone and naphthothiophene moieties form separate centrosymmetric dimers in crystal with parallel overlap of their pi-systems.

2.2.3.3. Crystal structure of methylated Boc animo thioxanthone 27.

The structure represents an equimolecular mixture of cis- and trans-isomers (relative to peptide bond). In both isomers, the carbomethoxy group is conjugated with the central thioxanthone moiety. The peptide moiety is not – it is rotated by 48 and 54°

relative to the thioxanthone group. The molecules of cis- and trans isomers alternate approximately parallel to each other in stacks along y direction

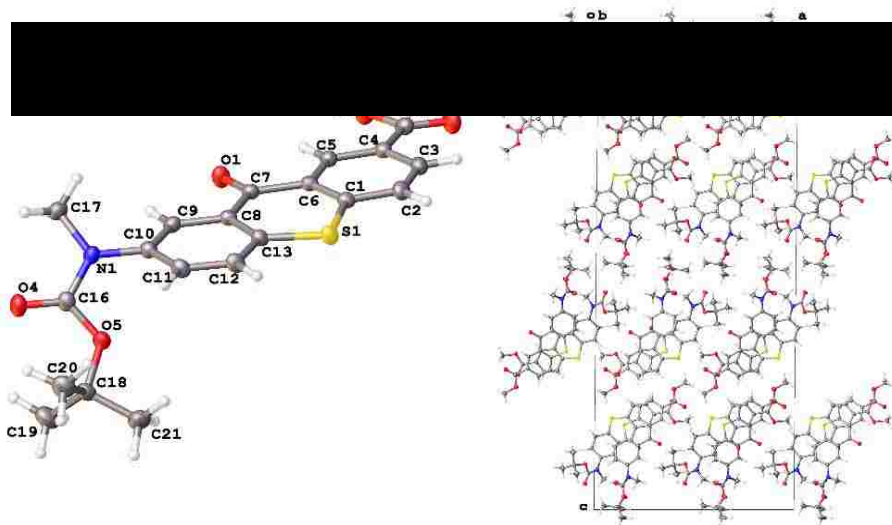
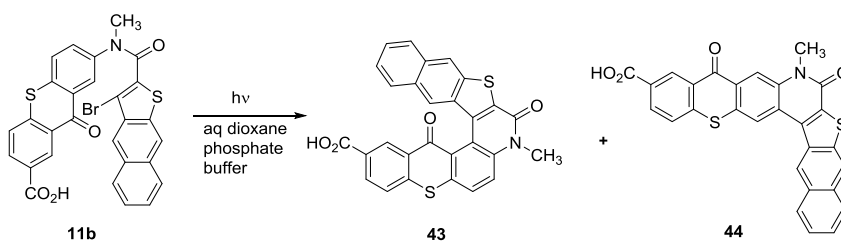


Figure 2.3. X-ray structure of methylated Boc amino thioxanthone **27**. (a. Crystal structure. b. Crystal packing.)

2.2.4. Photolyses

Direct photolysis of 1.52×10^{-3} M caged compound **11b** in 90% dioxane and 10% water containing 100 mM phosphate buffer at pH 7 with a Hanovia medium pressure mercury lamp gave nearly complete conversion (Scheme 2.7). A precipitate formed during photolysis. After acidification with 1 M HCl, the precipitate was isolated by filtration and appeared to be a single regioisomeric product by ^1H NMR analysis. ^1H NMR COSY



Scheme 2.5. Photolysis of direct-linked caged compound **11**.

clearly showed six cross peaks, one of which corresponded to a W-coupling, and the other five corresponded to five vicinal couplings (figure 2.5). Of the two possible regioisomers, the U-shaped regioisomer **43** would be most consistent with these findings, since four vicinal couplings should be observed for the L-shaped regioisomer **44**.

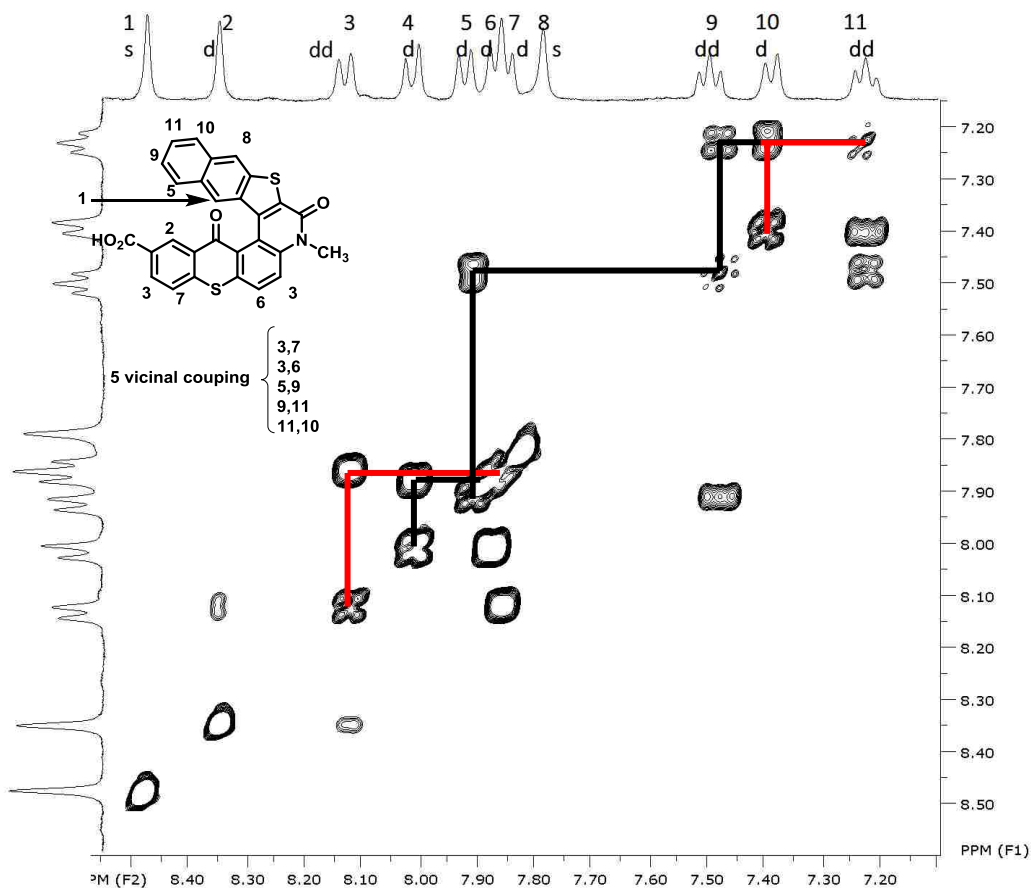
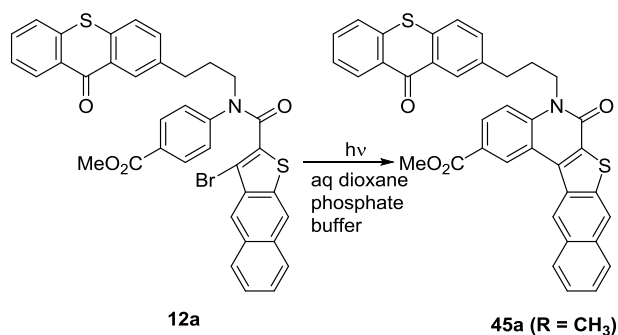
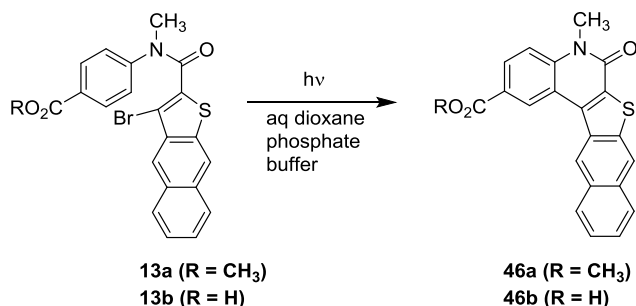


Figure 2.4. ^1H NMR COSY for photoproduct of compound **11b** in DMSO-d_6 .

Unfortunately, suitable crystals for an X-ray structure could not be obtained. Therefore, our structural assignment is not definitive. However, it should be noted that a structure analogous to **43**, i.e. compound **6**, was previously assigned based on COSY and X-ray crystallography for photolyses of the benzothiophene analogs such as **5**.



Direct photolysis of 10^{-3} M of the trimethylene linked naphthothiophenes **12a** in 95% dioxane and 5% water containing 100 mM phosphate buffer at pH 7 also gave precipitates, which likewise were isolated by filtration and identified by ^1H , ^{13}C NMR spectroscopy as **45a** (eq. 2.5). Similar photolyses were also performed for anilides **13a,b** to give photoproducts **46a,b** (eq. 2.6) All of these photolyses were cleanly carried out to nearly complete conversions of the reactants.



2.2.5. Absorption Spectroscopy.

2.2.5.1. The absorption spectrum of 11b and 43b.

The absorption spectrum of compound **11b** exhibits $\lambda_{\text{max}} = 390$ nm (ϵ 6000 $\text{M}^{-1} \text{cm}^{-1}$).

(Figure 2.6) The photoproduct also absorbs strongly at 390 nm (ϵ 5700 $\text{M}^{-1} \text{cm}^{-1}$). The

conversion was kept below 15% for the measurement of the quantum yield.

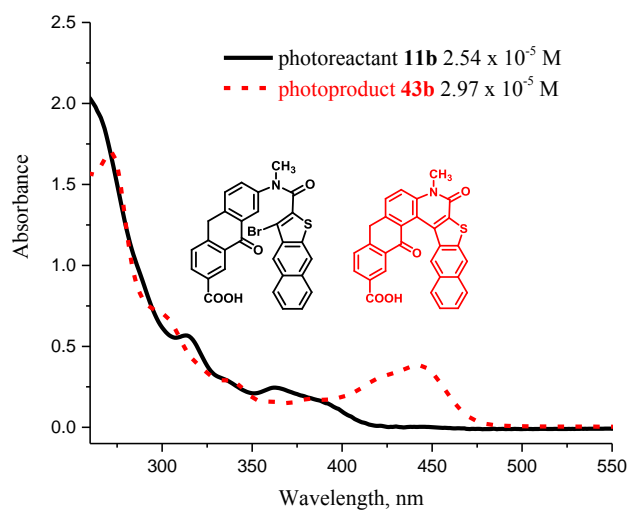


Figure 2.5. Absorption spectra of photoreactant **11b** (—) and photoproduct **43b** (----). Concentrations were 2.54×10^{-5} M and 2.97×10^{-5} M, respectively in dioxane containing 17% 100 mM phosphate buffer at pH 7.

2.2.5.2. The absorption spectrum of **12a** and its photoproduct.

The absorption spectrum of reactant **12a** exhibits $\lambda_{\max} = 390\text{nm}$ (ϵ 6000 $\text{M}^{-1} \text{cm}^{-1}$)

(Figure 2.7), while photoproduct has a structured band centered at $\lambda_{\max} = 390 \text{ nm}$ (ϵ 9900 $\text{M}^{-1} \text{cm}^{-1}$)

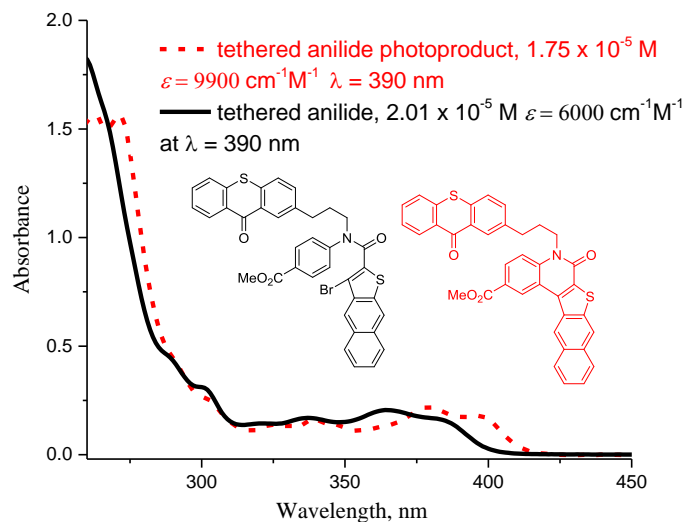


Figure 2.6. Absorption spectra of reactant **12a** (—) and photoproduct **45b** (----). Concentrations were 2.01×10^{-5} M and 1.75×10^{-5} M, respectively in dioxane containing 17% 100 mM phosphate buffer at pH 7.

2.2.5.3. The absorption spectrum of **13a**, its photoproduct and thioxanthone.

More important is the comparison of the absorption spectra of anilide **13a** to thioxanthone, which shows that ca. 80% of the light would likely be absorbed by the thioxanthone, when linked to the anilide via the trimethylene linker (Figure 2.8). This would imply that most of the photochemistry involves absorption of the light by the thioxanthone, which undergoes intersystem crossing with $\Phi_{isc} = 0.68^3$, followed by triplet excitation transfer from the thioxanthone triplet excited state ($E_T = 65 \text{ kcal mol}^{-1}$) of the naphthothiophene ($E_T = \text{ca. } 51 \text{ kcal mol}^{-1}$).⁶ Such triplet excitation transfer has been established on the basis of a computational study, which also shows that the ensuing photoreaction of **5** occurs in the triplet excited state.

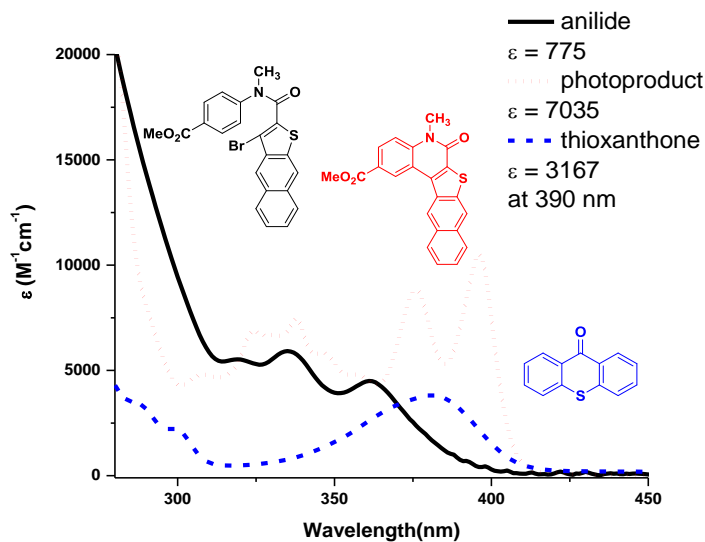


Figure 2.7. Absorption spectra of anilide 13a (—), photoproduct 46a (⋯), and thioxanthone (---).

2.2.5.4. Absorption spectra of trimethylene – linked thioxanone and an equimolar mixture of thioxanthone and anilide 13a.

The aforementioned assumes that the thioxanthone and the naphthothiophene components in **12a** are not strongly interacting or complexed. The comparison of the absorption spectrum **12a** to an equimolar mixture of anilide **13a** and thioxanthone shows that this is likely the case (Figure 2.7). The absorption spectrum mostly resembles the sum of the absorptions of the individual thioxanthone and anilide **13a** components.

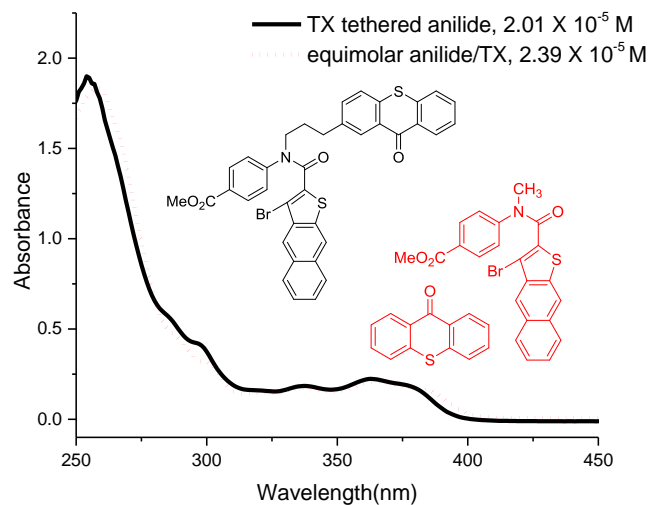


Figure 2.8. Absorption spectra of trimethylene – linked thioxanone **12a** (—) and an equimolar mixture of thioxanthone and anilide **13a** (.....).

2.2.5.5. The absorption spectrum of **13a** and xanthone.

The absorption spectrum of reactant **13a** exhibits $\lambda_{\max} = 361\text{nm}$ (ϵ 4500 $\text{M}^{-1} \text{cm}^{-1}$)

(Figure 2.10), while xanthone has a structured band centered at $\lambda_{\max} = 341 \text{ nm}$ (ϵ 8000

$\text{M}^{-1} \text{cm}^{-1}$).

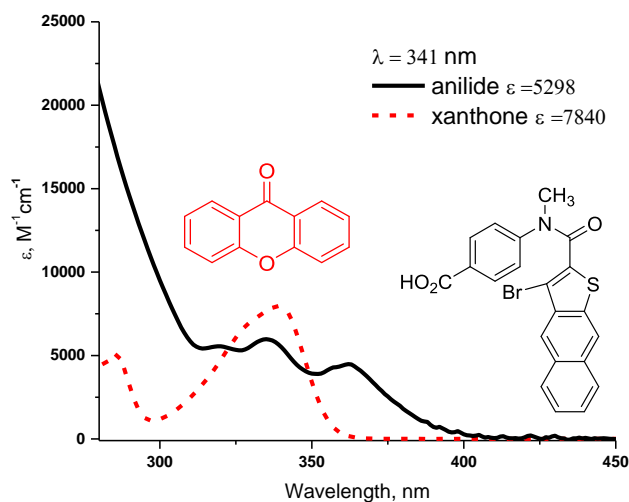


Figure 2.9. Absorption spectra of anilide **13b** (—) and thioxanthone (.....).

2.2.5.6. The absorption spectrum of **13a** and acriflavine.

Acriflavine absorbs strongly at 450 nm ($\epsilon = 24000 \text{ M}^{-1} \text{ cm}^{-1}$), where anilide **13a** is transparent. The absorption spectrum of reactant **13a** exhibits $\lambda_{\text{max}} = 361 \text{ nm}$ ($\epsilon = 4500 \text{ M}^{-1} \text{ cm}^{-1}$) (Figure 2.11).

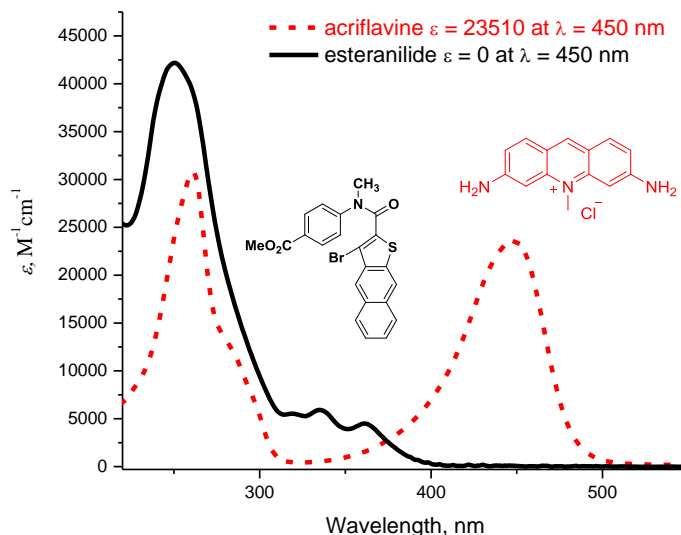
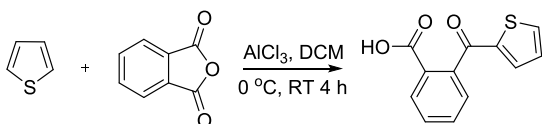


Figure 2.10. The Absorption spectra of anilide **12a** (—) and acriflavine (.....).

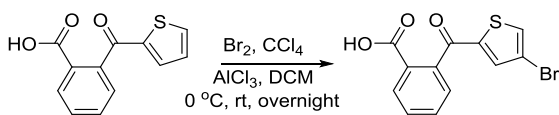
2.3. Experimental section.

Chemical and general method. Chemicals were purchased from Sigma-Aldrich, VWR, and Fisher Scientific. Compounds were used as received unless otherwise noted. The ^1H and ^{13}C NMR spectra were recorded on a Varian 300 or 400 spectrometer. Solutions required for the actinometry was prepared using the procedure reported by Zimmerman.⁸⁵ HRMS spectra were collected using a Shimadzu LCMS-IT-TOF instrument at the Department of Chemistry and Biochemistry UW-Milwaukee, Milwaukee, Wisconsin. Midwest Micro Lab, LLC, Indianapolis, Indiana 45250,

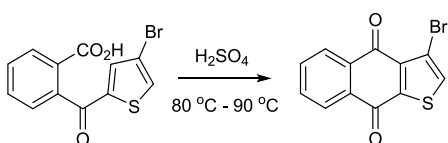
performed all elemental analyses. All melting point determinations were made with a Fisher-Johns melting point apparatus. UV absorption spectra were obtained using by a Cary 5000 UV spectrophotometer. GC-MS analysis was done using an Agilent 6850 GC-MS spectrometer with a HP-5 (5% phenylmethyl polysiloxane) column (30 m×0.32 mm×0.25 μ m). Crystal data sets were collected with an Oxford SuperNova diffractometer using Mo(K α) radiation at 100K.



2-(Thiophene-2-carbonyl)benzoic acid 14. The procedure was adapted from the literature.⁷⁸ To a solution of 9.00 g (67.5 mmol) of phthalic anhydride and 20.26 g (168.8 mmol) of AlCl₃ in 250 mL of anhydrous dichloromethane was added dropwise 5.11 g (67.5 mmol) of thiophene at 0 °C in 0.5 h. The reaction was stirred overnight at room temperature and then poured into HCl-ice mixture cautiously. The aqueous layer was extracted three times with 100 mL of dichloromethane. The combined extracts were washed with 5% NaOH solution. The aqueous hydroxide was acidified with concentrated HCl to pH 2. The mixture was cooled in an ice bath and filtered to give 13.4 g (86 %) of 2-(thiophene-2-carbonyl)benzoic acid **14** as colorless solid, mp 139-141 °C. The spectral data were as follows: ¹H NMR (300 MHz, CDCl₃) δ 8.08 (dd, J = 7.7, 1.4 Hz, 1H), 7.69 (dd, J = 4.9, 1.2 Hz, 1H), 7.65 (dd, J = 7.5, 1.4 Hz, 1H), 7.57 (td, J = 7.7, 1.4 Hz, 1H), 7.46 (dd, J = 7.5, 1.3 Hz, 1H), 7.25 (dd, J = 3.8, 1.3 Hz, 1H), 7.06 (dd, J = 4.9, 3.8 Hz, 1H); ¹³C NMR (400 MHz, CDCl₃) δ 189.2, 170.9, 144.3, 141.8, 134.7, 134.6, 133.1, 131.0, 129.9, 128.1, 127.9, 127.8.

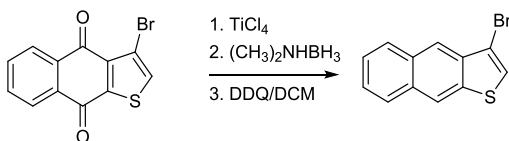


Preparation of 2-(4-bromothiophene-2-carbonyl)benzoic acid **15.** The procedure was adapted from reported literature.⁷⁹ To a solution of 7.70 g (33.2 mmol) of 2-(thiophene-2-carbonyl)benzoic acid and 13.3 g (99.6 mmol) of AlCl₃ in 100 mL of anhydrous CH₂Cl₂ was added dropwise 6.90 g (43.2 mmol) of bromine in 10 mL of carbon tetrachloride at 0 °C. The reaction was stirred overnight at room temperature for 2 days and then poured into HCl-ice mixture. The organic layer was filtered, and the collected crude was crystallized in 80% aqueous ethanol to give 9.12 g (88%) of 2-(4-bromothiophene-2-carbonyl)benzoic acid **15** as a colorless solid, mp 213-215 °C. HRMS (ESI/ IT-TOF) m/z: [M + H]⁺ Calcd for C₁₂H₇BrO₃S 310.9372; Found 310.9339: The spectral data were as follows: ¹H NMR (400 MHz, d₆-DMSO) δ 8.17 (d, *J* = 1.5 Hz, 1H), 7.99 (dd, *J* = 1.0, 7.6 Hz, 1H), 7.73 (ddd, *J* = 1.4, 7.4, 7.4 Hz, 1H), 7.68 (ddd, *J* = 1.4, 7.6, 7.6 Hz, 1H), 7.53 (dd, *J* = 1.0, 7.3 Hz, 1H), 7.24 (d, *J* = 1.4 Hz, 1H); ¹³C NMR (400 MHz, d₆-DMSO) δ 188.7, 167.01, 144.11, 140.7, 135.2, 134.5, 132.2, 130.1, 130.0, 129.9, 128.7, 127.5.



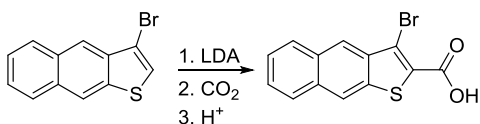
Preparation of 3-bromonaphtho[2,3-b]thiophene-4,9-dione **16.** 8.02 g (25.77 mmol) of the bromoketoacid **15** was heated in 100 mL of concentrated H₂SO₄ at 80 - 90 °C for 4 h. The reaction mixture was cautiously poured into ice once cooled to room temperature. The aqueous layer was extracted three times with 150 mL of dichloromethane. The organic layer was washed with saturated NaHCO₃, brine, dried

over MgSO_4 and concentrated to give 5.00 g (66%) of 3-bromonaphtho[2,3-b]thiophene-4,9-dione **16** as a yellow solid, mp 169-171 °C. HRMS (ESI/ IT-TOF) m/z : $[\text{M} + \text{H}]^+$ Calcd for $\text{C}_{12}\text{H}_5\text{O}_2\text{SBr}$ 292.9266; Found 292.9253. The spectra data were as follows: ^1H NMR (400 MHz, CDCl_3) δ 8.23-8.26 (m, 2H), 8.19-8.21 (m, 2H), 7.73-7.81 (m, 2H), 7.71 (s, 1H); ^{13}C NMR (400 MHz, CDCl_3) δ 178.0, 177.3, 146.4, 137.2, 134.4, 133.8, 133.6, 132.8, 132.7, 127.63, 126.8, 111.3.

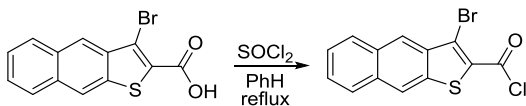


The preparation of 3-bromonaphtho[2,3-b]thiophene 18. The synthesis was followed previous literature.⁸⁰ 2.20 g (7.51 mmol) of 3-bromonaphtho[2,3-b]thiophene-4,9-dione **16** was dissolved in 20 mL of dichloromethane, cooled to 0 °C, and treated under stirring with the dropwise addition of 18.78 mmol of TiCl_4 . 1.11 g (18.78 mmol) of dimethylamine-borane in 5 mL of dichloromethane was added to the cold solution. The reaction mixture was allowed to warm to room temperature. The stirring was continued for 3 h. 1 N HCl was added cautiously to quench the reaction. Phases were separated and the aqueous layer was extracted twice with 20 mL of dichloromethane. The combined extracts were washed with saturated aqueous NaCl and dried over Na_2SO_4 . The solvent was removed, and crude product was dissolved in 20 mL of anhydrous dichloromethane and 4.26 g (18.78 mmol) of 2,3-Dichloro-5,6-dicyano-1,4-benzoquinone was added. The reaction mixture was stirred under N_2 atmosphere overnight and quenched with water. Phases were separated, and the aqueous layer was extracted twice with 10 mL of dichloromethane. The combined extracts were washed with saturated aqueous NaHCO_3 , saturated aqueous NaCl, and dried over Na_2SO_4 . Concentration in

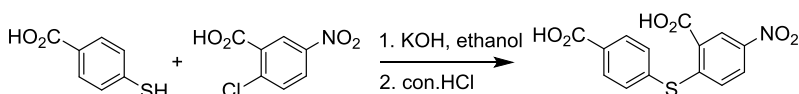
vacuo followed by chromatography on silica gel, eluting with hexane gave 1.38 g (63%) of 3-bromonaphtho[2,3-b]thiophene **18** as a colorless solid, mp 89-90 °C. The spectra data were as follows: ^1H NMR (400 MHz, CDCl_3) δ 8.32 (s, 1H), 8.29 (s, 1H), 8.02-8.04 (m, 1H), 7.89-7.92 (m, 1H), 7.51-7.53 (m, 2H), 7.50 (s, 1H); ^{13}C NMR (400 MHz, CDCl_3) δ 136.4, 136.12, 131.3, 131.0, 128.6, 127.2, 126.0, 125.5, 125.2, 121.8, 121.2, 107.3.



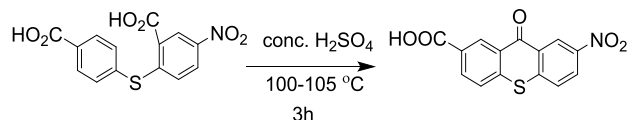
Preparation of 3-bromonaphtho[2,3-b]thiophene-2-carboxylic acid 19. 4.00 g (15.2 mmol) of 3-bromonaphtho[2,3-b]thiophene **18** was dissolved in 20 mL of anhydrous Tetrahydrofuran, cooled in acetone-dry ice bath and treated with the dropwise addition of 15.0 mL of 1 M Lithium diisopropylamide in THF under Nitrogen. The reaction was stirred for 1 h. Excess dry ice was cautiously added into the reaction mixture, followed by 2 h stirring at room temperature. The reaction was quenched with water and washed with diethyl ether to remove unreacted starting material. 1 N HCl solution was added to the aqueous solution until pH 2. The resulting yellow precipitate was filtered and dried to give 4.20 g (90.0 % Yield) of 3-bromonaphtho[2,3-b]thiophene-2-carboxylic acid **19** as a bright yellow solid, mp 320-321 °C. (The compound turned dark after this point.) HRMS (ESI/ IT-TOF) m/z : $[\text{M}]^+$ Calcd for $\text{C}_{13}\text{H}_7\text{O}_2\text{SBr}$ 305.9345; Found 305.9326. The spectra data were as follows: ^1H NMR (400 MHz, DMSO-d_6) δ 8.66 (s, 1H), 8.56 (s, 1H), 8.22 (m 1H), 8.03 (m, 1H), 7.67-7.53 (m, 2H); ^{13}C NMR (400 MHz, DMSO-d_6) δ 162.6, 137.6, 135.4, 133.0, 131.3, 130.9, 129.3, 127.7, 127.6, 126.5, 124.7, 122.1, 113.7.



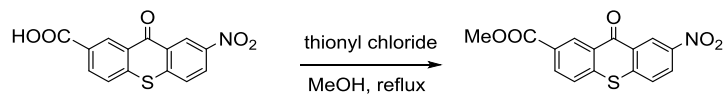
Preparation of 3-bromonaphtho[2,3-b]thiophene-2-carbonyl chloride **20.** The mixture of 1.17 g (3.80 mmol) of the acid **19**, 1.37 g (19.0 mmol) of thionyl chloride in 10 mL of anhydrous benzene was refluxed for 3 h. The reaction mixture was concentrated in vacuo, washed with cold hexane and further dried in vacuum to give 0.80 g (65%) of the acid chloride **20** as a yellow solid, which was used in the coupling reaction without further purification.



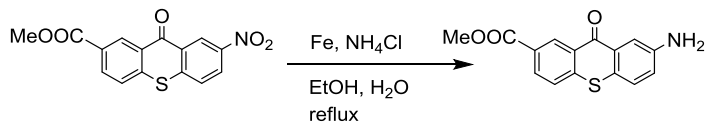
Preparation of 2-((4-carboxyphenyl)thio)-5-nitrobenzoic acid **21.** To a solution of 19.20 g (95.3 mmol) of 5-nitro-2-chlorobenzoic acid in 300 mL absolute ethanol was added 16.12 g (104.6 mmol) of 4-mercaptobenzoic acid and 14.04 g (250.2 mmol) of potassium hydroxide dissolved in 600 mL ethanol while stirring. The reaction was stirred under refluxing overnight. The concentrate of the reaction mixture was diluted with water and acidified with concentrated HCl to pH 2. The resulting solid was filtered and washed with water. The crude product was recrystallized with 80% aqueous ethanol to obtain 24.42 g (81%) of 2-((4-carboxyphenyl)thio)-5-nitrobenzoic acid **21** as light yellow crystals, mp 238-240 °C. HRMS (ESI/ IT-TOF) m/z: [M+H]⁺ Calcd for C₁₄H₉NO₆S 319.0078; Found 318.0070. The spectral data were as follows: ¹H NMR (400 MHz, DMSO-d₆) δ 8.62 (d, J = 2.7 Hz, 1H), 8.16 (dd, J = 9.0, 2.7 Hz, 1H), 8.05 (d, J = 8.5 Hz, 2H), 7.71 (d, J = 8.5 Hz, 2H), 6.91 (d, J = 9.0 Hz, 1H).; ¹³C NMR (400 MHz, DMSO-d₆): δ 167.34, 166.46, 151.11, 144.82, 136.59, 136.05, 132.86, 131.72, 128.44, 128.11, 127.39, 126.42



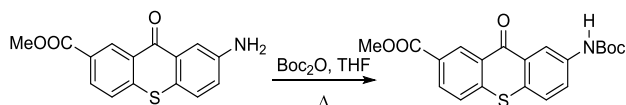
Preparation of 7-nitro-9-oxo-9H-thioxanthene-2-carboxylic acid 22. To 150 mL of concentrated sulphuric acid at 100 °C was added 20.54 g (64.4 mmol) of 2-((4-carboxyphenyl)thio)-5-nitrobenzoic acid **21**. The temperature of the mixture was maintained at 100-105 °C for 3 h. The reaction mixture was cooled to room temperature and poured onto 100 g of ice. The resulting precipitate was filtered, washed water, dried in air and washed with methanol to give 17.00 g (88%) of **22** as a yellow solid, mp 378-380 °C. HRMS (ESI/ IT-TOF) m/z: [M-H]⁻ Calcd for C₁₄H₇NO₅S 299.9972; Found 299.9971. The spectral data were as follows: ¹H NMR (400 MHz, DMSO-d₆) δ 9.10 (d, *J* = 2.6 Hz, 1H), 8.96 (d, *J* = 2.0 Hz, 1H), 8.53 (dd, *J* = 8.8, 2.6 Hz, 1H), 8.26 (dd, *J* = 8.4, 2.0 Hz, 1H), 8.20 (d, *J* = 8.8 Hz, 1H), 8.06 (d, *J* = 8.4 Hz, 1H).



Preparation of methyl 7-nitro-9-oxo-9H-thioxanthene-2-carboxylate 23. To the mixture of 5.00 g (16.6 mmol) of 7-nitro-9-oxo-9H-thioxanthene-2-carboxylic acid in 300 mL of anhydrous methanol was added dropwise 6.00 mL (83.0 mmol) of thionyl chloride at 0 °C. The reaction was refluxed overnight under nitrogen. The reaction mixture was filtered to give 3.66 g of crude ester **23**, which contains small amount of starting material. The crude product was used in next step without further purification. HRMS (ESI/ IT-TOF) m/z: [M+H]⁺ Calcd for C₁₅H₉NO₅S 316.0274; Found 316.0270.

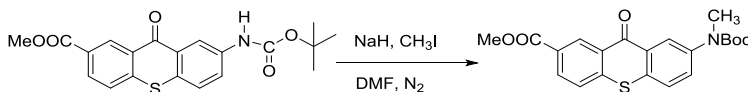


Preparation of methyl 7-amino-9-oxo-9H-thioxanthene-2-carboxylate 24. The procedure was adapted from a procedure reported by Steinmetz⁴ and Moon.³² A mixture of 5.00 g (ca. 15.9 mmol) of 7-nitro-9-oxo-9H-thioxanthene-2-carboxylate **23**, 5.00 g (100.0 mmol) of ammonium chloride, and 2.80 g (51.2 mmol) of iron in 600 mL of ethanol and 180 mL of water was refluxed overnight while mechanically stirring. The reaction was hot filtered through silica gel. The silica gel was washed several times with hot ethanol. The combined filtrate was concentrated in vacuo to remove ethanol. The product was extracted into chloroform, washed with saturated NaCl solution, dried over anhydrous sodium sulphate, concentrated via vacuo, and recrystallized in ethanol to give 1.80 g (ca. 40%) of 7-amino-9-oxo-9H-thioxanthene-2-carboxylate **24** as a yellow powder, mp 208-209 °C. HRMS (ESI/ IT-TOF) m/z: [M+H]⁺ Calcd for C₁₅H₁₁NO₃S 286.0532; Found 286.0522. The spectral data were as follows: ¹H NMR (400 MHz, CDCl₃) δ 9.24 (d, *J* = 1.9 Hz, 1H), 8.18 (dd, *J* = 8.5, 1.9 Hz, 1H), 7.90 (d, *J* = 2.7 Hz, 1H), 7.61 (d, *J* = 8.5 Hz, 1H), 7.40 (d, *J* = 8.5 Hz, 1H), 7.06 (dd, *J* = 8.6, 2.7 Hz, 1H), 4.03 – 3.94 (m, 5H); ¹³C NMR (400 MHz, CDCl₃) δ 179.3, 166.2, 145.7, 142.7, 131.6, 130.1, 128.4, 127.6, 127.1, 126.3, 125.2, 121.5, 113.5, 52.3.



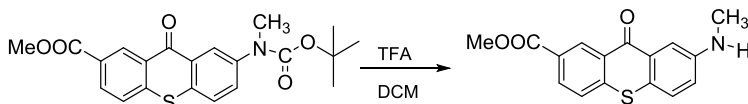
Preparation of tert-butyl (7-methyl-9-oxo-9H-thioxanthen-2-yl)carbamate 25. A mixture of 5.05 g (17.7 mmol) of methyl 7-amino-9-oxo-9H-thioxanthene-2-carboxylate and 15.15 g (70.10 mmol) in 20 mL of dioxane was stirred under refluxing

for 5 h. TLC was used to confirm the completion. The reaction mixture was then diluted with 20 mL of water and extracted 3 times with dichloromethane. The combined organic layer was washed with saturated NaCl solution, dried over anhydrous sodium sulfate, and concentrated in vacuo to give the crude. The crude was crystalized in ethanol to give 3.1 g (46%) of product **25** as a light-yellow powder, mp 190-192 °C. HRMS (ESI/ IT-TOF) m/z: [M+H]⁺ Calcd for C₂₀H₁₉NO₅S 386.1057; Found 386.1045. The spectral data were as follows: ¹H NMR (400 MHz, CDCl₃): δ 9.19 (d, *J* = 1.7 Hz, 1H), 8.29 (s, 1H), 8.18 (dd, *J* = 8.4, 1.9 Hz, 1H), 8.13 (s, 1H), 7.59 (d, *J* = 8.4 Hz, 1H), 7.51 (d, *J* = 8.8 Hz, 1H), 7.04 (s, 1H), 3.97 (s, 3H), 1.54 (s, 9H); ¹³C NMR (400 MHz, CDCl₃) δ 179.0, 166.1, 152.6, 142.3, 137.9, 132.0, 131.5, 130.1, 129.4, 128.3, 128.0, 126.9, 126.3, 124.1, 118.1, 81.2, 52.4, 28.3.

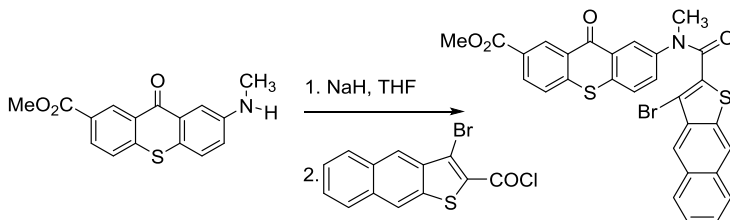


Preparation of methyl 7-((tert-butoxycarbonyl)(methyl)amino)-9-oxo-9H-thioxanthene-2-carboxylate 26. To a stirred solution of 1.33g (3.50 mmol) of methyl 7-((tert-butoxycarbonyl)amino)-9-oxo-9H-thioxanthene-2-carboxylate in 10 mL of anhydrous DMF was added 0.178 g (4.40 mmol) of NaH (60%) under N₂. The mixture was stirred for 30 min followed by drop wise addition of 0.74 g (5.2 mmol) of methyl iodide. After 24 h, the reaction mixture was diluted with 30 mL of water and extracted 3 times with 50 mL of ethyl acetate. The combined organic layers were concentrated via vacuo to give the crude product, which was crystalized in ethanol to give 0.73 g (54%) of methyl amide as a yellow powder, mp 141-142 °C. The spectral data as follows: ¹H NMR (400 MHz, CDCl₃) δ 9.25 (d, *J* = 1.9 Hz, 1H), 8.44 (d, *J* = 2.5 Hz, 1H), 8.24 (dd, *J* = 8.5, 1.9 Hz, 1H), 7.70 (d, *J* = 8.4 Hz, 1H), 7.65 (d, *J* = 8.4 Hz, 1H), 7.54 (d, *J* = 8.7 Hz, 1H),

3.99 (s, 3H), 3.38 (s, 3H), 1.49 (s, 9H). ^{13}C NMR (400 MHz, CDCl_3) δ 179.0, 166.1, 154.3, 142.9, 142.1, 132.7, 132.2, 131.6, 130.9, 129.4, 128.5, 128.3, 126.4, 126.1, 124.6, 81.1, 52.4, 37.1, 28.3.

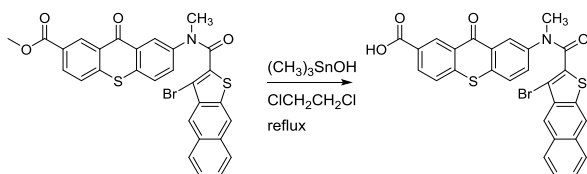


Preparation of methyl 7-(methylamino)-9-oxo-9H-thioxanthene-2-carboxylate 27. To a solution of 3.12 g (7.81 mmol) of Bocamino compound in 10 mL of dichloromethane was added 10 mL of TFA and the solution stirred at room temperature overnight. The reaction was then diluted with 50 mL of 3 M KOH. The resulting precipitate was filtered and washed with water to give 2.11 g (90%) of the deprotected amino compound as an orange powder, mp 178-180 °C. HRMS (ESI/ IT-TOF) m/z : $[\text{M} + \text{H}]^+$ Calc. for $\text{C}_{16}\text{H}_{13}\text{NO}_3\text{S}$ 300.0680; Found 300.0680. The spectral data were as follows: ^1H NMR (400 MHz, CDCl_3): δ 9.24 (d, $J = 2.0$ Hz, 1H), 8.16 (dd, $J = 8.4, 2.0$ Hz, 1H), 7.74 (d, $J = 2.7$ Hz, 1H), 7.60 (d, $J = 8.4$ Hz, 1H), 7.37 (d, $J = 8.6$ Hz, 1H), 6.98 (dd, $J = 8.6, 2.7$ Hz, 1H), 4.10 (s, 1H), 3.97 (s, 1H), 2.96 (s, 3H); ^{13}C NMR (400 MHz, CDCl_3): δ 179.4, 166.3, 148.4, 142.7, 131.6, 131.4, 130.1, 128.3, 127.5, 126.9, 126.2, 123.9, 120.0, 109.4, 52.3, 30.7.



Preparation of methyl 7-(3-bromo-N-methylnaphtho[2,3-b]thiophene-2-carboxamido)-9-oxo-9H-thioxanthene-2-carboxylate 11a. To a solution of 0.50 g (1.7 mmol) of amino thioxanthone **11a** in 20 mL of anhydrous THF was added cautiously

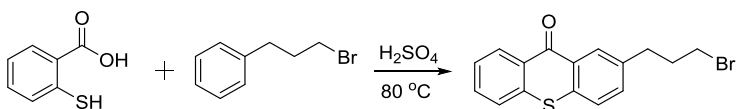
0.17 g (4.2 mmol) of NaH (60%) under nitrogen atmosphere. The mixture was stirred for 30 min before 0.62 g (1.86mmol) the acid chloride **20** was added slowly. The reaction was kept overnight. TLC was used to confirm the completion. The reaction mixture was then diluted with 20 mL of dichloromethane and filtered. Concentration of the filtrate in vacuo followed by column chromatography on silica gel, eluting with 30% ethyl acetate in hexane gave 0.69 g (70 % yield) of pure direct linked anilide ester **11a** as a light-yellow solid, mp 266-267 °C. HRMS (ESI/ IT-TOF) m/z: [M+H]⁺ Calcd for C₂₉H₁₈NO₄S₂Br 587.9933; Found 587.9931. The spectra data were as follows: ¹H NMR (400 MHz, CDCl₃) δ 9.19 (d, *J* = 1.9 Hz, 1H), 8.59 (d, *J* = 2.5 Hz, 1H), 8.19 (m, 3H), 7.94 (m, 1H), 7.83 (m, 1H), 7.56 (m, 2H), 7.52 – 7.38 (m, 3H), 3.96 (s, 3H), 3.63 (s, 3H); ¹³C NMR (400 MHz, CDCl₃) δ ¹³C NMR (75 MHz, CDCl₃) δ 178.6, 165.9, 163.4, 141.6, 141.5, 135.8, 135.4, 135.2, 133.4, 132.4, 132.1, 131.6, 131.1, 131.0, 129.6, 128.5, 128.4, 127.2, 127.1, 127.0, 126.5, 126.3, 125.8, 123.0, 121.1, 108.0, 52.5, 38.0.



4-(3-bromo-N-methylnaphtho[2,3-b]thiophene-2-carboxamido)benzoic acid

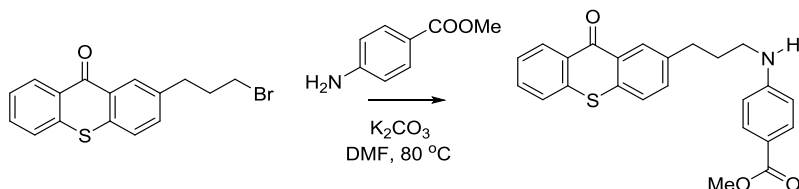
11b. The same ester demethylation procedure was adapted from previous literature⁸⁶. A solution of 0.50 g (0.85 mmol) of ester **11a** and 0.77 g (4.3 mmol) of trimethyl tin hydroxide in 20 mL of anhydrous dichloroethane was stirred at 80 °C. TLC was used to confirm the completion of the reaction. The reaction was added 1 N HCl solution until pH 2 once cooled to room temperature. The layers were separated, and aqueous layer was extract three times with 30 mL of ethyl acetate. The combined the organic layer were

washed with brine, dried over NaSO₄, and concentrated to give the crude product. The crude carboxylic acid product was washed with water, triturated with hot methanol, and washed with cold methanol to give 0.46 g (95%) of **11b** as a yellow solid, mp > 340 °C. (Compound turned dark after this point.) HRMS (ESI/ IT-TOF) m/z: [M-H]⁻ Calcd for C₂₈H₁₆NO₄S₂Br 571.9607; Found 571.9631. The spectra data were as follows: ¹H NMR (400 MHz, DMSO-*d*₆) δ 13.37 (br, 1H), 8.89(d, *J* = 1.8 Hz, 1H), 8.55 (s, 1H), 8.45 (s, 1H), 8.28 (s, 1H), 8.14 (dd, *J* = 8.5, 1.8 Hz, 1H), 8.09 (d, *J* = 8.0 Hz, 1H), 7.93 (d, *J* = 7.0 Hz, 1H), 7.87 (d, *J* = 8.5 Hz, 1H), 7.84 (s, 2H), 7.56 – 7.47 (m, 2H), 3.52 (s, 3H);



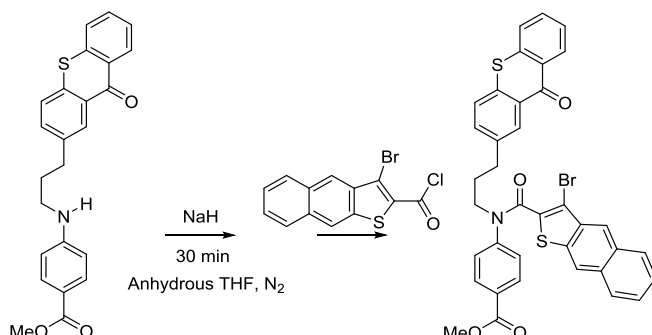
Preparation of 2-(3-bromopropyl)-9H-thioxanthen-9-one 31. The procedure was adapted from previous literature.⁸³ To a stirred 50 mL of concentrated sulfuric acid was added slowly 5.00 g (30.9 mmol) of thiosalicylic acid at room temperature. After being stirred for another 15 min at room temperature, the reaction was added 6.70 mL (123.6 mmol) 3-bromo-1-phenylpropane was slowly added within a period of 30 minute. The reaction mixture was stirred at room temperature for 2 h, and then slowly brought to 80 °C and stirred for another 24 h. The reaction was then slowly poured into 300 mL of ice cooled water and left to stand for about 2 h, forming a yellow precipitate. The yellow precipitate was filtered, washed with cold water to give the crude product. The aqueous solution was also extracted with dichloromethane to give another fraction of the crude product. Crystallization from ethanol gives 6.20 g (60.0 %) of compound **31** as needle-like crystals, mp 95-97 °C. HRMS (ESI/ IT-TOF) m/z: [M + H]⁺ Calcd for C₁₆H₁₃OSBr

332.9943; Found 332.9909. The spectra data were as follows: ^1H NMR (400 MHz, CDCl_3): δ 8.63 (d, $J = 8.1$ Hz, 1H), 8.46 (s, 1H), 7.66 – 7.44 (m, 5H), 3.42 (t, $J = 6.9$ Hz, 2H), 2.93 (t, $J = 6.9$ Hz, 2H), 2.25 (p, $J = 6.9$ Hz, 2H). ^{13}C NMR (400 MHz, CDCl_3): δ 179.9, 139.0, 137.29, 135.0, 133.1, 132.2, 129.9, 129.2, 129.2, 129.2, 126.2, 126.0, 33.8, 33.7, 32.8.



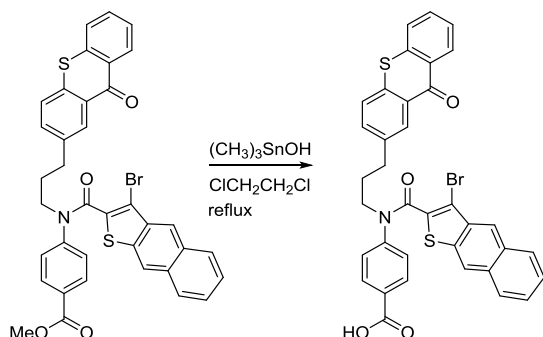
Preparation of methyl 4-((3-(9-oxo-9H-thioxanthen-2-yl)propyl)amino)benzoate **33.** To the mixture of 4.14 g (12.4 mmol) of 2-(3-bromopropyl)-9H-thioxanthen-9-one and 1.88 g (12.4 mmol) of methyl 4-aminobenzoate in 20 mL of anhydrous DMF was added 3.44 g (24.9 mmol) of K_2CO_3 under N_2 . The reaction was heated to 80 °C. After stirring for 24 h, the reaction was cooled to room temperature and poured to 20 mL of cold water. The mixture was extracted three times with 20 mL of dichloromethane. The combined organic layer was washed with water, brine and dried over sodium sulfate. Concentration in vacuum followed by recrystallization from ethanol gave 1.40 g (28.0 %) of compound **33** as a colorless solid, mp 177-178 °C. HRMS (ESI/IT-TOF) m/z : $[\text{M} + \text{H}]^+$ Calcd for $\text{C}_{24}\text{H}_{21}\text{NO}_3\text{S}$ 404.1315; Found 404.1272. The spectra data were as follows: ^1H NMR (400 MHz, CDCl_3): δ 8.63 (d, $J = 8.1$, 1H), 8.47 (s, 1H), 7.85 (d, $J = 8.8$ Hz, 2H), 7.65 – 7.57 (m, 2H), 7.55 – 7.44 (m, 3H), 6.53 (d, $J = 8.8$ Hz, 2H), 4.15 (broad, 1H), 3.84 (s, 3H), 3.23 (m, 2H), 2.88 (t, $J = 7.6$ Hz, 2H), 2.04 (p, $J = 7.6$ Hz, 2H). ^{13}C NMR (400 MHz, CDCl_3): δ 179.9, 167.3,

151.8, 139.8, 137.3, 134.9, 132.9, 132.2, 131.5, 129.9, 129.1, 128.9, 126.2, 126.2, 126.0, 118.2, 111.4, 51.5, 42.6, 32.9, 30.6.



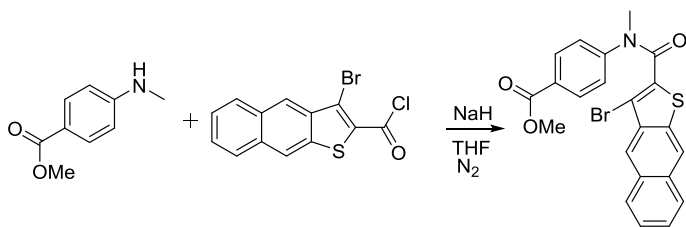
Methyl-4-(3-bromo-N-(3-(9-oxo-9H-thioxanthene-2-yl)propyl)naphtho[2,3-b]thiophene-2-carboxamido)benzoate 12a. The solution of 0.56 g (1.4 mmol) of the amine in 10 mL of anhydrous THF was added slowly 0.11 g (2.8 mmol) of 60% NaH under N₂. The reaction was stirred at room temperature for 30 min before the slow addition of 0.50g (1.5 mmol) 3-bromonaphtho[2,3-b]thiophene-2-carbonyl chloride. Thin layer chromatography was taken to confirm the completion of the reaction after stirring overnight under N₂. The reaction mixture was diluted with 20 mL of dry dichloromethane. The solid was filtered off. Concentration of the filtrate followed by chromatography on silica gel, eluting with AcOEt-hexane (2:8) gave 0.87 g (90 %) of the amide **12a** as a light-yellow solid, mp 190-191 °C. HRMS (ESI/ IT-TOF) m/z: [M + H]⁺ Calcd for C₃₇H₂₆NO₄S₂Br 692.0559; Found 692.0547. The spectra data were as follows: ¹H NMR (400 MHz, CDCl₃): δ 8.59 (d, *J* = 8.1 Hz, 1H), 8.38 (s, 1H), 8.17 (s, 1H), 8.11 (s, 1H), 7.91 (m, 3H), 7.79 (m, 1H), 7.58-7.51 (m, 2H), 7.49 – 7.40 (m, 5H), 7.32 (d, *J* = 8.8 Hz, 2H), 4.06 (t, *J* = 7.6 Hz, 2H), 3.79 (s, 3H), 2.85 (t, *J* = 7.6 Hz, 2H), 2.04 (p, *J* = 7.6 Hz, 2H). ¹³C NMR (400 MHz, CDCl₃): ¹³C NMR (101 MHz, cdcl₃) δ 179.6, 165.8, 162.9, 145.0, 139.3, 137.1, 135.5, 134.9, 134.7, 134.7, 133.5, 132.6, 131.9, 131.8, 130.9,

130.5, 130.4, 129.6, 129.1, 128.9, 128.8, 128.7, 128.3, 126.9, 126.9, 126.3, 125.9, 125.9, 125.8, 125.5, 122.8, 120.8, 107.9, 52.0, 49.6, 32.6, 29.1.



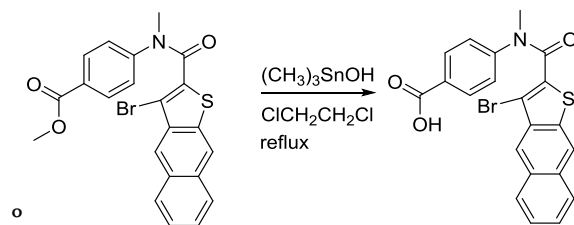
4-(3-bromo-N-(3-(9-oxo-9H-thioxanthen-2-yl)propyl)naphtho[2,3-

b]thiophene-2-carboxamido)benzoic acid 12b. The same ester demethylation procedure was adapted from demethylation of **11a**. A solution of 1.00 g (1.44 mmol) of ester **12a** and 1.31 g (7.28 mmol) of trimethyl tin hydroxide in 40 mL of anhydrous dichloroethane was stirred at refluxing. The work up was same with the demethylation of **11a**. The crude carboxylic acid was washed with water, triturated with hot methanol, and washed with cold methanol to give 0.75 g (89%) as a light yellow solid, mp 318-320 °C. HRMS (ESI/IT-TOF) m/z: [M+H]⁺ Calcd for C₃₂H₂₃NO₅S₂ 439.9951; Found 439.9929. The spectra data were as follows: ¹H NMR (400 MHz, DMSO-*d*₆) δ 12.99 (s, 1H), 8.59 (s, 1H), 8.32 (s, 1H), 8.15 (m, 1H), 7.99 (m, 1H), 7.82 (d, *J* = 8.2 Hz, 2H), 7.57 (m, 2H), 7.48 (d, *J* = 8.2 Hz, 2H), 3.48 (s, 3H); ¹³C NMR (400 MHz, DMSO-*d*₆) δ 162.5, 146.5, 135.6, 135.0, 134.9, 132.0, 131.2, 130.5, 128.9, 127.6, 127.2, 126.8, 126.4, 122.7, 122.1, 107.4, 37.8.



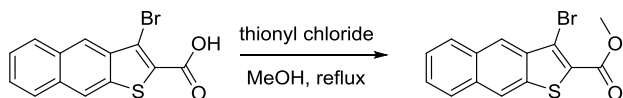
Methyl 4-(3-bromo-N-methylnaphtho[2,3-b]thiophene-2-

carboxamido)benzoate 13a. To a solution of 0.41 g (2.5 mmol) of commercially available methyl-4-(methylamino)benzoate in 10 mL of anhydrous THF was added 0.20 g (5.0 mmol) of NaH (60%) under nitrogen atmosphere. The mixture was stirred for 30 min before 0.90 g (2.7 mmol) the acid chloride **20** was added slowly. The reaction was kept overnight. TLC was used to confirm the completion. The reaction mixture was then diluted with 20 mL of dichloromethane and filtered. Concentration of the filtrate in vacuo followed by column chromatography on silica gel, eluting with 30% ethyl acetate in hexane gave 0.45 g (40 %) of pure benzanilide **13a** as a colorless solid, mp 279-280 °C. HRMS (ESI/ IT-TOF) m/z: [M]⁺ Calcd for C₂₂H₁₆NO₃SBr 454.0107; Found 454.0089. The spectra data were as follows: ¹H NMR (400 MHz, CDCl₃) δ 8.23 (s, 1H), 8.19 (s, 1H), 8.00 – 7.95 (m, 1H), 7.90 (d, J = 8.7 Hz, 2H), 7.88 – 7.84 (m, 1H), 7.50 (m, 2H), 7.36 – 7.30 (d, J = 8.7 Hz, 2H), 3.82 (s, 3H), 3.58 (s, 3H); ¹³C NMR (400 MHz, CDCl₃) δ 166.0, 163.2, 146.7, 135.8, 135.2, 133.5, 132.1, 131.1, 130.5, 128.8, 128.5, 127.1, 126.6, 126.1, 125.8, 123.1, 121.0, 108.2, 52.2, 37.8.



4-(3-bromo-N-methylnaphtho[2,3-b]thiophene-2-carboxamido)benzoic acid

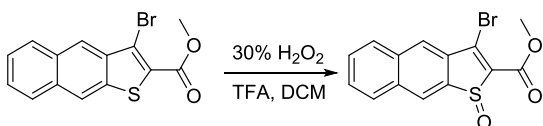
13b. The same ester demethylation procedure was adapted from previous literature⁸⁶. A solution of 1.00 g (2.20 mmol) of ester **13a** and 2.00 g (5.50 mmol) of trimethyl tin hydroxide in 40 mL of anhydrous dichloroethane was stirred at refluxing. The work up was same with the procedure for **11a**. The crude carboxylic acid **13b** was washed with water, triturated with hot methanol, and washed with cold methanol to give 0.87 g (90%) as a light yellow solid, mp > 300 °C. (The compound turned dark after this point.) HRMS (ESI/ IT-TOF) m/z: [M +H]⁺ Calcd for C₃₂H₂₃NO₅S₂ 439.9951; Found 439.9929. The spectra data were as follows: ¹H NMR (400 MHz, DMSO-*d*₆) δ 12.99 (s, 1H), 8.59 (s, 1H), 8.32 (s, 1H), 8.15 (m, 1H), 7.99 (m, 1H), 7.82 (d, *J* = 8.2 Hz, 2H), 7.57 (m, 2H), 7.48 (d, *J* = 8.2 Hz, 2H), 3.48 (s, 3H); ¹³C NMR (400 MHz, DMSO-*d*₆) δ 162.5, 146.5, 135.6, 135.0, 134.9, 132.0, 131.2, 130.5, 128.9, 127.6, 127.2, 126.8, 126.4, 122.7, 122.1, 107.4, 37.8.



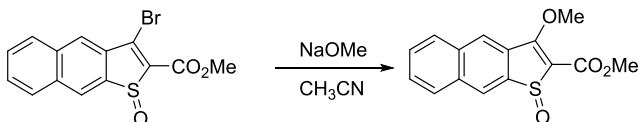
Preparation of methyl 3-bromonaphtho[2,3-b]thiophene-2-carboxylate **34**.

The mixture of 3.00 (9.80 mmol) of 3-bromonaphtho[2,3-b]thiophene-2-carboxylic acid in 250 mL of anhydrous methanol was added dropwise 3.56 mL (49.0 mmol) of thionyl chloride at 0 °C. The reaction was heated to refluxing and stirred for 24 h. After removal of the solvent, dichloromethane was added to the solid. The solution was washed with

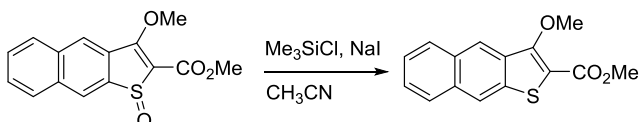
saturated NaHCO₃ aqueous solution, brine, and dried over Na₂SO₄. Concentration in vacuum gave 2.81 g (95%) of methyl 3-bromonaphtho[2,3-b]thiophene-2-carboxylate **34** as a brown solid, mp 147-149 °C. The spectral data were as follows: ¹H NMR (400 MHz, CDCl₃) δ 8.49 (s, 1H), 8.28 (s, 1H), 8.03 (m, 1H), 7.90 (m, 1H), 7.55 – 7.47 (m, 2H), 3.99 (s, 3H); ¹³C NMR (400 MHz, CDCl₃) δ 161.8, 137.3, 135.7, 133.9, 131.2, 128.9, 128.35, 127.1, 127.1, 125.8, 124.9, 121.0, 115.1, 52.8.



Preparation of methyl 3-bromonaphtho[2,3-b]thiophene-2-carboxylate 1-oxide 35. To a solution of 3.00 g (9.30 mmol) of methyl 3-bromonaphtho[2,3-b]thiophene-2-carboxylate in 30 mL of CH₂Cl₂ was added a mixture of 0.85 mL (8.4 mmol) of 30% H₂O₂ and 10 mL of trifluoroacetic acid at 5-10 °C with vigorous stirring. After being stirred at room temperature overnight, the reaction mixture was cautiously poured into saturated aqueous solution of NaHCO₃. The organic layer was separated, and the aqueous layer was extracted three times with 30 mL of CH₂Cl₂. The combined organic layer was washed with brine and dried with Na₂SO₄. Removal of the solvent in vacuum followed by column chromatography on silica gel, eluting with 10% ethyl acetate in hexane gave 2.75 g (88%) of methyl 3-bromonaphtho[2,3-b]thiophene-2-carboxylate 1-oxide **35** as a light yellow solid, mp 242-244 °C. HRMS (ESI/ IT-TOF) m/z: [M + H]⁺ Calcd for C₁₄H₉O₃SBr 336.9529; Found 336.9497. The spectral data were as follows: ¹H NMR (400 MHz, CDCl₃) δ 8.39 (s, 1H), 8.24 (s, 1H), 8.07 – 7.97 (m, 2H), 7.72-7.68 (m, 2H), 4.03 (s, 3H); ¹³C NMR (400 MHz, CDCl₃) δ 160.8, 139.2, 138.7, 137.9, 134.5, 134.4, 133.8, 129.6, 129.4, 129.1, 129.0, 128.0, 127.9, 53.1.

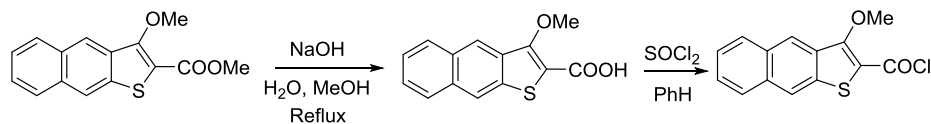


Preparation of methyl 3-methoxynaphtho[2,3-b]thiophene-2-carboxylate 1-oxide 36. To a solution of 4.86 g (14.4 mmol) methyl 3-bromonaphtho[2,3-b]thiophene-2-carboxylate 1-oxide in 20.0 mL of CH₃CN was added 1.94 g (36.0 mmol) of sodium methoxide under nitrogen. The reaction mixture was stirred at room temperature for 12 h. TLC was used to confirm the complete consumption of the starting material. The reaction mixture was diluted with 20.0 mL of water and extracted three times with CH₂Cl₂. The combined organic layers were washed with brine and dried over MgSO₄. Concentration in vacuo followed by column chromatography on silica gel, eluting with 20% ethyl acetate in hexane gave 1.05 g (26%) of methyl 3-methoxynaphtho[2,3-b]thiophene-2-carboxylate 1-oxide **36** as a yellow solid, mp 268-270 °C. HRMS (ESI/ IT-TOF) m/z: [M + H]⁺ Calcd for C₁₅H₁₂O₄S 289.0529; Found 289.0516. The spectra data were as follows: ¹H NMR (400 MHz, CDCl₃) δ 8.35 (s, 1H), 8.16 (s, 1H), 8.00 – 7.94 (m, 2H), 7.67 – 7.61 (m, 2H), 4.46 (s, 3H), 3.97 (s, 3H); ¹³C NMR (400 MHz, CDCl₃) δ 166.47, 161.97, 138.80, 134.62, 134.33, 131.35, 129.32, 129.05, 128.67, 128.57, 127.29, 124.39, 116.19, 63.25, 52.69.

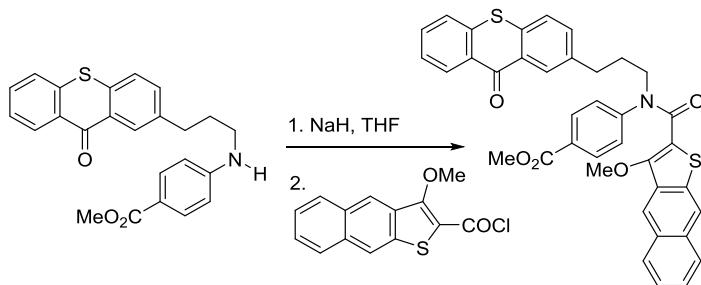


Preparation of methyl 3-methoxynaphtho[2,3-b]thiophene-2-carboxylate 37. To a stirred solution of 3-methoxynaphtho[2,3-b]thiophene-2-carboxylate 1-oxide (2.0 g, 6.8 mmol) and dry sodium iodide (2.03 g, 13.5 mmol) in 40 mL of dry acetonitrile was slowly added 1.70 mL (13.5 mmol) of chlorotrimethylsilane under Nitrogen. The reaction

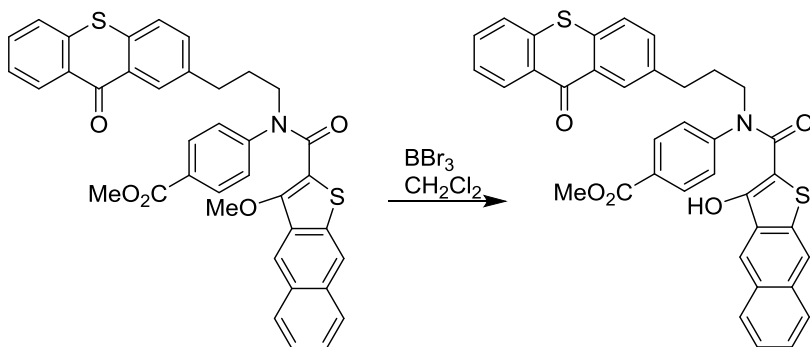
mixture was stirred at room temperature for 3 h. The reaction was quenched with 15 mL of water followed by addition of 60 mL of sodium thiosulfate aqueous solution (1M). The resulting mixture was extracted with CH₂Cl₂. The combined organic layers were washed with water, brine and dried over anhydrous sodium sulfate. Concentration in vacuo followed by recrystallization in methanol gave 0.98 g (53%) of methyl 3-methoxynaphtho[2,3-b]thiophene-2-carboxylate **37** as a light yellow solid, m.p. 178-180 °C. HRMS (ESI/ IT-TOF) m/z: [M + H]⁺ Calcd for C₁₅H₁₂O₃S 273.0580; Found 273.0568. The spectral data were as follows: ¹H NMR (400 MHz, CDCl₃) δ 8.43 (s, 1H), 8.24 (s, 1H), 8.01 (m, 1H), 7.90 (m, 1H), 7.57 – 7.44 (m, 2H), 4.25 (s, 3H); ¹³C NMR (400 MHz, CDCl₃) δ 162.2, 156.7, 134.6, 133.2, 132.9, 130.6, 128.8, 127.3, 126.7, 125.4, 122.2, 121.1, 115.3, 62.8, 52.3.



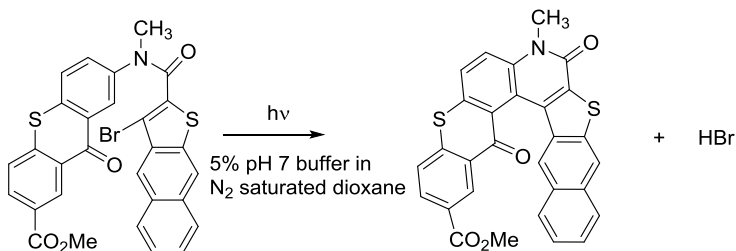
3-methoxynaphtho[2,3-b]thiophene-2-carbonyl chloride. The mixture of 0.50 g (1.8 mmol) methyl 3-methoxynaphtho[2,3-b]thiophene-2-carboxylate in 10 mL of 5% NaOH aqueous solution was refluxed overnight. The reaction was cooled to room temperature and acidified with concentrated HCl until pH 2. The resulting precipitate was filtered and dried to give the crude acid, which was refluxed with 2 mL of thionyl chloride in 10 mL of benzene for 4 h. The reaction mixture was concentrated in vacuum and further dried under vacuum pump to give 0.44 g (89%) of the acid chloride. The compound was used in the next step to couple with the tethered aniline **33**.



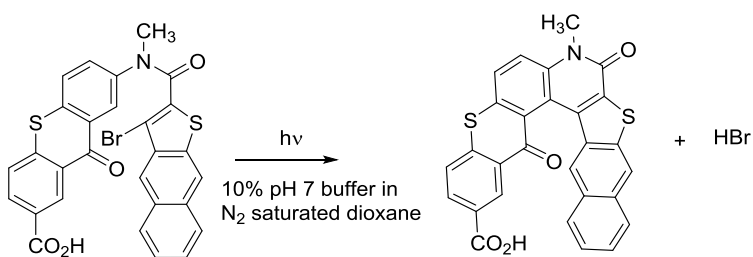
Methyl 4-(3-methoxy-N-(3-(9-oxo-9H-thioxanthen-2-yl)propyl)naphtho[2,3-b]thiophene-2-carboxamido)benzoate 40. To a solution of 0.50 g (1.2 mmol) of the tethered aniline **33** in 15 mL of anhydrous THF was added 0.10 g (2.5 mmol) of NaH (60%) under nitrogen atmosphere. The mixture was stirred for 30 min before 0.38 g (1.4 mmol) of the acid chloride **39** was added slowly. TLC was used to confirm the completion of the reaction after stirring overnight. The reaction mixture was then diluted with 20 mL of dichloromethane and filtered. Concentration of the filtrate in vacuo followed by column chromatography on silica gel, eluting with dichloromethane and then with 5% of Et₂O in dichloromethane gave 0.52 g (65 %) of pure caged compound **40** as a colorless solid, 195-196 °C. HRMS (ESI/ IT-TOF) m/z: [M+H]⁺ Calcd for C₃₈H₂₉NO₅S₂ 644.1560; Found 644.1569. The spectra data were as follows: ¹H NMR (400 MHz, CDCl₃) δ 8.61 (dd, *J* = 8.1, 1.5, 1H), 8.15 (s, 0H), 8.06 (s, 1H), 7.92 (d, *J* = 8.7 Hz, 1H), 7.90 – 7.87 (m, 1H), 7.80 (dd, *J* = 7.9, 1.7 Hz, 1H), 7.64 – 7.54 (m, 2H), 7.51 – 7.41 (m, 5H), 4.11 (s, 3H), 4.07 – 4.01 (m, 2H), 3.83 (s, 3H), 2.86 – 2.78 (m, 2H), 2.13 – 2.00 (m, 2H).



Preparation of methyl 4-(3-hydroxy-N-(3-(9-oxo-9H-thioxanthen-2-yl)propyl)naphtho[2,3-b]thiophene-2-carboxamido)benzoate **41.** To a solution of 1.50 g (2.40 mmol) of methoxy compound **40** in 30 mL of dichloromethane in a dry ice and acetone bath was slowly added a solution of 5.00 mL (5.00 mmol) of BBr₃ (1 M) in dichloromethane. The reaction mixture was stirred for 2 h and then slowly warmed to room temperature and stirred for 1 h. The reaction mixture was quenched by addition of 50 mL of water. The aqueous layer was separated and extracted three times with dichloromethane. The combined extracts were washed with saturated NaCl and dried over anhydrous MgSO₄. After removal of the solvent in vacuo, the crude solid was triturated with hot ethanol to obtain 1.17 g (78%) of compound **41** as a light-yellow solid, mp 202-204 °C. HRMS (ESI/ IT-TOF) m/z: [M + H]⁺ Calcd for C₃₇H₂₇NO₅S₂ 630.1403; Found 630.1407. ¹H NMR (300 MHz, CDCl₃) δ 13.31 (s, 1H), 8.61 (dd, *J* = 8.2, 1.2 Hz, 1H), 8.47 (s, 1H), 8.42 (d, *J* = 1.2 Hz, 1H), 8.18 (d, *J* = 8.5 Hz, 1H), 8.00 – 7.94 (m, 1H), 7.89 (s, 1H), 7.82 – 7.72 (m, 1H), 7.64 – 7.53 (m, 2H), 7.53 – 7.41 (m, 7H), 3.99 (m, 5H), 2.90 – 2.82 (m, 2H), 2.15 – 2.03 (m, 2H); ¹³C NMR (300 MHz, CDCl₃) δ ¹³C NMR (75 MHz, CDCl₃) δ 179.9, 167.4, 166.2, 162.4, 144.0, 139.6, 137.3, 135.3, 134.9, 133.6, 132.8, 132.2, 131.2, 131.0, 130.4, 130.1, 129.9, 129.5, 129.2, 129.1, 129.0, 129.0, 127.2, 126.7, 126.2, 126.2, 126.0, 125.2, 122.3, 120.2, 101.7, 52.5, 50.5, 32.9, 29.1.

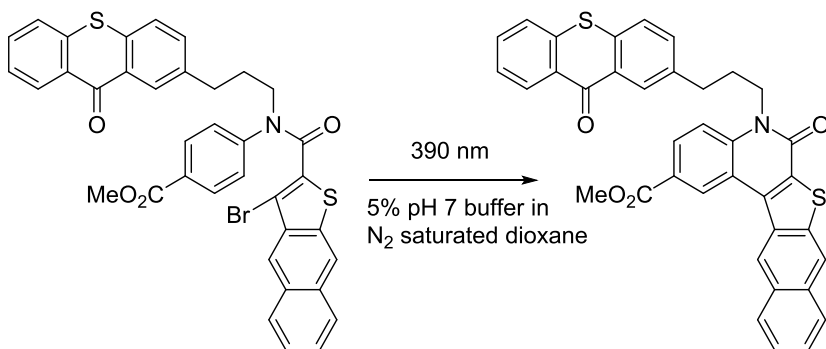


Photosynthesis of compound 43a. A solution of 0.25 mg (0.42 mmol, 5.3×10^{-3} M) of **11a** in 80 mL of 5% pH 7 buffer in N_2 saturated dioxane was irradiated with a 450 W Hanovia medium pressure mercury lamp with a Pyrex filter for 8 h. The solution was then concentrated in vacuo and the solid product was washed with water. The product was chromatographed on a silica gel (60-200 mesh) column eluting with 5% ether in dichloromethane to give 0.21 mg (99 %) of photoproduct **43a** as a yellow powder, mp > 350 °C. (Yellow compound turned dark at this point.) The spectra data were as follows: ^1H NMR (400 MHz, CDCl_3) δ 8.92 (d, $J = 1.9$ Hz, 1H), 8.49 (s, 1H), 8.40 (dd, $J = 8.4$, 1.9 Hz, 1H), 8.26 (s, 1H), 7.97 (d, $J = 8.4$ Hz, 1H), 7.88 (d, $J = 9.0$ Hz, 1H), 7.83 (d, $J = 8.4$ Hz, 1H), 7.77 (d, $J = 9.0$ Hz, 1H), 7.66 (d, $J = 8.4$ Hz, 1H), 7.56 (dd, $J = 7.5$ Hz, 1H), 7.41 (dd, $J = 7.5$ Hz, 1H), 4.00 (s, 3H), 3.94 (s, 3H); The solubility of the photoproduct was poor to give a decent carbon NMR.



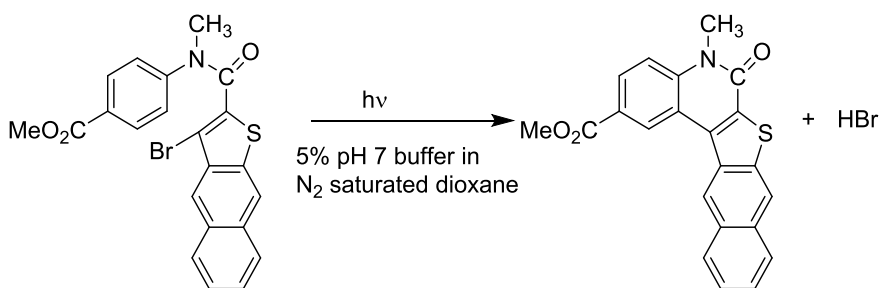
Photosynthesis of compound 43b. A solution of 0.18 mg (0.36 mmol, 3.6×10^{-3} M) of **11b** in 100 mL of 10% pH 7 buffer in N_2 saturated dioxane was irradiated with a 450 W Hanovia medium pressure mercury lamp with a Pyrex filter for 8 h. 0.5 mL of 1 N HCl was added to the reaction mixture. The solution was concentrated in vacuo until ca.

20 mL of solvent left. The precipitate was collected by filtration. The photoproduct was washed with dioxane and water before dried in vacuum to give 0.17 mg (97%) of photoproduct **43b** as a bright-yellow powder, mp > 350 °C. HRMS (ESI/ IT-TOF) m/z: [M + H]⁺ Calcd for C₂₈H₁₅NO₄S₂ 494.0515; Found 494.0480. The spectra data were as follows: ¹H NMR (400 MHz, DMSO-*d*₆) δ 13.39 (br, 1H), 8.76 (s, 1H), 8.60 (d, *J* = 1.9 Hz, 1H), 8.33 (dd, *J* = 8.4, 1.9 Hz, 1H), 8.25 (s, 1H), 8.22 (d, *J* = 9.0 Hz, 1H), 8.15 (d, *J* = 8.4, 1H), 8.12 (d, *J* = 9.0, 1H), 8.07 (d, *J* = 8.4 Hz, 1H), 7.66 (d, *J* = 8.3 Hz, 1H), 7.64 – 7.58 (dd, *J* = 8.4, 7.6 Hz, 1H), 7.45 (dd, *J* = 8.3, 7.6 Hz, 1H), 3.94 (s, 3H); ¹³C NMR (75 MHz, DMSO-*d*₆) δ 182.1, 167.0, 157.7, 140.1, 139.0, 137.6, 135.7, 135.7, 134.9, 132.8, 132.4, 132.1, 131.7, 130.5, 130.0, 129.1, 127.9, 127.7, 127.5, 127.3, 127.1, 126.3, 125.7, 122.1, 115.6, 31.0.



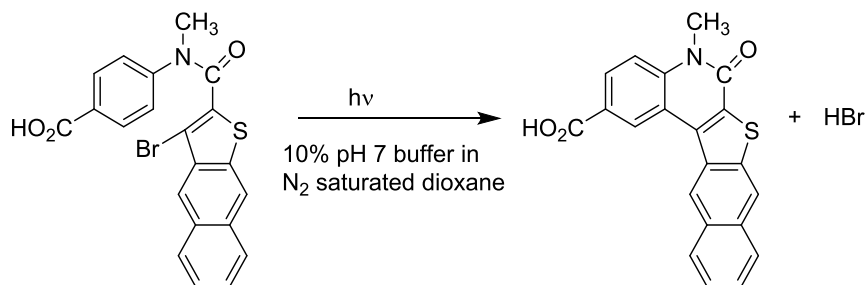
Photosynthesis of compound 46a. A solution of 0.30 mg (0.43 mmol, 4.3×10^{-3} M) of **11a** in 100 mL of 5% pH 7 buffer in N₂ saturated dioxane was irradiated with a 450 W Hanovia medium pressure mercury lamp with a Pyrex filter for 5 h. The solution was then concentrated in vacuo and the solid product was washed with water. The product was chromatographed on a silica gel (60-200 mesh) column eluting with dichloromethane and then 5% ether in dichloromethane to give 0.26 mg (97 %) of photoproduct **46a** as a light yellow powder, mp 255-256 °C. HRMS (ESI/ IT-TOF) m/z:

$[M + H]^+$ Calcd for $C_{37}H_{25}NO_4S_2$ 612.1298; Found 612.1332. The spectra data were as follows: 1H NMR (400 MHz, $CDCl_3$) δ 9.18 (d, $J = 1.8$ Hz, 1H), 8.83 (s, 1H), 8.48 (dd, $J = 8.1, 1.5$ Hz, 1H), 8.30 (d, $J = 1.8$ Hz, 1H), 8.23 (s, 1H), 8.07 (dd, $J = 8.9, 1.8$ Hz, 1H), 7.95 (d, $J = 8.1$ Hz, 1H), 7.80 (d, $J = 8.1$ Hz, 1H), 7.55 – 7.43 (m, 3H), 7.38 (m, 2H), 7.35 – 7.28 (m, 3H), 4.44 (t, $J = 7.3$ Hz, 2H), 3.99 (s, 3H), 2.93 (t, $J = 7.3$ Hz, 2H), 2.23 (p, $J = 7.3$ Hz, 2H); ^{13}C NMR (101 MHz, $CDCl_3$) δ 179.5, 166.2, 158.1, 140.2, 139.0, 138.9, 137.1, 134.7, 134.4, 134.4, 132.6, 132.0, 131.8, 130.9, 129.7, 129.2, 129.2, 128.9, 128.8, 128.5, 127.0, 126.8, 126.0, 125.9, 125.9, 125.8, 125.5, 124.9, 123.9, 121.6, 118.8, 115.1, 52.4, 42.3, 32.7, 27.8.



Photosynthesis of compound 46a. A solution of 0.24 mg (0.52 mmol, $5.2 \times 10^{-3} M$) of **13a** in 100 mL of 5% pH 7 buffer in N_2 saturated dioxane was irradiated with a 450 W Hanovia medium pressure mercury lamp with a Pyrex filter for 5 h. The solution was then concentrated in vacuo and the solid product was washed with water. The product was chromatographed on a silica gel (60-200 mesh) column eluting with dichloromethane and then 5% ether in dichloromethane to give 0.19 mg (97 %) of photoproduct **46a** as a light-yellow solid, mp > 300 °C. The spectra were as follows: 1H NMR (300 MHz, $CDCl_3$) δ 9.57 (d, $J = 1.9$ Hz, 1H), 9.27 (s, 1H), 8.50 (s, 1H), 8.27 (dd,

$J = 8.9, 1.9$ Hz, 1H), 8.24 – 8.14 (m, 1H), 8.02 – 7.92 (m, 1H), 7.68 – 7.53 (m, 3H), 4.08 (s, 3H), 3.94 (s, 3H); Solubility was poor to take ^{13}C NMR.



Photosynthesis of compound 46b. A solution of 0.19 mg (0.43 mmol, 5.31×10^{-3} M) of **13a** in 80 mL of 10% pH 7 buffer in N_2 saturated dioxane was irradiated with a 450 W Hanovia medium pressure mercury lamp with a Pyrex filter for 5 h. The work up was followed as with compound **43b**. The photoproduct was washed with dioxane and water before dried in vacuum to give 0.15 mg (97%) of photoproduct **46b** as a bright-yellow solid, mp > 310 °C. HRMS (ESI/ IT-TOF) m/z: $[\text{M} + \text{H}]^+$ Calcd for $\text{C}_{21}\text{H}_{13}\text{NO}_3\text{S}$ 360.0689; Found 360.0651. The spectra were as follows: ^1H NMR (400 MHz, $\text{DMSO}-d_6$) δ 9.30 (s, 1H), 9.09 (s, 1H), 8.62 (s, 1H), 8.12 (d, $J = 8.9$ Hz, 2H), 7.98 (d, $J = 8.1$ Hz, 1H), 7.74 (d, $J = 8.9$ Hz, 1H), 7.66 – 7.52 (m, 2H), 3.78 (s, 3H); Solubility was poor to take ^{13}C NMR.

CHAPTER 3.

PHOTOCHEMISTRY OF THE SYSTEM INVOLVING THIOXANTHONE AND NAPHTHOTHIOPHENE-2-CARBOXAMIDE

3.1. Introduction.

In this chapter, we continue to study the photochemistry of three caged compounds synthesized in chapter 2 (Figure 2.1): (1) the thioxanthone chromophore is

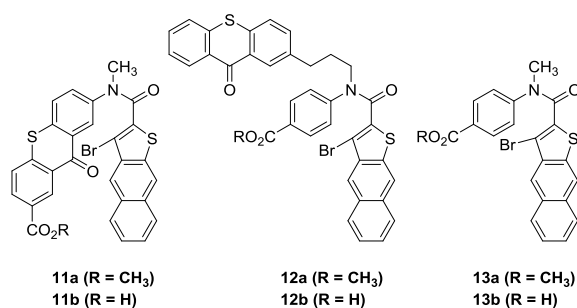


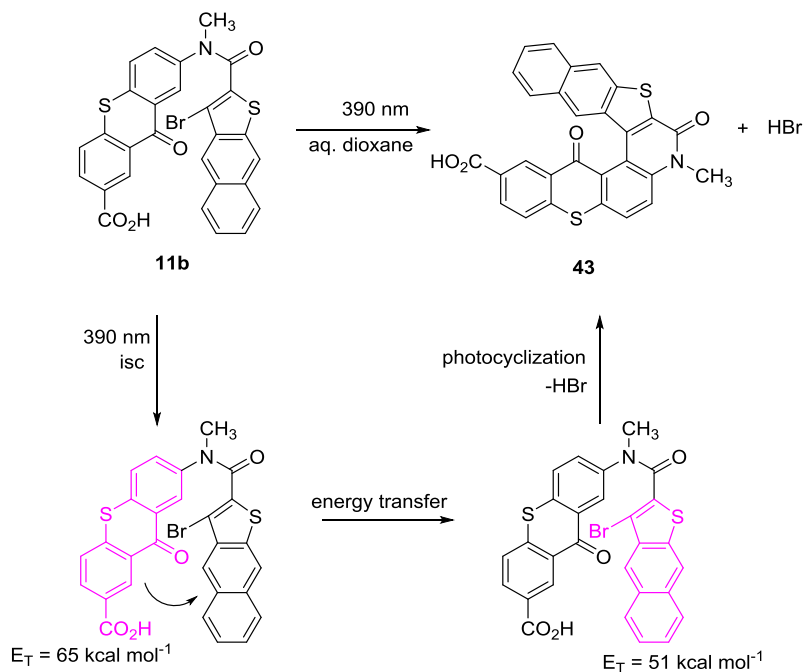
Figure 2.1. Three cases under study.

directly attached to the naphthothiophene-2-carboxamide at the amide nitrogen (compound **11**), (2) the thioxanthone chromophore is tethered to the amide nitrogen via a trimethylene linkage (compound **12**), and (3) the thioxanthone bimolecularly sensitizes the photochemistry of the naphthothiophene-2-carboxamide **13**. These studies include quantum yields of photolysis of **11**, **12** and **13**, determination of rate constants and lifetimes through quenching experiments for both photolysis of **12a** and **13a**. The analysis of the corresponding Stern-Volmer plots from both experiments give similar triplet lifetime for the anilide moiety. Relative high quantum yield has been observed for the trimethylene-linked system **12a** compared to that of direct-linked system **11**. This provides us with possibilities to expel more basic leaving group such as carboxylate and hydroxide.

3.2. Results

3.2.1. Quantum Yields.

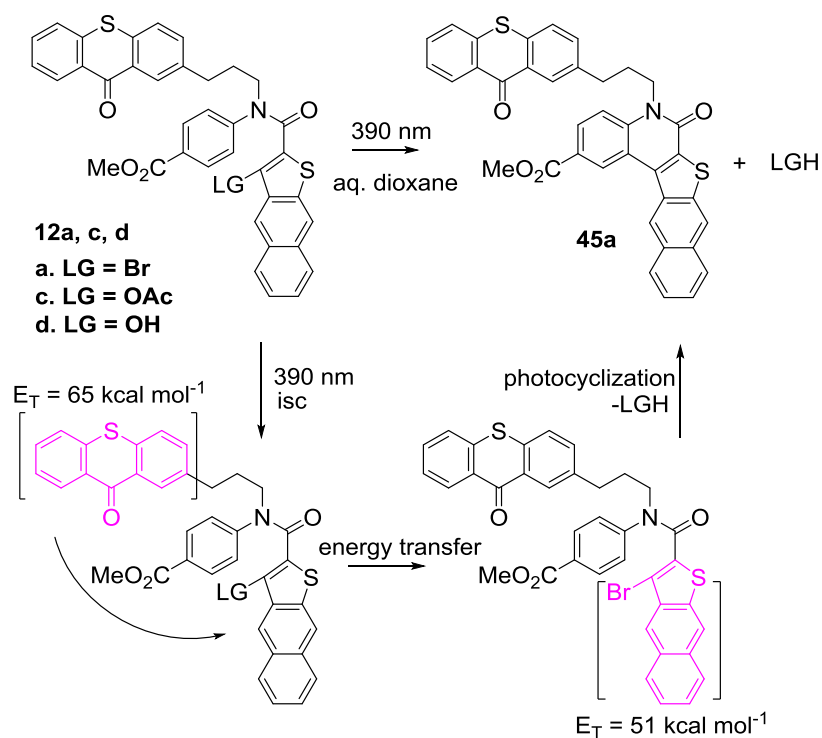
In the case where the thioxanthone chromophore is directly attached to the naphthothiophene-2-carboxamide at the amide nitrogen (Scheme 3.1), the quantum yield for direct photolysis of **11** at 390 nm in dioxane containing 20% water with 100 mM phosphate buffer at pH 7 is 0.07.



Scheme 3.1. Photolysis of **11b**.

Upon irradiation, thioxanthone absorbs light and gets excited to its singlet state which undergoes intersystem crossing to its triplet state. (Scheme 3.1). Triplet energy transfer from thioxanthone chromophore to the naphthothiophene gives the triplet naphthothiophene, which undergoes photocyclization to expel Br^- as a leaving group along with the deprotonation.

For the system where thioxanthone and the naphthothiophene-2-carboxamide are connected via a trimethylene linker, the photolysis was conducted under same condition with **11**. Upon the irradiation, exothermic triplet energy transfer from thioxanthone to naphthothiophene moiety results in the photocyclization of the **11** to form photoproduct **45a** with the expulsion of leaving groups (OH^- , OAc^- and Br^-).

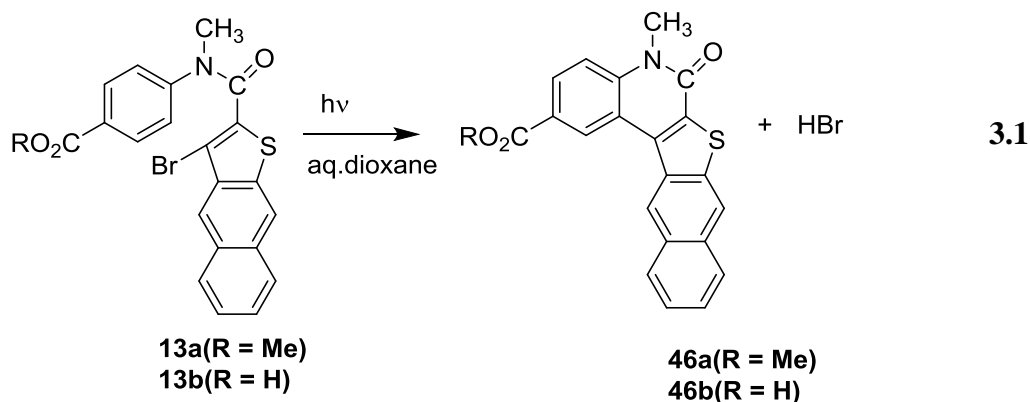


Scheme 3.2. Photolysis of **12** with various leaving groups.

Quantum yields for trimethylene linked thioxanthone – naphthothiophenes **12a** and **d** are 0.13 and 0.004, respectively. An important point is that the quantum yield for **12a** is double that found for **11b**, where $\Phi = 0.070$.

In addition, the quantum yields for photolysis of **12a** at 390 nm under same solvent condition is essentially identical to **13a, b**, which has $\Phi = 0.13$ and 0.15,

respectively (eq. 3.1), despite the fact that the former photoreactivity requires a triplet excitation transfer step from the thioxanthone to the naphthothiophene moiety.



Naphthothiophene absorbs strongly at 361 nm to produce a singlet excited state which intersystem crosses to give the triplet state. The triplet anilide cyclizes to expel HBr. Further quenching studies with the known triplet quencher ferrocene on **12a** and **13a** confirm that the triplet excited state is responsible for the photochemistry.

3.2.2. Quenching Studies.

3.2.2.1. Quenching of photolysis of compound **12a** with ferrocene.

Quenching studies were performed to establish whether the photochemistry of **12a** ($E_T = \text{ca. } 51 \text{ kcal mol}^{-1}$ in protic solvent⁶) indeed occurred primarily in the triplet excited state. The photochemistry was not quenched by 1,2-diphenyl-1-propene. However, when ferrocene ($E_T = 43 \text{ kcal mol}^{-1}$ ⁸⁷) was used, the Stern-Volmer plot (Figure 3.1) was obtained.

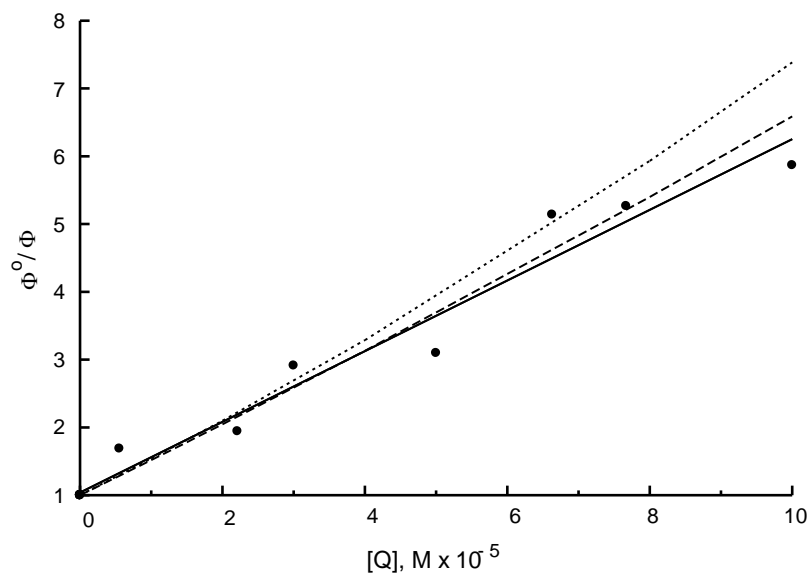
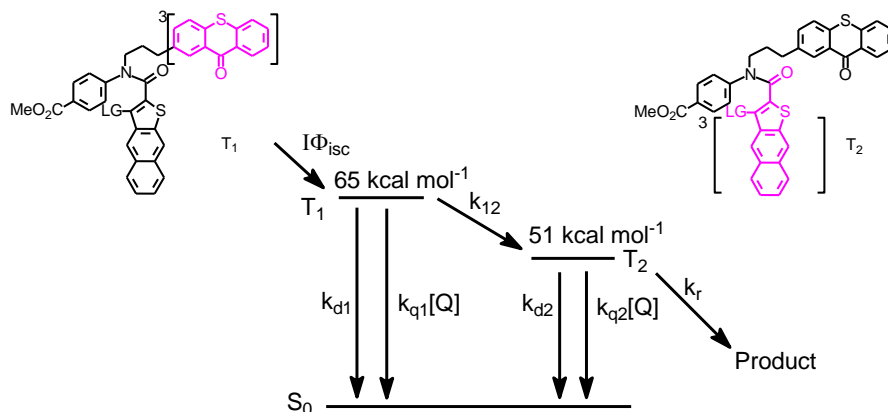


Figure 3.1. Stern-Volmer plot for quenching of the photochemistry of **12a** by ferrocene. Fit of the data to a line (—), calculated curves (eq. 3.2) for $\tau_1 = 200$ ns (- - -) or $\tau_1 = 500$ ns (·····) using $\tau_2 = 11.5$ μ s.

The quenching of **12a** by ferrocene can be analyzed within the context of Scheme 8. Most of the photochemistry is expected to involve initial excitation of the thioxanthone, which undergoes intersystem crossing with $\Phi_{isc} = 0.68^{88}$. Triplet excitation transfer from thioxanthone triplet donor (T_1) to the lower energy triplet excited state of the naphthothiophene (T_2) would lead to the observed photochemistry.



If both T_1 and T_2 are quenched by the ferrocene, the Stern-Volmer plot should exhibit quadratic behavior that follows eq.3.2. However, the quadratic behavior in the quenching data in Figure 3.1 is practically imperceptible. The reason for this is likely due to experimental error that results in significant scatter of the data. Furthermore, the very likely short-lifetime for T_1 must also be considered. The lifetime τ_1 of T_1 will very likely be shortened by the rapid rate of highly exothermic triplet energy transfer to give T_2 , which is estimated to lie ca. 13 kcal mol⁻¹ below T_1 . If the $k_{q1}\tau_1$ term in eq. 3.2 is very small, negligible as compared to $k_{q2}\tau_2$, the plot will appear to be essentially linear with slope $k_{q2}\tau_2$.

$$\frac{\Phi^\circ}{\Phi} = (1 + k_{q1}\tau_1[Q])(1 + k_{q2}\tau_2[Q]) \quad 3.2$$

In other words, the Stern-Volmer plot will reflect primarily quenching of the longer lived excited state T_2 , i.e., the excited state localized on the naphthothiothiophene-2-carboxanilide. A simple linear fit of the data gave a slope = $5.05 \times 10^4 \text{ M}^{-1}$ ($R^2 = 0.9750$). That slope represents the lifetime for T_2 , which is 11.5 μs taking $k_q = 4.4 \times 10^9 \text{ M}^{-1} \text{ s}^{-1}$. The k_{q1} and k_{q2} values of $4.4 \times 10^9 \text{ M}^{-1} \text{ s}^{-1}$ can be estimated from the Debye equation using the

viscosity of 20% H₂O and 80% dioxane reported in the literature.⁸⁹ For purposes of illustration in Figure 3.1, we also show the calculated curve that results from eq. 3.2 for arbitrary values for $\tau_1 = 200$ ns or 500 ns using $\tau_2 = 11.5$ μ s, latter of which corresponds to the slope from the linear fit of the data. Due to the scatter in the data, we were unable to perform a quadratic fit of the data without using a negative $k_q\tau$ value as an adjustable parameter in eq. 3.2.

It should be noted that the long-lived component with $\tau_2 = 11.5$ μ s corresponds closely to the triplet excited state lifetime of the naphthothiophene-2-carboxanilide **13a**. The lifetime for **13a** of $\tau_2' = 11.1$ μ s is obtained from the slope of the Stern-Volmer plot using ferrocene as the quencher ((Figure 3.1).

3.2.2.2. Queching of anilide **13a** with ferrocene.

Quenching experiment with ferrocene was conducted on **13a** to give a Stern-Volmer plot. (Figure 3.2)

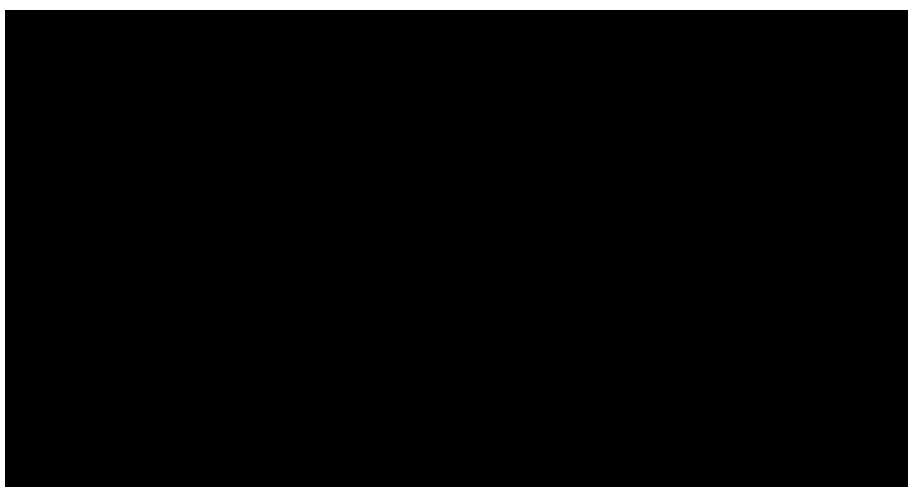


Figure 3.2. Stern-Volmer plot for quenching of the photochemistry of **13a** by ferrocene.

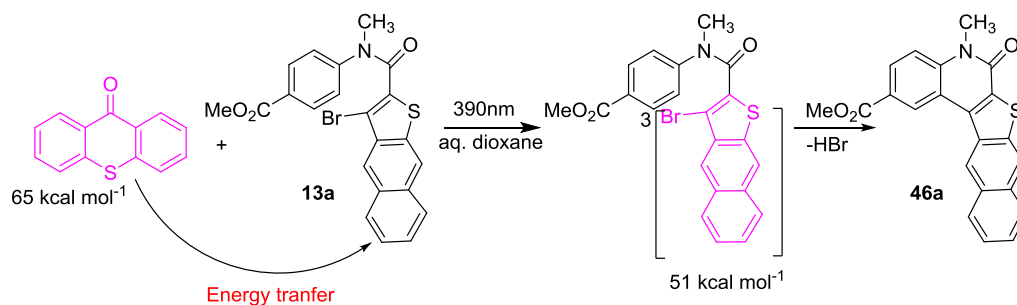
The Stern-Volmer slope for quenching by ferrocene was $k_q\tau_2 = 4.87 \times 10^4 \text{ M}^{-1}$. Taking $k_q = 4.4 \times 10^9 \text{ M}^{-1} \text{ s}^{-1}$ in aq dioxane, the triplet lifetime is $\tau_2 = 11.1 \text{ }\mu\text{s}$. This lifetime for the triplet excited state of anilide **13a** is very similar to the lifetime of $11.5 \text{ }\mu\text{s}$ previously calculated from quenching of the compound **12a**.

3.2.2.3. Quenching of photolysis of compound **12a** with *trans*-1,2-diphenylpropene.

A quenching study with *trans*-1,2-diphenylpropene ($50 - 51 \text{ kcal mol}^{-1}$ ⁹⁰) as the triplet excited state quencher was attempted with trimethylene – linked thioxanthone compound **12a**. Quenching of the photoreaction was not detectable by any decrease in quantum yields for product formation with $1.00 \times 10^{-3} \text{ M}$ *trans*-1,2-diphenylpropene. Evidently the inability to quench would likely be due to a low quenching rate of the quencher resulting from its triplet excited state energy not being low enough for the quenching process to be exothermic.

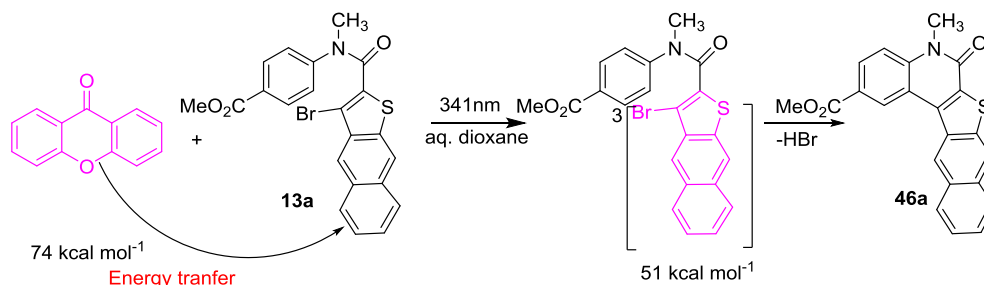
3.2.3. Intermolecular sensitized photolysis with thioxanthone as the sensitizer.

The thioxanthone sensitized photolysis of 0.0060 M **13a** gave $\Phi = 0.13$ in dioxane with 17% water containing 100 mM buffer at pH 7 (Scheme 3.4). The concentration of thioxanthone of 0.020 M was sufficiently high to absorb $> 99\%$ of the incident light. The quenching of thioxanthone should be completely efficient at the concentration of quencher used, given the long lifetime of $13.3 \text{ }\mu\text{s}$ of the sensitizer. Thus, the intermolecular triplet energy transfer to **13a** from the initially excited thioxanthone gives the same quantum yield for product as the case when the energy transfer is intramolecular with **12a**. The photochemistry of anilide **13a** is important since it resembles the moiety that accepts the triplet energy in compound **12a**.



Scheme 3.3. Intermolecular sensitized photolysis of thioxanthone with naphthothiophene-2-carboxanilide **13a**.

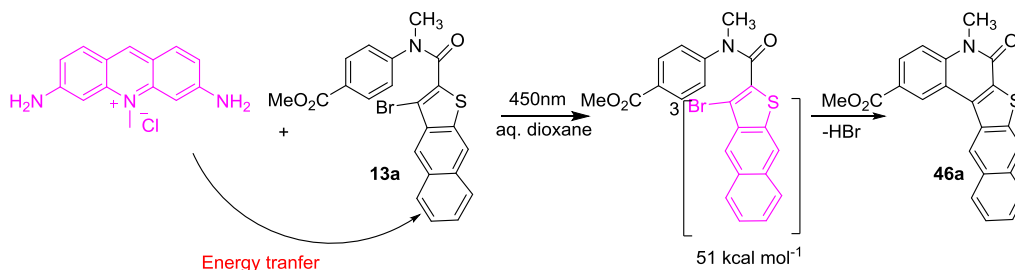
3.2.4. Intermolecular Sensitized Photolysis with xanthone as the sensitizer.



Scheme 3.4. Intermolecular sensitized photolysis of xanthone and anilide **13a**.

A xanthone sensitized photolysis was also performed (Scheme 3.5). The quantum yield $\Phi_{isc} = 1.0$ for xanthone, while $\Phi_{isc} = 0.68$ for thioxanthone. Thus, a higher quantum yield for sensitized photolysis was expected for xanthone. The sensitized photolysis of 6.0×10^{-4} M naphthothiophene-2-carboxanilide **13a** with xanthone ($E_T = 74$ kcal/mol⁹¹) gave $\Phi = 0.14$ after correction for the 8% of the light that was absorbed directly by **13a**. Absorption spectroscopy showed that the sensitizer and **13a** absorb light at the same wavelength of 341 nm. Therefore, the concentration of the sensitizer of 5.0×10^{-3} M was chosen to absorb 92% of the light. The need for a correction for light absorbed means the experimental error in the quantum yield will be much greater than for the thioxanthone sensitized photolysis

3.2.5. Intermolecular Sensitized Photolysis with acriflavine as the sensitizer.



Scheme 3.5. Intermolecular sensitized photolysis of acriflavine and anilide **13a**.

Anilide **13a** allows the use of sensitizers that absorb at substantially longer wavelengths than thioxanthone. One such sensitizer would be acriflavine, which has $\lambda_{\text{max}} = 440\text{-}450\text{ nm}$ (ϵ $2.40 - 3.00 \times 10^4\text{ M}^{-1}\text{ cm}^{-1}$ ^{7,92}). Its triplet excited state energy ($E_{\text{T}} = 51\text{ kcal mol}^{-1}$) is similar to **13a**, and its triplet lifetime is exceptionally long at $150\text{ }\mu\text{s}$. The chief defect with acriflavine is its somewhat low triplet yield, $\Phi_{\text{isc}} = 0.16$.

With $1.00 \times 10^{-3}\text{ M}$ acriflavine and $1.20 \times 10^{-3}\text{ M}$ anilide **13a** photolysis at 450 nm produced photoproduct **46a** with 5% conversion indicated by $^1\text{H NMR}$ spectroscopy. Considering the long lifetime for the triplet excited state of acriflavine, the concentration of anilide quencher is sufficient to completely quench the acriflavine triplet excited state, provided that $k_{\text{q}} > \text{ca. } 10^7\text{ M}^{-1}\text{ s}^{-1}$. Normally $k_{\text{q}} = 10^9 - 10^{10}\text{ M}^{-1}\text{ s}^{-1}$ when quenching is diffusion controlled, which would be true if the triplet energy transfer is at 4 kcal mol^{-1} exothermic.⁹³ In the present case the magnitude of k_{q} will be much less given the similar triplet energies of sensitizer and the quencher. In addition, it seems possible that a contributing factor for the relative low efficiency could be the rather low Φ_{isc} ⁹⁴ for acriflavine.

3.3. Discussion

The photochemistry of **11** – **13** occurs in the triplet excited state. This was established by the ease of quenching of the photoreactivity **12a** and anilide **13a** by the triplet quencher,⁸⁷ ferrocene. In addition, the photoreactivity of benzothiophenes **1**,¹ **5**,² and **7**³⁷ was also readily quenched, in those cases by cyclohexadiene as the triplet quencher. Computational studies of the photochemistry of **5** show that electrocyclic ring closure of **5** requires an initial triplet excitation transfer from the initial triplet excited state of the thioxanthone to generate the triplet excited state localized on the benzothiophene ring system. Subsequent electrocyclization generates a triplet biradical intermediate, which converts to a lower energy singlet biradical that spontaneously gives closed shell product. Intermediate **2** should be viewed as a singlet biradical that has zwitterionic character.¹

Most of the photoreactivity of trimethylene – linked thioxanthone **12a** involves initial excitation of thioxanthone, which intersystem crosses to give a triplet excited state with $\Phi_{isc} = 0.68$.³ Prior to electrocyclization, triplet energy transfer is required to produce the triplet excited state of the naphthothiophene. The electrocyclization is expected to give an intermediate with zwitterionic character. Expulsion of the leaving group with loss of a proton would then furnish **46a** as the photoproduct. The overall quantum yield for the sequence of steps is $\Phi = 0.13$.

The quantum yield for **12a** can be compared to $\Phi = 0.13$ for thioxanthone sensitized photolysis, for which the triplet energy transfer is intermolecular. The overall quantum yield can be considered the product of the efficiencies for the three steps that are involved, i.e., $\Phi = \Phi_{isc} \Phi_{et} \Phi_r$ where Φ_{isc} is the intersystem crossing efficiency, Φ_{et} is the

energy transfer efficiency, and Φ_r is the efficiency for the ensuing reaction. It is reasonable that $\Phi_{et} \approx 1$ for the intermolecular energy transfer process, because of its exothermicity. Given $\Phi_{isc} = 0.68$, then the calculated $\Phi_r \approx 0.19$.

The value for $\Phi_r = 0.19$ may also be applicable to the tethered compound **12a** which has $\Phi = 0.13$. Given that $\Phi_{isc} = 0.68$, the tethered compounds undergo completely efficient triplet excitation transfer.

In addition, for **13a** $\Phi = 0.13$ for direct photolysis. According to the quenching studies, the triplet excited state is involved in this photoreaction. If $\Phi_r = 0.19$, then one can calculate that $\Phi_{isc} = 0.68$. A similar value must hold for the direct photolysis of **12a**. Triplet yields of this magnitude are not unreasonable, considering that the heavy atom, Br, present as the leaving group will promote intersystem crossing. With no bromide present, values for Φ_{isc} are 0.66 for anthracene and 0.80 for naphthalene, both for polar solvent.³⁸

The Φ_r obtained above can also be compared to that obtained from xanthone sensitized photolysis of acid **13b**, where $\Phi_{isc} = 1.0$. Xanthone has $E_T = 74 \text{ kcal mol}^{-1}$, which would make the energy transfer highly exothermic such that $\Phi_{et} = 1.0$. Moreover, the long lifetime $\tau = 17.9 \text{ } \mu\text{s}$ in polar solvent³⁸ means that relatively low concentrations of anilide quencher can completely quench the triplet excited state of xanthone. The fact that xanthone and anilide absorb at similar wavelengths in the 340 nm region meant that the relative concentrations of the two had to be adjusted to insure that the sensitizer absorbed most of the incident light, which in this case was 92%, thus necessitating a correction for the 8% of the light absorbed by the anilide. From the observed sensitized quantum yield of 0.14, $\Phi_r = 0.14$ is calculated. The difference in the calculated Φ_r for

13b for the xanthone sensitized photolysis vs. the thioxanthone intra- or intermolecular sensitized photolyses may be attributable to experimental error, which is larger for the xanthone sensitization.

The exothermic energy transfer from triplet thioxanthone to generate the naphthothiophene-2-carboxanilide triplet excited state should be quite fast. This is borne out by the quenching with ferrocene, which gives an approximately linear Stern-Volmer plot with slope that is essentially identical to that for quenching of anilide **13a**. Such energy transfer will of course shorten the lifetime of the thioxanthone component in **12a**, and in the limit, if that lifetime τ_1 were negligible, the Figure 3 quenching would appear to be essentially linear. However, for purposes of discussion, if $\tau_1 = 500$ ns, the plot shown in Figure 3 would perhaps show some perceptible quadratic curvature.

Considering that the intrinsic lifetime of triplet thioxanthone is 13.3 μs ($k_d = 7.7 \times 10^4 \text{ s}^{-1}$), such a 500 ns lifetime would correspond to a $k_{12} = 1.92 \times 10^6 \text{ s}^{-1}$ for the energy transfer step. The efficiency Φ_{et} would be nearly unity in that case. It seems likely that the rate constant k_{12} would be even larger than that for exothermic energy transfer, since rate constants of 10^8 to 10^9 s^{-1} have been established for bichromophoric systems with flexible tethers of < 5 atoms separating the chromophores.⁹⁵ This would suggest that $\tau_1 < 10$ ns would not be unlikely.

In the studies of tethered bichromophoric systems considerable evidence supports through-bond energy transfer as the primary mechanism the triplet energy transfer for relatively short tethers of four or fewer atoms.⁹⁵ For longer flexible tethers up to 14 atoms that have been studied, the rate constants for energy transfer remain remarkably high and do not fall below 10^8 s^{-1} . In these latter examples a through space interaction

predominates for the energy transfer. The orientation of the chromophores relative to the spacer bond may play a role in the shorter tethers, which in part might explain the much lower efficiencies observed when thioxanthone is attached to the carboxamide nitrogen in **11**. There may also be an adverse substituent effect that discourages electrocyclization of the thioxanthone and naphthothiophene rings.

The above points however are belied by the fact that with a 4-benzoyl group attached to the anilide phenyl group the overall quantum yield is $\Phi = 0.15$.¹ Swapping a thioxanthone chromophore in place of the 4-benzoylphenyl group would mean Φ_{isc} becomes 0.68, dropping Φ to 0.1. E_T would decrease from ca. 69 kcal mol⁻¹ to 65 kcal mol⁻¹, which would lower the rate constant for energy transfer and potentially decrease the overall efficiency. Assuming any geometrical requirements are similar, the further decrease in Φ to ca. 0.06 with thioxanthone might be attributable to a substituent effect, which has yet to be experimentally delineated.

3.4. Conclusions.

For **11b** $\Phi = 0.070$ where the thioxanthone chromophore is attached directly to nitrogen of the naphthothiophene-2-carboxamide. Despite the 14 kcal mol⁻¹ exothermic triplet energy transfer from chromophoric group to the lower energy naphthothiophene triplet excited state energy acceptor, there is only a two-fold improvement in efficiency as compared to the analogous benzothiophene ring system **5**, where the triplet excitation transfer is 4 kcal mol⁻¹ endothermic. Significant improvement in overall efficiency for the photoreactivity is achieved when the triplet excitation transfer is facilitated by a through – bond mechanism by linking the thioxanthone chromophore via a trimethylene

linker, as in structures **12a**, for which $\Phi = 0.14$. Here the photoreactivity should be essentially the same as that for the sensitized photolysis of the unlinked system involving anilides **13a,b** with thioxanthone, which is planned. According to a computational study,² the mechanism for these photoreactions involves electrocyclization in the triplet excited state of the naphthothiophene with the phenyl group attached to the 2-carboxamide nitrogen. The resultant triplet diradical then intersystem crosses to a ground state intermediate that is thought to have zwitterionic character. Expulsion of the leaving group attached to the C-3 position of the thiophene ring produces the observed photoproducts.

The naphthothiophene-2-carboxanilide system appears to be inherently less efficient in undergoing electrocyclization and leaving group expulsion in the triplet excited state as compared to the analogous benzothiophene-2-carboxanilides **9**. For the latter case $\Phi = 0.23$ for direct photolysis. Previous studies showed that attaching bromine to the C-6 position of the benzothiophene ring increases the quantum yield to 0.33. A heavy atom effect increases the intersystem crossing efficiency and hence, the quantum yield. Quantum yields as high as 0.41 are observed in thioxanthone sensitized photolyses of anilide **7**.

The advantage of having the naphthothiophene ring system as triplet energy acceptor is its relatively low triplet energy, which will allow incorporation of chromophores that absorb at longer wavelengths with attendant lowering of the energies of the triplet excited states. Experiments have been conducted using acriflavine as a sensitizer, in which case the triplet energy transfer from acriflavin to naphthothiophene will be bimolecular. The rate of energy transfer will be $k_q[Q]$ where k_q is the bimolecular

rate constant for triplet energy transfer to the naphthothiophene and $[Q]$ is the naphthothiophene concentration. Since the triplet energy of acriflavin is 51 kcal mol^{-1} and about the same as that for the naphthothiophene, the rate constant k_q will be less than the value of $10^9 - 10^{10} \text{ M}^{-1} \text{ s}^{-1}$ expected for diffusion-controlled quenching when the energy transfer is at least 4 kcal mol^{-1} exothermic. The photoproduct **46a** observed for $[Q] = 1.20 \times 10^{-4} \text{ M}$ with a 5% conversion. The successful sensitized photolysis provide possibility to expel leaving groups with a single molecule system with brominated acriflavine tethered to the anilide. In this system the intersystem quantum yield could have been improved and give a higher overall quantum efficiency.

3.5. Experimental Section.

3.5.1. Potassium Ferrioxalate Actinometry.

Ferrioxalate Preparation ($\text{K}_2\text{Fe}(\text{C}_2\text{O}_4)_3 \cdot 3\text{H}_2\text{O}$). The method was adapted from the procedure developed by Hatchard and Parker.⁹⁶ To 250 mL of 1.5 M aqueous solution of FeCl_3 (101.4 g of hexahydrate in 250 mL of solution) was added to 750 mL of 1.5 M aqueous solution of $\text{K}_2\text{C}_2\text{O}_4$ monohydrate (207.3 g in 750 mL of solution). The mixture was shaken vigorously and allowed to cool to room temperature in a dark flask. The solid green crystals were filtered and dried at $45 \text{ }^\circ\text{C}$ overnight. The product was used after recrystallized with warm water three times.

Phenanthroline Preparation. A solution of 0.1% 9,10-phenanthroline in deionized water (1.0909 g in 1000 mL) was prepared.

Buffer solution. The buffer solution was 600 mL of 1N sodium acetate (49.25 g of sodium acetate in 600 mL of H₂O), 360 mL of 1N H₂SO₄ (27.9 mL of concentrated H₂SO₄ in 100 mL solution) and water was added to give a total volume of 1000 mL

Actinometry solution. A 0.006 M ferrioxalate solution was prepared with 2.947 g of potassium ferrioxalate and 600 mL of H₂O, followed by addition of 100 mL of 1N H₂SO₄. The solution was diluted to 1000 mL

3.5.2. Determination of light output (LOP).

1. Certain volume (V_1) of actinometry solution was pipetted in to the cell equal to that of the samples to be irradiated.

2. Actinometry solution was irradiated for a recorded period of time(T).

3. Mixed the irradiated actinometry solution thoroughly and pipetted an aliquote (V_2) to a 25 mL volumetric flask (V_3). The amount of the aliquote depends on the irradiation time. Often used 1 to 3 mL for the main cell and 5 to 10 mL for the side cell for a 30 to 120 min irradiation time in this project.

4. 3 mL of buffer solution and 4.5 mL of phenanthroline solution were added into the flask.

5. Diluted the solution to the mark with deionized water, mix.

6. Prepared a blank sample following 3-5 with a volume nonirradiated actinometer(V_4).

7. The absorbances of the solution 5 and 6 vs deionized water at 510 nm were measured and the difference per mL was calculated as A

8. The LOP was calculated as follows:

$$LOP(mEh^{-1}) = \frac{[Fe^{2+}]V_1 V_3}{\Phi_\lambda T} = \frac{AV_1 V_3}{\epsilon d \Phi_\lambda V_2 T} \quad 3.3$$

A absorbance (mL^{-1}) at 510 nm of irradiated actinometer solution corrected for absorption of blank.

d path length (cm) of absorption cell used in measurement of A.

ϵ . Extinction coefficient of ferrous 1,10-phenanthroline complex at 510 nm (ca. $1.11 \times 10^4 \text{ mol}^{-1} \text{ cm}^{-1}$).

Φ_λ Quantum yield of ferrous production at wavelength of light used in the photolysis.

9. The splitting ratio is obtained by irradiating the main cell and the side cell with no sample cell in between (see Figure 3.7 below).

$$LOP_{\text{sample cell}} = \text{splitting ratio} \times LOP_{\text{side cell}} - LOP_{\text{back cell}} \quad 3.4$$

$$\text{Splitting ratio} = \frac{LOP_{\text{main cell}}}{LOP_{\text{side cell}}} \quad 3.5$$

$$\text{Quantum yield, } \Phi = \frac{\text{mmol of product}}{LOP_{\text{sample cell}} T} \quad 3.6$$

3.5.3. General Procedure for Quantum Yield Determination.

A semi-micro optical bench was used for quantum yield determinations, which was similar to the apparatus described by Zimmerman.⁸⁵ Light from a 200 W high-pressure mercury lamp was passed through an Oriel monochromator, which was set to a wavelength of either 310 nm or 395 nm. The light was collimated through a lens. A fraction of the light was diverted 90° by a beam splitter to a 42.5 mL side quartz cylindrical cell containing an actinometer. The photolysate was contained in a 37.5 mL

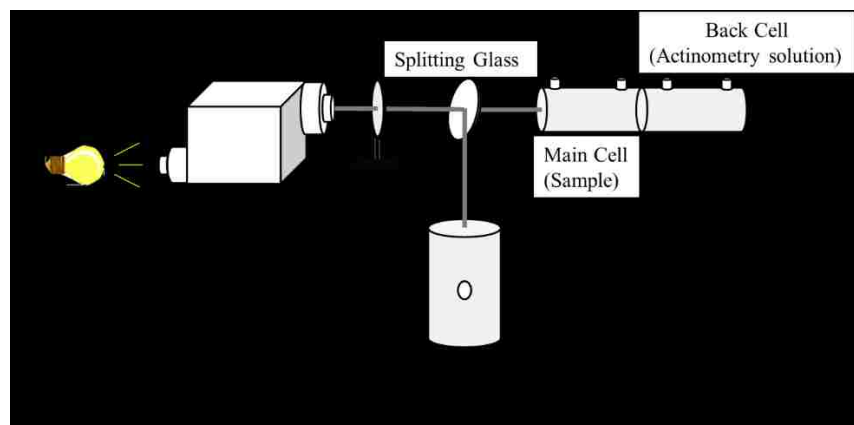


Figure 3.3. Depiction of Semi-micro optical bench set up for quantum yield determination.

quartz cylindrical cell placed in the light path. Behind the photolysate was mounted a quartz cylindrical cell containing 42.5 mL of actinometer. Light output was monitored by ferrioxalate actinometry using the splitting ratio technique. All quantum yields reported were the average of two or more independent runs

3.5.4. Preparation of 100 mM KH_2PO_4 buffer pH 7 solution.

To a 100 mL of water was added 1.35 g of KH_2PO_4 . The solution was then adjusted to pH 7 by dropwise addition of 1 M KOH.

3.5.5. Photochemical Studies.

Quantum Yields for Acids 11b. A 1.00×10^{-3} M solution acid **12a** in 20% aq dioxane containing 100 mM phosphate buffer in a 37.5 mL cell was flushed with nitrogen for ca. 30 min in the dark. The sample was sealed and photolyzed at 390 nm for 120 min. Light absorbed was determined by performing ferrioxalate actinometry. At the end of the

photolysis, 0.5 mL of 1 M HCl was added to the solution, which was concentrated in vacuo in the dark. The concentrate was then freeze dried for 2 h and dried under vacuum overnight in the dark. The photoproduct was dissolved in d_6 -DMSO and quantified by ^1H NMR analysis using DMF as an internal standard by integrating the N-CH₃ signal at 3.91 ppm.

Quantum Yields for Esters 12a, c. A 1.5×10^{-3} M solution of each of the thioxanthone-linked esters **12a, c** in 17% aq dioxane containing 100 mM phosphate buffer in a 37.5 mL cell was flushed with nitrogen for ca. 30 minute in the dark. Each sample was sealed and photolyzed at 390 nm for 60-180 min. Light absorbed was determined by performing ferrioxalate actinometry. The solution was concentrated in vacuo. The concentrate was freeze dried for 2 h and dried under vacuum overnight in the dark. Photoproduct was dissolved in CDCl₃ and a known amount of benzyl methyl ether (CH₂ and CH₃ peaks) was added as internal standard. The photoproduct was quantified by ^1H NMR analysis by integrating each of the three CH₂ signals of **45a** at 4.46, 2.95 and 2.25 ppm and averaging.

Quantum yields for compound 13a. A 1.0×10^{-3} M solution of **13a** in 17% aq dioxane containing 100 mM phosphate buffer in a 37.5 mL cell was flushed with nitrogen for ca. 30 minute in the dark. The sample was sealed and photolyzed at 390 nm for 90 min. Light absorbed was determined by performing ferrioxalate actinometry. The solution was concentrated in vacuo. The concentrate was freeze dried for 2 h and dried under vacuum overnight in the dark. The photoproduct was dissolved CDCl₃ and a known amount of benzyl methyl ether (CH₂ and CH₃ peaks) was added as an internal standard. The photoproduct was quantified by ^1H NMR by integrating each of the three

CH signals of **45a** at 8.91, 8.48 and 8.25 ppm and averaging relative to the CH₂ and CH₃ of the internal standard.

Quenching of the direct photolysis of tethered anilide ester 12a by ferrocene.

The general procedure for determining product quantum yields was used. A stock solution of 0.240 g (0.377 mmol, 1.26×10^{-3} M) of thioxanthone-linked ester **12a** in 300 mL dioxane containing 17% aqueous 100 mM phosphate buffer was prepared. Samples of 37.5 mL were flushed with nitrogen for 40 min in the dark followed. Ferrocene was added to give final concentrations of quencher of 0.00 M, 5.53×10^{-6} M, 2.21×10^{-5} M, 3.00×10^{-5} M, 4.42×10^{-5} M, 5.00×10^{-5} M, 6.63×10^{-5} M, 7.76×10^{-5} M, 1.00×10^{-4} M. Samples were sealed and photolyzed at 390 nm for 60-120 min. Light absorbed was determined by performing ferrioxalate actinometry. The photolysate was concentrated in vacuo in the dark. The concentrate was then freeze dried for 2 h and dried under vacuum overnight in the dark. Photoproduct was dissolved in CDCl₃ and a known amount of benzyl methyl ether (CH₂ and CH₃ peaks) was added as internal standard. The photoproduct was quantified by ¹H NMR analysis by integrating each of the three CH₂ signals of **45a** at 4.46, 2.95 and 2.25 ppm and averaging.

Quenching of the direct photolysis of anilide 13a by ferrocene. The general procedure for determining product quantum yields was used. A stock solution of 0.196 g (0.431 mmol, 1.44×10^{-3} M) of anilide ester **13a** in 300 mL dioxane containing 17% aqueous 100 mM phosphate buffer was prepared. Samples of 37.5 mL were flushed with nitrogen for 40 min in the dark. Ferrocene was added to give final concentrations of quencher of 0.00 M, 1.52×10^{-5} M, 2.00×10^{-5} M, 4.39×10^{-5} M, 7.76×10^{-5} M, 6.50×10^{-5} M, 7.76×10^{-5} M, and 2.20×10^{-4} M. Samples were sealed and photolyzed at 390 nm

for 60-120 min. Light absorbed was determined by performing ferrioxalate actinometry. After photolysis, ca. 0.5 mL of 1 M HCl was added and the photolysate was concentrated in vacuo in the dark. The concentrate was then freeze dried for 2 h and dried under vacuum overnight in the dark. Photoproduct was dissolved in CDCl₃ and a known amount of benzyl methyl ether (CH₂ and CH₃ peaks) was added as internal standard. The photoproduct was quantified by ¹H NMR analysis by integrating each of the three CH signals of **46a** at 8.91, 8.48, 9.22 and 8.25 ppm and averaging.

Quenching of the direct photolysis of tethered anilide 12a by 1,2-diphenylpropene. The general procedure for determining product quantum yields was used. A stock solution of 0.240 g (0.377 mmol, 1.26 x 10⁻³ M) of thioxanthone-linked ester **12a** in 300 mL dioxane containing 17% aqueous 100 mM phosphate buffer was prepared. Samples of 37.5 mL were flushed with nitrogen for 40 min in the dark followed by addition of 1,2-diphenylpropene solution via syringe to give final concentrations of quencher of 0.00 M, 1.00 x 10⁻³ M, 1.40 x 10⁻³ M. Samples were sealed and photolyzed at 390 nm for 60-120 min. Light absorbed was determined by performing ferrioxalate actinometry. The photolysate was concentrated in vacuo in the dark. The concentrate was then freeze dried for 2 h and dried under vacuum overnight in the dark. Photoproduct was dissolved in CDCl₃ and a known amount of benzyl methyl ether (CH₂ and CH₃ peaks) was added as internal standard. The photoproduct was quantified by ¹H NMR analysis by integrating each of the three CH₂ signals of **45a** at 4.46, 2.95 and 2.25 ppm and averaging.

Intermolecular sensitized photolysis of anilide 13a with thioxanthone as the sensitizer. The general procedure for determining product quantum yields was used. A

stock solution of 2.00×10^{-2} M of thioxanthone in dioxane containing 10% aqueous 100 mM phosphate buffer was prepared. Samples of 37.5 mL were flushed with nitrogen for 40 min in the dark followed by addition of naphthothiophene-2-carboxanilide **13a** to give the final concentration of anilide **13a** of 1.00×10^{-2} M. The sample was sealed and photolyzed at 390 nm for 90 min. The photoproduct was dissolved CDCl_3 and a known amount of benzyl methyl ether (CH_2 and CH_3 peaks) was added as an internal standard. The photoproduct was quantified by ^1H NMR by integrating each of the three CH signals of **47a** at 8.91, 8.48 and 8.25 ppm and averaging relative to the CH_2 and CH_3 of the internal standard.

Intermolecular sensitized photolysis of anilide 13a with xanthone as the sensitizer. The general procedure for determining product quantum yields was used. A stock solution of 5.0×10^{-3} M of xanthone in dioxane containing 17% aqueous 100 mM phosphate buffer was prepared. Samples of 37.5 mL were flushed with nitrogen for 40 min in the dark followed by addition of naphthothiophene-2-carboxanilide **13a** to give the final concentration of anilide **13a** of 6.00×10^{-5} M. The sample was sealed and photolyzed at 341 nm for 90 min. The photoproduct was dissolved CDCl_3 and a known amount of benzyl methyl ether (CH_2 and CH_3 peaks) was added as an internal standard. The photoproduct was quantified by ^1H NMR by integrating each of the three CH signals of **47a** at 8.91, 8.48 and 8.25 ppm and averaging relative to the CH_2 and CH_3 of the internal standard.

Intermolecular sensitized photolysis of anilide 13a with acriflavine as the sensitizer. General procedure for product quantum yield was used. A stock solution of 1.0×10^{-3} M of acriflavine in 200 mL of dioxane containing 17% aqueous 100 mM

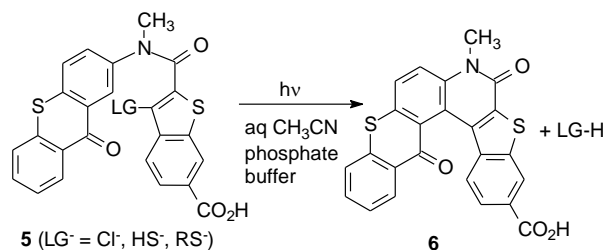
phosphate buffer was prepared. The anilide **12a** was dissolved in 37.5 mL of the stock solution to give the final concentration of anilide of 1.00×10^{-3} M. After flushing in the dark with nitrogen for ca. 40 min, the sample was irradiated at 450 nm for 2.5 h. Light absorbed by the photolysate was determined by ferrioxalate actinometry. The photolysis was concentrated in vacuo in the dark and freeze dried for 2 h and further dried overnight under vacuum in the dark. The dried sample was dissolved in d_6 -DMSO and a known amount of DMF was added to each as an internal standard. The yield of photoproduct **46a** was determined by $^1\text{H-NMR}$ analysis by integration of the N-CH₃ signal of photoproduct at 3.81 ppm relative to the DMF methyl groups signals.

APPENDIX 1.

SYNTHESIS OF 3-BROMO-7-OXO-7H-CYCLOPENTA [1,2-b:4,3-b']DITHIOPHENE-2-CARBOXYLIC ACID WITH POTENTIAL TO BE SENSITIZED WITH CHROMOPHORE THAT ABSORBS AT LONGER WAVELENGTH.

4.1. Introduction

The major finding of the photochemical study of benzothiophene-2-carboxamides **5** with thioxanthone attached to the amide nitrogen (eq. 2.1) was that the



electrocyclization of the benzothiophene ring with thioxanthone occurred in the triplet excited state subsequent to intersystem crossing of the thioxanthone. Computational studies showed that triplet excitation transfer from the thioxanthone to the benzothiophene ring system is a prerequisite to electrocyclization. The problem is that this triplet energy transfer is an endothermic process. Thioxanthone has $E_T = 65 \text{ kcal mol}^{-1}$ while the benzothiophene triplet excited state as the energy acceptor is estimated to lie 4 kcal mol^{-1} higher in energy. Although later studies involving analysis of Stern-Volmer quenching of the reaction showed that this energy transfer process is a reversible process with $K_{\text{eq}} = 0.058$, the reaction is still highly efficient with Φ values as high as 0.4 since the product of $K_{\text{eq}} \times k_r$ is competitive with the relatively slow decay of the thioxanthone triplet excited state. Here k_r is the rate of electrocyclization, which can be

determined through the use of Stern-Volmer quenching with cyclohexadiene, an efficient triplet excited state quencher.

Additional provisions are needed to insure the electrocyclization involving thiophenes is efficient when energy transfer must take place after initial excitation of a chromophore. For thioxanthone it should be attached to the amide nitrogen via a trimethylene linker so that the triplet excitation transfer occurs efficiently via a through – bond mechanism. Other linkers may be satisfactory for energy transfer to be efficient, but we did not explore beyond the one example. We do know that directly attaching the thioxanthone to the amide nitrogen leads to inefficient photoreactivity for reasons that are not well understood.

Thioxanthone may be among the longest wavelength chromophores that can be used with benzothiophene as triplet energy acceptor. Use of chromophores with lower energy triplet excited states than thioxanthone are expected to have reduced rate constants for energy transfer and overall lower efficiencies for reaction, as the triplet energy transfer becomes increasingly endothermic. Further advances in extending the photolysis wavelength will require a thiophene ring system with a rather lower E_T .

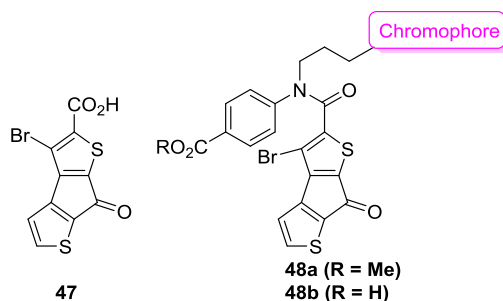
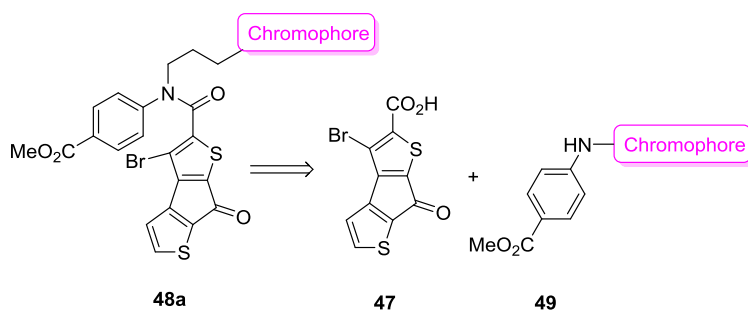


Figure 4.1. Compound **47** and its corresponding caged compound.

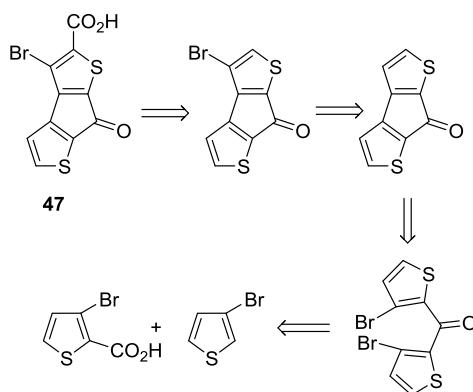
Efforts thus far focused on use of the naphthothiophene ring system with $E_T = 51$ kcal mol⁻¹, as exemplified by structures **11-13**. This thiophene ring system would allow longer wavelength chromophores with rather low values for E_T . (figure 4.1) However, significant time was also spent attempting to develop another chromophore with an even lower E_T . Efforts focused on synthesis of cyclopentadithiophene-7-one **47** as a chromophore. This triplet energy acceptor was very attractive, because of its low $E_T = 38$ kcal mol⁻¹ and rather long 1.7 ms lifetime. Cyclopentadithiophene-7-one **47** would be coupled with a suitable amine **49** to produce structure **48**, which has a chromophore that is attached via a trimethylene linker (Scheme 4.1). The chromophore itself would have a long wavelength absorption band and a lowest energy triplet excited state that lies above 38 kcal mol⁻¹ such that triplet energy transfer would be exothermic.



Scheme 4.1. Retrosynthesis of **48a**

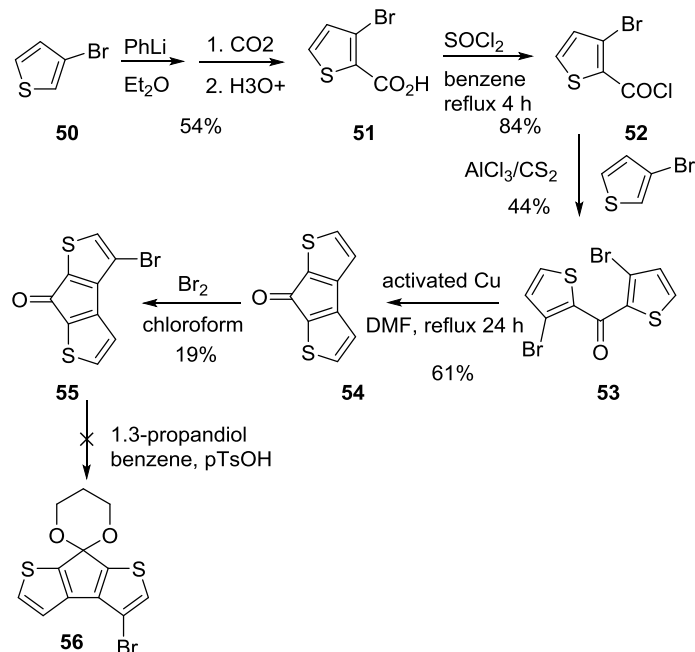
4.2. Results

The retrosynthetic analysis of **47** is shown in Scheme 4.2. The synthesis starts with the carboxylation at the C-2 position of the 3-bromothiophene (Scheme 4.3). Phenyllithium was used to deprotonate the C-2 position **50**, which was reacted with



Scheme 4.2. Retrosynthesis of compound **47**.

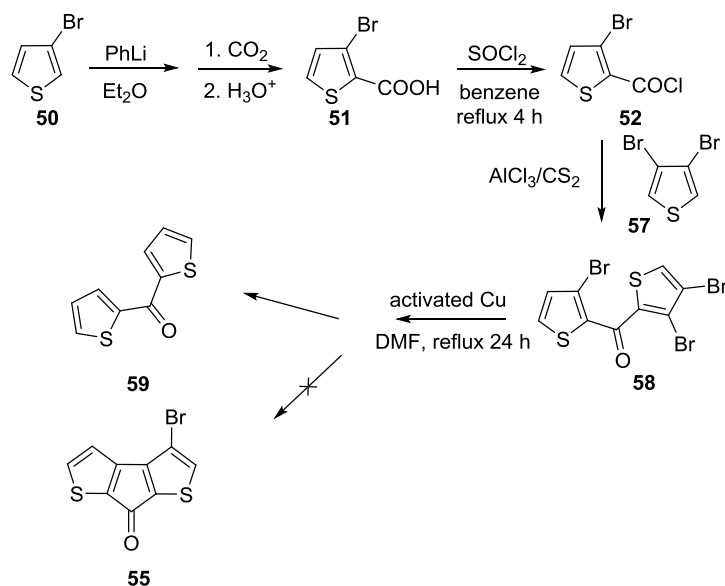
CO₂ to give **51** in 54%. After conversion to acid chloride **52**, Friedel Crafts acylation of **50** using standard methods produced the dithienylketone **53**. Intramolecular coupling⁹⁷ using an activated copper⁹⁸ catalyst in DMF gave **54** in 63%. The DMF is used in this step to allow use of a high reaction temperature for the coupling reaction. The yield of this step is 63.1%. Various amounts of byproducts are observed, possibly due to the debromination of **53** during the coupling reaction. The cyclized product **54** was reacted with bromine in dry chloroform to give monobromide **55** in 19% along with an unidentified dibromide byproduct.⁷⁹



Scheme 4.3. Attempted synthesis of **47**.

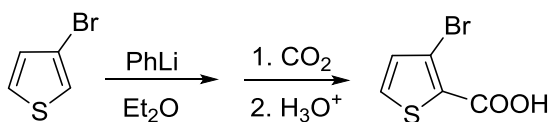
Ketalization of the carbonyl group in **56** was believed to be necessary for subsequent carboxylation at the C-2 position of **55**. However, an attempt to make **56** by refluxing **55** with 1,3-propanediol and toluene sulfonic acid in toluene with use of a Dean Stark trap failed. Virtually no water from dehydration of **55** was observed in the trap. However, the reactant **55** was not be recovered in decent yield. At this point the synthesis of **47** was abandoned.

As a side note, an attempt was made to use 3,4-dibromothiophene to obtain **58** (Scheme 4.4). In principle, this would have allowed the next to last bromination step in Scheme 4.3 to be omitted. However, the attempted coupling reaction of compound **58** resulted in only complete debromination to furnish **59** and no **55** was observed as a product by NMR spectroscopy.



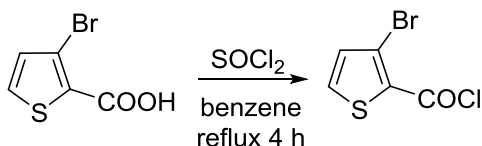
Scheme 4.4. Original attempted synthesis of **47**

4.3. Experimental Section.

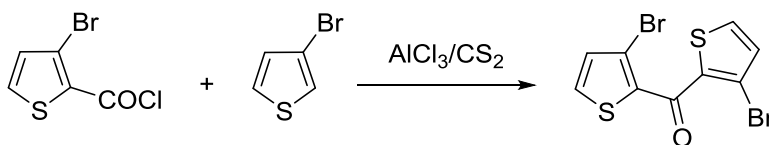


Preparation of 3-bromothiophene-2-carboxylic acid 51. To a stirred mixture of 1.80 g (259 mmol) of lithium and 10 mL of anhydrous diethyl ether was added dropwise 21.20 g (131.9 mmol) of bromobenzene in 40 mL of anhydrous diethyl ether under nitrogen. The reaction was stirred until little lithium was left. To a solution of 20.22 g (128.1 mmol) of 3-bromothiophene in 20 mL of diethyl ether was added cautiously the above reaction mixture through glass wool to filter the excess lithium. The reaction was heated to refluxing for 4 h. To a 500 mL flask full of dry ice was added slowly the above reaction mixture. The reaction was kept for 0.5 h and then warmed slightly to become a completely liquid. To the reaction was added cautiously 10 % HCl until pH 2. The mixture was cooled in an ice bath and then filtered to give off-white crude, which

crystallized into 14.49 g (54.5 %) of 3-bromothiophene-2-carboxylic acid as a colorless solid **51**, mp 190 - 193 °C. The spectra data were as follows: ^1H NMR (400 MHz, CDCl_3) δ 7.15 (d, $J = 5.2$ Hz, 2H), 7.57 (d, $J = 5.2$ Hz, 2H); ^{13}C NMR (400 MHz, CDCl_3) δ 118.78, 126.75, 132.90, 133.47, 165.86.

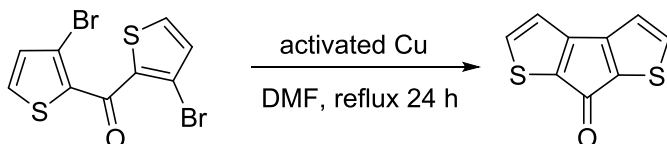


Preparation of 3-bromothiophene-2-carbonyl chloride 52. To a solution of 4.38 g (21.2 mmol) of the acid **51** in 30 mL of benzene was added slowly 15.10 g (127.9 mmol) of thionyl chloride at 0 °C. The reaction was heated to reflux and stirred for 4 h. Benzene was distilled out and the residue was recrystallized in hexane to give 4.01 g (84.1 %) of 3-bromothiophene-2-carbonyl chloride **52** as light-yellow needles, mp 62 - 63 °C. The spectra data were as follows: ^1H NMR (400 MHz, CDCl_3) δ 7.22 (d, $J = 5.3$ Hz, 2H), 7.70 (d, $J = 5.3$ Hz, 2H).

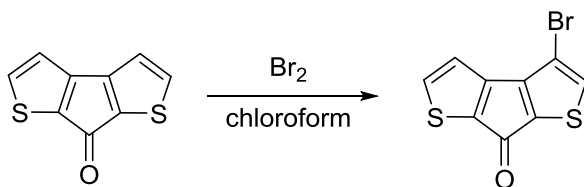


Preparation of the bis(3-bromothiophen-2-yl)methanone 53.⁹⁷ To a mixture of 5.76 g (43.2 mmol) of AlCl_3 in 20 mL of carbon disulfide was added dropwise 6.40 g (28.3 mmol) of 3-bromothiophene-2-carbonyl chloride in 20 mL carbon disulfide followed by the dropwise addition of 4.80 g (29.4 mmol) of 3-bromothiophene in 20 mL of carbon disulfide at -3 °C. The reaction was stirred at 0 °C for 0.5 h and then at room temperature for 2.5 h. To the reaction mixture added cautiously 10 % HCl until pH 2. The aqueous layer was extracted three times with 50 mL of chloroform. The combined

extracts were washed with saturated NaHCO_3 solution, water and brine, and then dried with magnesium sulfate. Concentration in vacuo followed by recrystallization in ethanol gave 4.42 g (44.2 %) of 3-bromothiophene-2-carbonyl chloride **53** as a yellow solid, mp 93 - 95 °C. $^1\text{H NMR}$ (400 MHz, CDCl_3) δ 7.12 (d, $J = 5.1$ Hz, 2H), 7.58 (d, $J = 5.1$ Hz, 2H).



Preparation of 7H-cyclopenta[1,2-b:4,3-b']dithiophen-7-one **54.**⁹⁷ A solution of 3.30 g (9.40 mmol) of bis(3-bromothiophen-2-yl)methanone and 1.80 of activated copper powder³³ in 20 mL of anhydrous DMF was heated to reflux for 24 h under nitrogen. The reaction mixture was cooled and filtered. The solid was washed with ether. The filtrate was diluted with 100 mL of water and extracted 3 times with 100 mL of ether. The combined extracts were washed with 10 % HCl and water, and then dried with magnesium sulfate. Concentration in vacuo followed by chromatography on silica gel, eluting with AcOEt-hexane (1:9) gave 1.10 g (61.3 %) of 7H-cyclopenta[1,2-b:4,3-b']dithiophen-7-one **54** as red needles. The spectra data were as follows: $^1\text{H NMR}$ (400 MHz, CDCl_3) δ 6.88 (d, $J = 4.6$ Hz, 2H), 7.56 (d, $J = 4.6$ Hz, 2H).



Preparation of 3-bromo-7H-cyclopenta[1,2-b:4,3-b']dithiophen-7-one **55.**⁷⁹

To a solution of 2.20 g (11.4 mmol) of **54** in 20 mL of anhydrous chloroform was added dropwise 1.14 g (7.1 mmol) of bromine at 0 °C under nitrogen. The reaction was stirred

at room temperature overnight. The solvent was removed by vacuum and the residue was purified by chromatograph on silica gel, eluting with EtOAc-hexane (5:5) to give 0.59 g (19.0 %) of 3-bromo-7H-cyclopenta[1,2-b:4,3-b']dithiophen-7-one **55** as a red solid. The spectra data were as follows: ^1H NMR (400 MHz, CDCl_3) δ 6.85 (d, $J = 4.6$ Hz, 1H), 6.94 (s, 1H), 7.57 (d, $J = 4.6$ Hz, 1H).

APPENDIX 2.

X-RAY CRYSTALLOGRAPHY

Table 5.1. Crystal data and structure refinement for direct-linked cage compound **11b**.

Identification code	stein1a
Empirical formula	C ₃₀ H ₂₂ NO ₅ S ₃ Br
Formula weight	652.58
Temperature/K	99.8(3)
Crystal system	triclinic
Space group	P-1
a/Å	8.7105(3)
b/Å	12.6691(4)
c/Å	13.5257(5)
α/°	69.189(3)
β/°	83.682(3)
γ/°	82.071(3)
Volume/Å ³	1378.89(8)
Z	2
ρ _{calc} /cm ³	1.572
μ/mm ⁻¹	4.513
F(000)	664
Crystal size/mm ³	0.2485 × 0.1962 × 0.1219
Radiation	CuKα (λ = 1.54184)
2θ range for data collection/°	7 to 148.5
Index ranges	-10 ≤ h ≤ 10, -15 ≤ k ≤ 15, -16 ≤ l ≤ 16
Reflections collected	26508
Independent reflections	5504 [R _{int} = 0.0280, R _{sigma} = 0.0177]
Data/restraints/parameters	5504/0/365
Goodness-of-fit on F ²	1.058
Final R indexes [I ≥ 2σ (I)]	R ₁ = 0.0570, wR ₂ = 0.1543
Final R indexes [all data]	R ₁ = 0.0606, wR ₂ = 0.1580
Largest diff. peak/hole / e Å ⁻³	2.29/-0.96

Table 5.2. Crystal data and structure refinement for tethered caged compound **12a**.

Identification code	stein1b
Empirical formula	C ₃₇ H ₂₆ BrNO ₄ S ₂
Formula weight	692.62
Temperature/K	100.15
Crystal system	monoclinic
Space group	P2 ₁ /c
a/Å	10.72938(7)
b/Å	25.05384(13)
c/Å	11.69011(8)
α/°	90
β/°	93.2255(6)
γ/°	90
Volume/Å ³	3137.47(3)
Z	4
ρ _{calc} /cm ³	1.466
μ/mm ⁻¹	3.375
F(000)	1416
Crystal size/mm ³	0.356 × 0.215 × 0.197
Radiation	CuKα (λ = 1.54184)
2θ range for data collection/°	7.06 to 141.18
Index ranges	-12 ≤ h ≤ 12, -30 ≤ k ≤ 30, -13 ≤ l ≤ 13
Reflections collected	28815
Independent reflections	5943 [R _{int} = 0.0178, R _{sigma} = 0.0106]
Data/restraints/parameters	5943/0/407
Goodness-of-fit on F ²	1.025
Final R indexes [I ≥ 2σ (I)]	R ₁ = 0.0451, wR ₂ = 0.1119
Final R indexes [all data]	R ₁ = 0.0454, wR ₂ = 0.1121
Largest diff. peak/hole / e Å ⁻³	1.84/-1.64

Table 5.3. Crystal data and structure refinement for methylated Boc animo thioxanthone 27.

Identification code	stein1h
Empirical formula	C ₂₁ H ₂₁ NO ₅ S
Formula weight	399.45
Temperature/K	100.15
Crystal system	monoclinic
Space group	I2/a
a/Å	21.2630(3)
b/Å	6.87078(11)
c/Å	53.6836(7)
α/°	90
β/°	90.4883(13)
γ/°	90
Volume/Å ³	7842.52(19)
Z	16
ρ _{calc} /cm ³	1.353
μ/mm ⁻¹	0.198
F(000)	3360
Crystal size/mm ³	0.682 × 0.379 × 0.068
Radiation	MoKα (λ = 0.71073)
2θ range for data collection/°	6.926 to 59.452
Index ranges	-29 ≤ h ≤ 28, -9 ≤ k ≤ 9, -73 ≤ l ≤ 74
Reflections collected	46346
Independent reflections	9982 [R _{int} = 0.0306, R _{sigma} = 0.0291]
Data/restraints/parameters	9982/0/515
Goodness-of-fit on F ²	1.041
Final R indexes [I ≥ 2σ (I)]	R ₁ = 0.0515, wR ₂ = 0.1315
Final R indexes [all data]	R ₁ = 0.0678, wR ₂ = 0.1436
Largest diff. peak/hole / e Å ⁻³	0.85/-0.28

APPENDIX 3.**NMR SPECTRA**

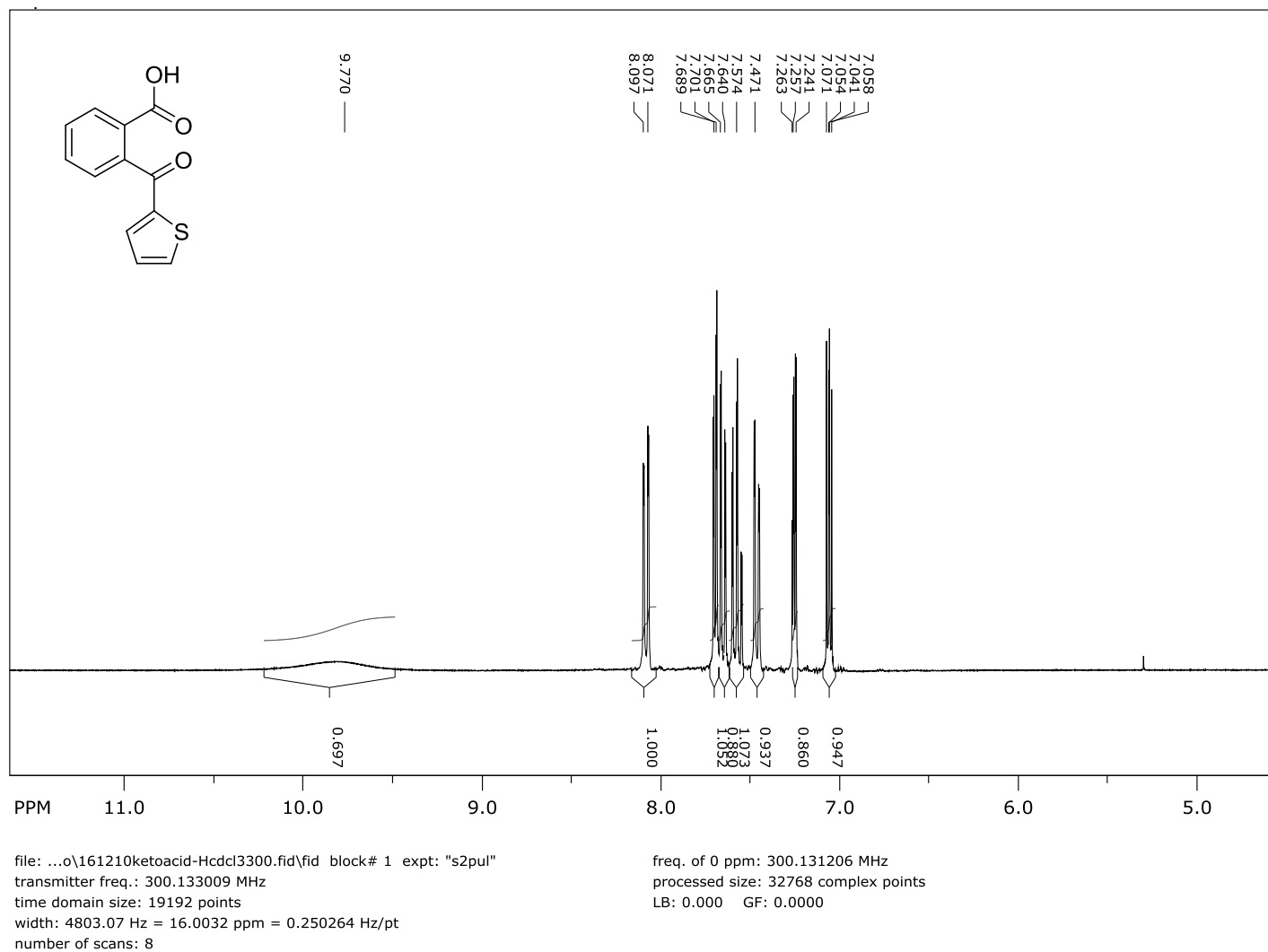


Figure 1. ¹H NMR Spectra of Compound 14 in CDCl₃.

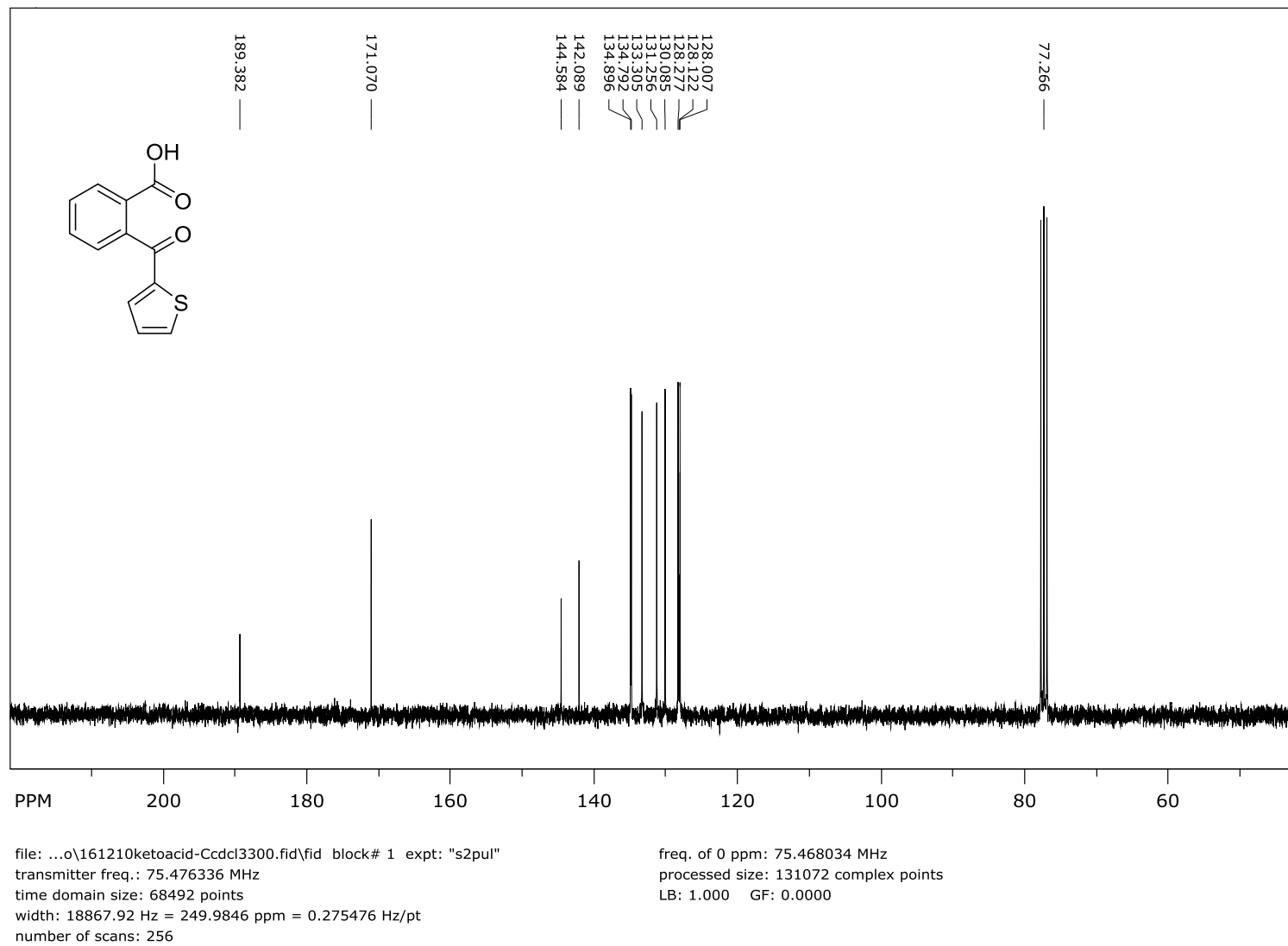


Figure 2. ¹³C NMR Spectra of Compound 14 in CDCl₃

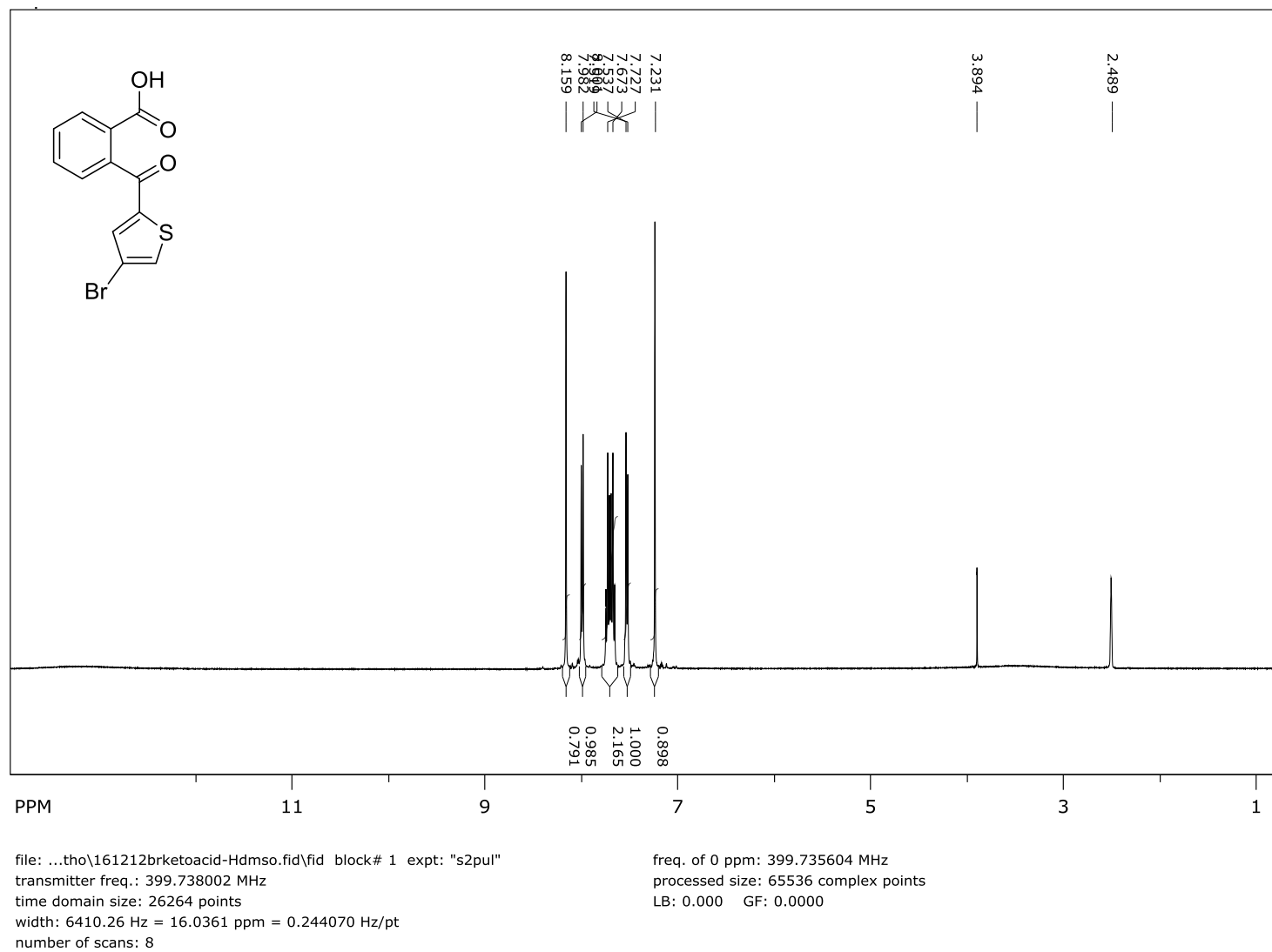


Figure 3. ¹H NMR Spectra of Compound 15 in DMSO-d₆.

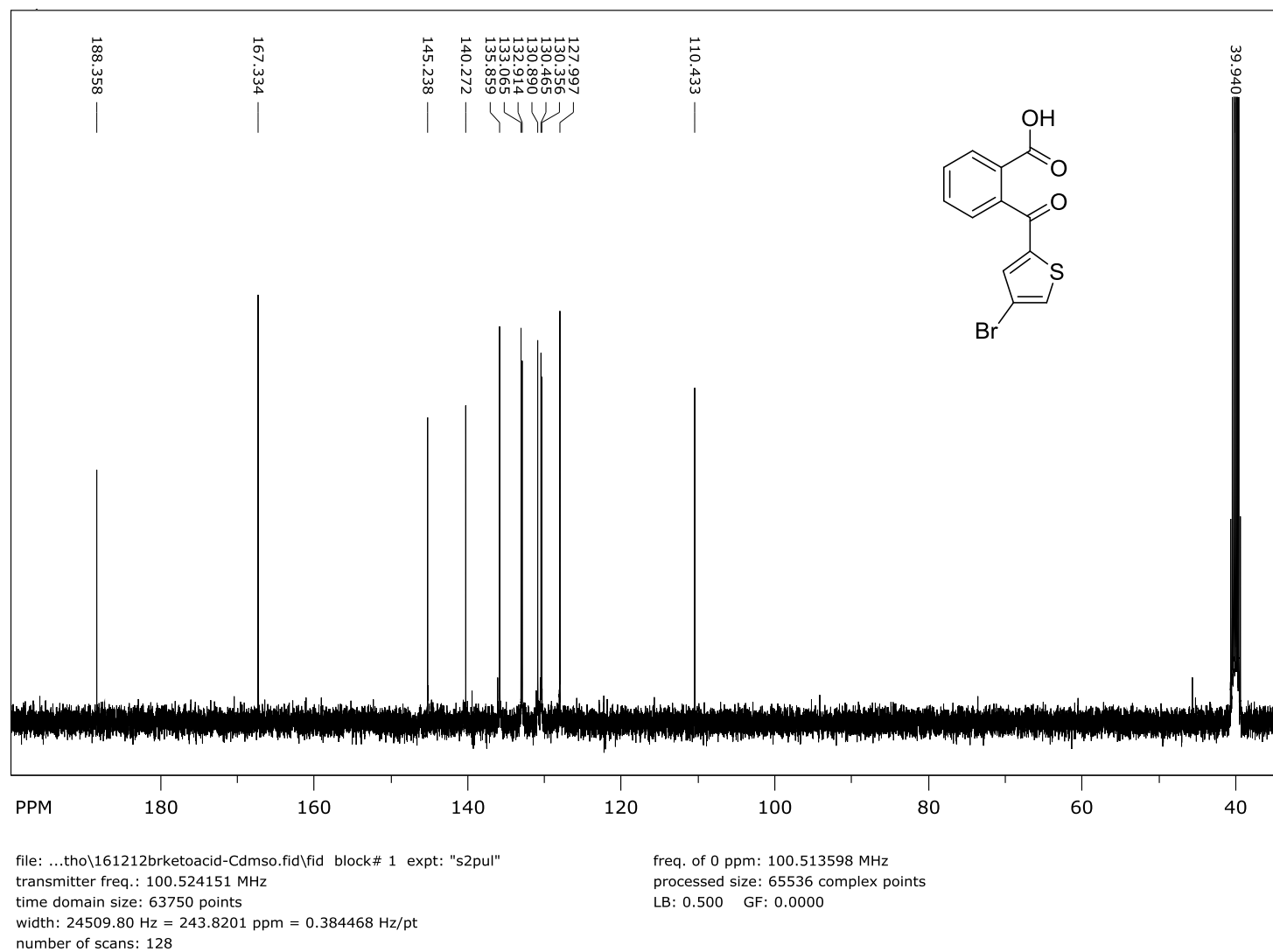


Figure 4. ^{13}C NMR Spectra of Compound **15** in DMSO-d_6

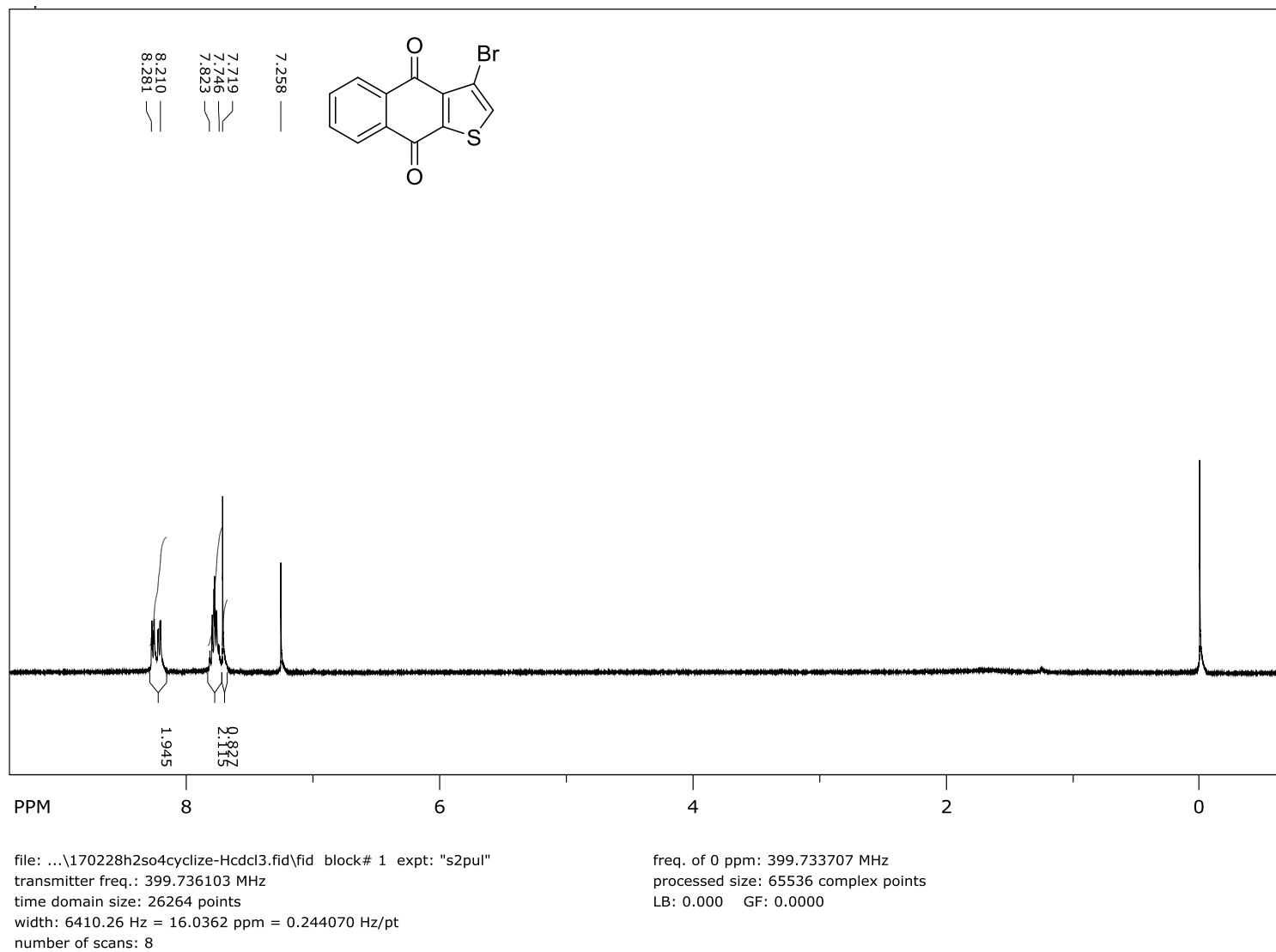


Figure 5. ^1H NMR Spectra of Compound **16** in CDCl_3

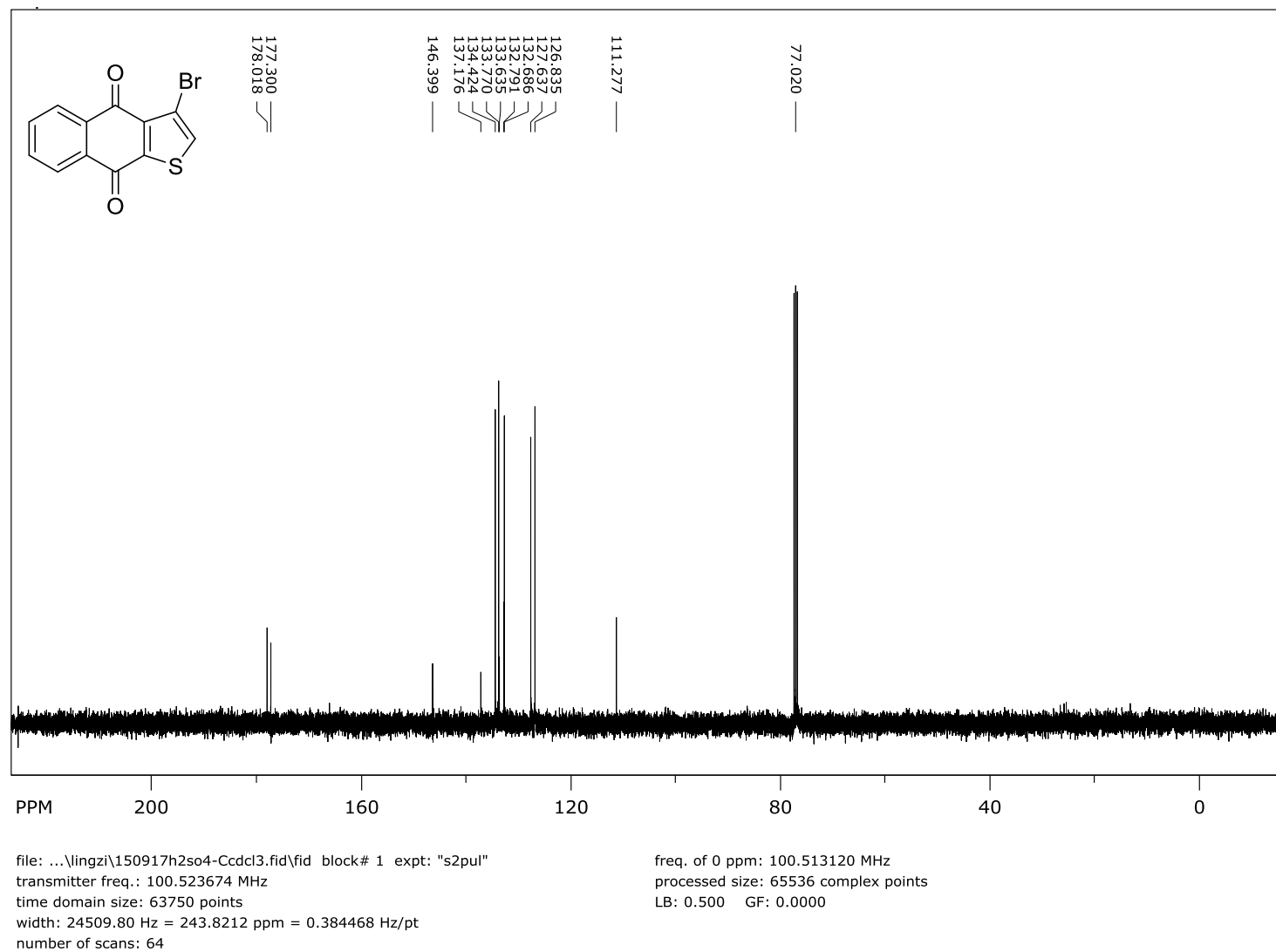


Figure 6. ¹³C NMR Spectra of Compound 16 in CDCl₃

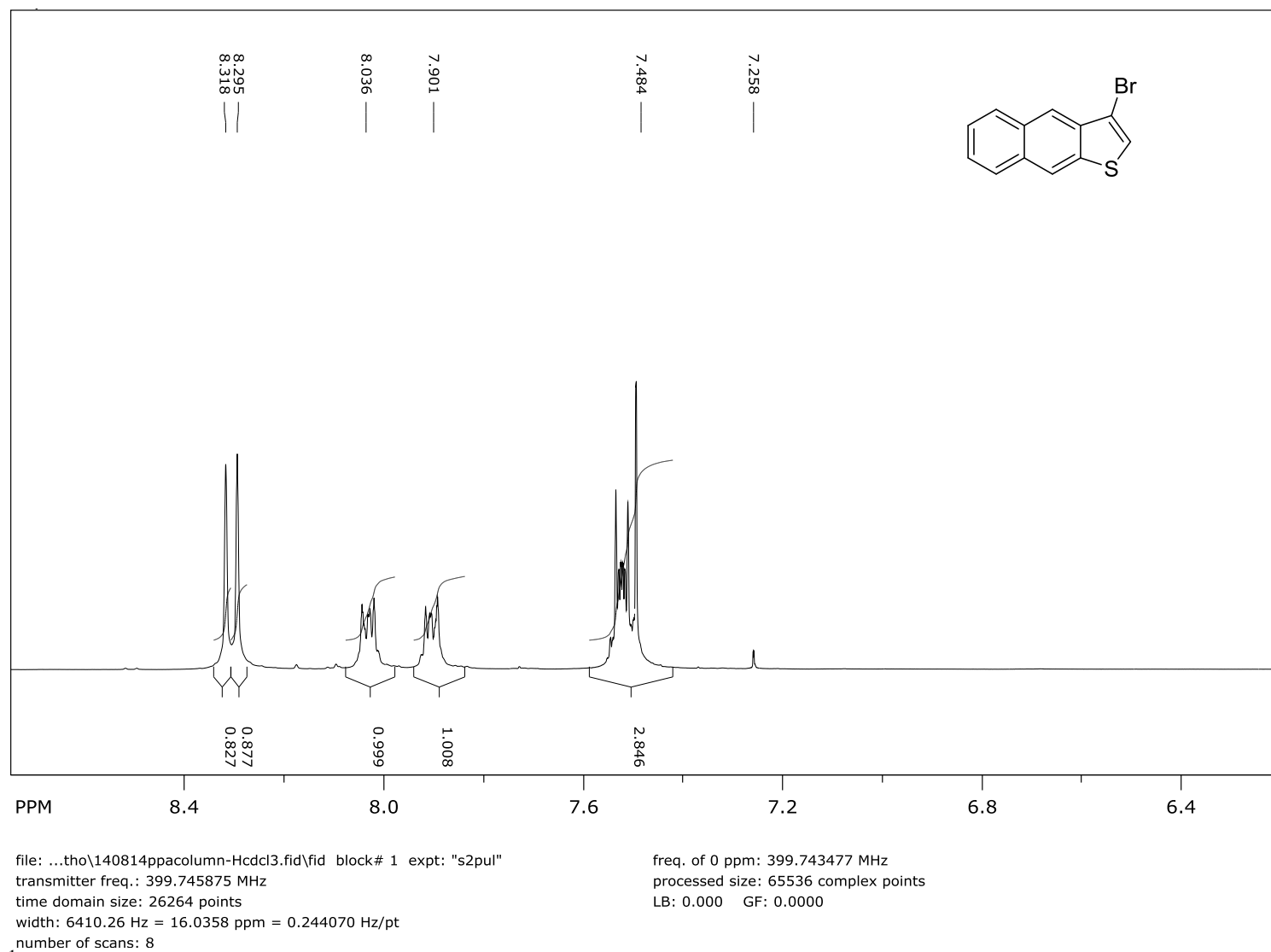


Figure 7. ^1H NMR Spectra of Compound **18** in CDCl_3

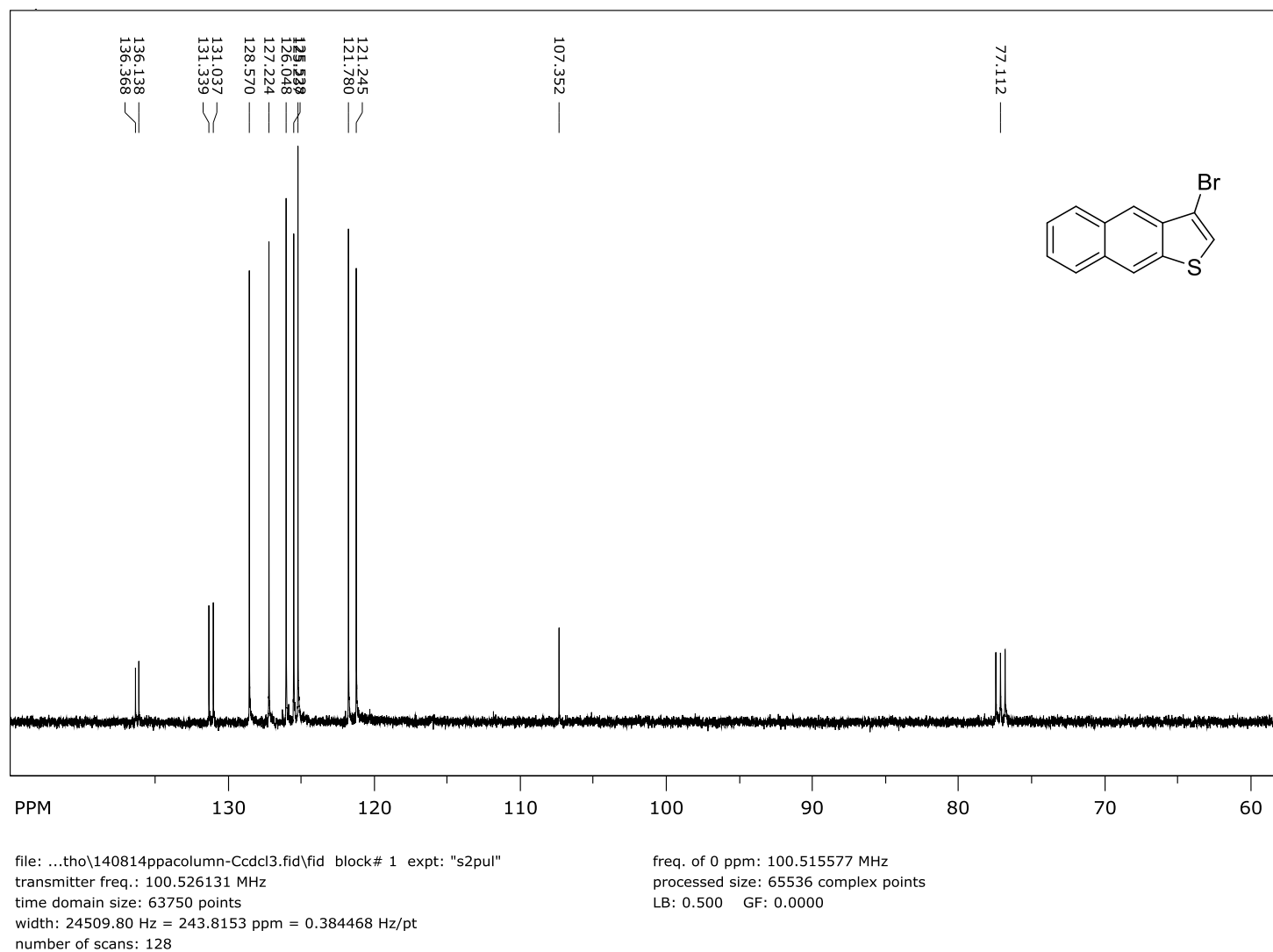


Figure 8. ^{13}C NMR Spectra of Compound **18** in CDCl_3

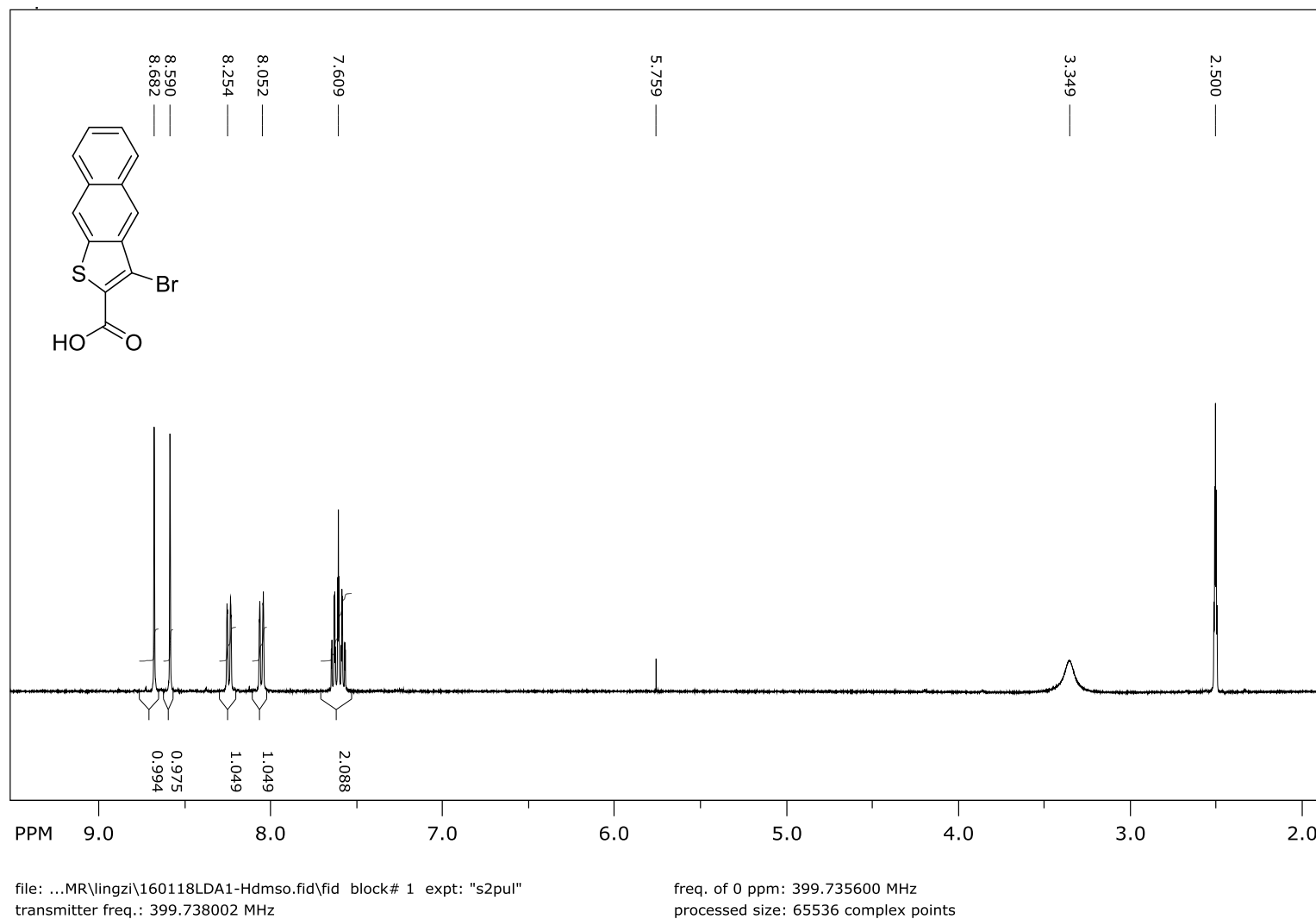


Figure 9. ¹H NMR Spectra of Compound **19** in DMSO-*d*₆.

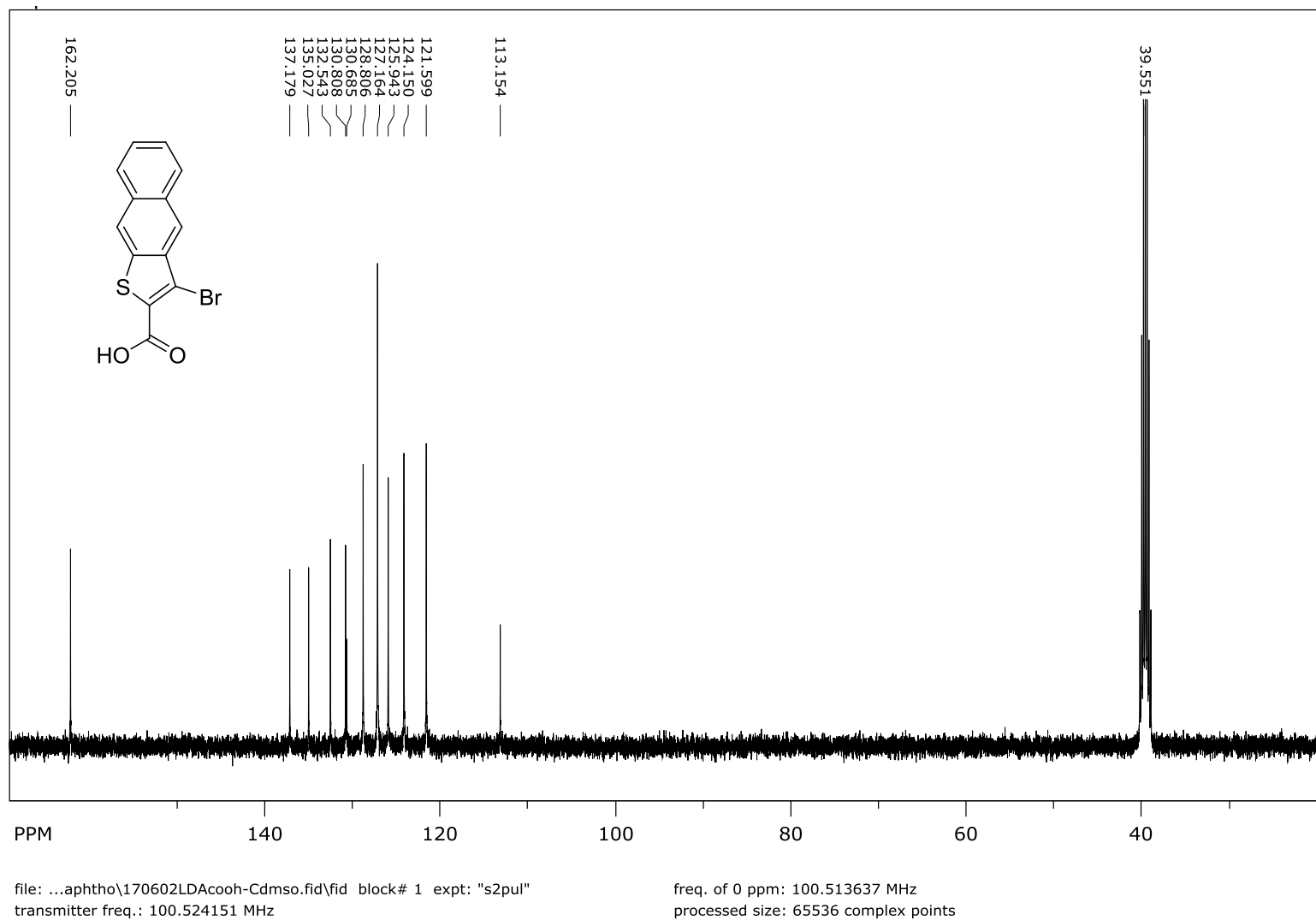


Figure 10. ^{13}C NMR Spectra of Compound **19** in $\text{DMSO-}d_6$

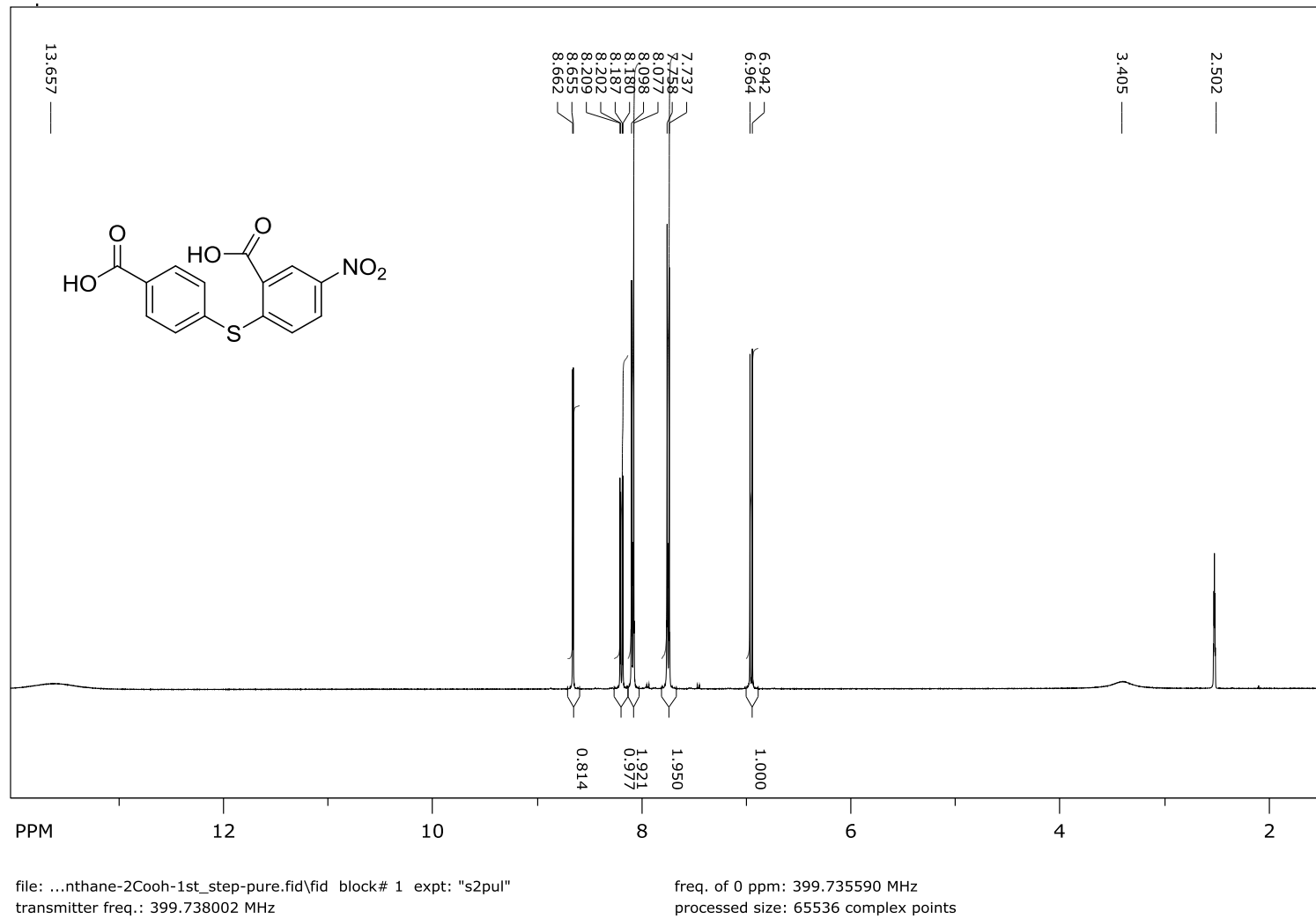


Figure 11. ^1H NMR Spectra of Compound **22** in $\text{DMSO-}d_6$.

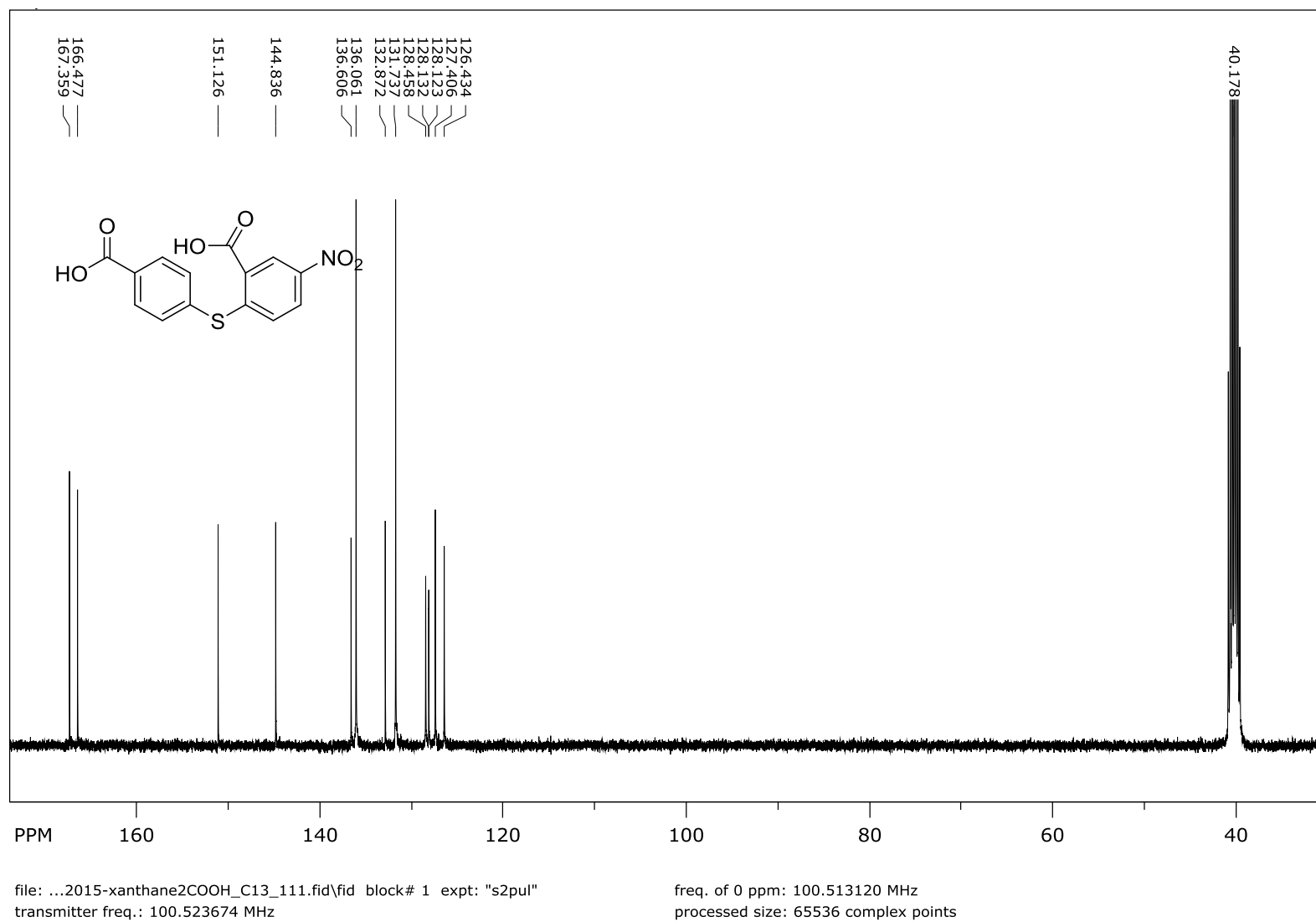


Figure 11. ^{13}C NMR Spectra of Compound **22** in $\text{DMSO-}d_6$.

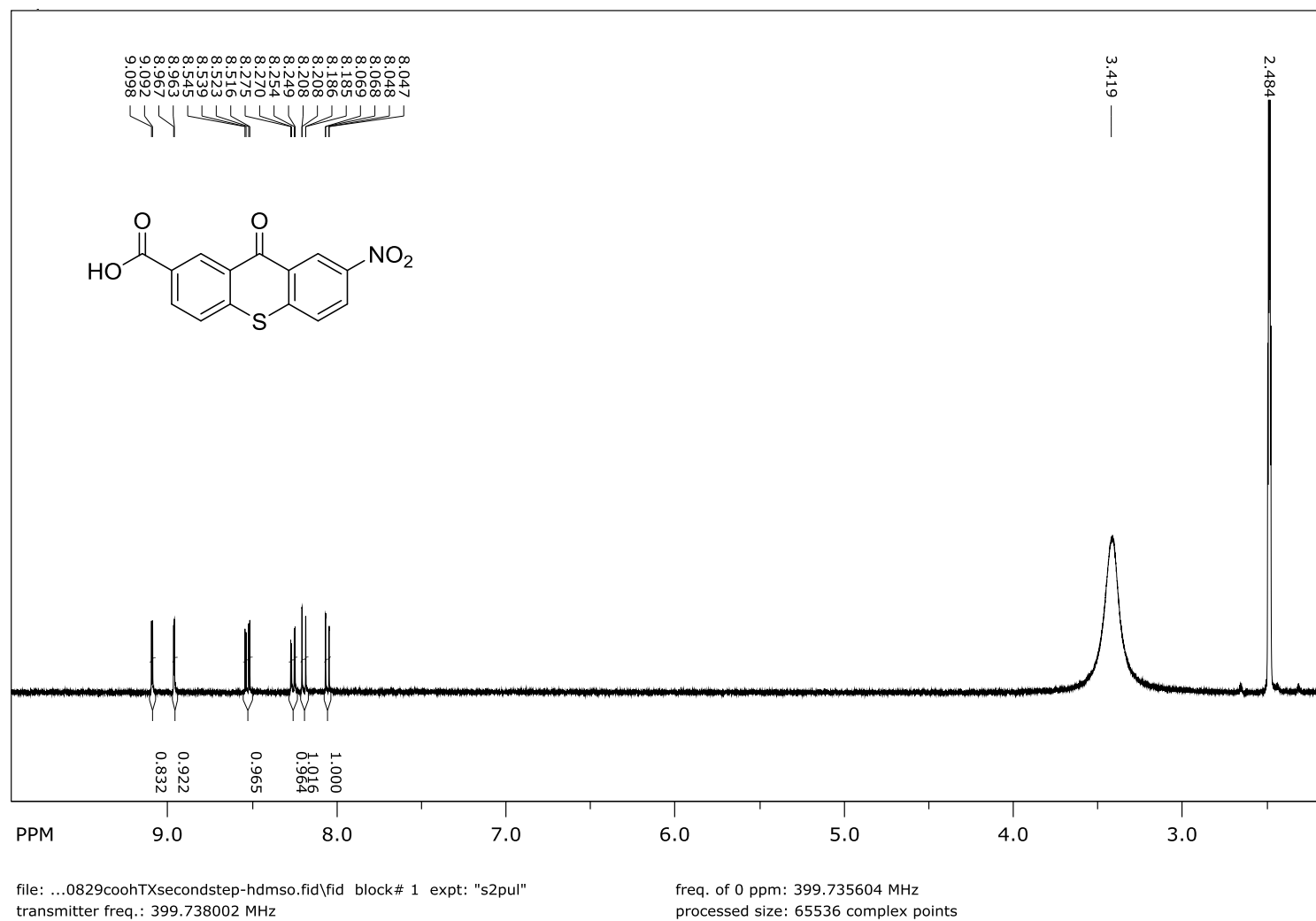


Figure 12. ^1H NMR Spectra of Compound **23** in $\text{DMSO-}d_6$.

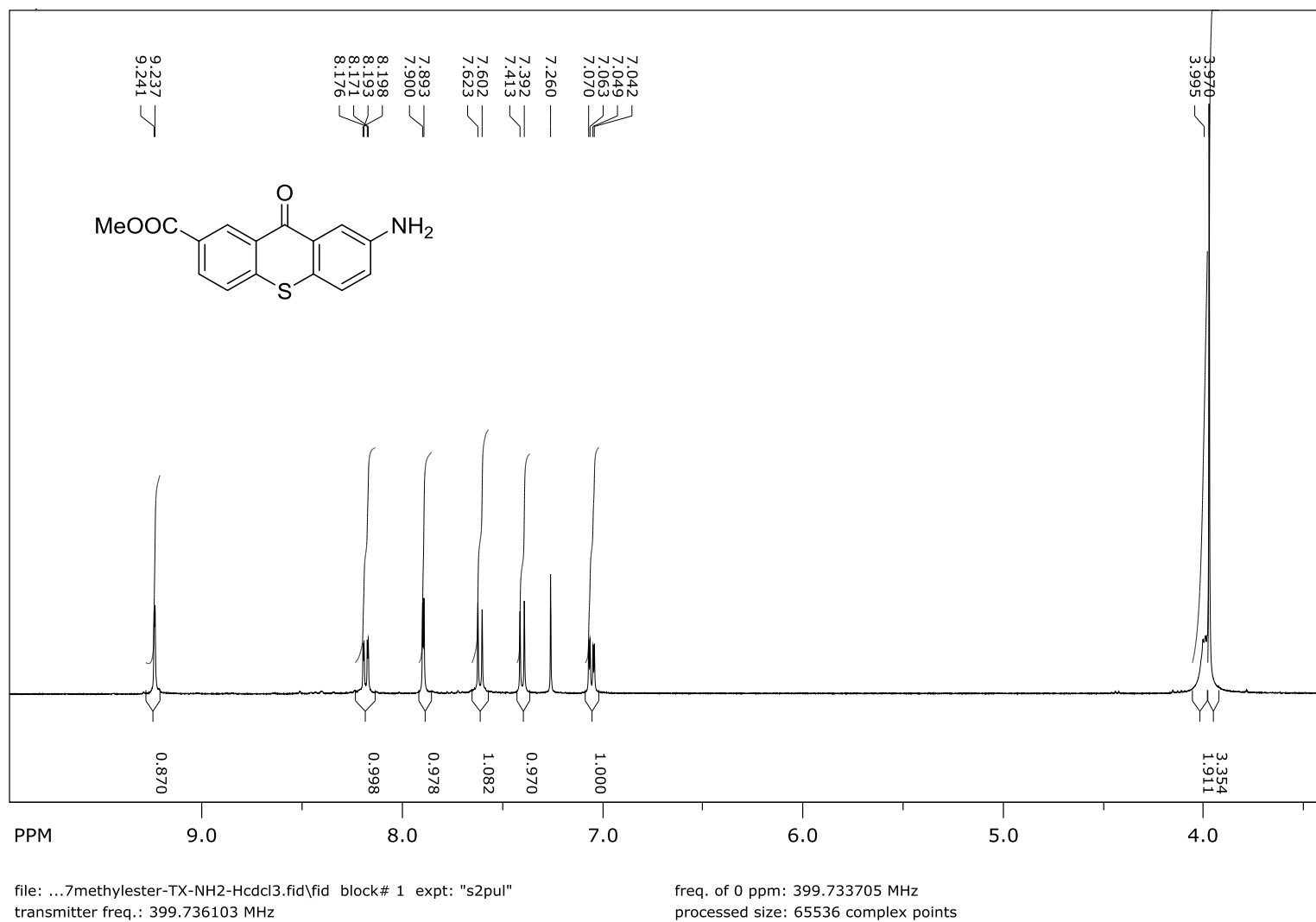


Figure 13. ^1H NMR Spectra of Compound **25** in CDCl_3 .

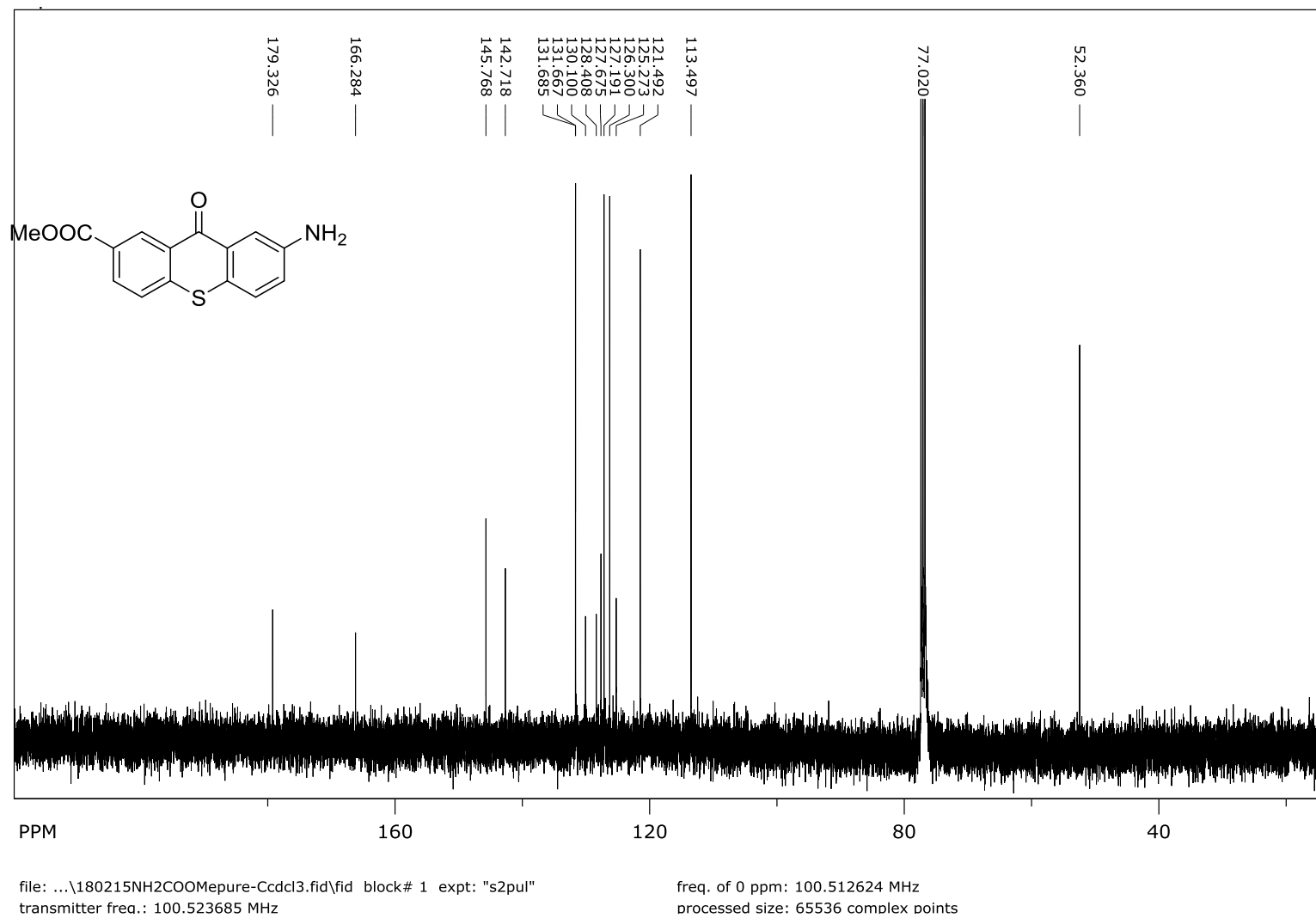
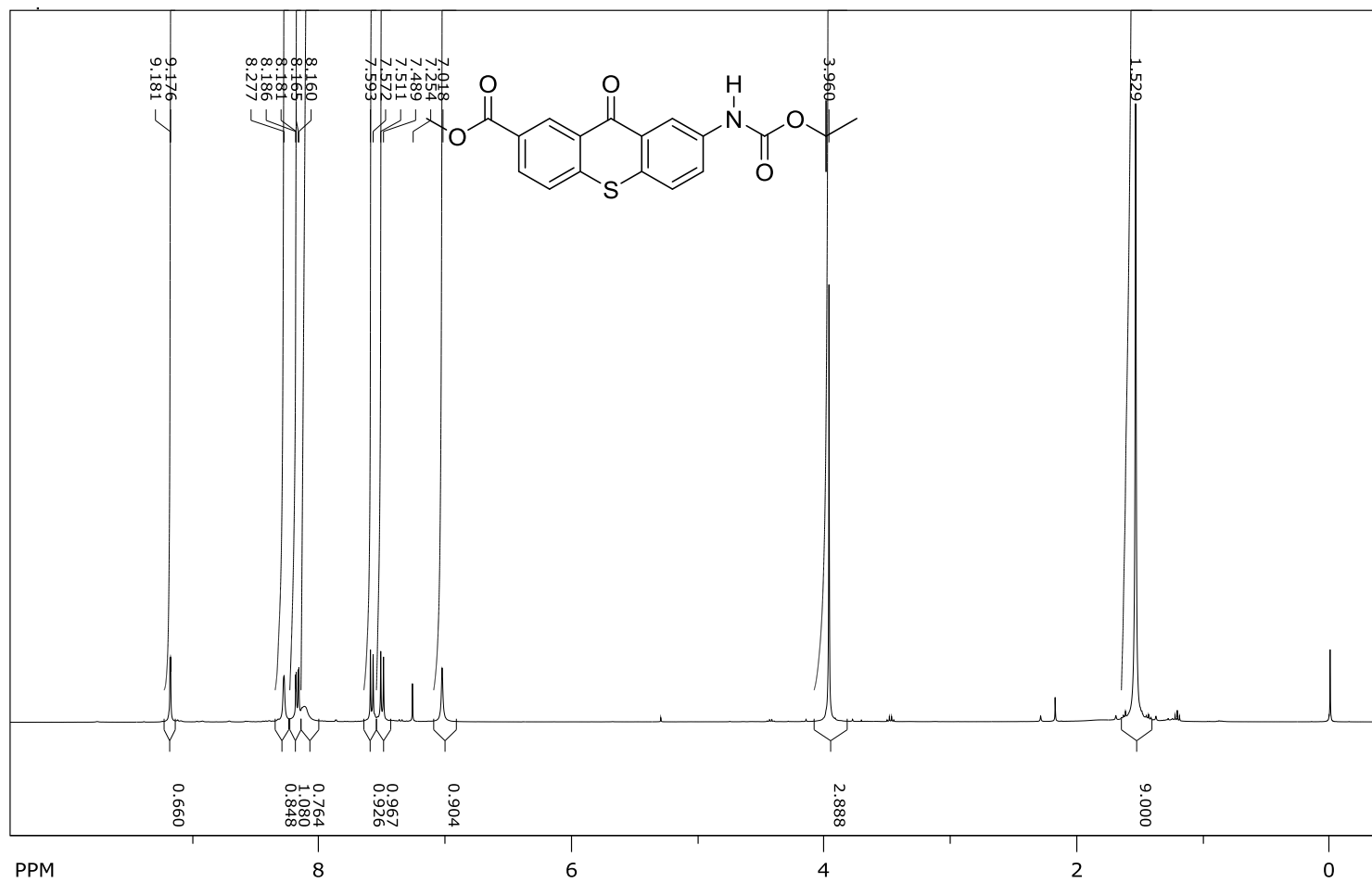


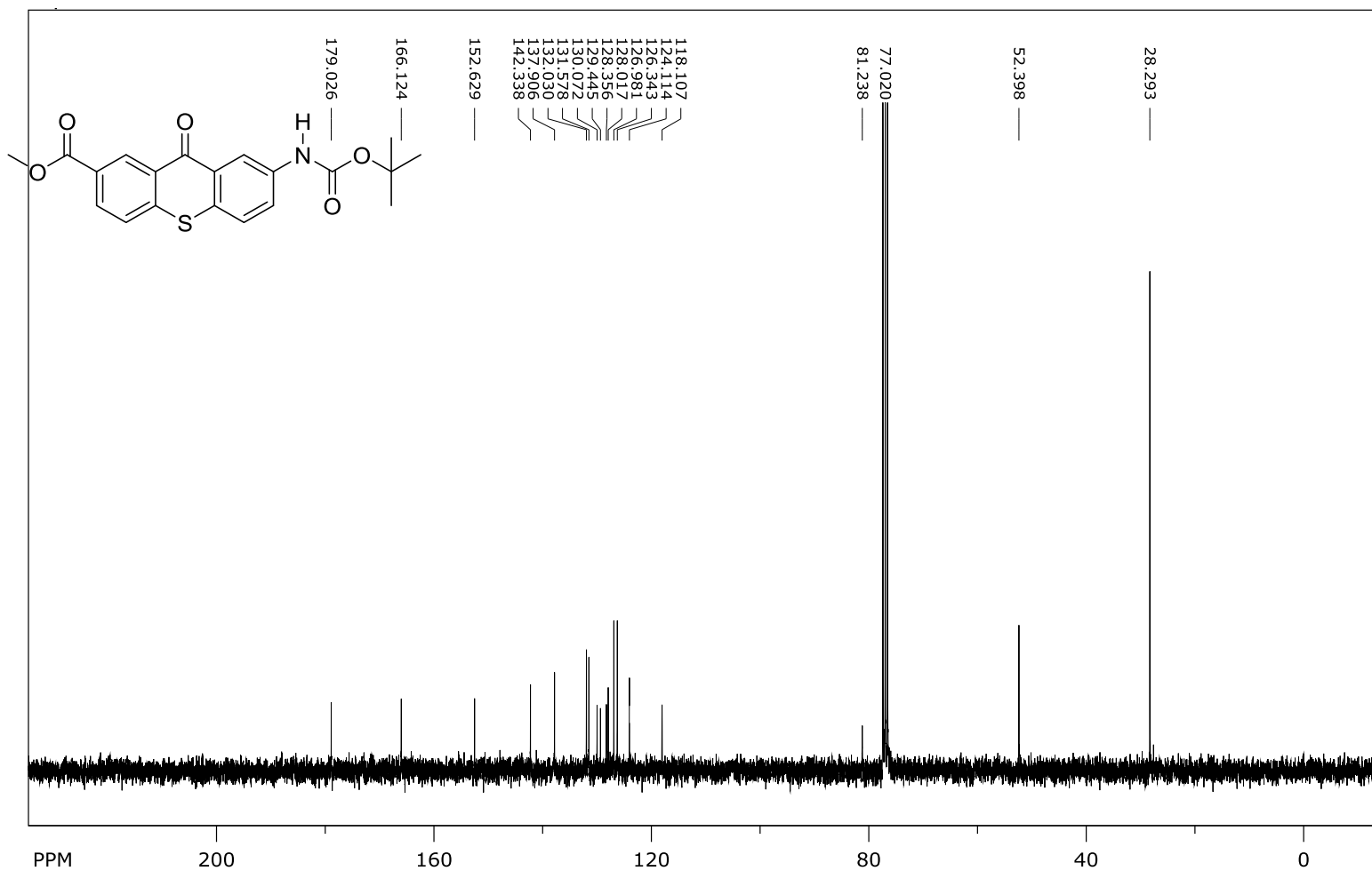
Figure 14. ^{13}C NMR Spectra of Compound **25** in CDCl_3



file: ...016-xanthane-ester-boc-1H.fid\fid block# 1 expt: "s2pul"
transmitter freq.: 399.736103 MHz

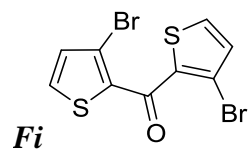
freq. of 0 ppm: 399.733706 MHz
processed size: 65536 complex points

Figure 15. ¹H NMR Spectra of Compound **26** in CDCl₃



file: ...\\180515BOcNHCOOMeTX-Ccdcl3.fid\\fid_block# 1 expt: "s2pul"
transmitter freq.: 75.476336 MHz

freq. of 0 ppm: 75.468051 MHz
processed size: 131072 complex points



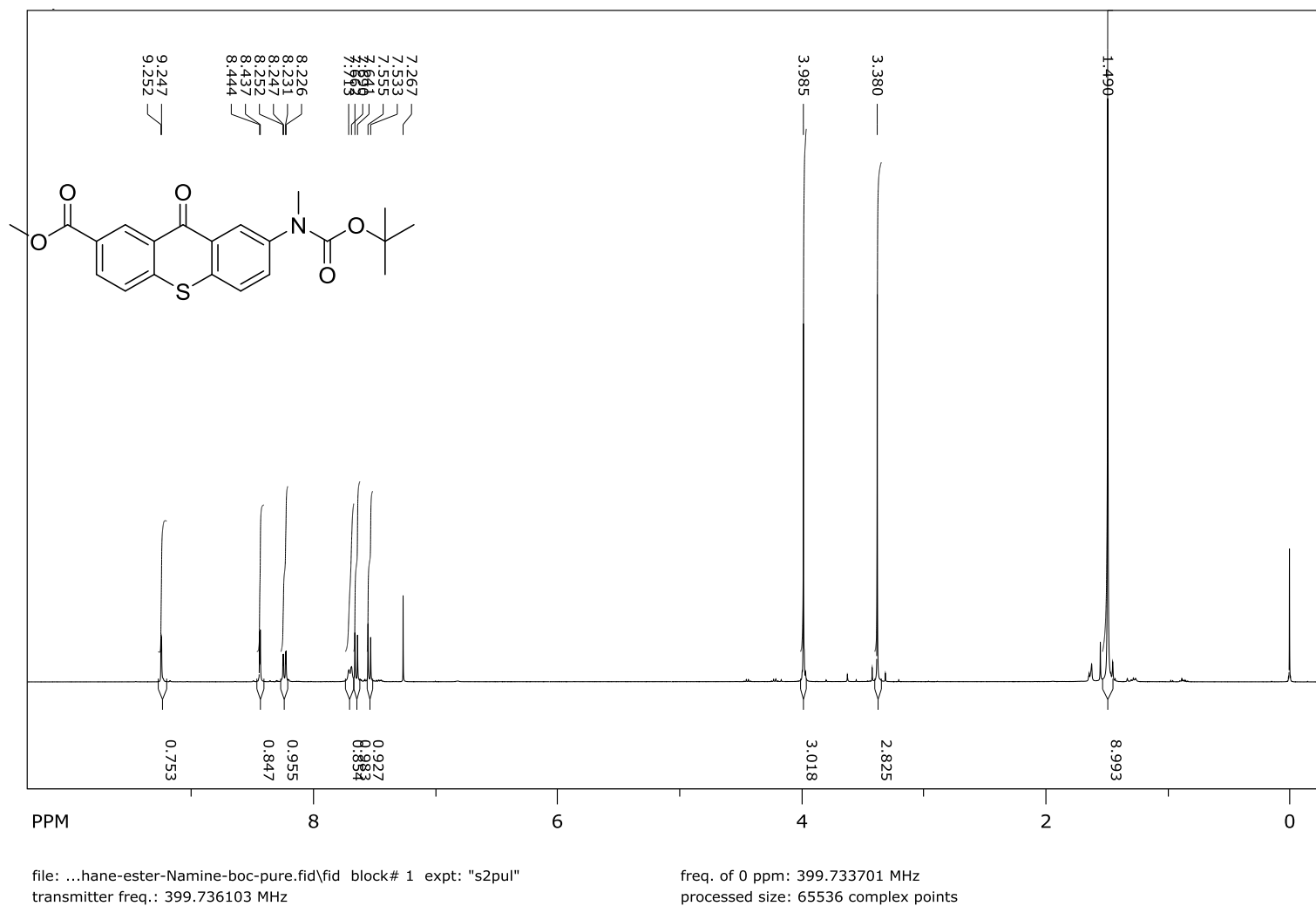


Figure 16. ^1H NMR Spectra of Compound **27** in CDCl_3

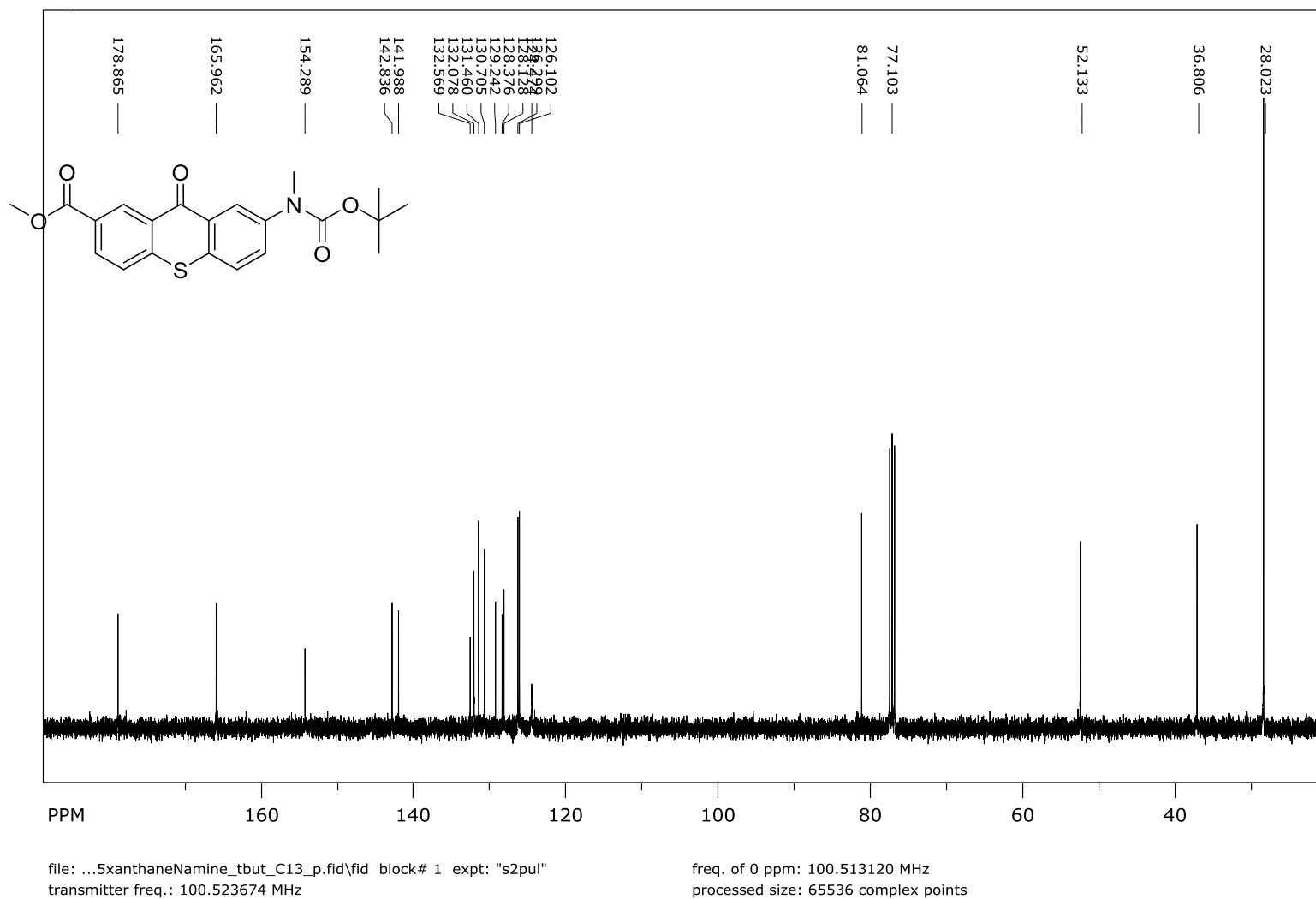


Figure 17. ^1H NMR Spectra of Compound **27** in CDCl_3

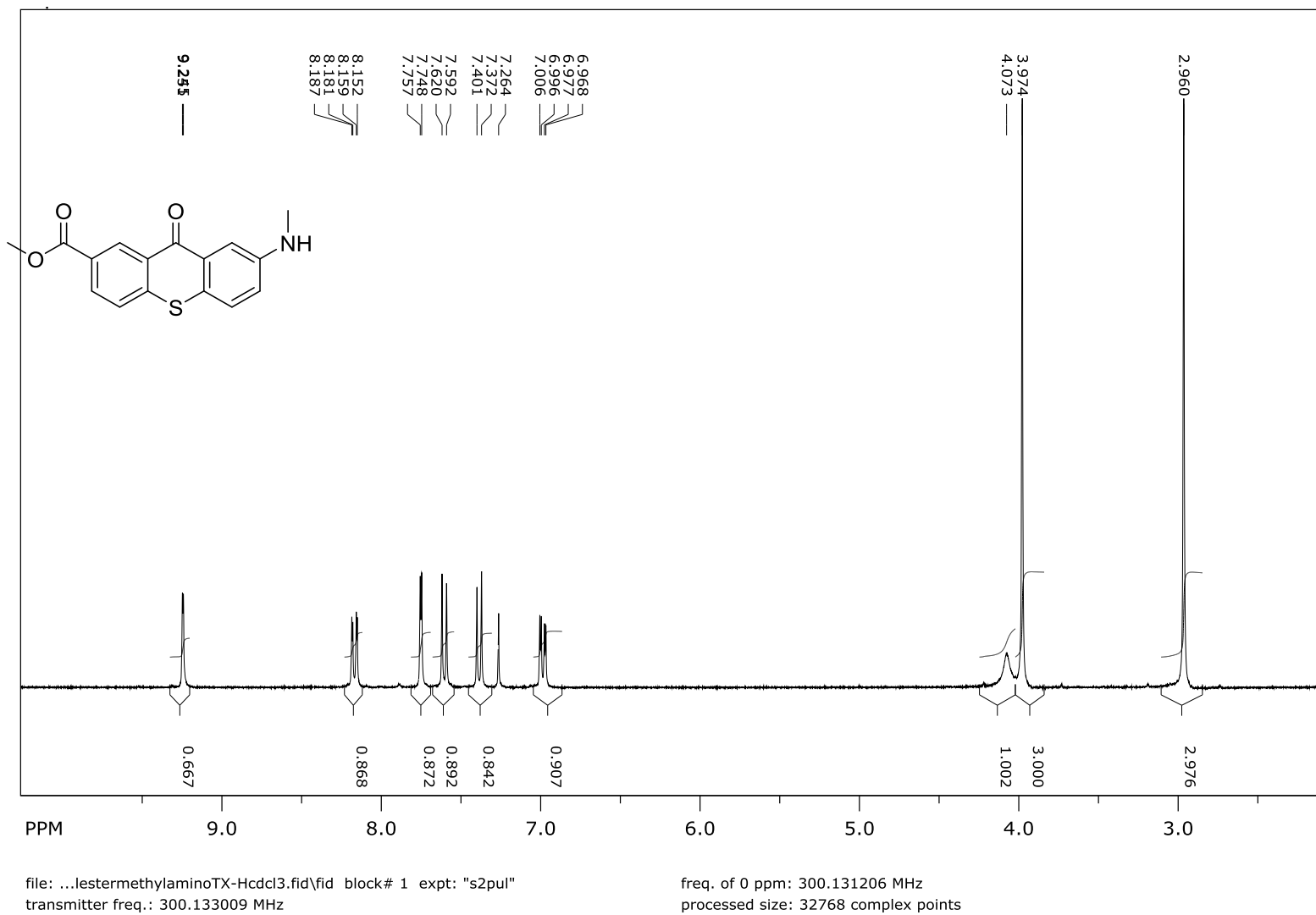


Figure 18. ¹H NMR Spectra of Compound **28** in CDCl₃

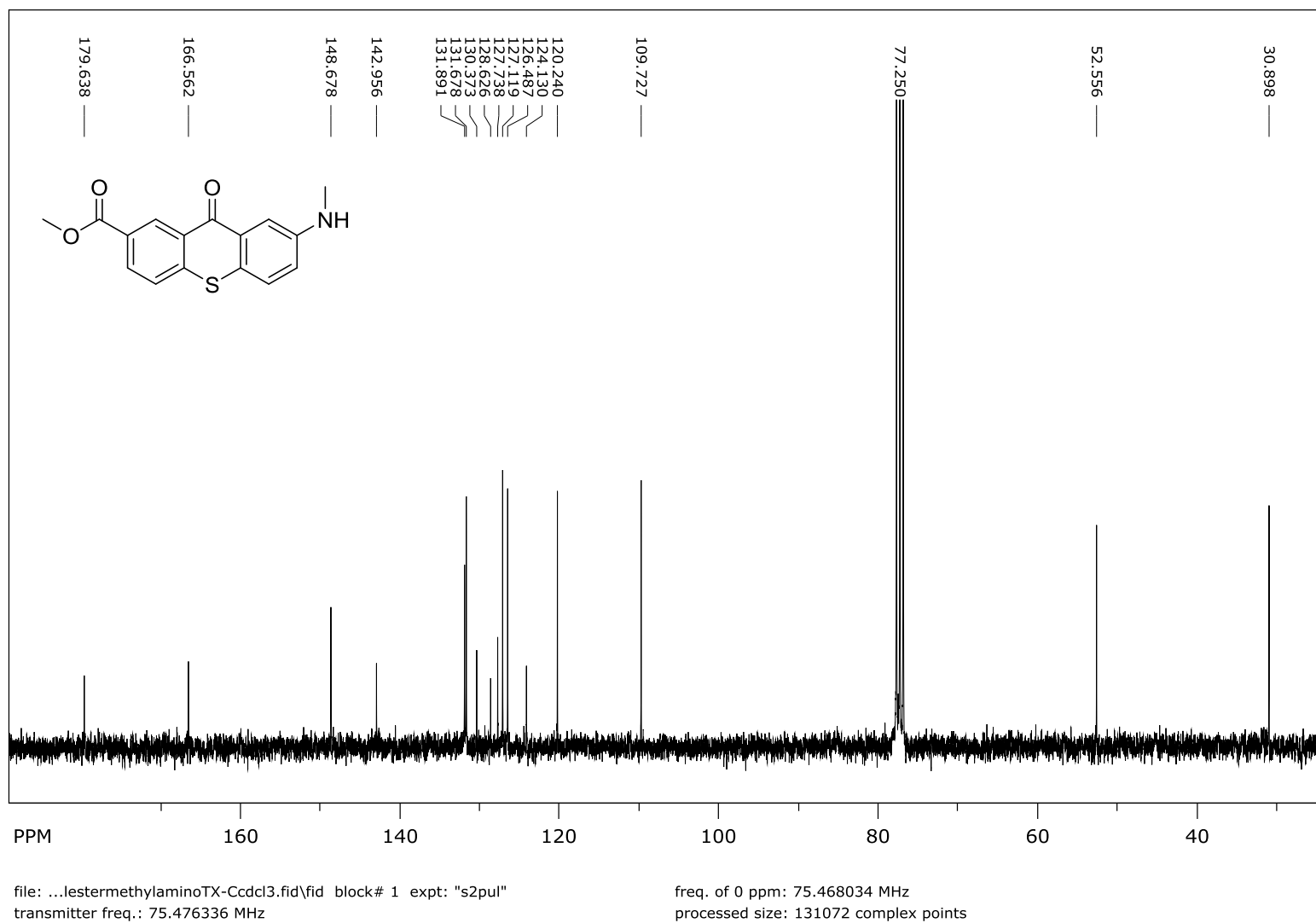
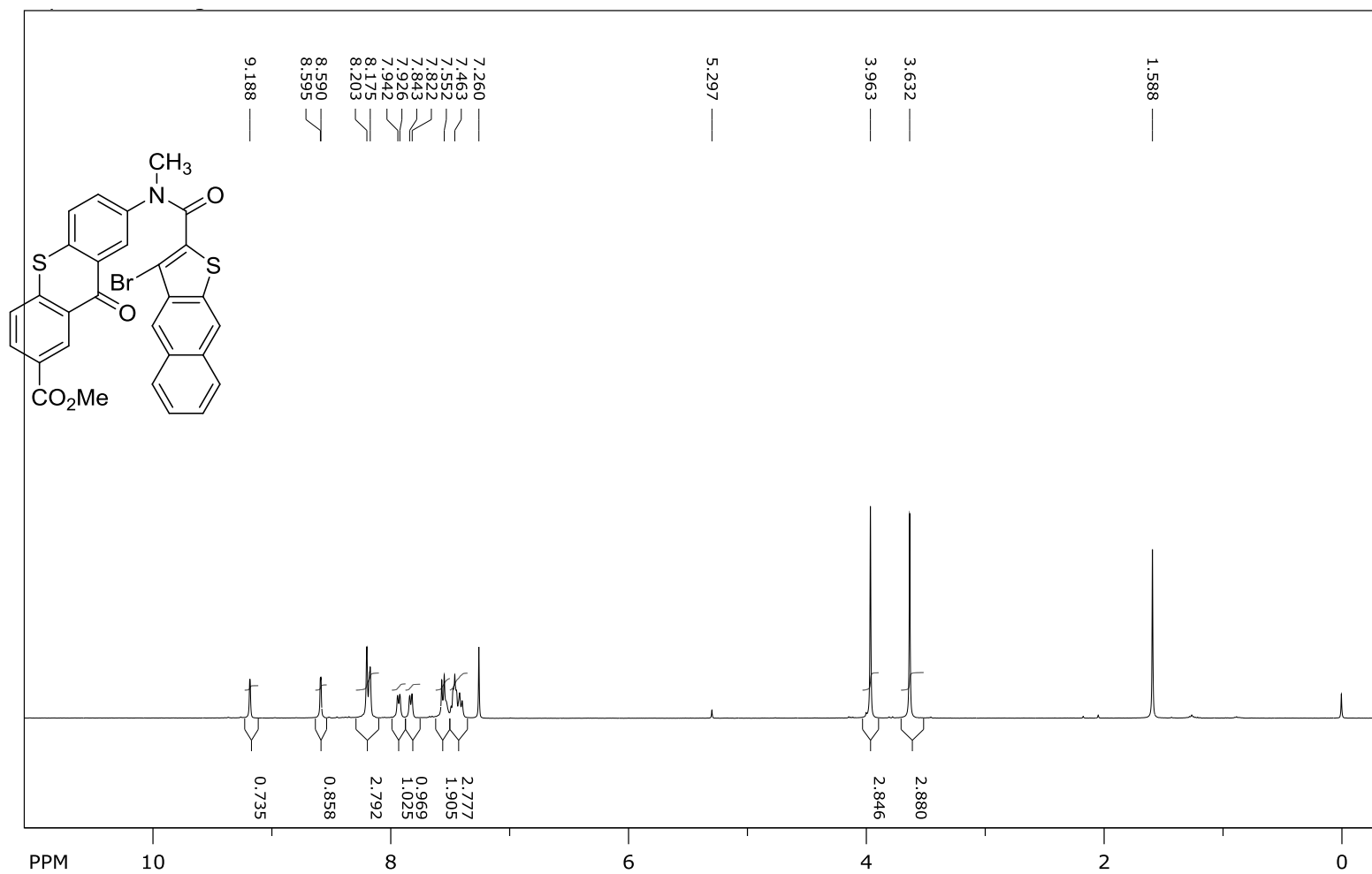


Figure 19. ^{13}C NMR Spectra of Compound **28** in CDCl_3



file: ...rigidTXanilideester-hcdcl3.fid\fid block# 1 expt: "s2pul"
transmitter freq.: 399.734149 MHz

freq. of 0 ppm: 399.731745 MHz
processed size: 32768 complex points

Figure 20. ^1H NMR Spectra of Compound 11a in CDCl_3

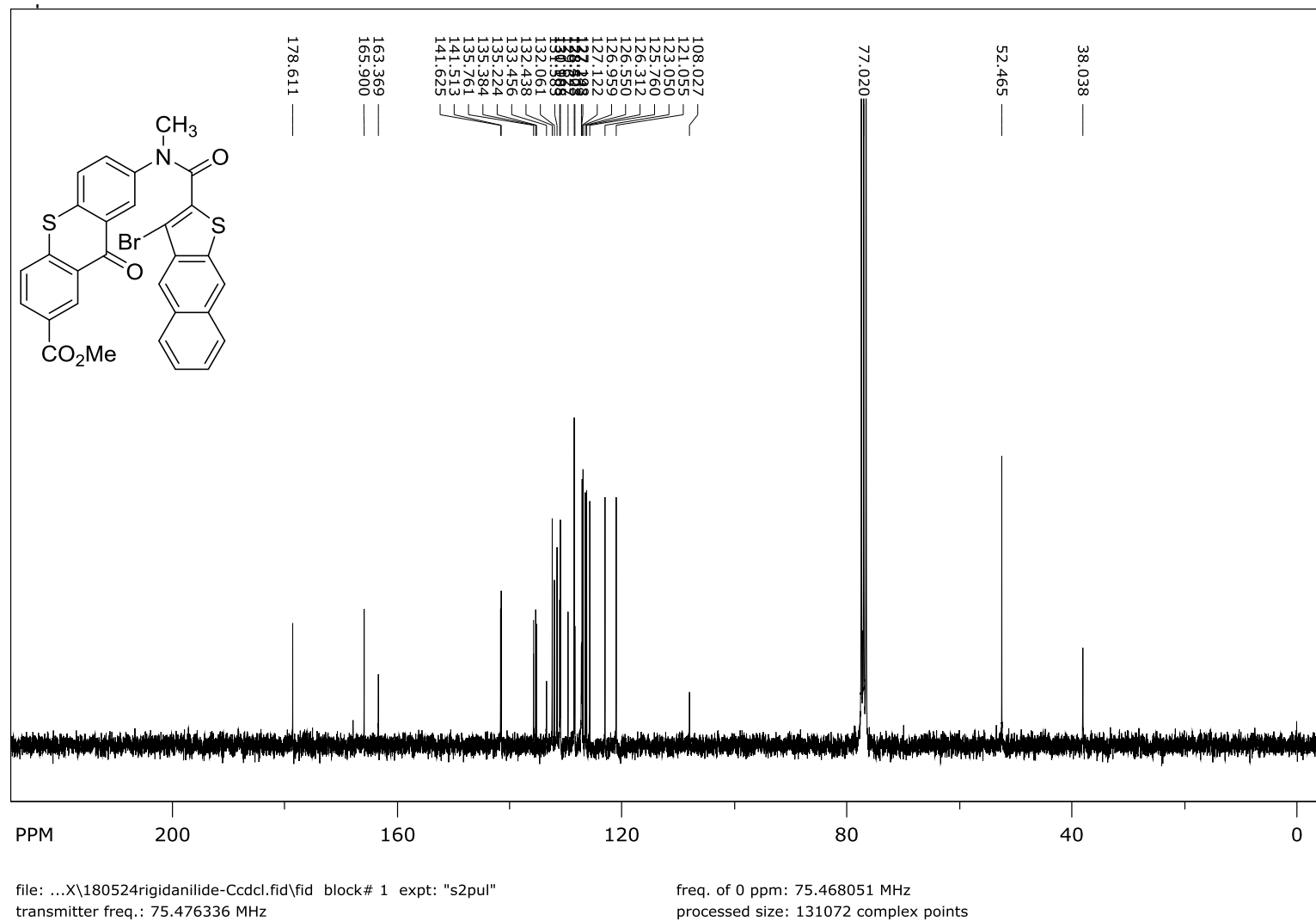
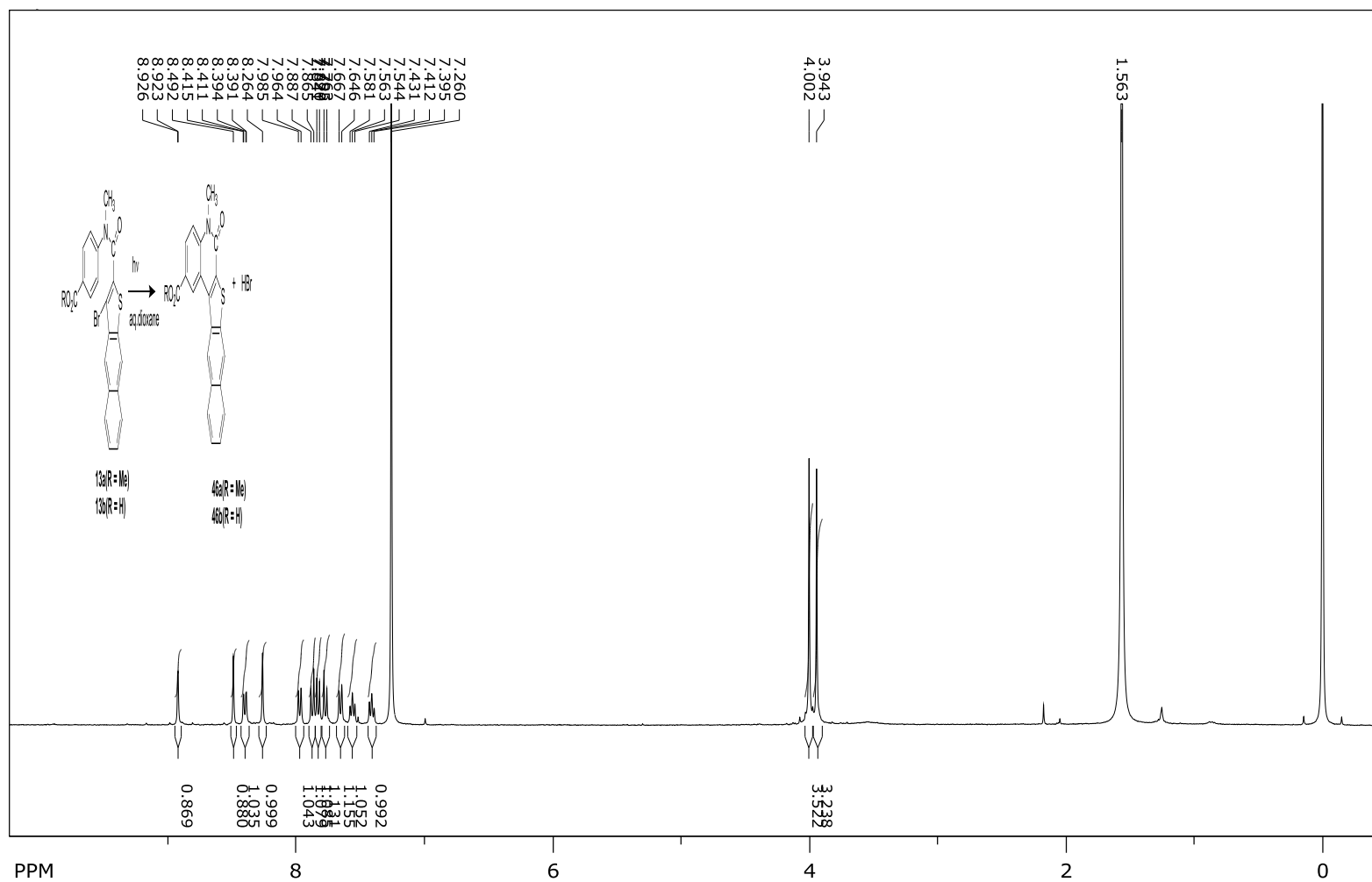


Figure 21. ^{13}C NMR Spectra of Compound **11a** in CDCl_3



file: ...idanilideesterprod1-Hcdcl3.fid\fid_block# 1 exp: "s2pul"
 transmitter freq.: 399.734149 MHz

freq. of 0 ppm: 399.731745 MHz
 processed size: 32768 complex points

Figure 22. ¹H NMR Spectra of Compound **43a** in CDCl₃.

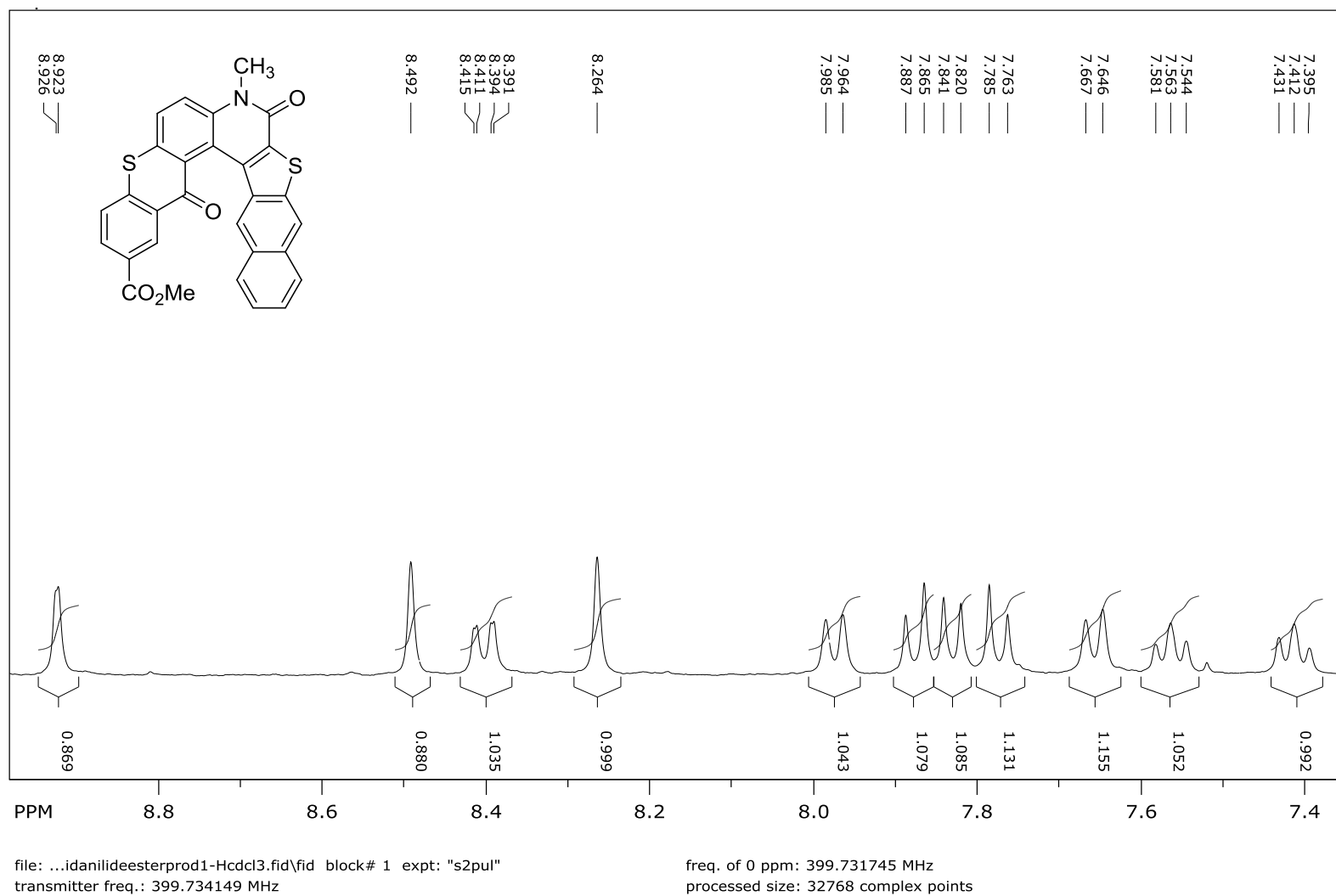


Figure 23. Expanded (8.90 – 7.30 ppm) ¹H NMR Spectra of Compound **43a** in CDCl₃

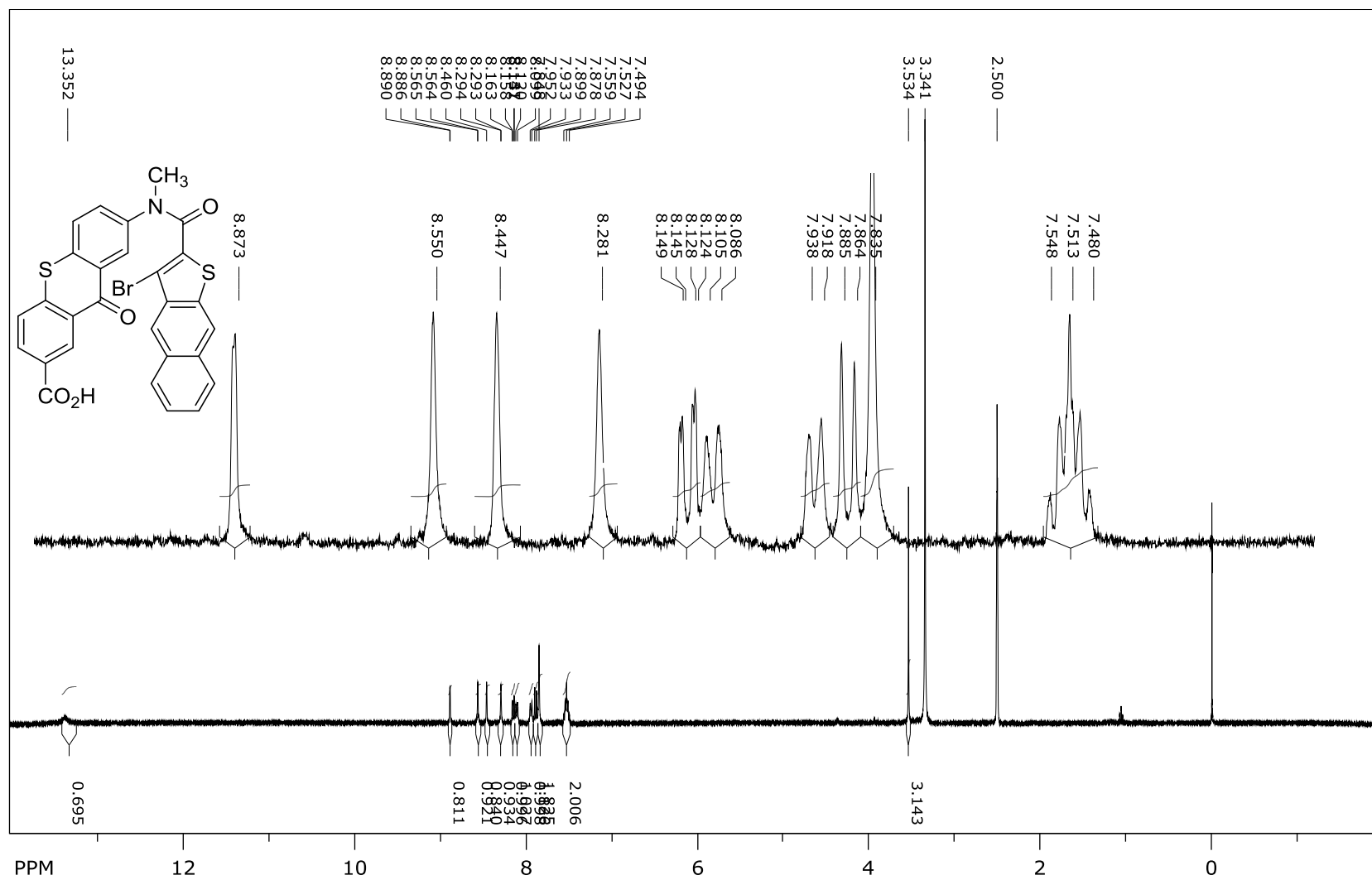
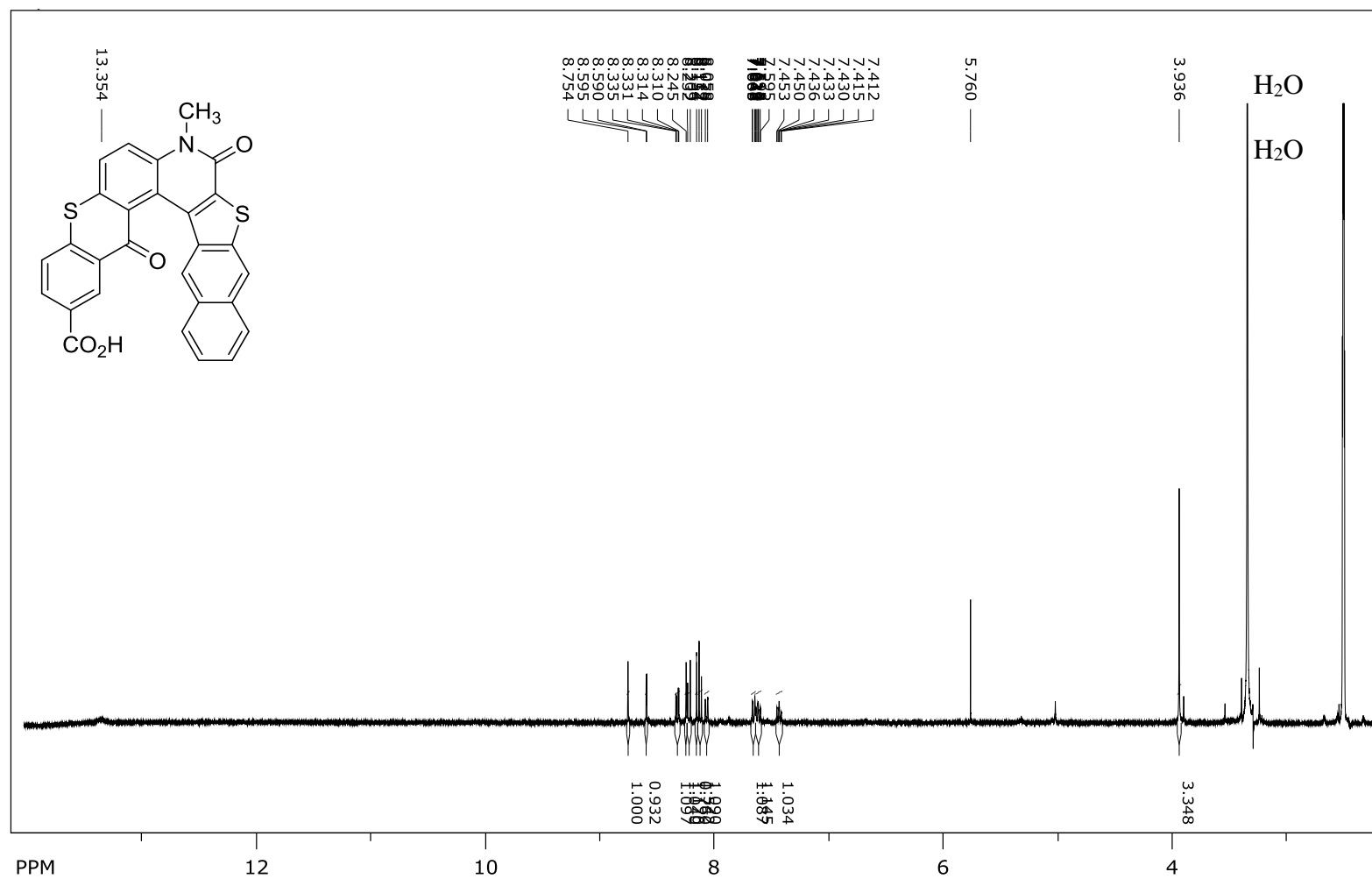


Figure 24. ¹H NMR Spectra of Compound 11b in DMSO-*d*₆.



file: ...160328dmsophtlworkup-Hdmsol.fid block# 1 expt: "s2pul"
 transmitter freq.: 399.738002 MHz

freq. of 0 ppm: 399.735598 MHz
 processed size: 65536 complex points

Figure 25. ¹H NMR Spectra of Compound **43b** in DMSO-*d*₆.

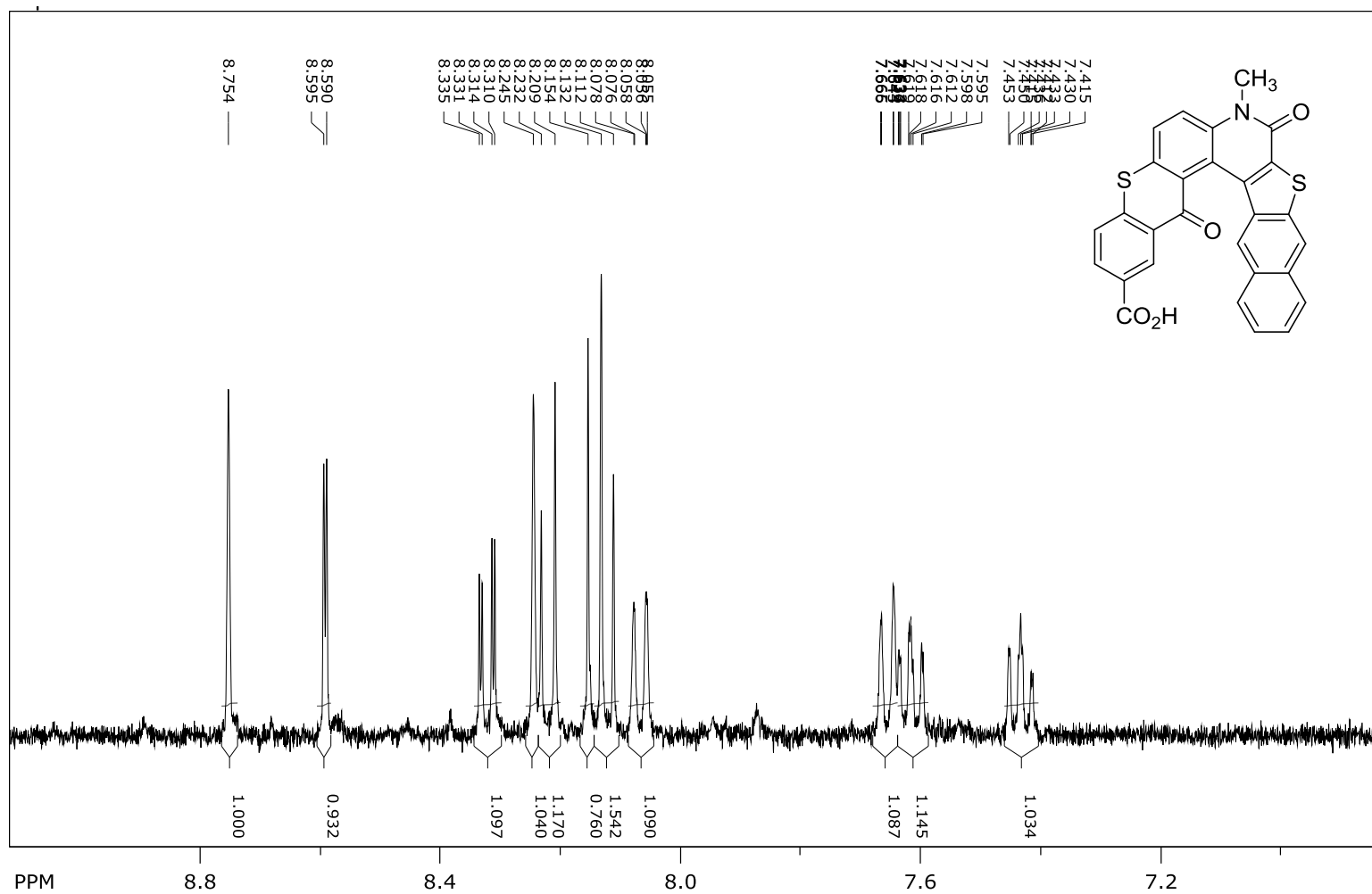
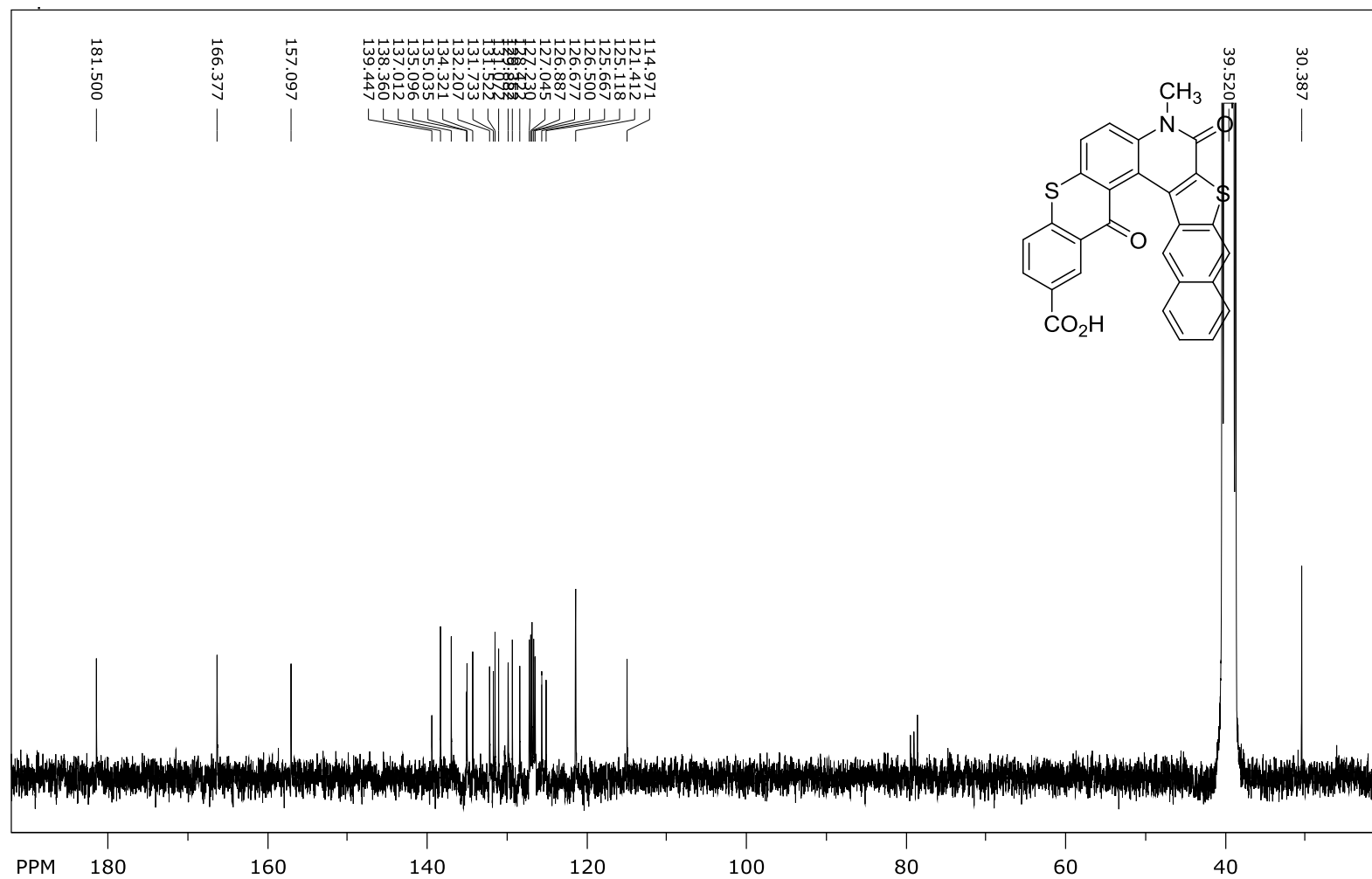


Figure 26. Expanded (8.80 – 7.20 ppm) ^1H NMR Spectra of Compound **43a** in $\text{DMSO-}d_6$



file: ...\\180529rigidcoohprod-Cdms0.fid\\fid_block# 1_expt: "s2pul"
transmitter freq.: 75.476694 MHz

freq. of 0 ppm: 75.468440 MHz
processed size: 131072 complex points

Figure 27. ^{13}C NMR Spectra of Compound **43b** in $\text{DMSO-}d_6$

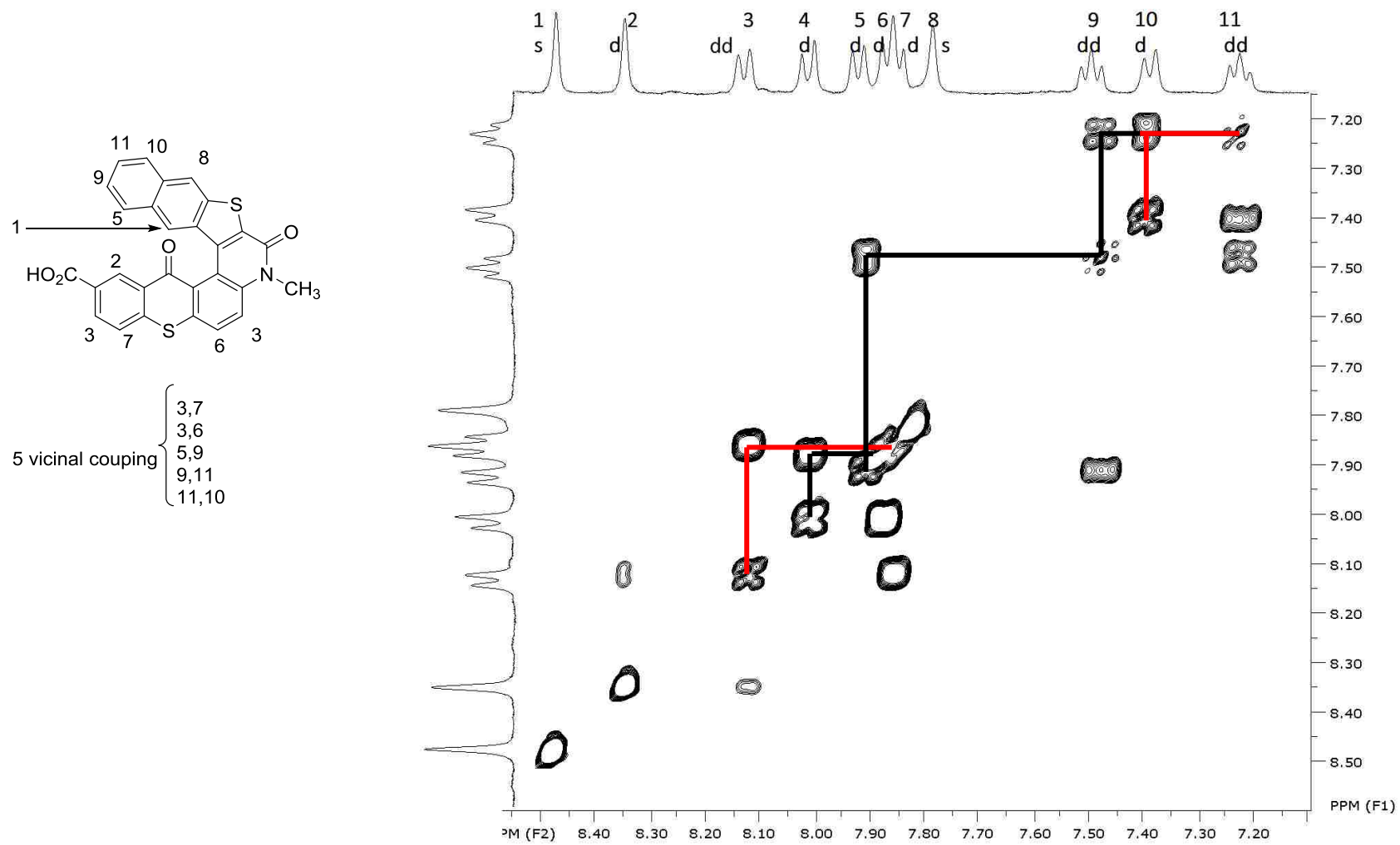


Figure 28. Cosy Spectra (400 MHz) of Compound **43b** in DMSO-*d*₆

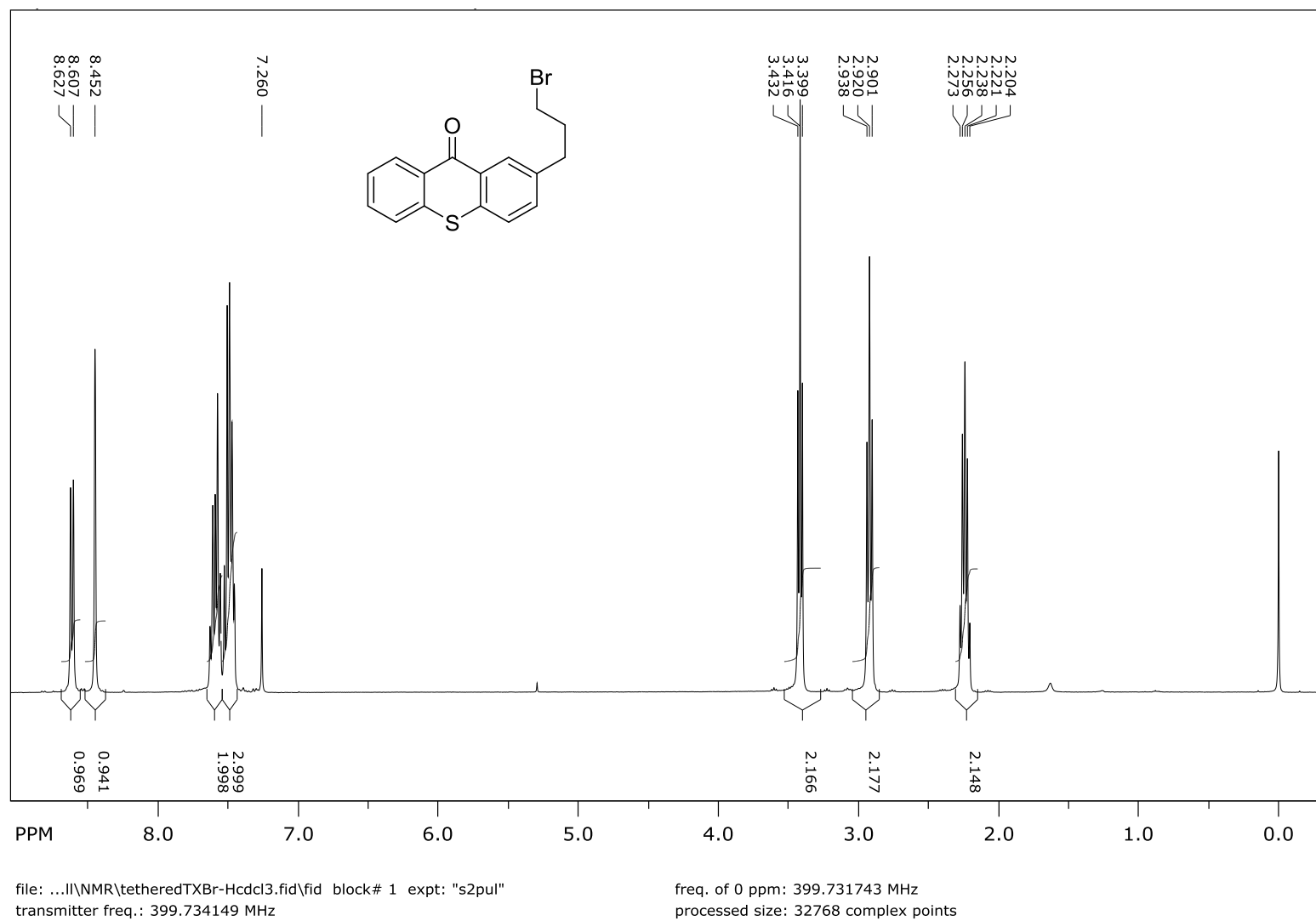
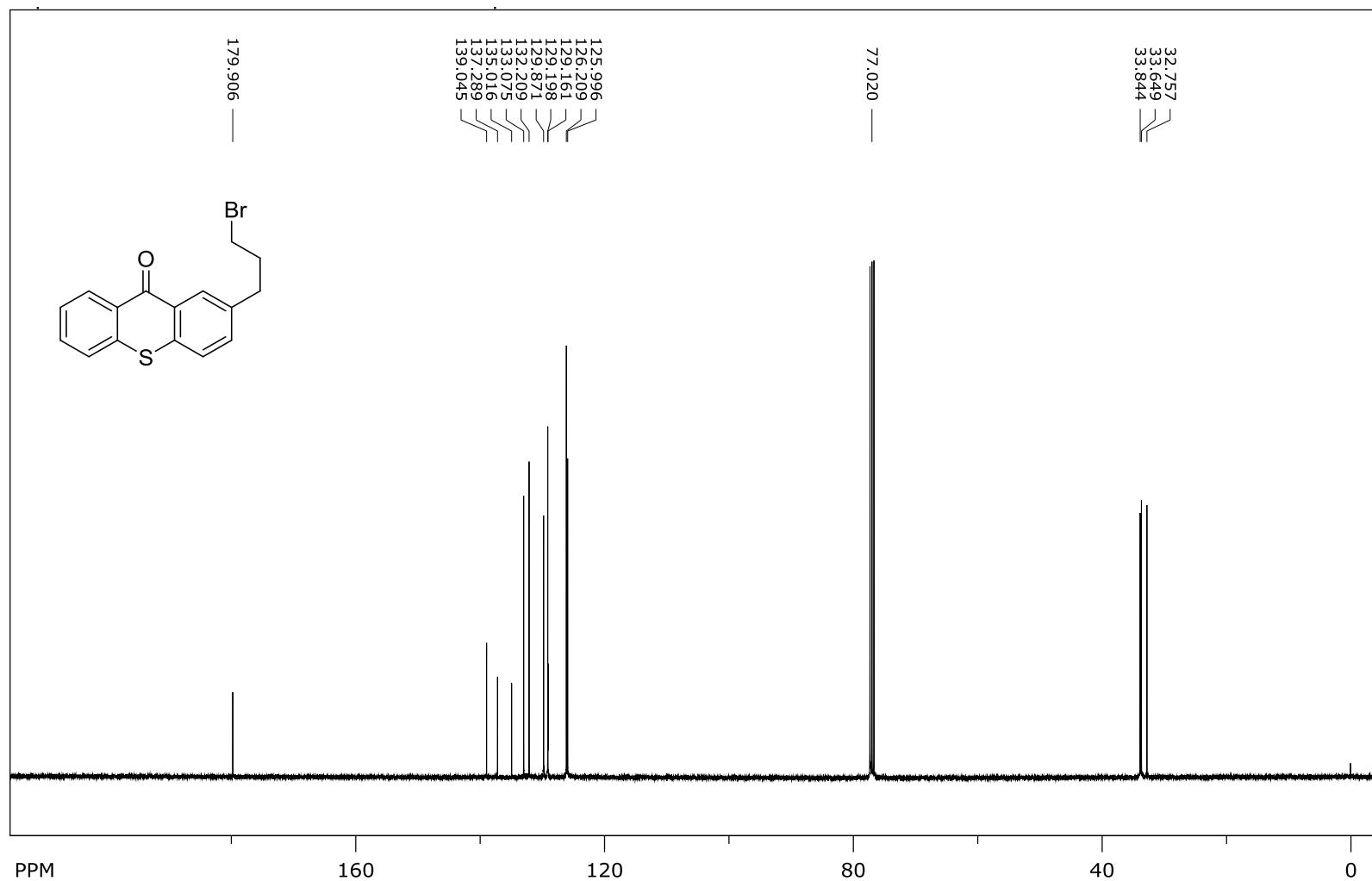


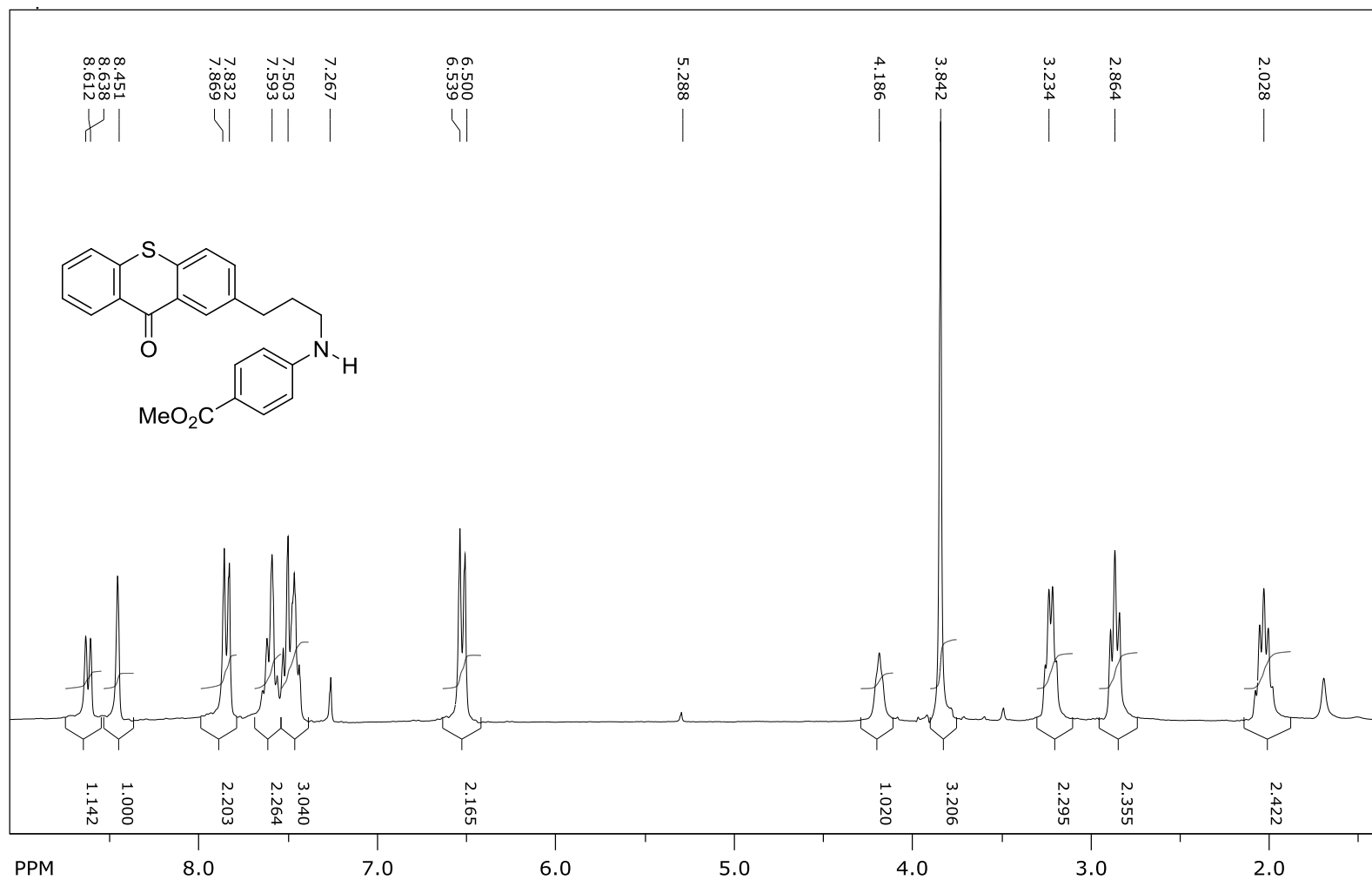
Figure 29. ^1H NMR Spectra of Compound 31 in CDCl_3



file: ...NMR\tetheredTXBrcon-Cdcl3.fid\fid block# 1 expt: "s2pul"
transmitter freq.: 100.523685 MHz

freq. of 0 ppm: 100.512627 MHz
processed size: 65536 complex points

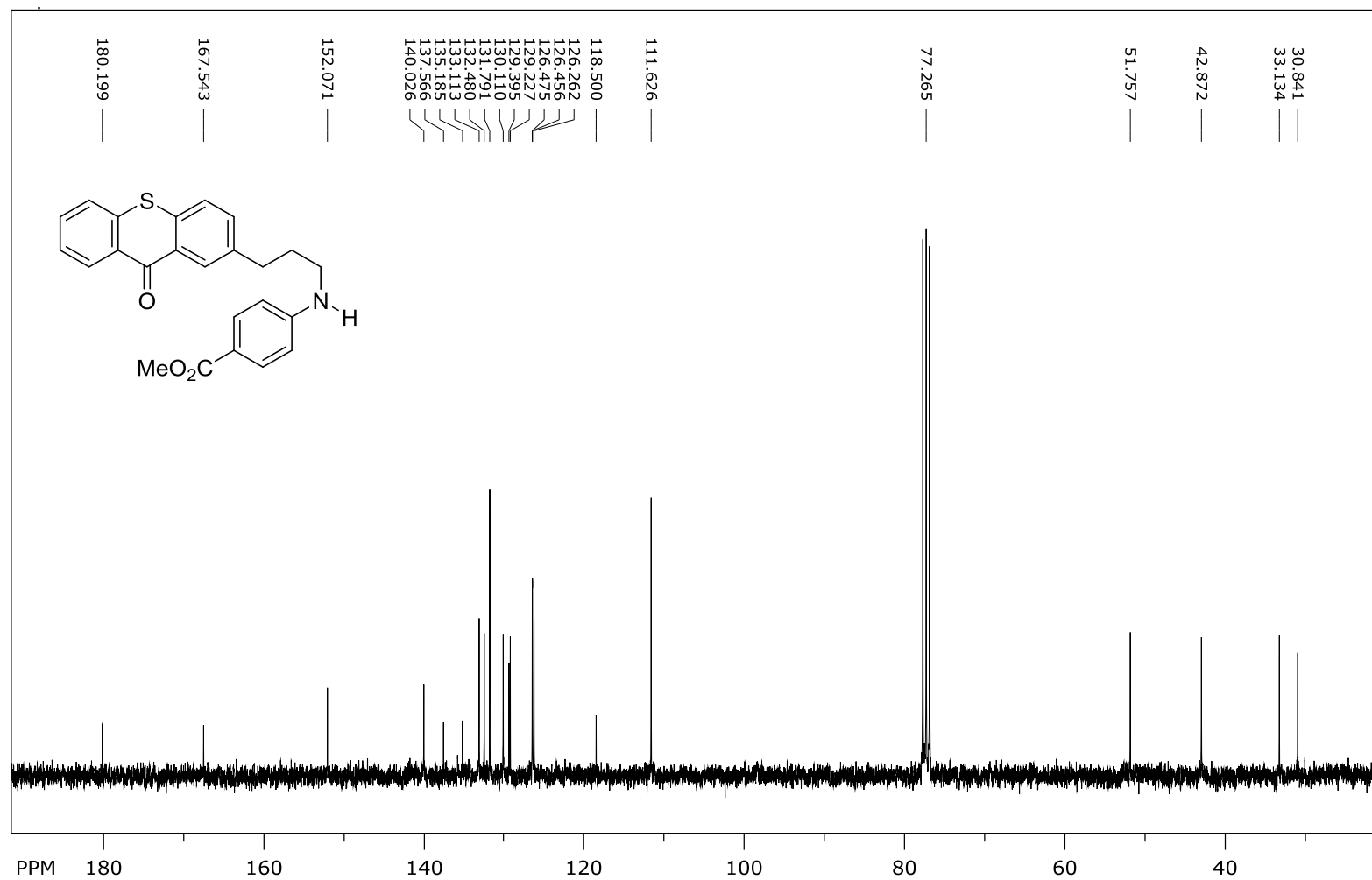
Figure 30. ^{13}C NMR Spectra of Compound **31** in CDCl_3



file: ...170220tetheredamine-Hcdcl3.fid\fid block# 1 expt: "s2pul"
transmitter freq.: 300.133009 MHz

freq. of 0 ppm: 300.131205 MHz
processed size: 32768 complex points

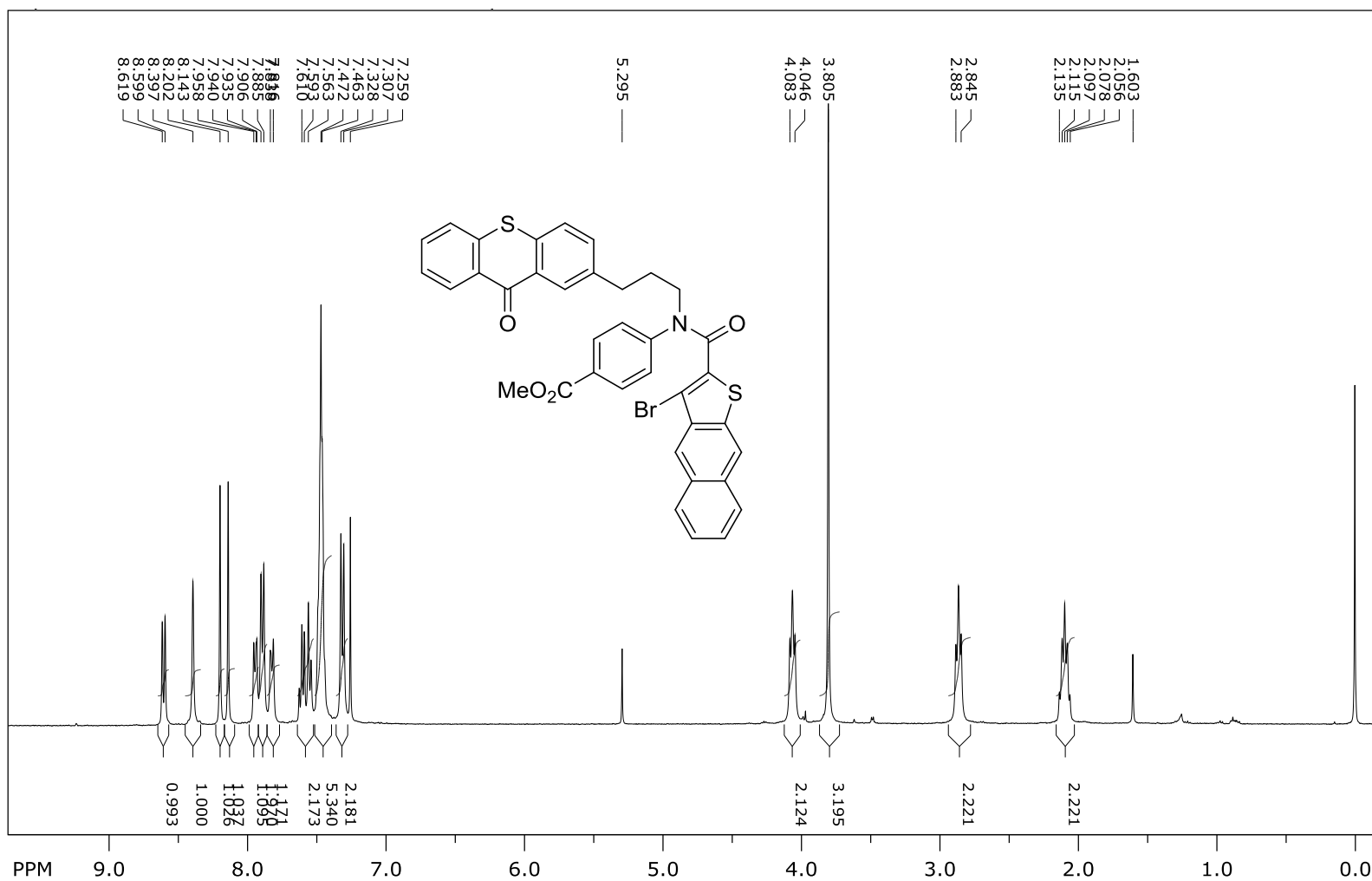
Figure 31. ^1H NMR Spectra of Compound **33** in CDCl_3



file: ...170220tetheredamine-Ccdcl3.fid\fid block# 1 expt: "s2pul"
transmitter freq.: 75.476336 MHz

freq. of 0 ppm: 75.468034 MHz
processed size: 131072 complex points

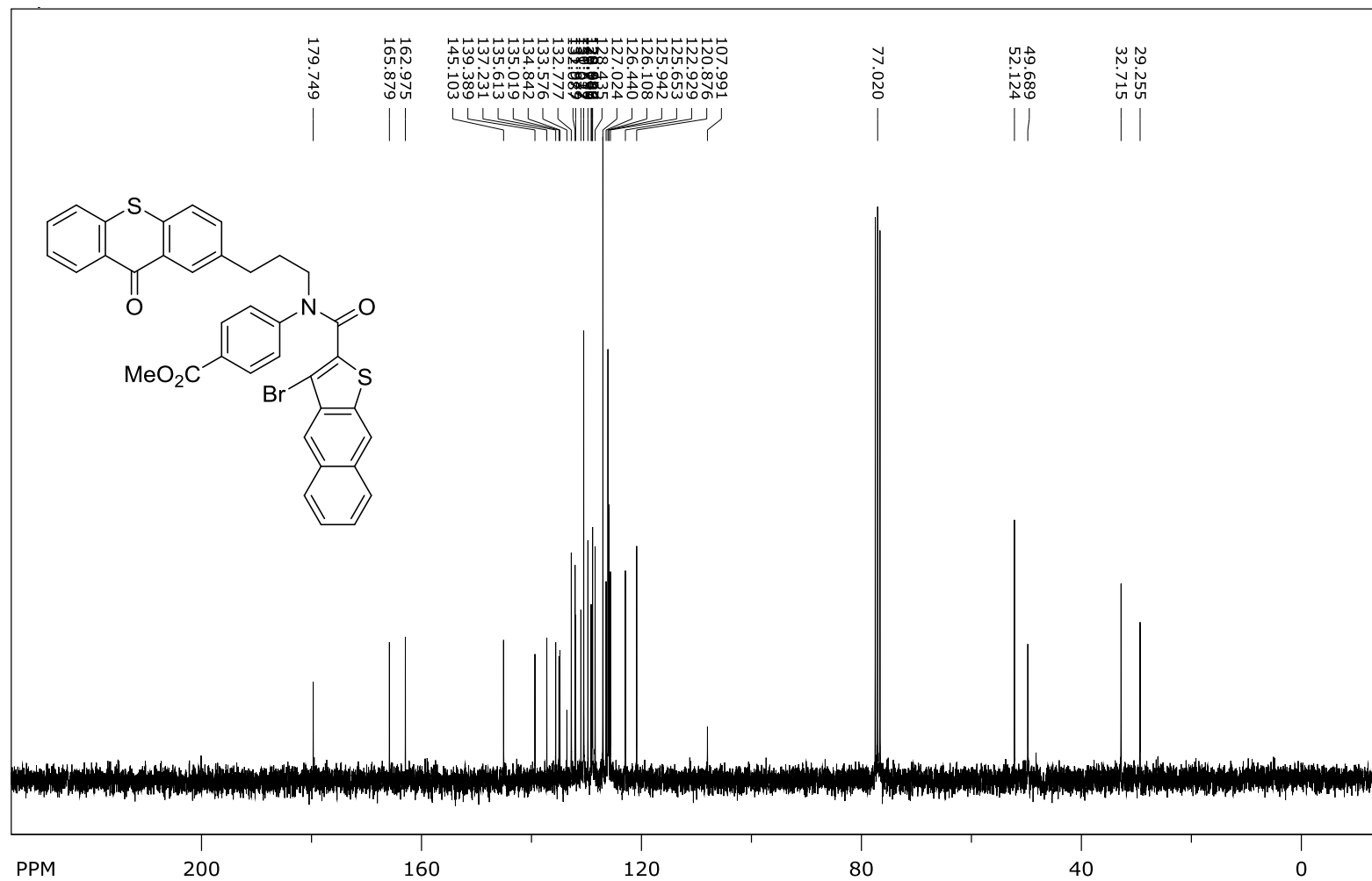
Figure 32. ¹³C NMR Spectra of Compound 33 in CDCl₃



file: ...redesteranilideLGBR-hcdcl3.fid\fid block# 1 expt: "s2pul"
 transmitter freq.: 399.734149 MHz

freq. of 0 ppm: 399.731743 MHz
 processed size: 32768 complex points

Figure 33. ¹H NMR Spectra of Compound 12 in CDCl₃



file: ...MR\180405tetheredBr-ccdcl3.fid\fid block# 1 expt: "s2pul"
transmitter freq.: 75.476336 MHz

freq. of 0 ppm: 75.468056 MHz
processed size: 131072 complex points

Figure 34. ^{13}C NMR Spectra of Compound 12 in CDCl_3

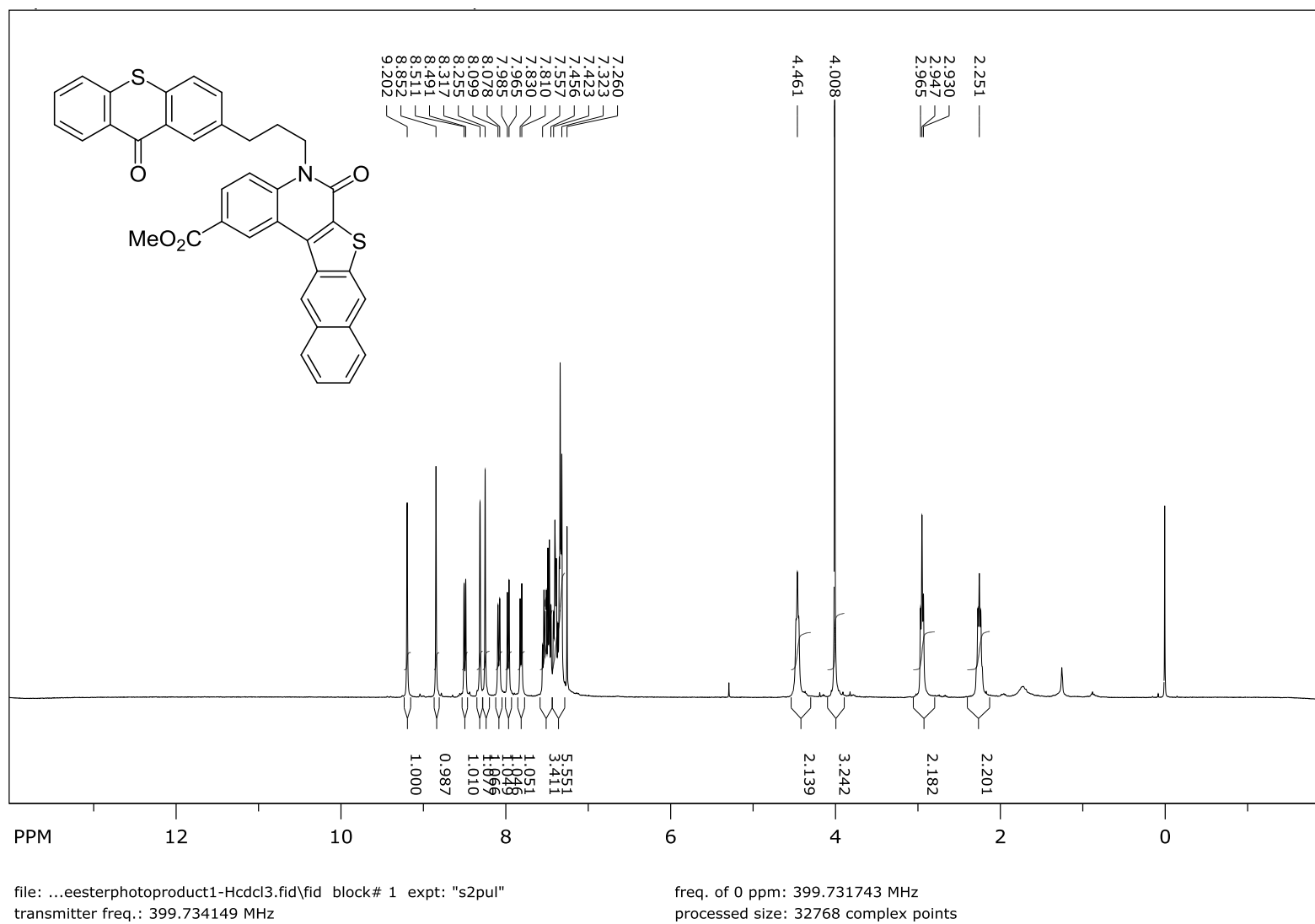
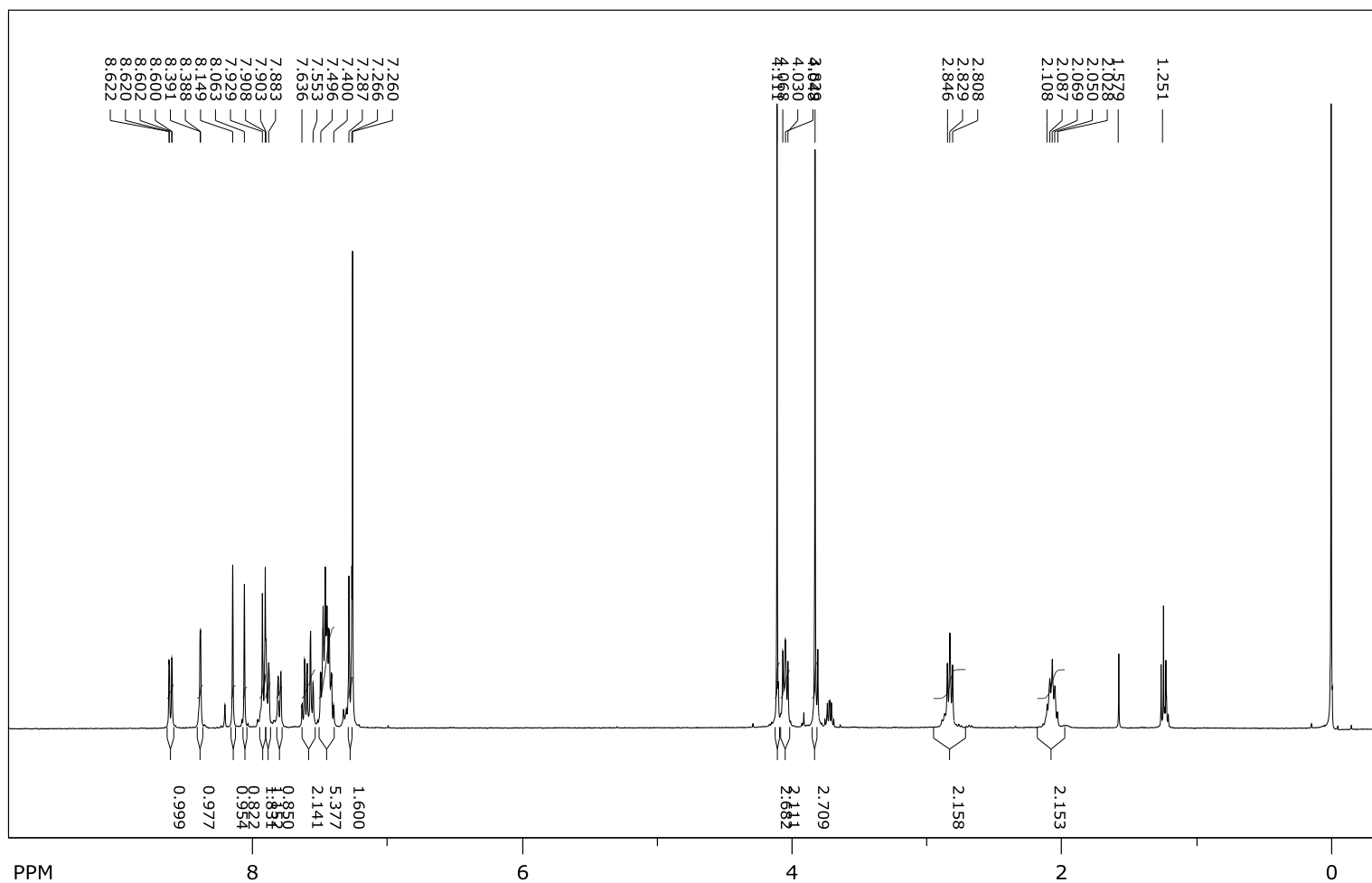


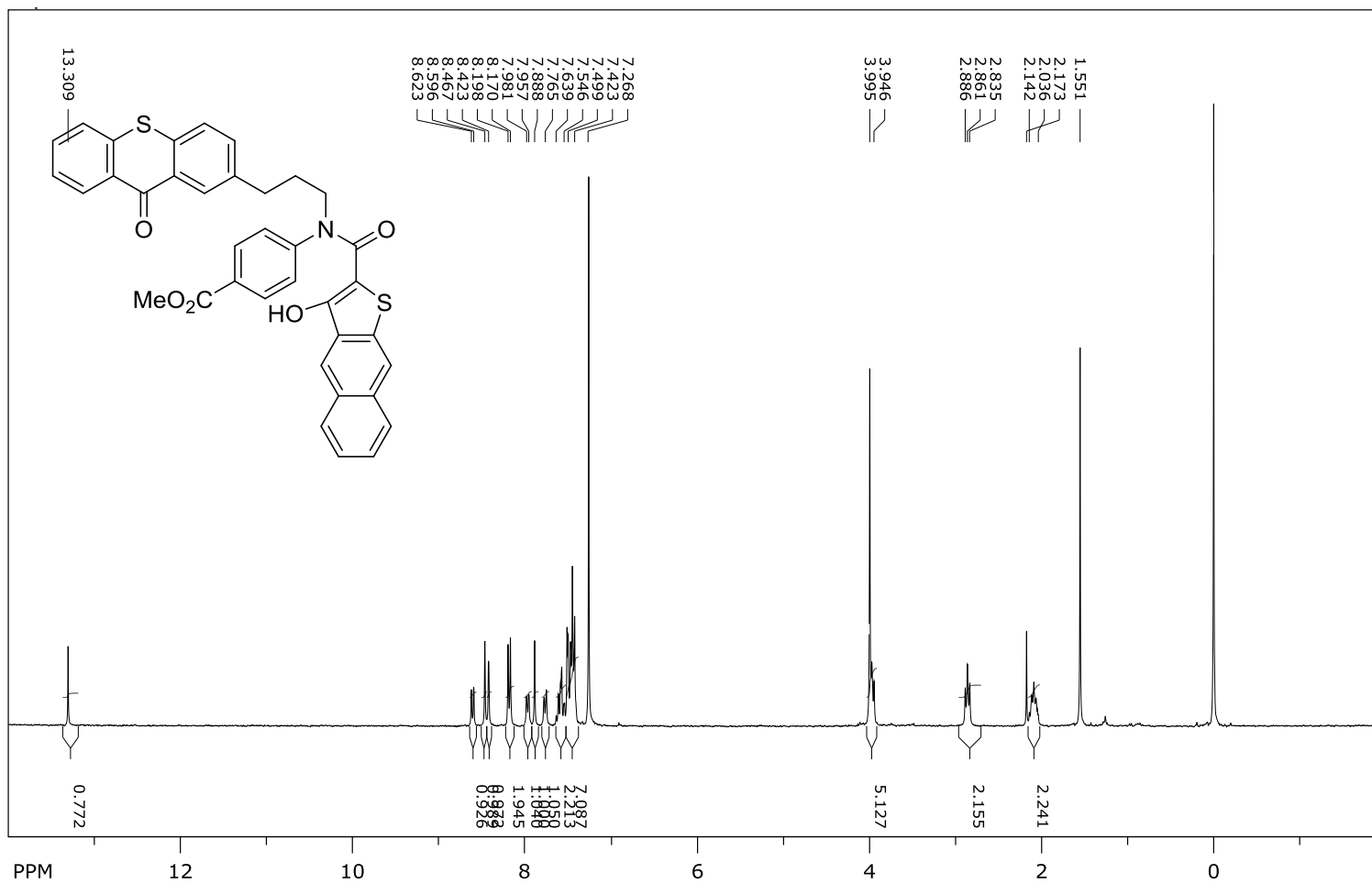
Figure 35. ^1H NMR Spectra of Compound **45** in CDCl_3



file: ...8tetheredesterOMeLG-Hcdcle.fid\fid block# 1 expt: "s2pul"
 transmitter freq.: 399.734149 MHz

freq. of 0 ppm: 399.731743 MHz
 processed size: 32768 complex points

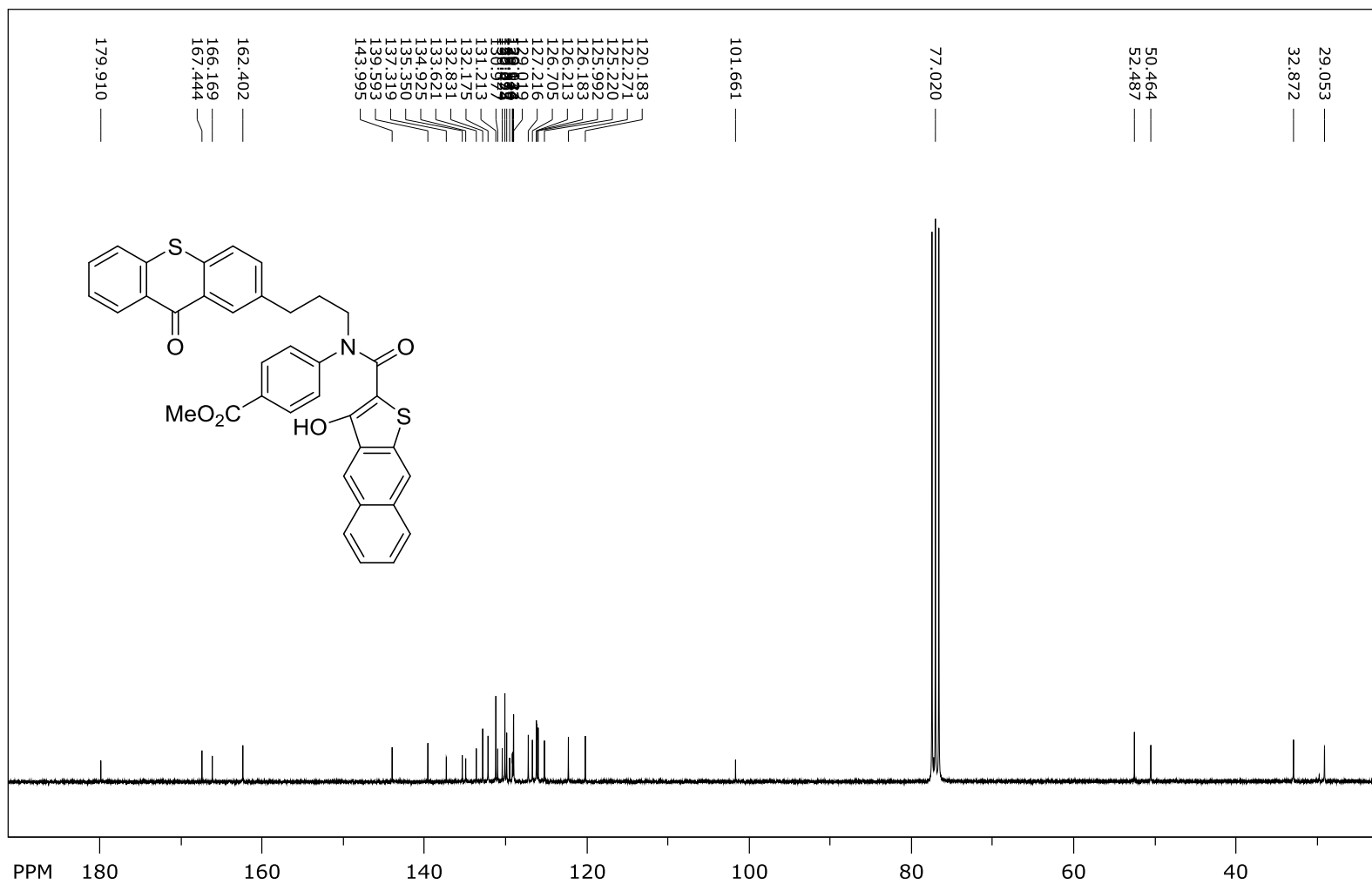
Figure 37. ^1H NMR spectra of compound **40** in CDCl_3 .



file: ...MR\180403tetheredOH-Hcdcl3.fid\fid block# 1 expt: "s2pul"
 transmitter freq.: 300.133009 MHz

freq. of 0 ppm: 300.131207 MHz
 processed size: 32768 complex points

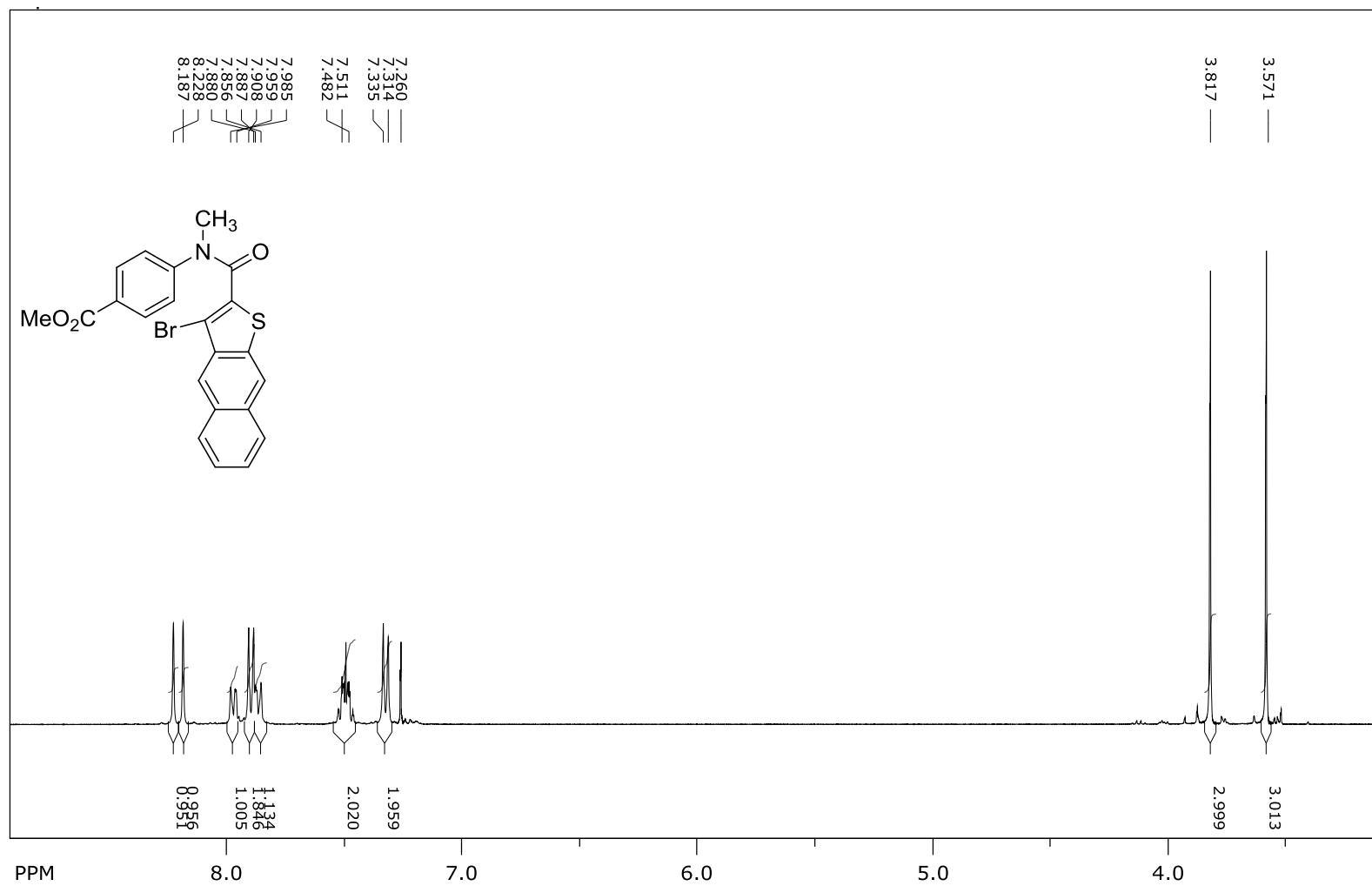
Figure 38. ^1H NMR Spectra of Compound **41** in CDCl_3



file: ...0404tetheredesterOH-Ccdcl3.fid\fid block# 1 expt: "s2pul"
 transmitter freq.: 75.476336 MHz

freq. of 0 ppm: 75.468051 MHz
 processed size: 131072 complex points

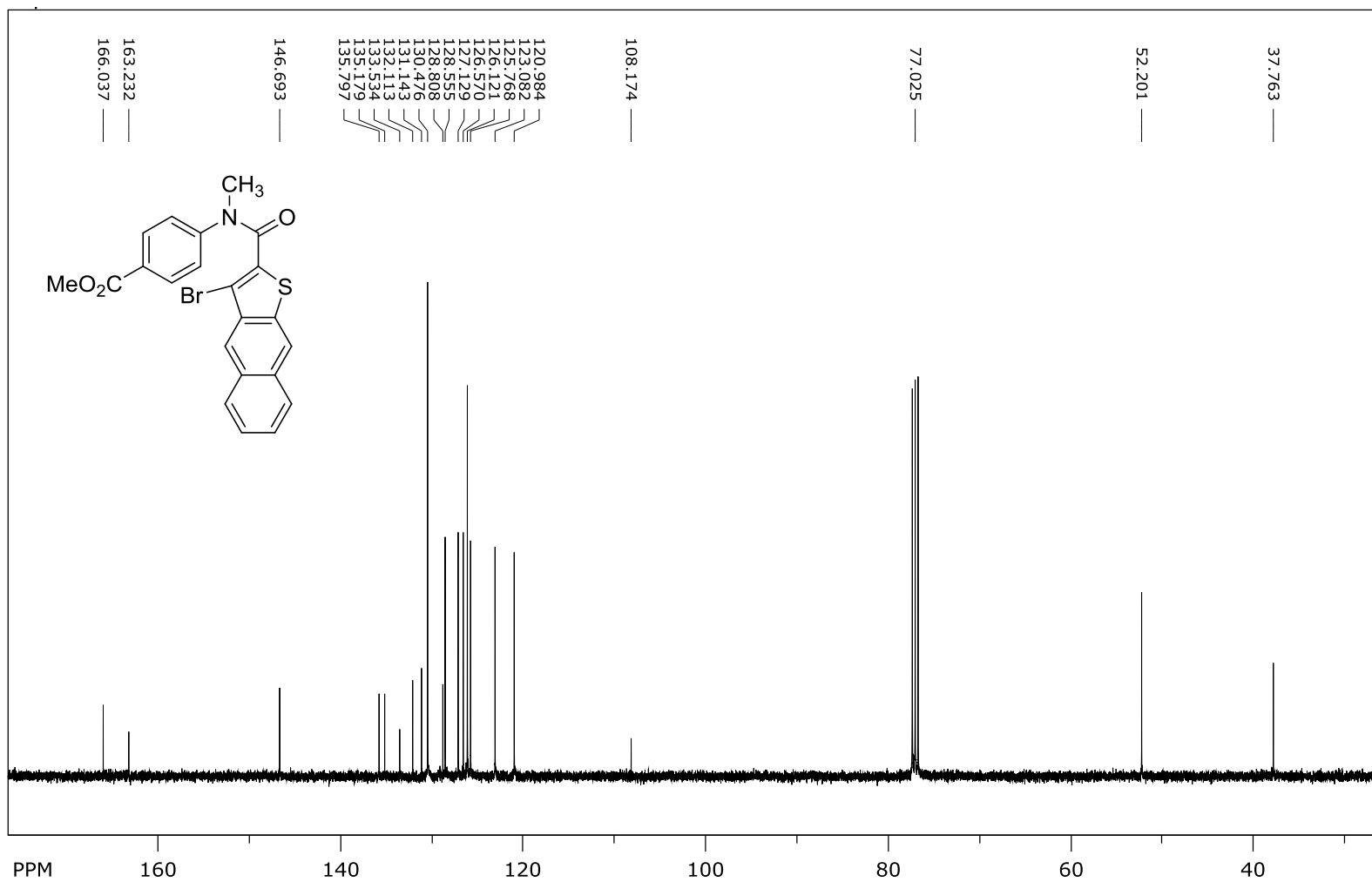
Figure 39. ^{13}C NMR Spectra of Compound **41** in CDCl_3



file: ...esteranilidenaphtho-Hcdcl3.fid\fid block# 1 expt: "s2pul"
transmitter freq.: 399.736103 MHz

freq. of 0 ppm: 399.733704 MHz
processed size: 65536 complex points

Figure 40. ^1H NMR Spectra of Compound **13a** in CDCl_3



file: ...esteranilidenaphtho-Ccdcl3.fid\fid block# 1 expt: "s2pul"
transmitter freq.: 100.523674 MHz

freq. of 0 ppm: 100.513120 MHz
processed size: 65536 complex points

Figure 41. ¹³C NMR Spectra of Compound **13a** in CDCl₃

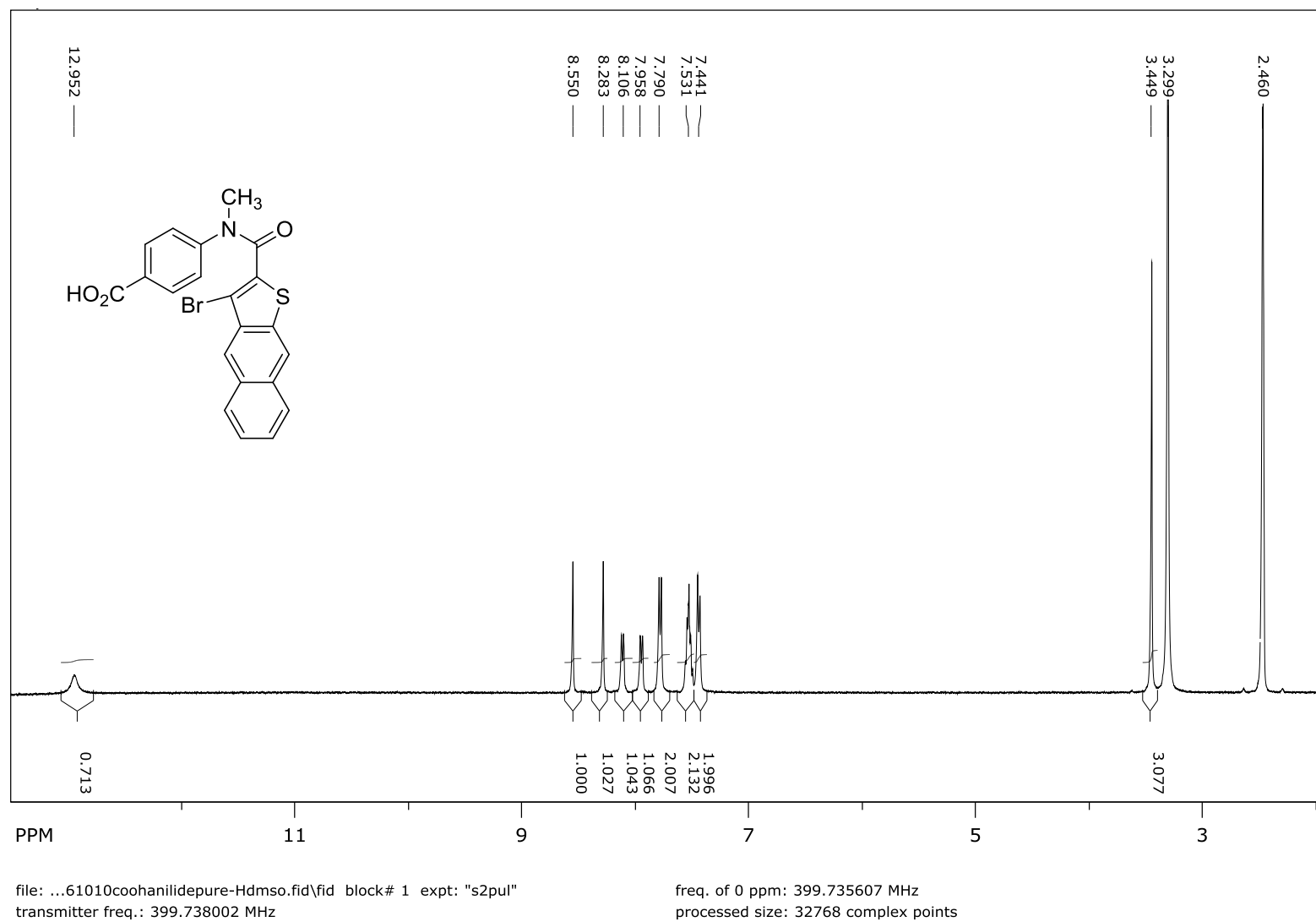
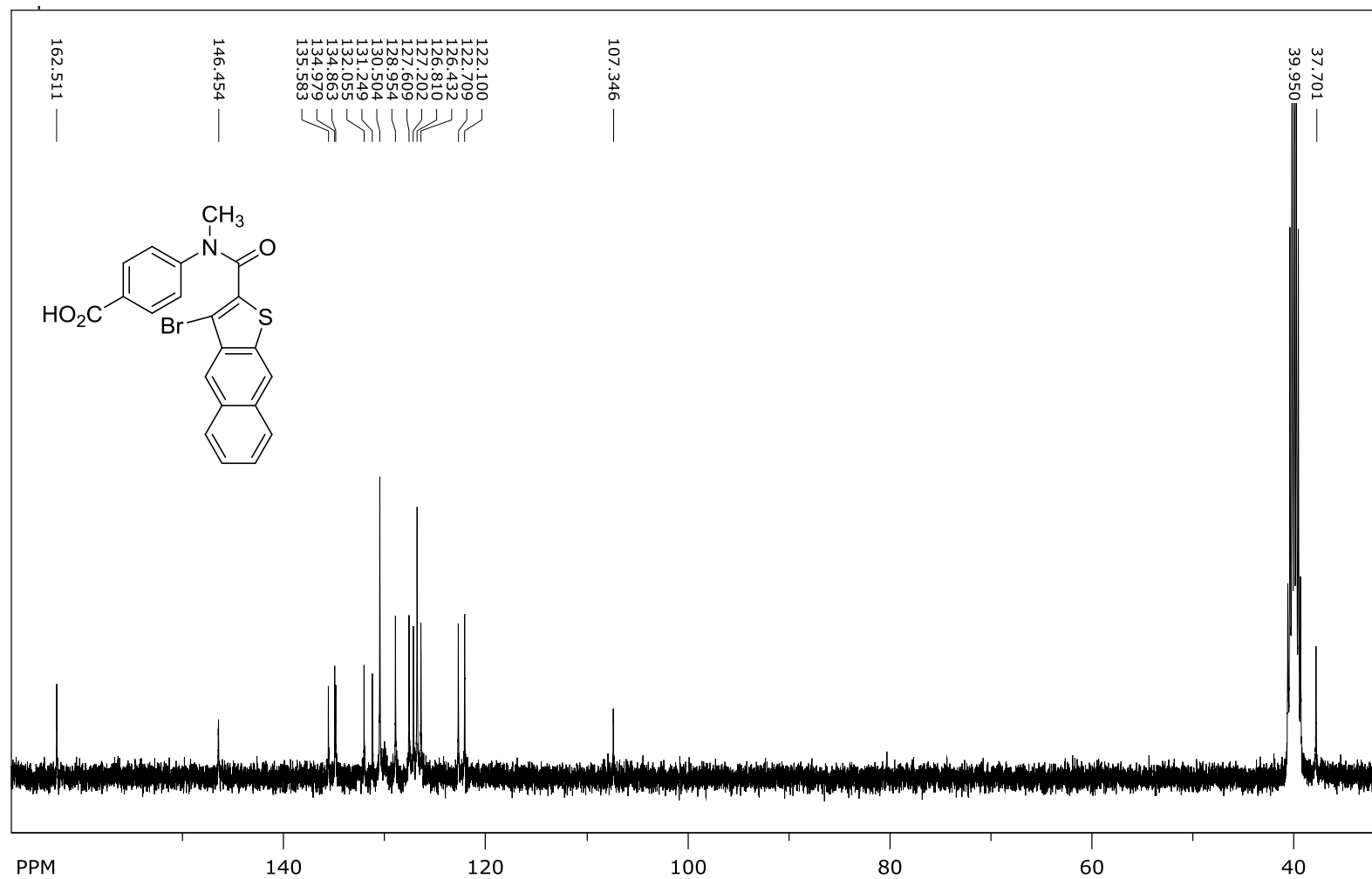


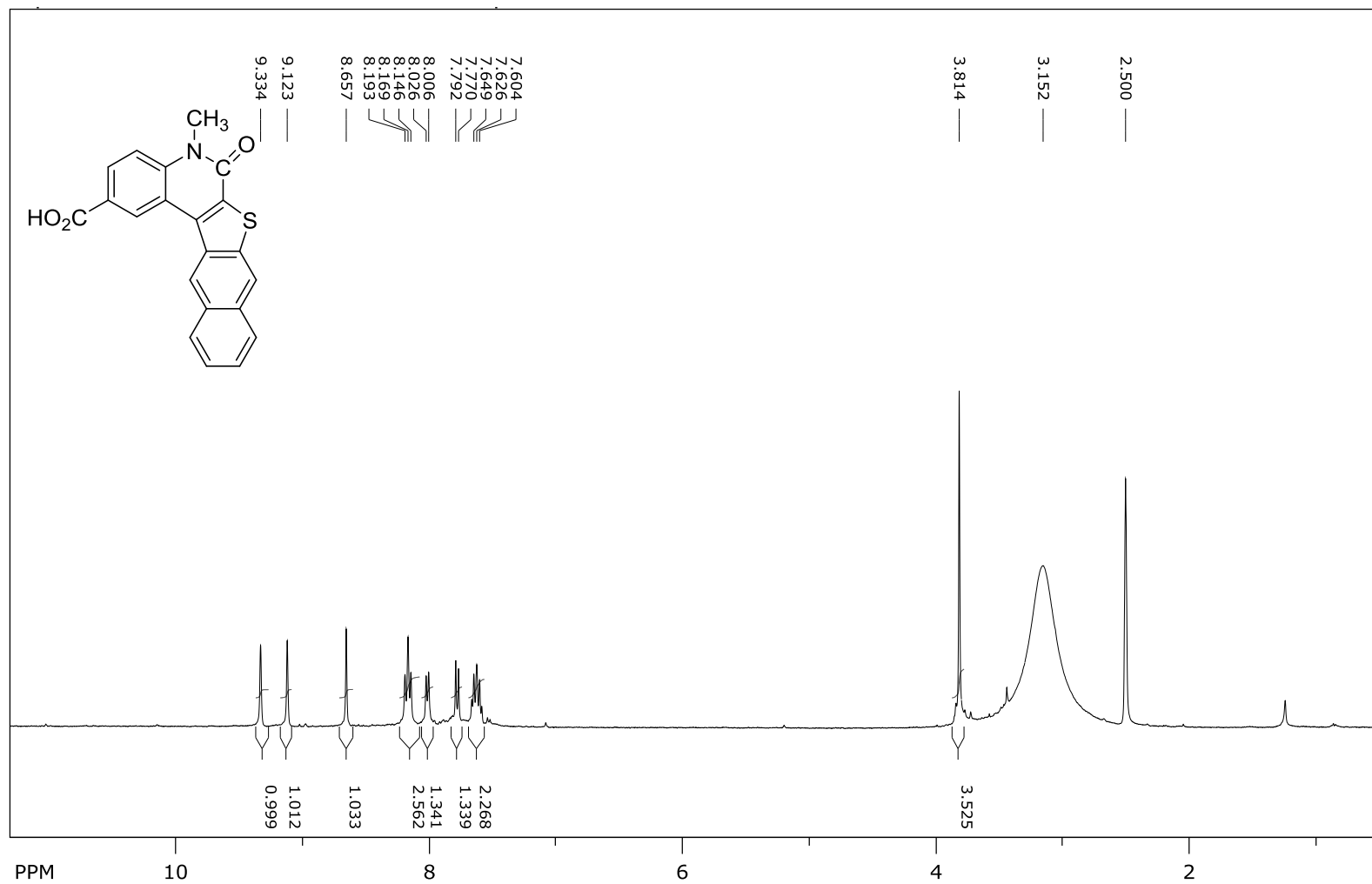
Figure 42. ^1H NMR Spectra of Compound **13b** in $\text{DMSO-}d_6$.



file: ...de\161010coohanilide-Cdms0.fid\fid block# 1 expt: "s2pul"
transmitter freq.: 100.524151 MHz

freq. of 0 ppm: 100.513598 MHz
processed size: 65536 complex points

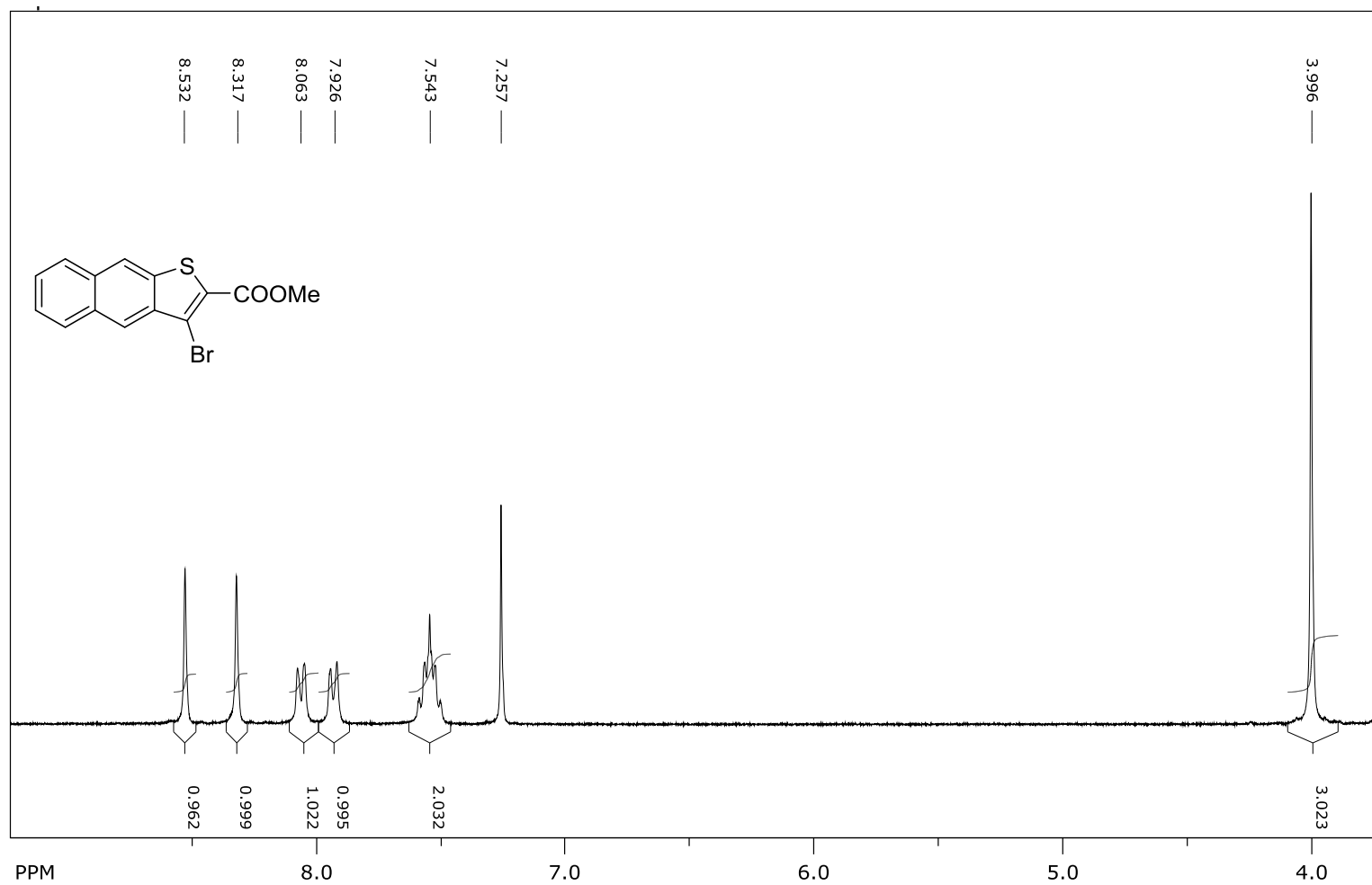
Figure 43. ^{13}C NMR Spectra of Compound **13b** in $\text{DMSO-}d_6$.



file: ...anilidephotoproduct-Hcdcl3.fid\fid_block# 1 expt: "s2pul"
 transmitter freq.: 399.736048 MHz

freq. of 0 ppm: 399.733635 MHz
 processed size: 32768 complex points

Figure 44. ^1H NMR Spectra of Compound **46b** in $\text{DMSO-}d_6$.



file: ...218metylesterbrnaph-hcdcl3.fid\fid block# 1 expt: "s2pul"
transmitter freq.: 300.133009 MHz

freq. of 0 ppm: 300.131208 MHz
processed size: 32768 complex points

Figure 46. ^1H NMR Spectra of Compound **34** in CDCl_3 .

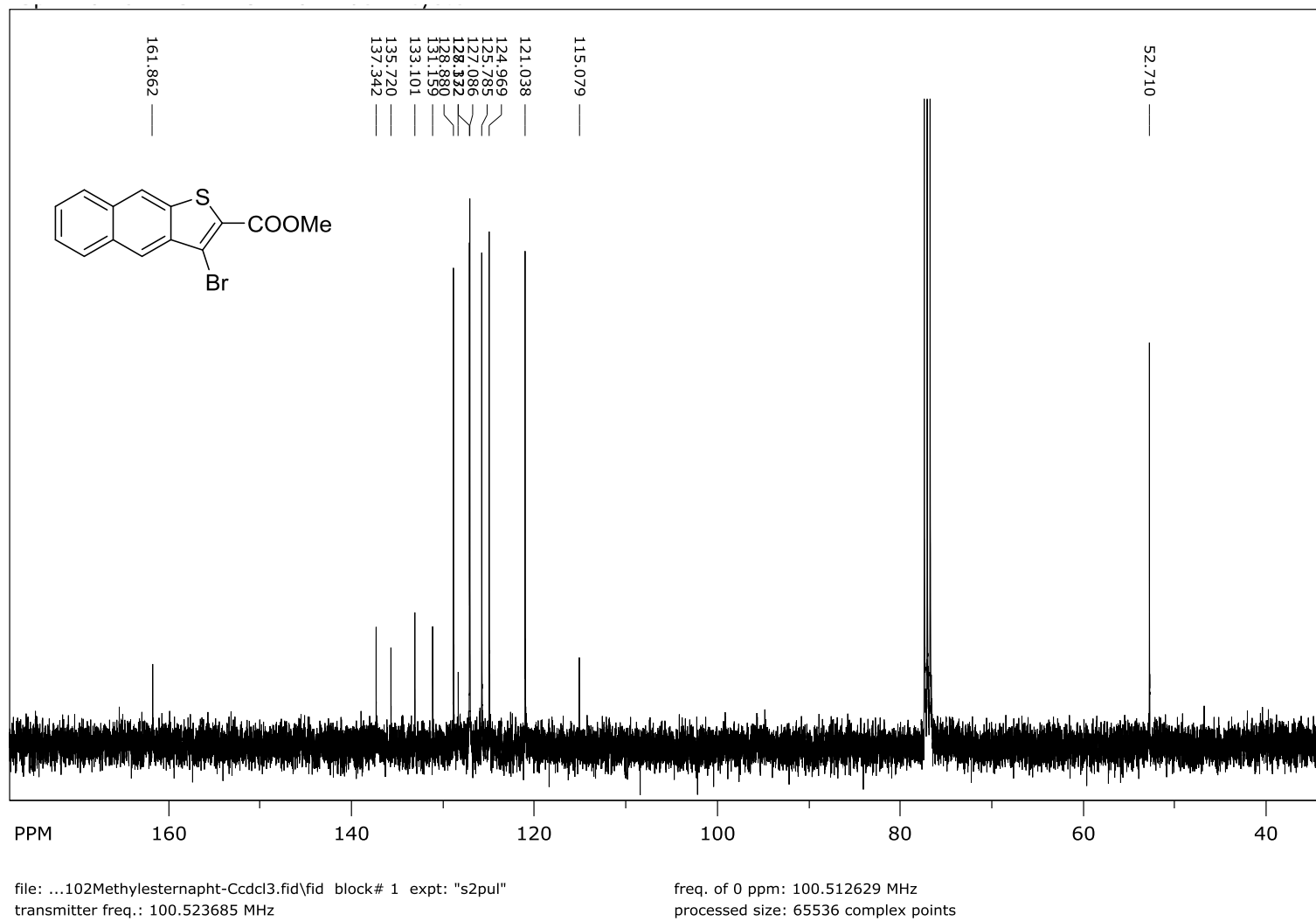
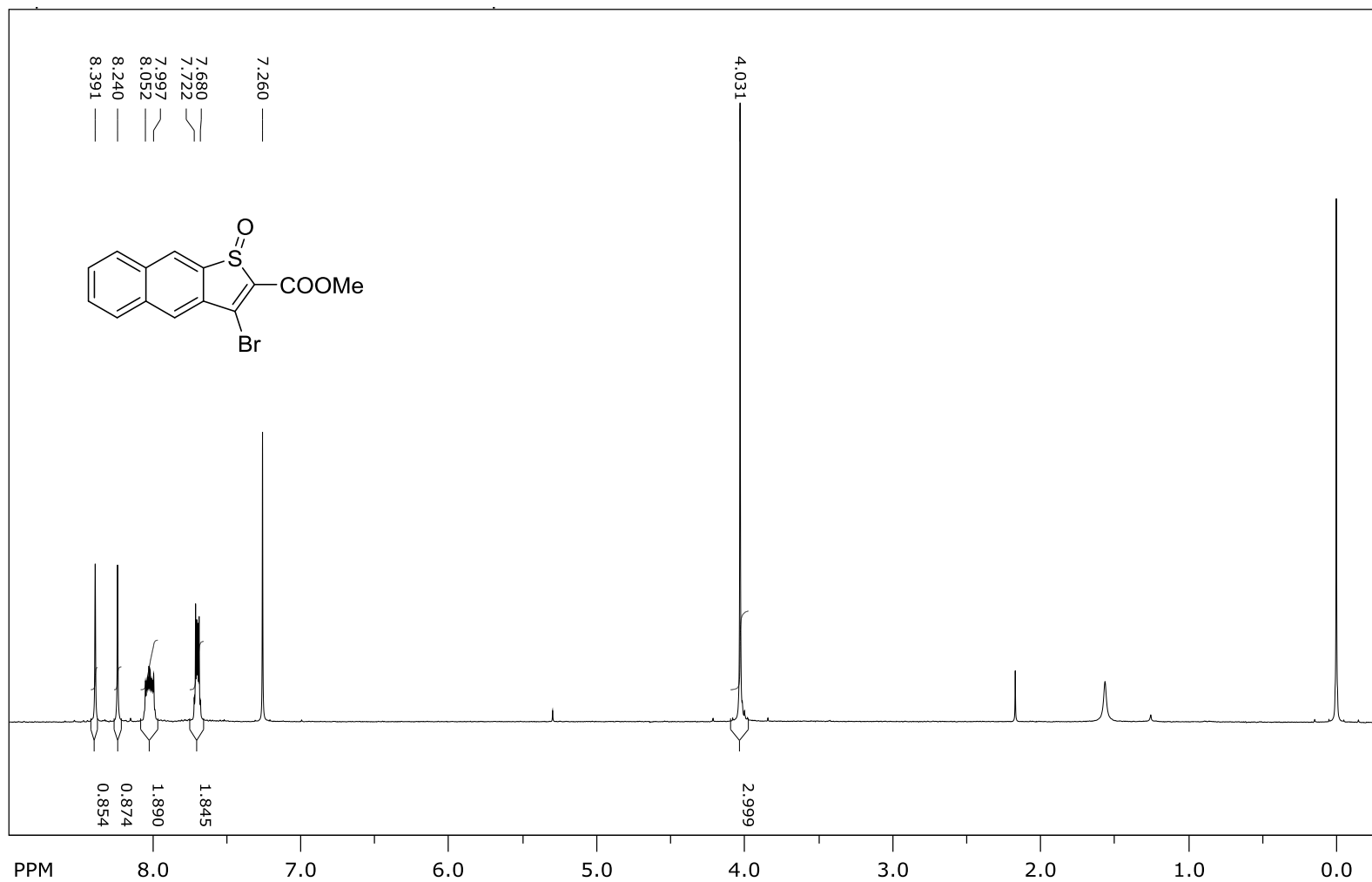


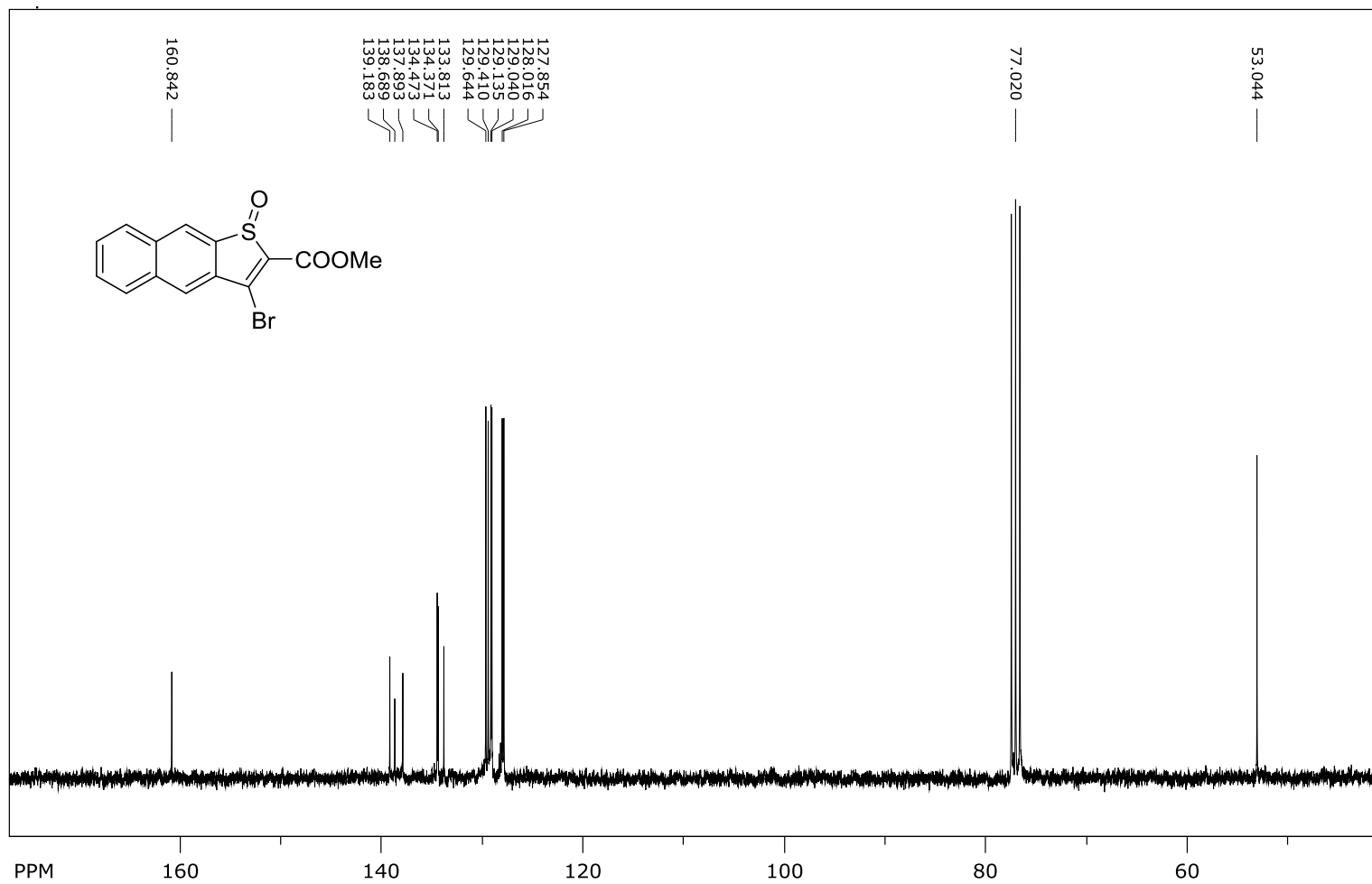
Figure 47. ¹³C NMR Spectra of Compound 34 in CDCl₃.



file: ...NMR\180122sulfoxide-hcdcl3.fid\fid block# 1 expt: "s2pul"
transmitter freq.: 399.734149 MHz

freq. of 0 ppm: 399.731743 MHz
processed size: 32768 complex points

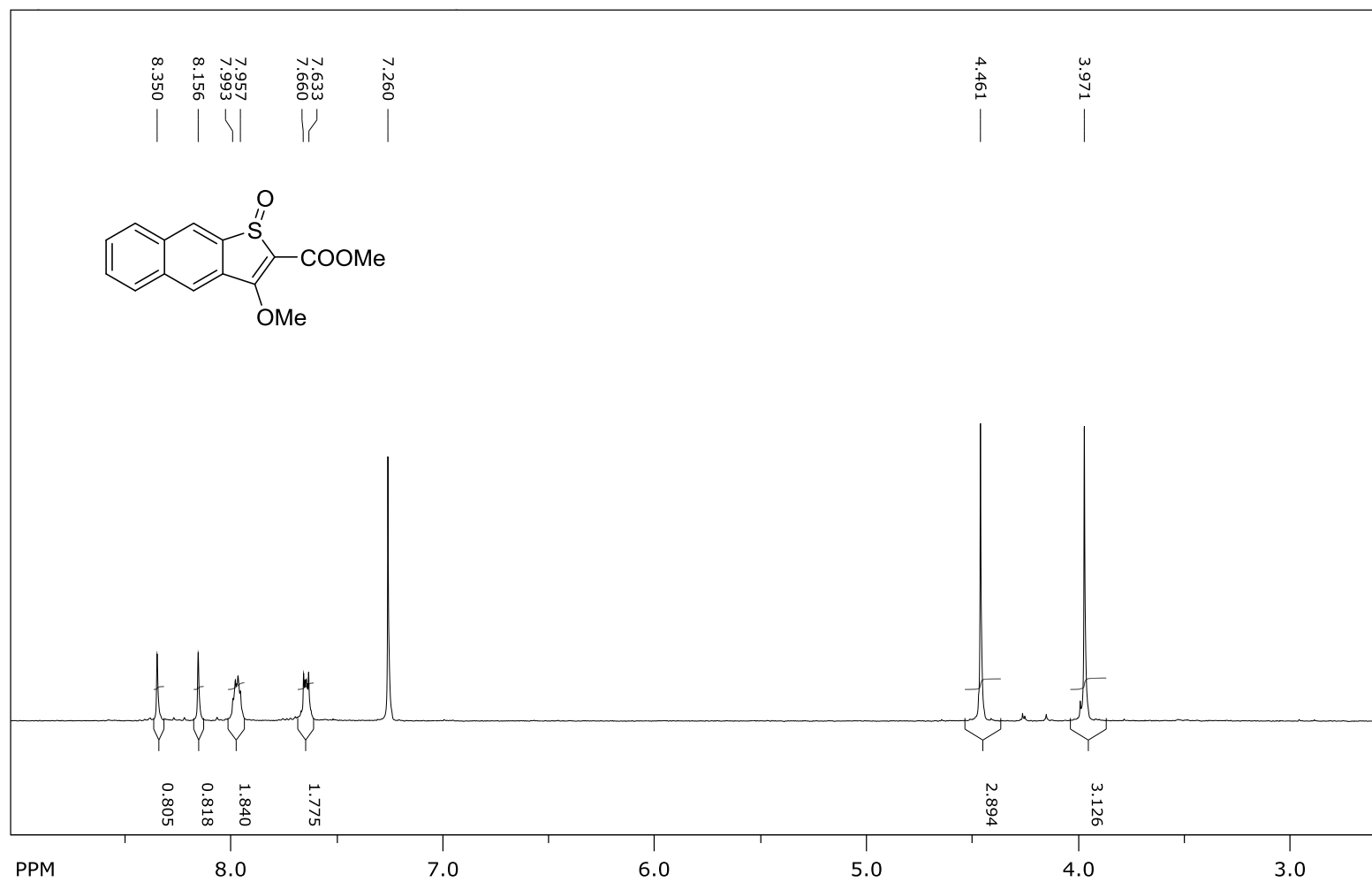
Figure 48. ^1H NMR Spectra of Compound 35 in CDCl_3 .



file: ...NMR\180125sulfoxide-Cdcl3.fid\fid block# 1 expt: "s2pul"
transmitter freq.: 75.476336 MHz

freq. of 0 ppm: 75.468055 MHz
processed size: 131072 complex points

Figure 49. ¹³C NMR Spectra of Compound 35 in CDCl₃



file: ...\\NMR\171226omesub-hcdcl3.fid\fid_block# 1_expt: "s2pul"
transmitter freq.: 399.734149 MHz

freq. of 0 ppm: 399.731743 MHz
processed size: 32768 complex points

Figure 50. ¹H NMR Spectra of Compound 36 in CDCl₃.

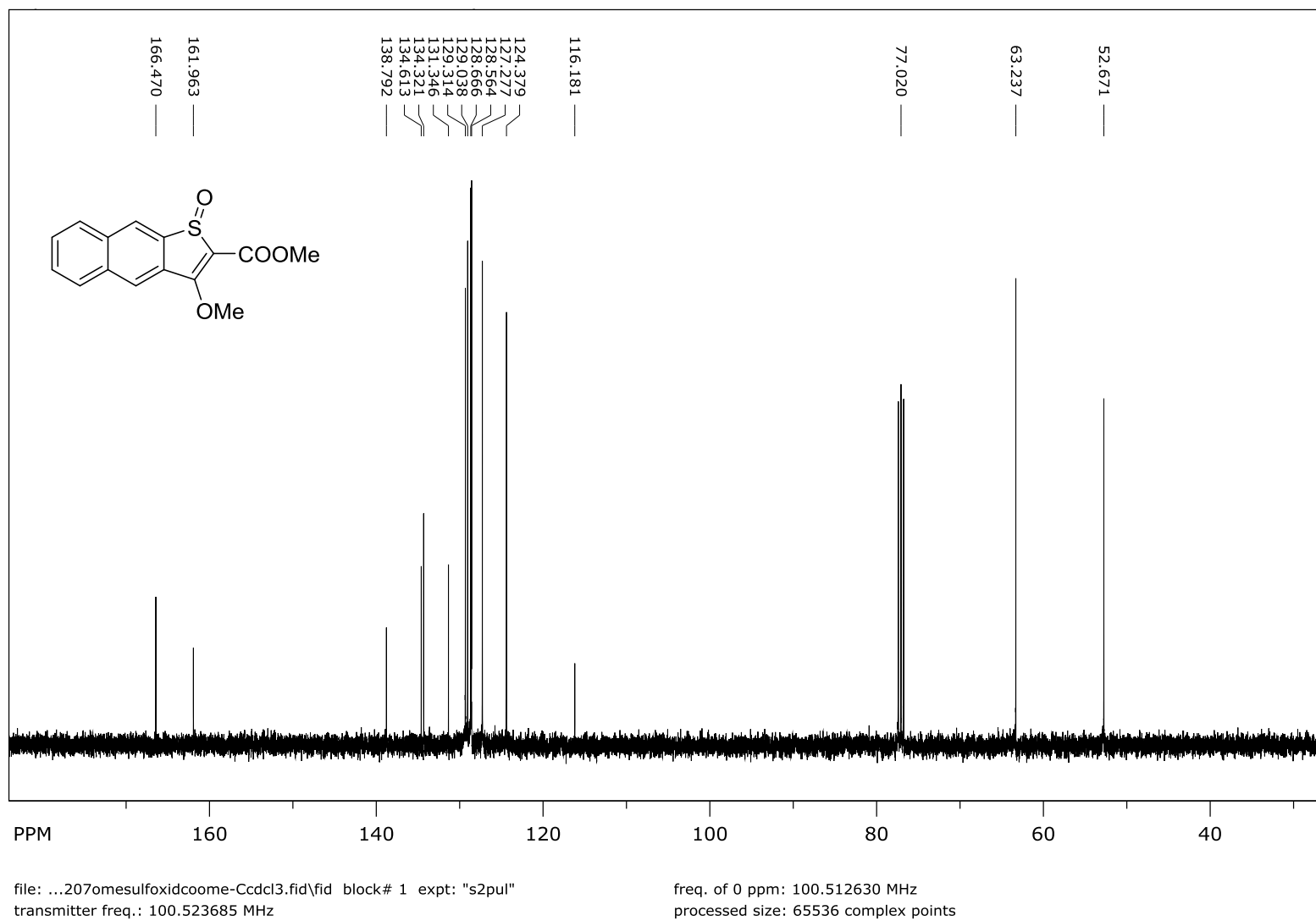
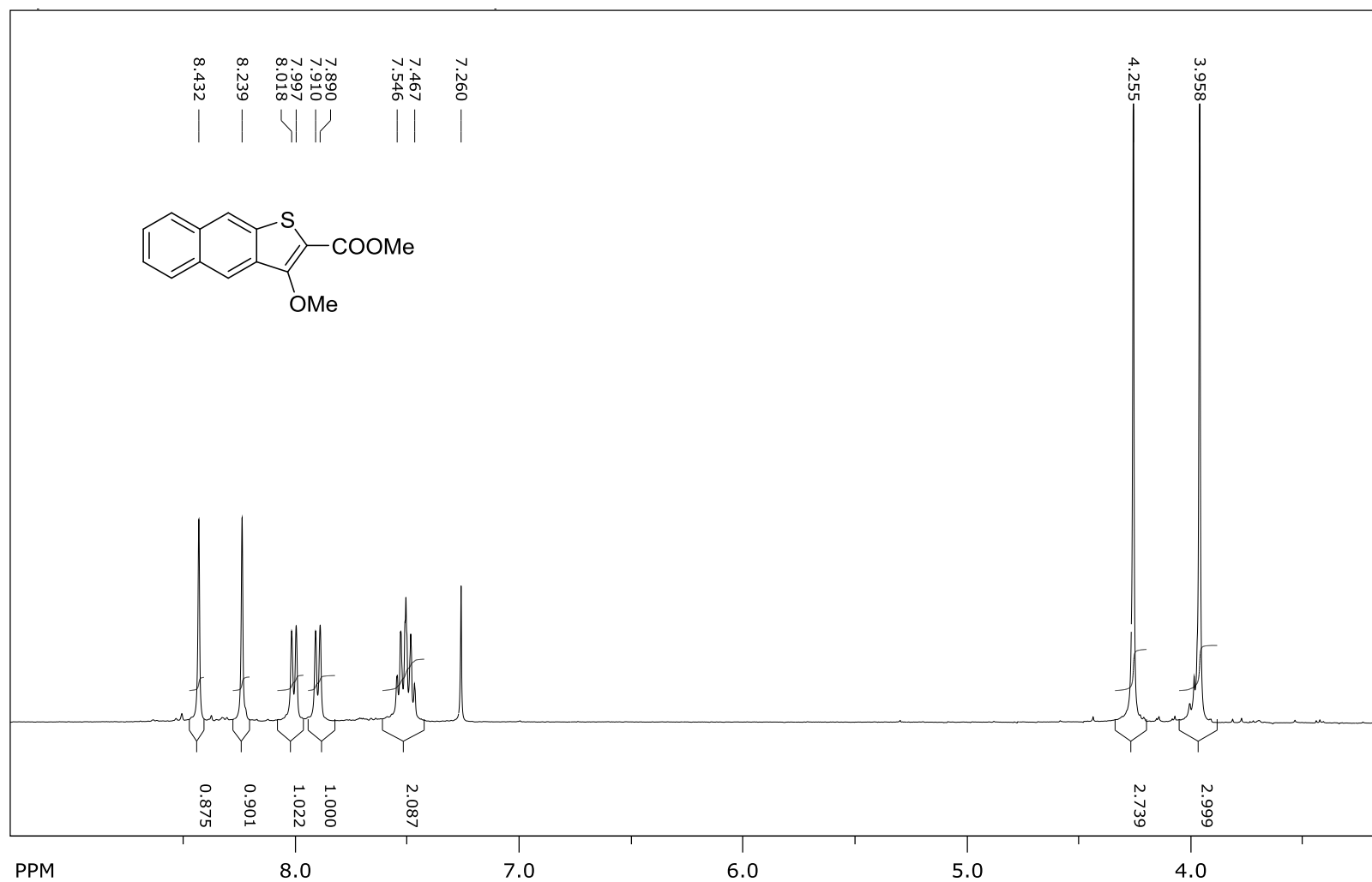


Figure 51. ^{13}C NMR Spectra of Compound 36 in CDCl_3 .



file: ...NMR\180121OMeCOOMe1-Hcdcl3.fid\fid block# 1 expt: "s2pul"
transmitter freq.: 399.736048 MHz

freq. of 0 ppm: 399.731742 MHz
processed size: 32768 complex points

Figure 52. ¹H NMR Spectra of Compound 37 in CDCl₃.

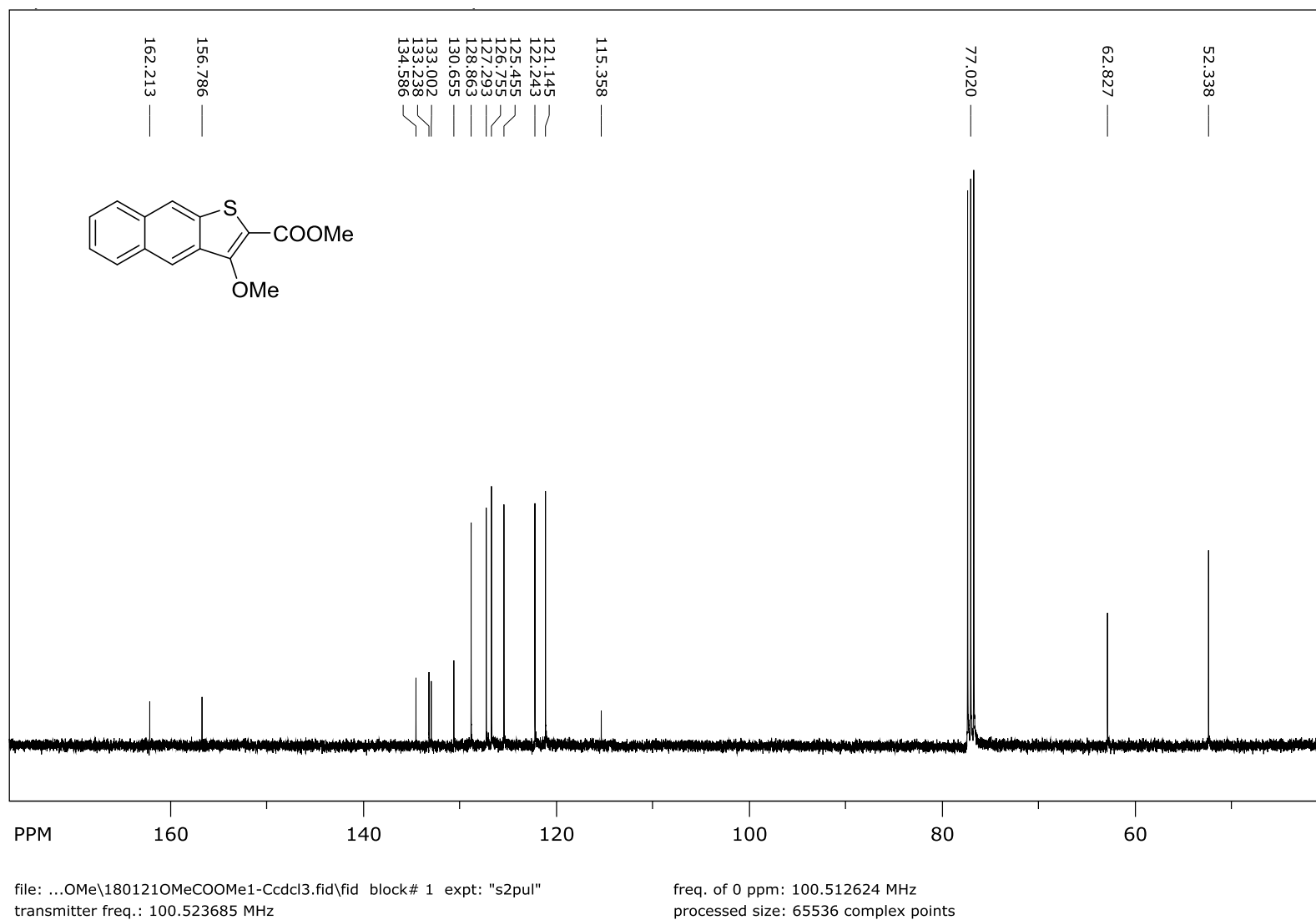
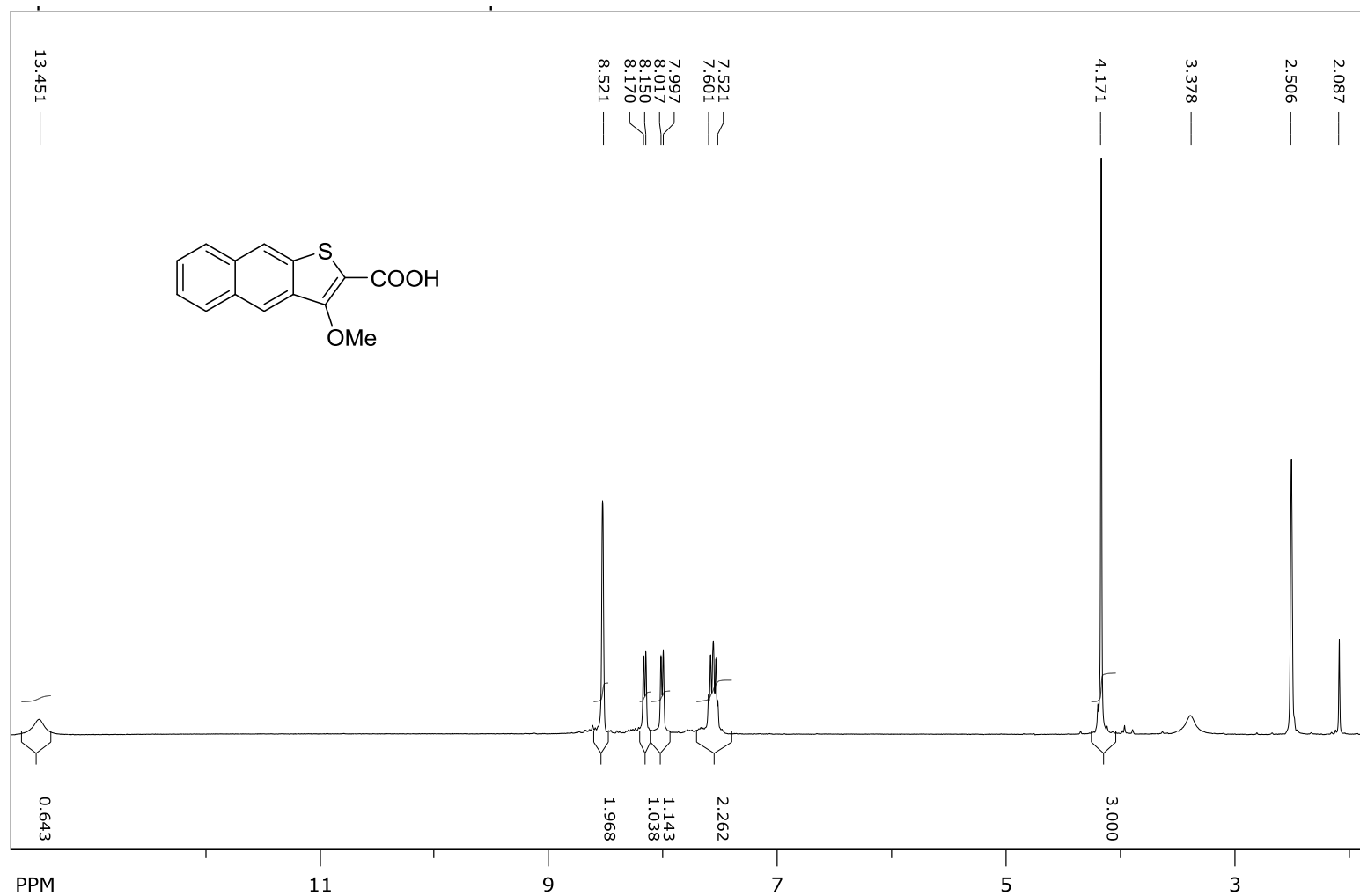


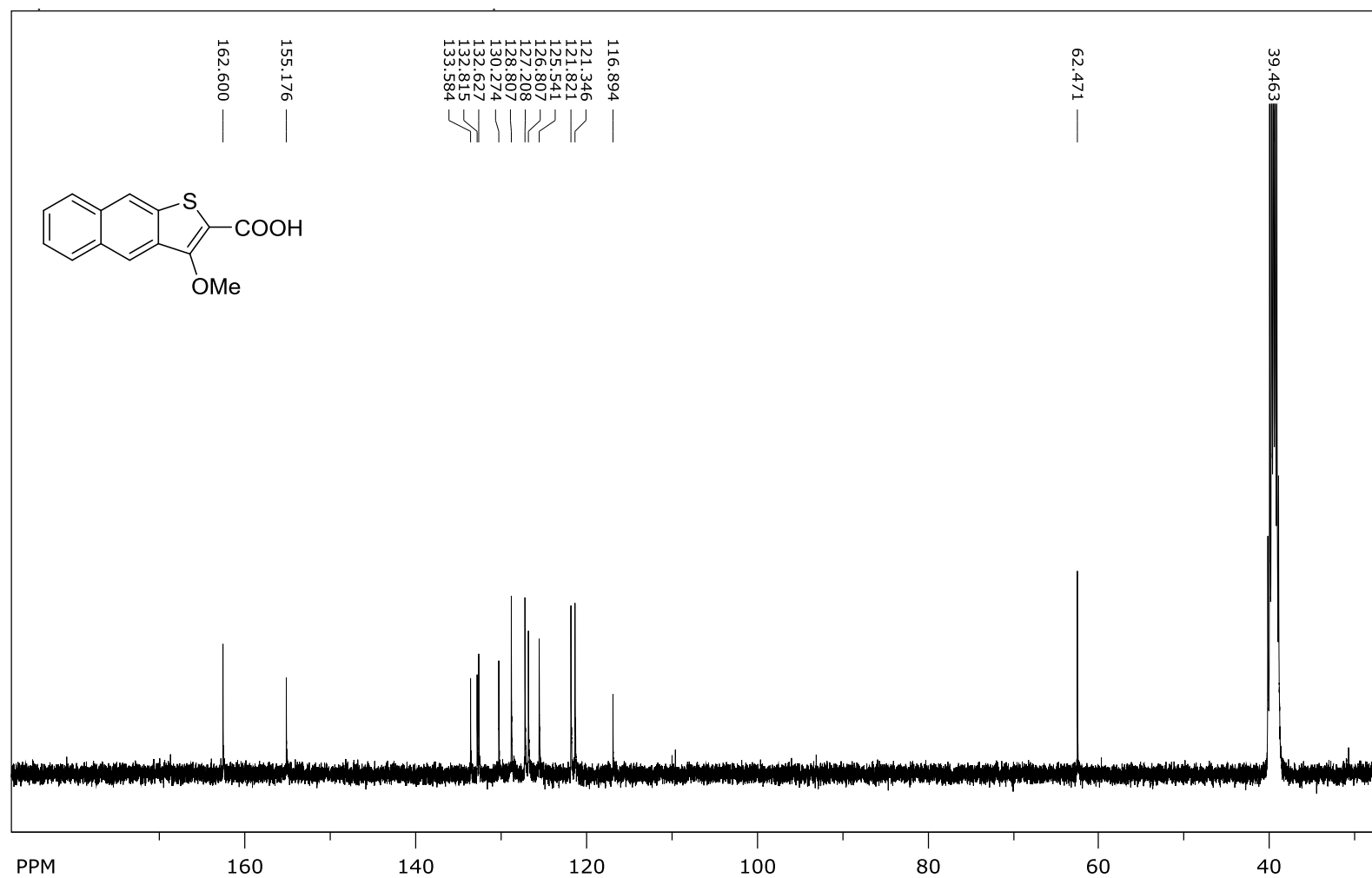
Figure 53. ^{13}C NMR Spectra of Compound **37** in CDCl_3 .



file: ...ho-OMe\180120OMeCOOH-Hdmsol.fid block# 1 expt: "s2pul"
transmitter freq.: 399.736048 MHz

freq. of 0 ppm: 399.733633 MHz
processed size: 32768 complex points

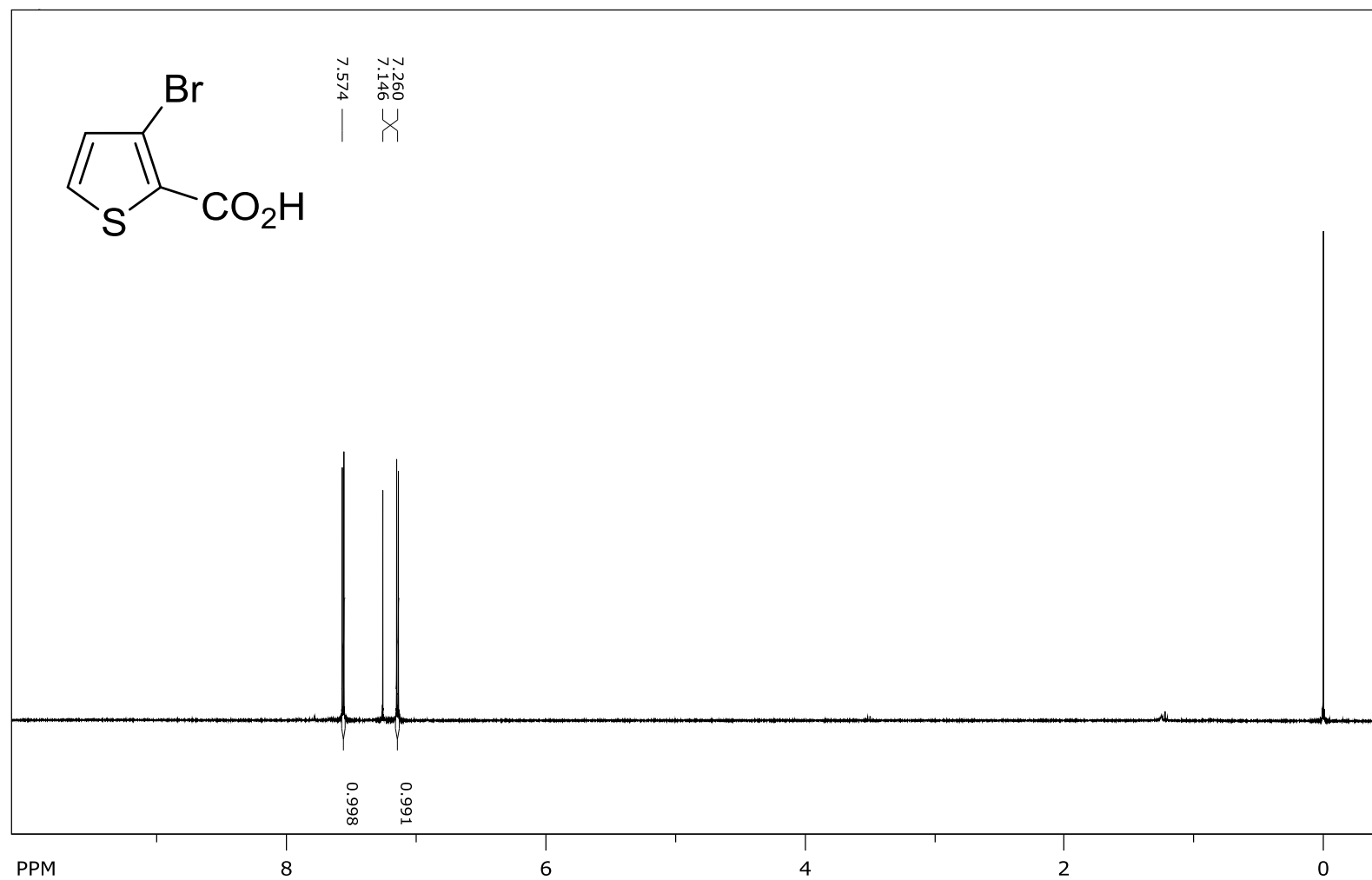
Figure 54. ^1H NMR Spectra of Compound **38** in CDCl_3 .



file: ...o-OMe\180121OMeCOOH1-Cdms0.fid\fid block# 1 expt: "s2pul"
transmitter freq.: 100.524163 MHz

freq. of 0 ppm: 100.513147 MHz
processed size: 65536 complex points

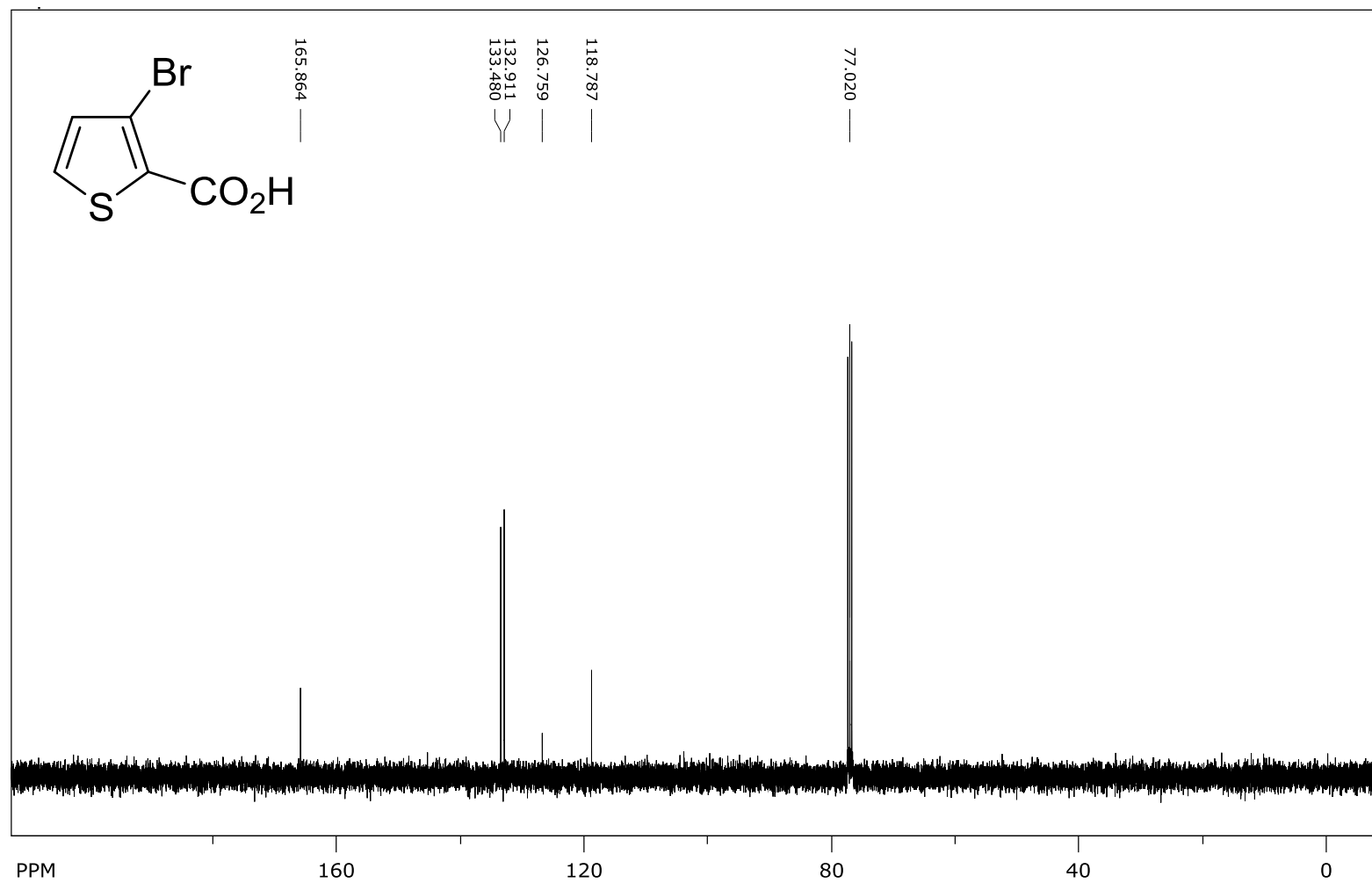
Figure 55. ¹³C NMR Spectra of Compound **38** in CDCl₃.



file: ...ingzi\3-bromothiopheneCOOH.fid\fid block# 1 expt: "s2pul"
transmitter freq.: 399.745875 MHz

freq. of 0 ppm: 399.743476 MHz
processed size: 65536 complex points

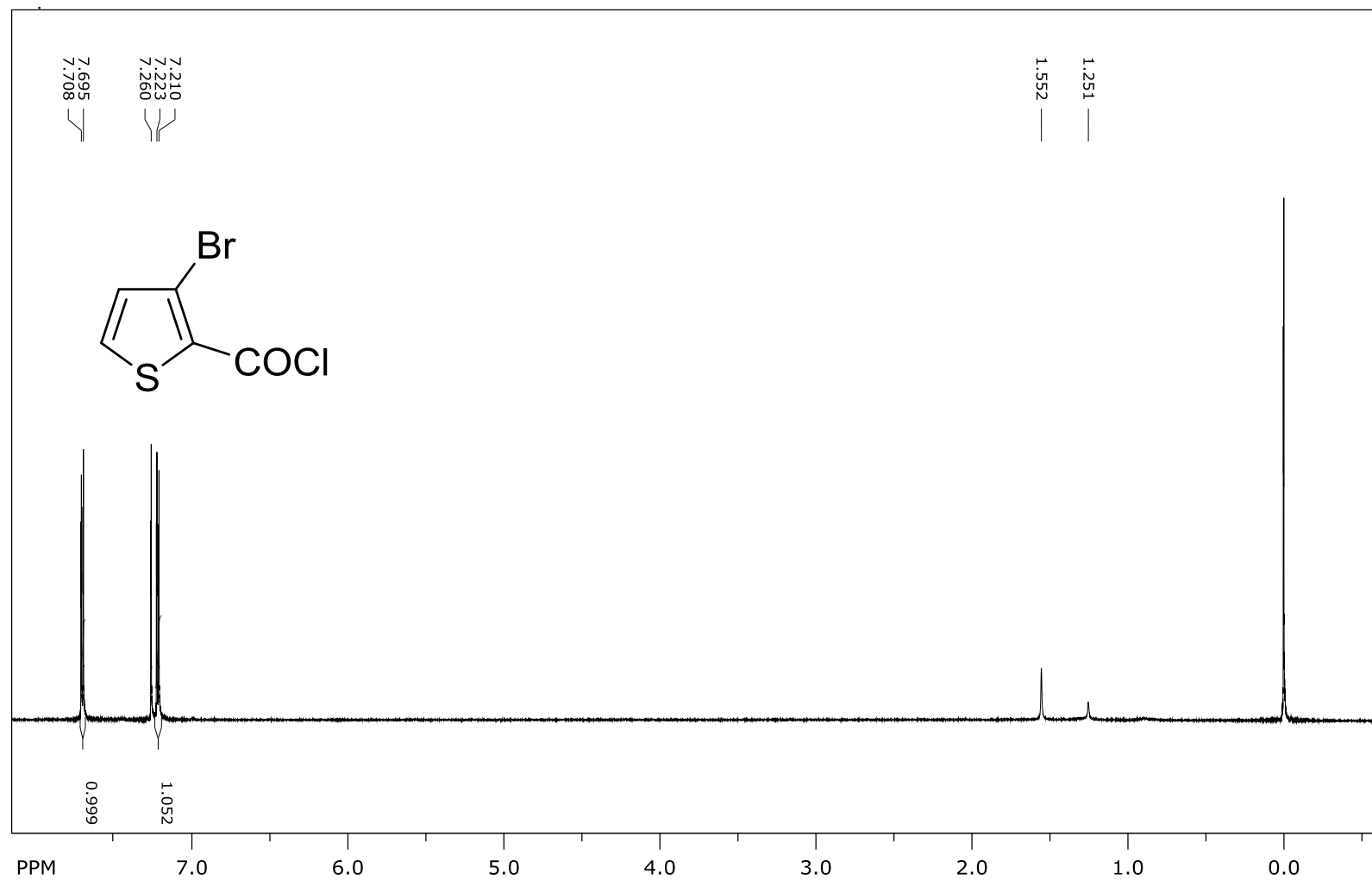
Figure 56. ^1H NMR spectra of compound **51** in CDCl_3 .



file: ...13bromothiopheneCOOHcarbon.fid\fid_block# 1 expt: "s2pul"
transmitter freq.: 100.526131 MHz

freq. of 0 ppm: 100.515575 MHz
processed size: 65536 complex points

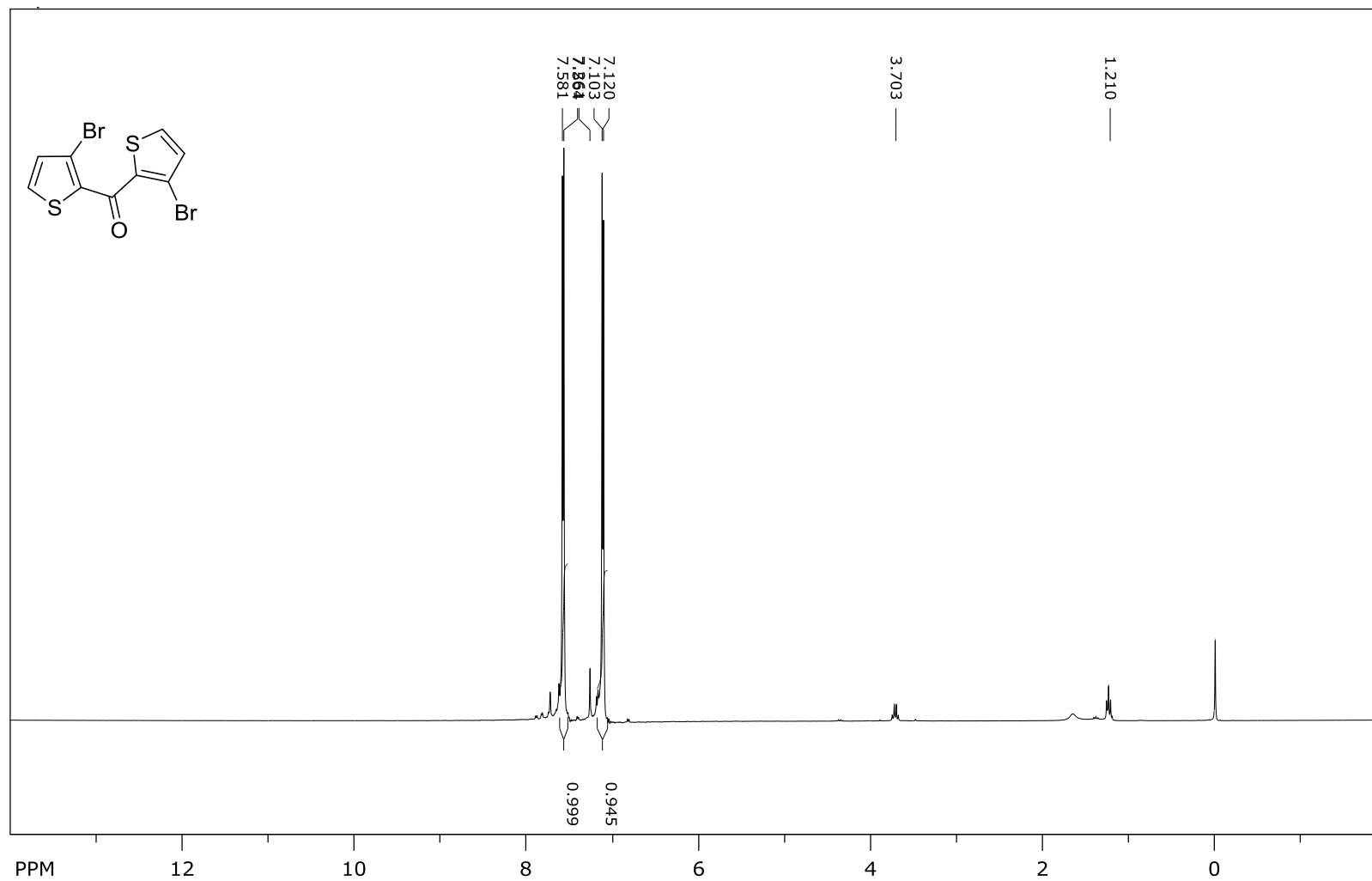
Figure 57. ^{13}C NMR spectra of compound **51** in CDCl_3 .



file: ...i steinmet1\hexanewashCOCl.fid\fid block# 1 expt: "s2pul"
transmitter freq.: 399.745875 MHz

freq. of 0 ppm: 399.743475 MHz
processed size: 65536 complex points

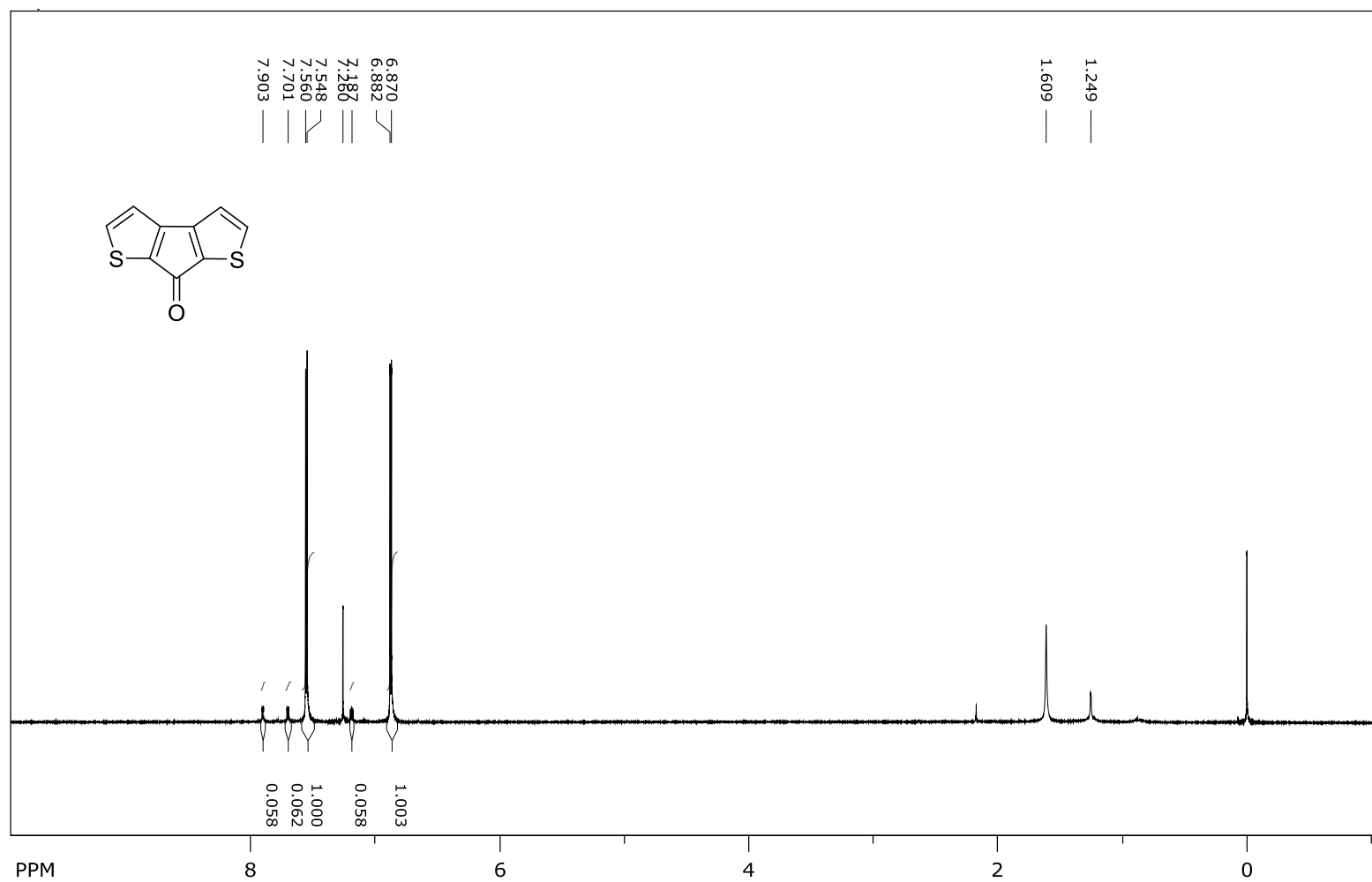
Figure 58. ¹H NMR spectra of compound **52** in CDCl₃.



file: ... lab comp\lingzi\130910f-c.fid\fid block# 1 expt: "s2pul"
transmitter freq.: 300.133009 MHz

freq. of 0 ppm: 300.131207 MHz
processed size: 32768 complex points

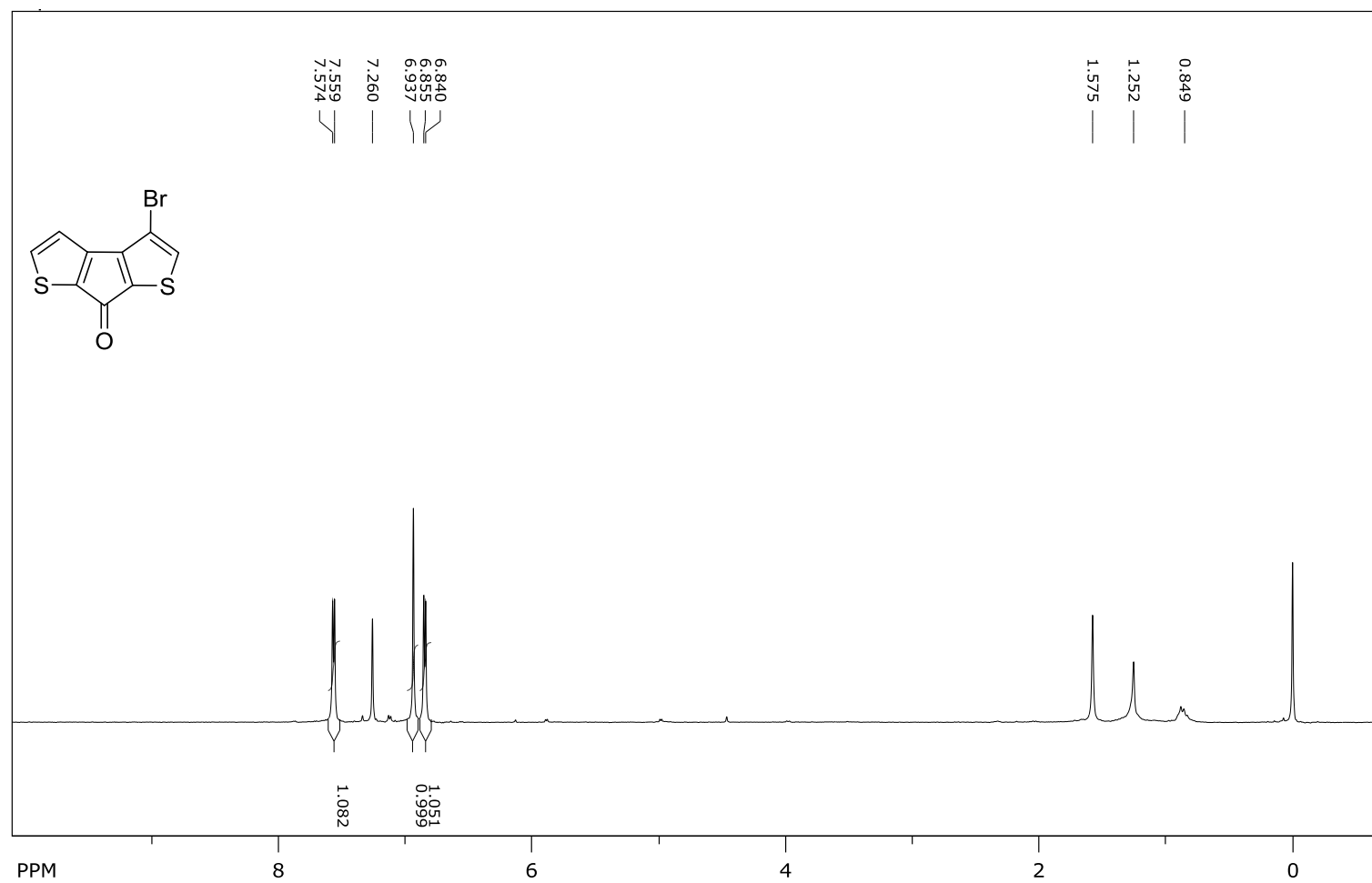
Figure 59. ¹H NMR spectra of compound 53 in CDCl₃.



file: ...gzi\080713bronzecolumn2-5H.fid\fid block# 1 expt: "s2pul"
transmitter freq.: 399.745875 MHz

freq. of 0 ppm: 399.743476 MHz
processed size: 65536 complex points

Figure 60. ^1H NMR spectra of compound **54** in CDCl_3 .



file: ...zi\130927brominationcolumn.fid\fid block# 1 expt: "s2pul"
transmitter freq.: 300.133009 MHz

freq. of 0 ppm: 300.131207 MHz
processed size: 32768 complex points

Figure 61. ¹H NMR spectra of compound 55 in CDCl₃.

BIBLIOGRAPHY

- (1) Sarker, M.; Shahrin, T.; Steinmetz, M. G. *Org. Lett.* **2011**, *13* (5), 872–875.
- (2) Sarker, M. I.; Shahrin, T.; Steinmetz, M. G.; Timerghazin, Q. K. *Photochem. Photobiol. Sci.* **2013**, *12* (2), 309–322.
- (3) Allonas, X.; Ley, C.; Bibaut, C.; Jacques, P.; Fouassier, J. P. *Chem. Phys. Lett.* **2000**, *322* (6), 483–490.
- (4) Melo, J. S. De; Rodrigues, L. M.; Serpa, C.; Arnaut, L. G.; Ferreira, I. C. F. R.; Queiroz, M. R. P. *Photochem. Photobiol.* **2003**, *77* (2), 121–128.
- (5) Wex, B.; Kaafarani, B. R.; Danilov, E. O.; Neckers, D. C. *J. Phys. Chem. A* **2006**, *110* (51), 13754–13758.
- (6) Zander, M.; Jacob, J.; Lee, M. L. *Z. Naturforsch* **1987**, *42* (7), 735–738.
- (7) Tiffe, H. W.; Matzke, K. H.; Thiessen, G. *Histochemistry* **1977**, *77*, 63–77.
- (8) Becker, R. S.; Favaro, G.; Poggi, G.; Romani, A. *J. Phys. Chem.* **1995**, *99* (5), 1410–1417.
- (9) McGall, G. H.; Barone, A. D.; Diggelmann, M.; Fodor, S. P. A.; Gentalen, E.; Ngo, N. *J. Am. Chem. Soc.* **1997**, *119* (22), 5081–5090.
- (10) Bochet, C. G. *J. Chem. Soc. Perkin Trans. 1* **2002**, No. 2, 125–142.
- (11) Falvey, D.; Sundararajan, C. *Photochem. Photobiol. Sci.* **2004**, *3* (9), 831–838.
- (12) Canepari, M.; Nelson, L.; Papageorgiou, G.; Corrie, J. E. T.; Ogden, D. J. *Neurosci. Methods* **2001**, *112* (1), 29–42.
- (13) Ellis-Davies, G. C. R. *Nat. Methods* **2007**, *4* (8), 619–628.
- (14) Ellis-Davies, G. C.; Kaplan, J. H.; Barsotti, R. J. *Biophys. J.* **1996**, *70* (2), 1006–1016.
- (15) Barltrop, J. A.; Schofield, P. *Tetrahedron Lett.* **1962**, No. 16, 697–699.
- (16) Go, M. A.; To, M.-S.; Stricker, C.; Redman, S.; Bachor, H.-A.; Stuart, G. J.; Daria, V. R. *Front. Cell. Neurosci.* **2013**, *7* (December), 1–9.
- (17) Ellis-Davies; C.R., G. *Beilstein J. Org. Chem.* **2013**, *9* (1), 64–73.
- (18) Callaway, E. M. *Curr. Biol.* **1994**, *4* (11), 1010–1012.

- (19) Tang, X.; Zhang, J.; Sun, J.; Wang, Y.; Wu, J.; Zhang, L. *Org. Biomol. Chem.* **2013**, *11* (45), 7814.
- (20) Pinheiro, A.; Baptista, P.; Lima, J. C. *Nucleic Acids Res.* **2008**, *36* (14), 1–7.
- (21) *Modern Molecular Photochemistry for Organic Molecules*; 2008; Vol. 108.
- (22) Ellis-Davies, G. C. R.; Barsotti, R. J. *Cell Calcium* **2006**, *39* (1), 75–83.
- (23) Ellis-Davies, G. C.; Kaplan, J. H. *Proc. Natl. Acad. Sci. U. S. A.* **1994**, *91* (1), 187–191.
- (24) Kasai, H. *Trends Neurosci.* **1999**, *22* (2), 88–93.
- (25) Shigeri, Y.; Tatsu, Y.; Yumoto, N. *Pharmacol. Ther.* **2001**, *91* (2), 85–92.
- (26) Riggsbee, C. W.; Deiters, A. *Trends Biotechnol.* **2010**, *28* (9), 468–475.
- (27) Ando, H.; Furuta, T.; Tsien, R. Y.; Okamoto, H. *Nat. Genet.* **2001**, *28* (4), 317–325.
- (28) Furuta, T.; Noguchi, K. *TrAC - Trends Anal. Chem.* **2004**, *23* (7), 511–519.
- (29) Zou, K.; Cheley, S.; Givens, R. S.; Bayley, H. *J. Am. Chem. Soc.* **2002**, *124* (28), 8220–8229.
- (30) Kaplan, J. H.; Forbush, B.; Hoffman, J. F. *Biochemistry* **1978**, *17* (10), 1929–1935.
- (31) Pratap, P. R.; Dediu, O.; Nienhaus, G. U. *Biophys. J.* **2003**, *85* (6), 3707–3717.
- (32) Monroe, W. T.; McQuain, M. M.; Chang, M. S.; Alexander, J. S.; Haselton, F. R. *J. Biol. Chem.* **1999**, *274* (30), 20895–20900.
- (33) Sheehan, J. C.; Umezawa, K. *J. Org. Chem.* **1973**, *38* (21), 3771–3774.
- (34) Lester, H. A.; Erbonne, J. M. N. *Ann. Rev. Biophys. Bioeng* **1982**, *11* (84), 151–175.
- (35) Kanaoka, Y.; Itoh, K.; Hatanaka, Y.; Flippen, J. L.; Karle, I. L.; Witkop, B. *J. Org. Chem.* **1975**, *40* (20), 3001–3003.
- (36) Kudo, H.; Castle, R. n. *J. Heterocycl. Chem.* **1985**, *22*, 211–214.
- (37) Ndzeidze, G. Photoremovable Protecting Groups Based on Electrocyclization with Leaving Group Expulsion Via a Proposed Zwitterion, Marquette University, 2018.
- (38) Murov, S. L. .; Carmichael, I.; Hug, G. L. *Handbook of Photochemistry*, 2nd ed.; Marcel Dekker: New York, 1993.

- (39) Turro, N. J.; V.Ramamurthy; Scaiano, J. C. *Principles of Molecular Photochemistry: an introduction.*, 1st ed.; Jeanette Stiefel, Ed.; Sausalito, 2009.
- (40) Wöll, D.; Walbert, S.; Stengele, K. P.; Albert, T. J.; Richmond, T.; Norton, J.; Singer, M.; Green, R. D.; Pfleiderer, W.; Steiner, U. E. *Helv. Chim. Acta* **2004**, *87* (1), 28–45.
- (41) Wöll, D.; Laimgruber, S.; Galetskaya, M.; Smirnova, J.; Pfleiderer, W.; Heinz, B.; Gilch, P.; Steiner, U. E. *J. Am. Chem. Soc.* **2007**, *129* (40), 12148–12158.
- (42) Barltrop, J. A.; Plant, P. J.; Schofield, P. *Chem. Commun.* **1966**, 822–823.
- (43) Kla, P.; Bochet, C. G.; Givens, R.; Rubina, M.; Popik, V.; Kostikov, A.; Wirz, J. *Chem. Rev.* **2013**, *113* (1), 119–191.
- (44) Kohl-Landgraf, J.; Buhr, F.; Lefrancois, D.; Mewes, J. M.; Schwalbe, H.; Dreuw, A.; Wachtveitl, J. *J. Am. Chem. Soc.* **2014**, *136* (9), 3430–3438.
- (45) Il'ichev, Y. V.; Wirz, J. *J. Phys. Chem. A* **2000**, *104* (33), 7856–7870.
- (46) Pelliccioli, A. P.; Wirz, J. *Photochem. Photobiol. Sci.* **2002**, *1* (7), 441–458.
- (47) Montanari, S.; Paradisi, C.; Scorrano, G. *J. Org. Chem.* **1999**, *64* (10), 3422–3428.
- (48) Sheehan, J. C.; Wilson, R. M. *J. Am. Chem. Soc.* **1964**, *86* (23), 5277–5281.
- (49) Givens, R. S.; Matuszewski, B.; M, R. S.; Athey, P. S. *J. Am. Chem. Soc.* **1990**, *112*, 6016–6021.
- (50) Givens, R. S.; Matuszewski, B. *J. Am. Chem. Soc.* **1984**, *106*, 6860–6861.
- (51) Corrie, J. E. T.; Furuta, T.; Givens, R. S.; Yousef, A. L.; Goeldner, M. *Photoremovable Protecting Groups Used for the Caging of Biomolecules*; 2005; Vol. 1999.
- (52) Givens, R. S.; Heger, D.; Hellrung, B.; Kamdzhilov, Y.; Mac, M.; Conrad, P. G.; Cope, E.; Lee, J. I.; Mata-Segreda, J. F.; Schowen, R. L.; Wirz, J. *J. Am. Chem. Soc.* **2008**, *130* (11), 3307–3309.
- (53) Hagen, V.; Bendig, J.; Frings, S.; Eckardt, T.; Helm, S.; Reuter, D.; Kaupp, U. B. **2001**, *40* (6), 1045–1048.
- (54) Suzuki, A. Z.; Watanabe, T.; Kawamoto, M.; Nishiyama, K.; Yamashita, H.; Ishii, M.; Iwamura, M.; Furuta, T. *Org. Lett.* **2003**, *5* (25), 4867–4870.
- (55) Schade, B.; Hagen, V.; Schmidt, R.; Herbrich, R.; Krause, E.; Eckardt, T.; Bendig, J. *J. Org. Chem.* **1999**, *64* (25), 9109–9117.
- (56) Wang, S. S. H.; Augustine, G. J. *Neuron* **1995**, *15* (4), 755–760.

- (57) Activity, L. P.; Rossi, F. M.; Margulis, M.; Kao, J. P. Y.; Rossi, F. M.; Margulis, M.; Tang, C.; Kao, J. P. Y. *J. Biol. Chem.* **1997**, *272*, 32933–32939.
- (58) Grewer, C. **2000**, 2063–2070.
- (59) Muralidharan, S.; Nerbonne, J. M. *J. Photochem. Photobiol. B Biol.* **1995**, *27*, 123–137.
- (60) Gee, K. R.; Niu, L.; Schaper, K.; Jayaraman, V.; Hess, G. P. **1999**, 3140–3147.
- (61) Breitinger, H. A.; Wieboldt, R.; Ramesh, D.; Carpenter, B. K.; Hess, G. P. **2000**, 5500–5508.
- (62) Ellis-Davies, G. C. R. *Chem. Rev.* **2008**, *108*, 1603–1613.
- (63) Ellis-Davies, G. C. R. **2003**, *360*, 226–238.
- (64) Adams, S. R.; Kao, J. P. Y.; Gryniewicz, G.; Minta, A.; Tsien, R. Y. *J. Am. Chem. Soc.* **1988**, *110* (10), 3212–3220.
- (65) Geibel, S.; Barth, A.; Amslinger, S.; Jung, A. H.; Burzik, C.; Clarke, R. J.; Givens, R. S.; Fendler, K. **2000**, *79* (September), 1346–1357.
- (66) Fendler, B. K.; Hartung, K.; Nagel, G.; Bamberg, E. *Methods Enzymol.* **1998**, *291*, 289–306.
- (67) Fendler, K.; Dro, S.; Epstein, W.; Bamberg, E.; Altendorf, K. **1999**, 1850–1856.
- (68) Ellman, B. J. O. N.; Mendel, D.; Anthony-cahill, S.; Christopher, J. N. O. R. E. N.; Schultz, P. G. **1991**, *202* (1989).
- (69) Miller, J. C.; Silverman, S. K.; England, P. M.; Dougherty, D. A.; Lester, H. A. *Neuron* **1998**, *20*, 619–624.
- (70) Merrifield, R. B. *J. Am. Chem. Soc.* **1963**, *85* (14), 2149–2154.
- (71) Merrifield, B. *Methods Enzymol.* **1997**, *289* (1951), 3–13.
- (72) Tatsu, Y.; Shigeri, Y.; Sogabe, S.; Yumoto, N.; Yoshikawa, S. *Biochem. Biophys. Res. Commun.* **1996**, *693*, 688–693.
- (73) Tang, X.; Dmochowski, I. *J. Mol. BioSyst.* **2007**, *3* (2), 100–110.
- (74) Chaulk, S. G.; MacMillan, A. M. *Nucleic Acids Res.* **1998**, *26* (13), 3173–3178.
- (75) Ndzeidze, G. N.; Li, L.; Steinmetz, M. G. *J. Org. Chem.*
- (76) Higa, T.; Krubsack, A. J. *J. Org. Chem.* **1976**, *41* (21), 3399–3403.

- (77) Curie, J.; Curie, P. *J. Chem. Inf. Model.* **1977**, *53*, 21.
- (78) Lindley, W. A.; MacDowell, D. W. H.; Petersen, J. L. *J. Org. Chem.* **1983**, *1700* (9), 4419–4421.
- (79) Alvarez-Insua, A. S.; Conde, S.; Corral, C. *J. Heterocycl. Chem.* **1982**, *19*, 713–719.
- (80) Dehmlow, E. V.; Niemaiin, T.; Kraft, A. *Synth. Commun.* **1996**, *26* (8), 1467–1472.
- (81) Tang, M. L.; Okamoto, T.; Bao, Z. *J. Am. Chem. Soc.* **2006**, *128*, 16002–16003.
- (82) Amstutz, E. D.; Neumoyer, C. R. *J. Am. Chem. Soc.* **1947**, *69*, 1925–1929.
- (83) Niu, S.; Schneider, R.; Vidal, L.; Balan, L. *Nanoscale* **2013**, *5* (14), 6538.
- (84) David, E.; Perrin, J.; Pellet-Rostaing, S.; Fournier Dit Chabert, J.; Lemaire, M. *J. Org. Chem.* **2005**, *70* (9), 3569–3573.
- (85) Zimmerman, H. *Mol. Photochem* **1971**, *3* (3), 281–292.
- (86) Nicolaou, K. C.; Estrada, A. A.; Zak, M.; Lee, S. H.; Safina, B. S. *Angew. Chemie - Int. Ed.* **2005**, *44* (9), 1378–1382.
- (87) Kikuchi, M.; Kikuchi, K.; Kokubun, H. *Bull. Chem. Soc. Jpn.* 1974, pp 1331–1333.
- (88) Neumann, M. G.; Gehlen, M. H.; Encinas, M. V.; Allen, N. S.; Corrales, T.; Peinado, C.; Catalina, F. *J. Chem. Soc. Faraday Trans.* **1997**, *93* (8), 1517–1521.
- (89) Omota, L.; Iulian, O.; Ciocîrlan, O.; Nita, I. *Rev. Roum. Chim* **2008**, *53* (11), 977–988.
- (90) Herkstroeter, W. G.; Hammond, G. S. *J. Am. Chem. Soc.* **1966**, *88* (21), 4769–4777.
- (91) Zimmerman, H. E.; E.Caufield, C.; King, R. K. *J. Am. Chem. Soc.* **1985**, *107* (25), 7724–7732.
- (92) Gupta, V. S.; Kraft, S. C.; Samuelson, J. S. *J. Chromatogr. A* **1967**, *26* (0), 158–163.
- (93) Wagner, P. J.; Kochevar, I. *J. Am. Chem. Soc.* **1968**, *958* (6), 2232–2238.
- (94) Das, S.; Rajesh, C. S.; Suresh, C. H.; Thomas, K. G.; Ajayaghosh, A.; Nasr, C.; Kamat, P. V.; George, M. V. *Macromolecules* **1995**, *28* (12), 4249–4254.
- (95) Klan, P.; Wagner, P. J. *J. Am. Chem. Soc.* **1998**, *120* (9), 2198–2199.

- (96) Hatchard, C. G.; Parker, C. A. *Proc. R. Soc. A Math. Phys. Eng. Sci.* **1956**, 235 (1203), 518–536.
- (97) Rawson, G.; Wynberg, H. *J. Chem. Soc. C* **1970**, 0, 273–277.
- (98) Kleiderer, E. C.; Adams, R. *J. Am. Chem. Soc.* **1933**, 55 (10), 4219–4225.